GEAP-3785

NUCLEAR SUPERHEAT PROJECT

Eighth Quarterly Progress Report, April–June 1961

By
R. T. Pennington

March 1962
[DTI Issuance Date]

Atomic Power Equipment Department
General Electric Company
San Jose, California

UNITED STATES ATOMIC ENERGY COMMISSION • DIVISION OF TECHNICAL INFORMATION

LEGAL NOTICE

Printed in USA. Price $4.00. Available from the Office of Technical Services, Department of Commerce, Washington 25, D. C.

USAEC Division of Technical Information Extension, Oak Ridge, Tennessee

GEAP-3785

REACTOR TECHNOLOGY

NUCLEAR SUPERHEAT PROJECT

EIGHTH QUARTERLY PROGRESS REPORT

April - June, 1961

prepared for

THE U.S. ATOMIC ENERGY COMMISSION

under

CONTRACT NO. AT(04-3)-189, PROJECT AGREEMENT #13

by

R. T. Pennington

Atomic Power Equipment Department

GENERAL ELECTRIC COMPANY

San Jose, California

CONTRIBUTORS

R. T. Pennington	Project Engineer Nuclear Superheat Project

S. F. Armour
H. N. Bass
F. J. Brutschy
N. V. Buikema
M. R. Carrothers
J. T. Cochran
C. O. Coffer
R. M. Cohen
F. A. Comprelli
M. L. Couchman
E. L. Esch
T. F. Evans
M. D. Fitzsimmons
G. G. Gaul
V. E. Hazel
K. Hikido
R. L. Holladay
H. F. Johnston
C. R. Jones
R. Kinney
S. Levy
M. F. Lyons
J. McClaughry
I. L. Marburger
J. E. Morlock
T. B. Murdock
P. Novak
W. L. Pearl
G. T. Peterson
G. R. Pflasterer
E. E. Polomik
W. R. Raymont
A. B. Reynolds
M. B. Reynolds
G. F. Rieger
J. I. Riesland
C. H. Robbins
J. M. Roberts
J. S. Rowe
S. G. Sawochka
R. A. Schmidt
C. M. Schields
M. Siegler
C. N. Spalaris
A. Sylvester
H. E. Townsend
C. H. Warneke
F. G. Warzek
L. I. Van Torne
B. Wolfe

TABLE OF CONTENTS

TABLE OF CONTENTS (CON'T)

TABLE OF CONTENTS (CON'T)

LIST OF ILLUSTRATIONS

LIST OF TABLES

1.0 INTRODUCTION AND SUMMARY

1.1 Introduction

This is the eighth of a series of quarterly reports which will cover the progress and results from the conceptual design, economic evaluations and research and development work performed by the General Electric Company as part of the Nuclear Superheat Project under Contract AT(04-3)-189, Project Agreement No. 13. The following list of progress reports and topical reports have been published as a result of this work.

GEAP-3290, First Quarterly Progress Report, July - September, 1959

GEAP-3319, Superheat Process Tube Heat Transfer Tests

GEAP-3371, Second Quarterly Progress Report, October - December, 1959

GEAP-3387, Fabrication, Irradiation and Evaluation of Superheat Fuel Elements

GEAP-3468, Third Quarterly Progress Report, January - March, 1960

GEAP-3538, Fourth Quarterly Progress Report, April - June, 1960

GEAP-3563, Interim Report on Steam Dryer Development

GEAP-3564, Results of Air-Water Steam-Water Tests on Primary Steam Separators - October, 1960

GEAP-3581, Fifth Quarterly Progress Report, July - September, 1960

GEAP-3589, Economic Study for 300 MW(e) Separate Superheat Reactor

GEAP-3590, Economic Study of the Mixed Spectrum Superheater

GEAP-3591, Manufacture of the Adhesive Bonded AEC Superheat Critical Fuel

GEAP-3633, Economic Study for 300 MW(e) Once-Thru Superheat Reactor

GEAP-3686, Sixth Quarterly Progress Report, October - December, 1960

GEAP-3698, Erosion Experiments of Powder Compacted Uranium Dioxide Under Dynamic Steam Flow

GEAP-3703, Heat Transfer Coefficients with Annular Flow During "Once-Through" Boiling of Water to 100 Per Cent Quality at 800, 1100, and 1400 psi

GEAP-3724, Seventh Quarterly Progress Report, January - March, 1961

GEAP-3737, Flood Safety of The Mixed Spectrum Superheater

GEAP-3739, Plastic Strain in Thin Fuel Element Cladding Due to UO_2 Thermal Expansion

Section I of the First Quarterly Report (GEAP-3290) presented a description of the Nuclear Superheat Project including objectives, approach to the problem and expected results by individual task. The following tabulation of task titles is listed for easy reference.

TASK A - Conceptual Design and Program Evaluation

TASK B - Fuel Technology

TASK C - Materials Development

TASK D - Experimental Physics

TASK E - Coolant Chemistry

TASK F - Heat Transfer

TASK G - Mechanical Development

TASK H - SADE & E SADE

TASK J - Mixed Spectrum Superheat Study

1.2 Summary

The following section provides a brief summary of significant results by task.

1.2.1 TASK A - Conceptual Design and Program Evaluation

Nuclear physics parametric studies on the use of erbium burnable poison in superheat fuel were completed. These studies indicate that significant amounts of control can be accomplished which

may result in acceptability of "gray" control rods with associated reduction in maximum rod worth and power perturbations. The enrichment penalty due to residual poison in the range of 12,000 to 18,000 MWD/T is in the neighborhood of one-third to one-half of 1 percent.

Work was completed on the study of safety and control problems for a Separate Superheater Power Plant. As a result of these studies a control and safety system has been established and is reported in Section 2.2.

1.2.2 TASK B - Fuel Technology

On May 24, 1961, SH-4B element was removed from the SADE facility in the VBWR reactor. The SH-4B element is an .028 inch stainless steel clad annular fuel element fabricated with 4.5 percent enriched UO_2 pellets. Two defects were found in the fuel element during the post-irradiation examination in the Radioactive Materials Laboratory. Details of operating conditions and results of detailed RML examinations are reported in Section 3.0. On June 2, 1961, SH-4 fuel element was installed in the SADE loop. This fuel element is identical to the previous SH-4B element except that the enrichment is $3\frac{1}{2}$ percent instead of $4\frac{1}{2}$ percent. At this reporting date the performance of the SH-4 fuel element has been satisfactory.

Additional capsules were irradiated in the Trail Cable facility in the GETR during this reporting period. In addition, a topical report, GEAP-3739, "Plastic Strain in Thin Fuel Element Cladding Due to UO_2 Thermal Expansion" was issued. A summary of the significant conclusions on this report is included in Section 3.0.

Development work was continued on zirconium process tubes, stainless steel annular process tubes, fuel element plenum supports and flow spacers.

1.2.3 TASK C - Materials Development

Work was initiated to determine an acceptable level of stainless steel tubing defects for use in superheat fuel cladding. Material samples of stainless steel tubing for use in nondestructive testing were ordered. Stress corrosion samples were exposed over 1,000 hours to determine stress corrosion cracking characteristics. No failures were observed after 1,000 hours in 1050°F superheated steam with 17 p.p.m. oxygen, 2.5 p.p.m. hydrogen from water having less than 0.03 p.p.m. cloride ion.

Difficulties in the procurement of equipment for in-reactor strain cycle tests have resulted in a schedule delay for this program. Alternate mechanical cycling concepts are being studied to minimize further program delays.

1.2.4 TASK D - Experimental Physics

All experimental measurements in the VAL critical facility were completed during this reporting period.

Thermal utilization and conversion ratio were measured on four superheat fuel configurations. Analytical work done to resolve discrepancies between experimental measurements and nuclear physics predictions based on a standard analytic model has been successful in resolving the discrepancies reported in the last quarterly report. A prime source of these discrepancies has been postulated to be the omission of the spatial variation in thermal spectrum.

By providing a semi-imperical "patch" to account for a spectral shift, good agreement was obtained between experimental and calculated values. The methods proposed for this modification in calculation techniques are discussed in detail in Section 5.0.

Initial criticality was attained on June 28 for the VESR preliminary critical. Parameters included in the present analysis are critical size, multiplication of the fuel core for various controls distribution, flooding effects, temperature effects, void coefficient, fuel element worth and power distribution.

1.2.5 TASK E - Coolant Chemistry

Exposures for 500 hours, 1,000 hours and 2,465 hours under dynamic heat transfer conditions with controlled superheat environment were completed on type 304 stainless steel. Measured corrosion rates are reported in Section 6.0.

Samples of steam entering and leaving the SADE loop during the period between January 15 and May 5 indicated that the SH-4B fuel element was not releasing significant quantities of iodine or fission gases. On May 24 comparison of condensate from steam entering and leaving SADE showed gross quantities of radioactive iodine apparently from the defect in SH-4B. Operating records of the VBWR stack monitor and release rates of fission gases from the VBWR during steady power operation are reported. A reactor water analysis of the VBWR reactor during the period from January 25 to May 9 and other measurements made on coupons inserted in the SADE effluent steam line are reported in Section 6.0. These measurements indicate that the SH-4B fuel element developed a defect during high power operation.

1.2.6 TASK F - Heat Transfer

A topical report, GEAP-3703, "Heat Transfer Coefficients with Annular Flow During 'Once-Through' Boiling of Water to 100 Per Cent Quality at 800, 1100, and 1400 psi" was issued.

The second phase of heat transfer work on experimental determination of heat transfer coefficients with superheated steam at high mass blow rates was initiated. Three data runs were obtained with steam flow inside of a 0.370 inch I.D. circular tube. Data is under reduction to establish correlation with other published data.

1.2.7 TASK G - Mechanical Development

All steam separator development work during the reporting period was applied to the radial vane type primary separator. The capacity of the two vane radial separator model was measured to be about five times that of a free surface separator over an equal area. At about 20,000 ft^3/hr of 1,000 psig saturated steam-water flow, a full circle of radial vanes was found to operate with moisture carry-over of 6 percent and vapor carry-under of 0.2 percent by weight.

Work is continued on the test program to determine the feasibility and performance characteristics of a temperature actuated mechanism which would provide a removable seal between superheat fuel element assembly and inlet-exit steam manifolding.

1.2.8 TASK H - SADE AND E-SADE

1.2.8.1 SADE

Fuel element SH-4B was irradiated in the SADE loop during this reporting period until it was removed from the SADE loop on May 24 after a cladding defect developed. Fuel

element SH-4 was reinserted in the loop on June 9 and has been operating satisfactorily since that time. Design conditions for SH-4 and SH-4B fuel elements are reported. The design conditions and a description of the defective fuel test on SH-1 fuel element are reported.

Drawings of special equipment and orders for materials were placed for the NUSU fuel element. Safeguards analysis on the NUSU fuel element was initiated and proposed operating conditions recommended.

1.2.8.2 E-SADE

Progress on the design and procurement of equipment for the E-SADE loop has been delayed due to systems changes required as a result of the safeguards analysis. The detailed designs of the first fuel assembly for installation in the E-SADE loop were finalized and are reported. The safeguard report for the E-SADE system was completed and forwarded to the AEC. The entire safeguards report has been included in Section 11.0.

1.2.9 TASK J - MIXED SPECTRUM SUPERHEAT REACTOR

Work was iniated on the design of a small prototype reactor to demonstrate the important features of a mixed spectrum superheater. The results of thermo hydraulics, nuclear physics, and safety aspects of fast core melt down are reported.

Work was initiated on the study of a critical experiment design to demonstrate the nuclear characteristics of a mixed spectrum superheater.

During this reporting period work was completed on a preliminary hazards review for the Mixed Spectrum Superheater. This information is reported in detail in Section 10.7.

2.0 TASK A - CONCEPTUAL DESIGN

2.1 Burnable Poison Study for Separate Superheater Reactors

2.1.1 Introduction

A physics parametric study of the use of erbium burnable poison in fuel was completed during the quarter. The reference design used for the study was the 300 MW(e) Separate Superheater (as reported in GEAP-3589). The following parameters were investigated as a function of initial erbium content, enrichment and burnup life: required total control rod worth, maximum control rod worth, flooding and unflooding reactivity changes in the hot and cold conditions, respectively, and the net reactivity change with temperature. In addition to these variables which influence reactor safety, the cost penalty associated with erbium as a burnable poison was assessed.

2.1.2 Conclusions

It appears that very significant amounts of control can be accomplished in a separate superheater through the use of natural erbium oxide intimately mixed with the uranium oxide fuel. By controlling a major portion of the excess reactivity with erbia, one should be able to use 304 stainless or similar "grey" control rods with associated reductions in maximum rod worth and power perturbations. The reactivity addition encountered upon a maximum worth rod ejection could be reduced by at least a factor of 2.

The enrichment penalty due to residual poison (unburned erbium) is in the neighborhood of one third to one half of one percent over the range of 12,000 to 18,000 MWD/T discharge exposure. This corresponds to an increase in fuel costs for the erbium-containing fuel of about 0.2 mills/kw-hr on the Separate Superheater Reactor

basis alone or about 0.05 mills/kw-hr on the total plant basis (assuming 18,000 MWD/T discharge exposure).

It is very difficult to assess capital cost differences for erbium-containing fuels due to the complexity of having the slope of reactivity versus exposure curves also dependent on exposure. This makes the achievement of a flat radial power distribution (by outside-in fuel movement) considerably more difficult for the erbium fuel than for the fuel without erbium which essentially has a constant reactivity versus burnup slope. This does not appear to be an insurmountable problem at the present time, but more analysis work must be done before this question can be resolved. The fact that the erbium-fueled core can use "grey" rods will help the over-all power peaking factor considerably.

2.1.3 Summary

A new analytical model derived by G. T. Petersen which accounts for spatial variation of the thermal neutron spectrum in the fuel-moderator cell has had a profound effect in counterbalancing the strong negative temperature coefficient that was previously associated with erbium-loaded cores. The interaction of the neutron spectrum shift with the effective erbium to uranium cross section ratio as a function of temperature as presently calculated with the new analytical model yields a net reactivity change (cold to hot) of approximately one or two percent Δk (negative). Due to the elimination of the large temperature reactivity effect, significant amounts of control can now be accomplished for the hot and cold reactor conditions through the use of erbium (see Figures 2.1 and 2.2). Previous calculations, in which the neutron spectrum shift was omitted, indicated unusually high cold reactivities were required

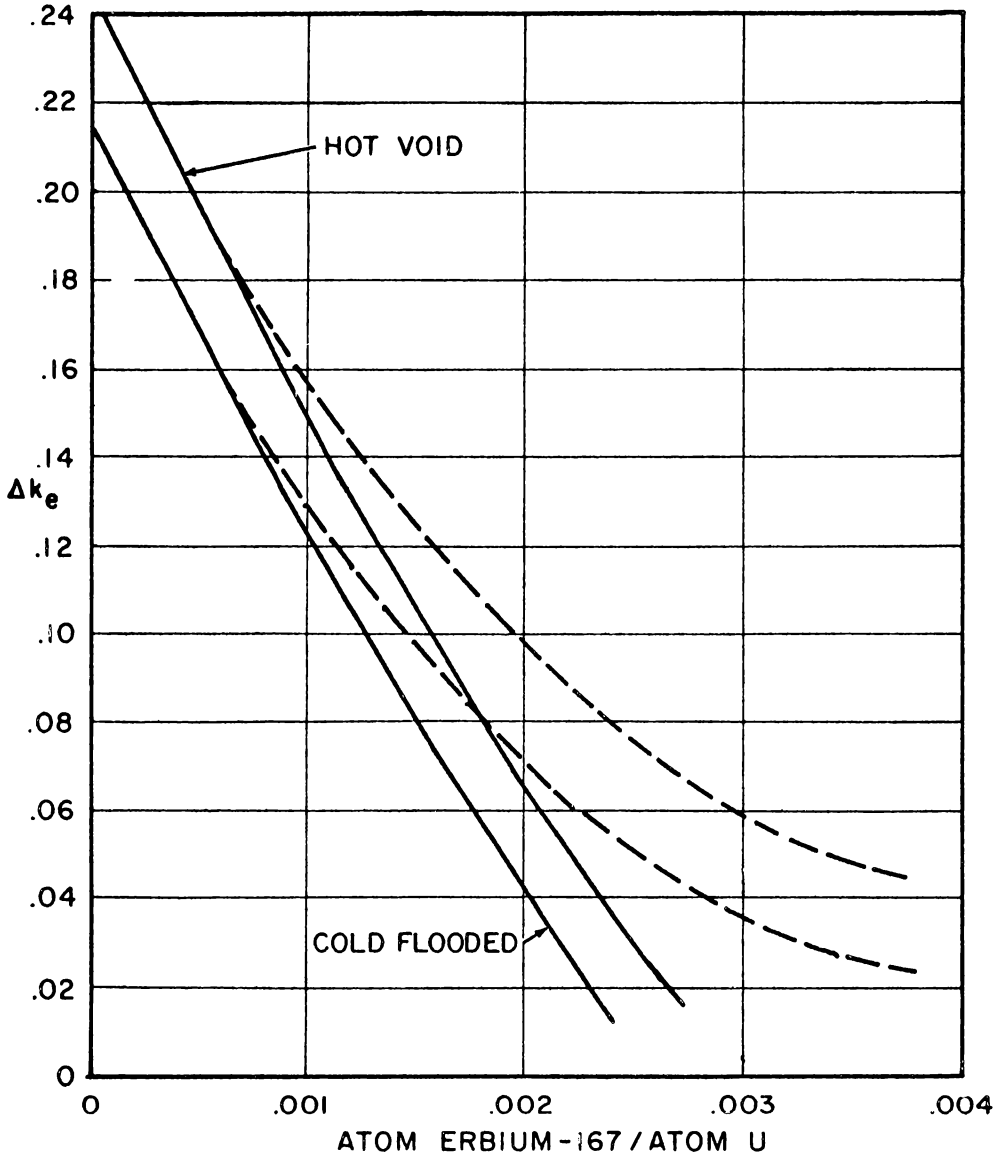

NOTE:

SOLID LINE — BEGINNING OF LIFE EXPOSURE
DASHED LINE — ALL FUEL AT EXPOSURE WHERE k IS MAXIMUM
Δk_e INCLUDES 3 % SHUTDOWN MARGIN

REQUIRED CONTROL STRENGTH VS. ERBIUM-167 CONTENT
FOR W/F = 2.6 AND % ENRICHMENT = 2.6

FIGURE 2.1

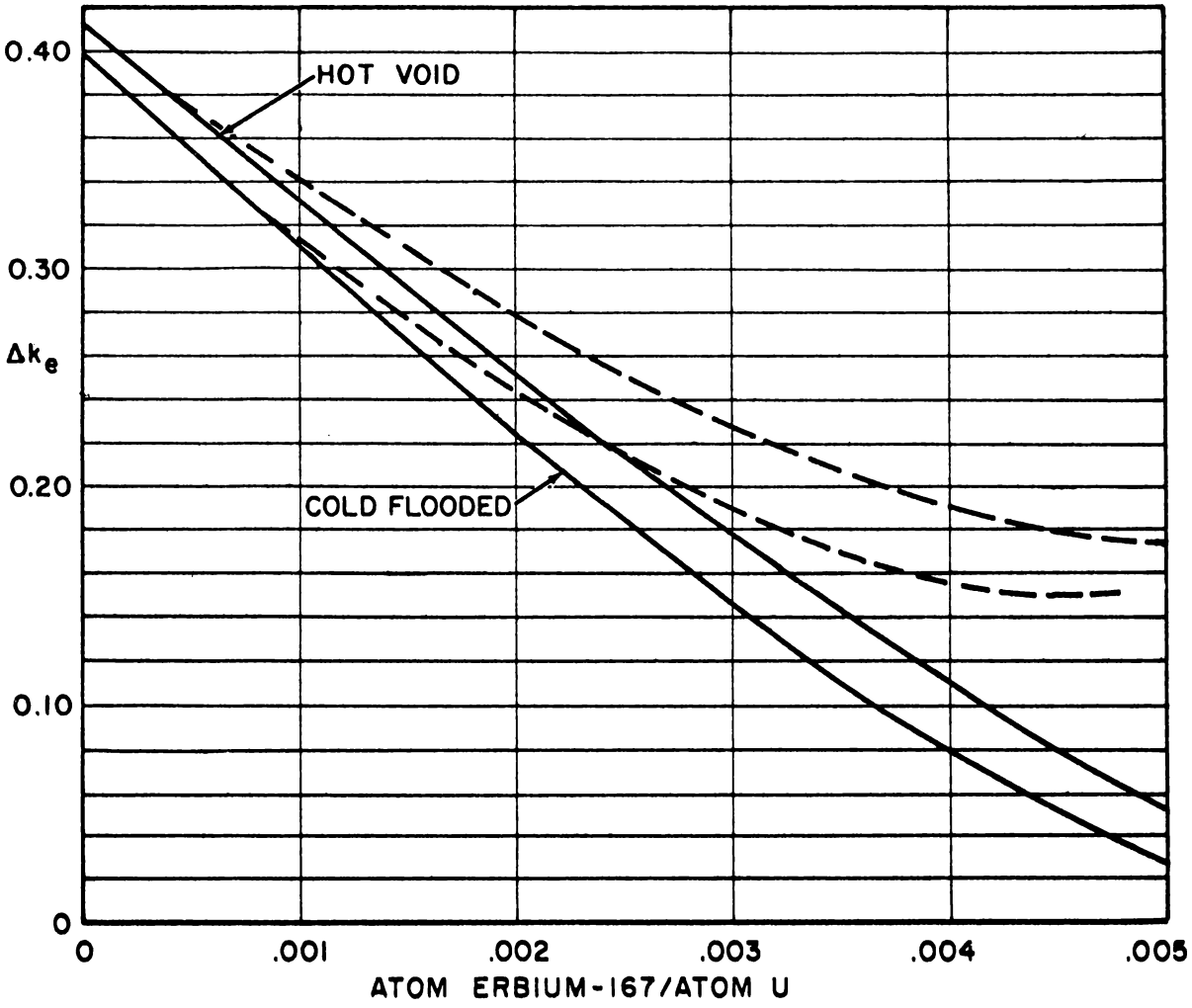

NOTE:

SOLID LINE – BEGINNING OF LIFE EXPOSURE

DASHED LINE – ALL FUEL AT EXPOSURE WHERE k IS MAXIMUM

Δk_e INCLUDES 3 % SHUTDOWN MARGIN

REQUIRED CONTROL STRENGTH VS. ERBIUM-167 CONTENT FOR W/F = 2.6, U-235 ENRICHMENT = 4.5 %

FIGURE 2.2

for a given discharge exposure, making cold control rod strengths marginal for even modest exposures.

The delegation of significant amounts of control to erbium will allow the use of "grey" rods. For example, to meet the discharge exposure of 12,000 MWD/T, the control strength requirements including a 3% shutdown margin when .00175 atom erbium-167/atom U is incorporated in the fuel will be under 9% Δk_c in the cold flooded condition. This can be adequately met with 304 stainless or Inconel X control rods, provided a control blade thickness of about 0.3 inches is used.

Significant improvement in the calculated hot flooding reactivity effect has been made through the use of erbium by virtue of the lower reactivity worth of the erbia-containing fuel (see Table 2.2). Erbium additions were found to have negligible effects on cold unflooding reactivity.

The use of erbium-containing fuel along with "grey" rods will reduce the magnitude of the control rod ejection and fuel bundle insertion accidents. The control rod ejection reactivity can be reduced by at least a factor of 2 in the hot operating condition. "Grey" rods should also reduce the local power peaking factors, although work up to now has not included any calculation of what the local power peaking changes would be.

Zero-dimensional burnup study results were used in one-dimensional diffusion theory calculations to determine differences in characteristics between fuel with and without erbium. Equilibrium cores were determined for multi-batch, shuffled reloading. Cores incorporating a single-batch mode of reloading were burned in several exposure steps to end of life. The effect of control rods on the power distributions obtained was not taken into account.

The single-batch reloading scheme showed large enrichment penalties and poor power peaking characteristics for the erbium fuel over the non-erbium fuel. From these results (which were for homogeneous cores) single-batch operation of erbium fuels should be eliminated from consideration unless spatial variation of enrichment and erbium is allowed.

The multi-batch equilibrium cores were found to give about a half of one percent enrichment penalty. This figure is a little high for the cases discharging fuel at 12,000 MWD/T as the erbium content of the fuel is a little too much (.0025 atoms erbium-167/atom U) and could be reduced to .00175 atom erbium-167/atom U.

The enrichment penalty will affect the depletion, reprocessing, and use charge contributions to the fuel costs. The total difference in fuel costs between fuels with erbium and those without, for a SHR core discharging fuel at 18,000 MWD/T, is 0.2 mills/kw-hr on the SHR basis alone, or 0.05 mills/kw-hr on the total plant basis. These costs are based on a schedule which includes the recent government price reduction.

In addition to fuel cost differences, there also is the possibility of capital cost differences between fuels with and without erbium should there be any differences in specific power density that these fuels can attain.

From Figure 2.4 we see that a fairly optimum power distribution can be maintained over a good range of spatial reactivity distributions. Thus, although the problem of finding a flat radial power distribution for erbia containing fuels will be much more difficult than that for fuels without erbium (as can be seen from Tables 2.4, 2.5, and 2.6) it is felt, particularly in the light of the ability to use grey rods and thus minimize local peaking for erbia fuels, that erbia-containing fuel might

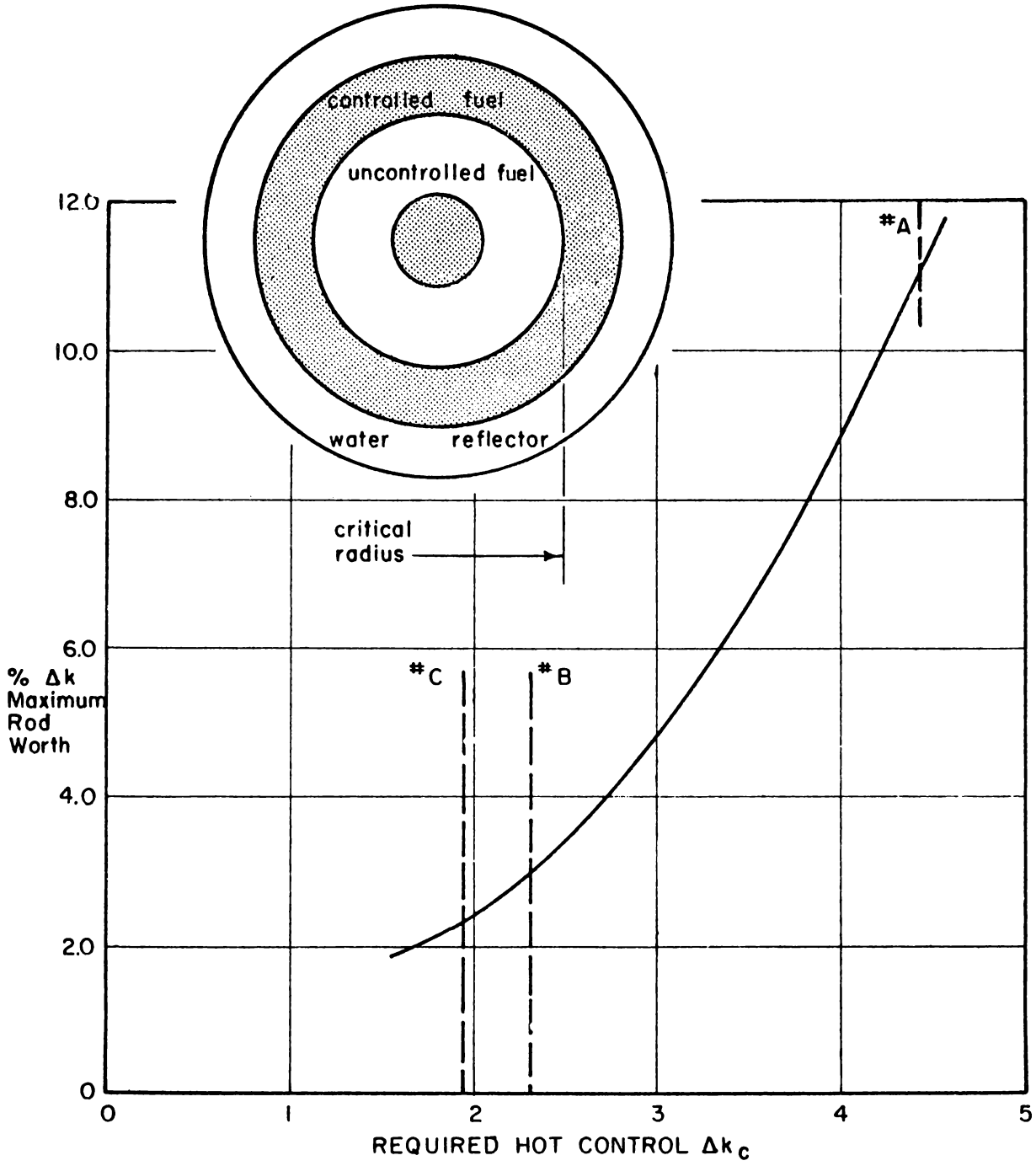

NOTE:

Δk CONTROL AT:	CRITICAL RADIUS
#A	38.0 cm
#B	47.5 cm
#C	58.9 cm

MAXIMUM ROD WORTH VS. HOT CONTROL STRENGTH

FIGURE 2.3

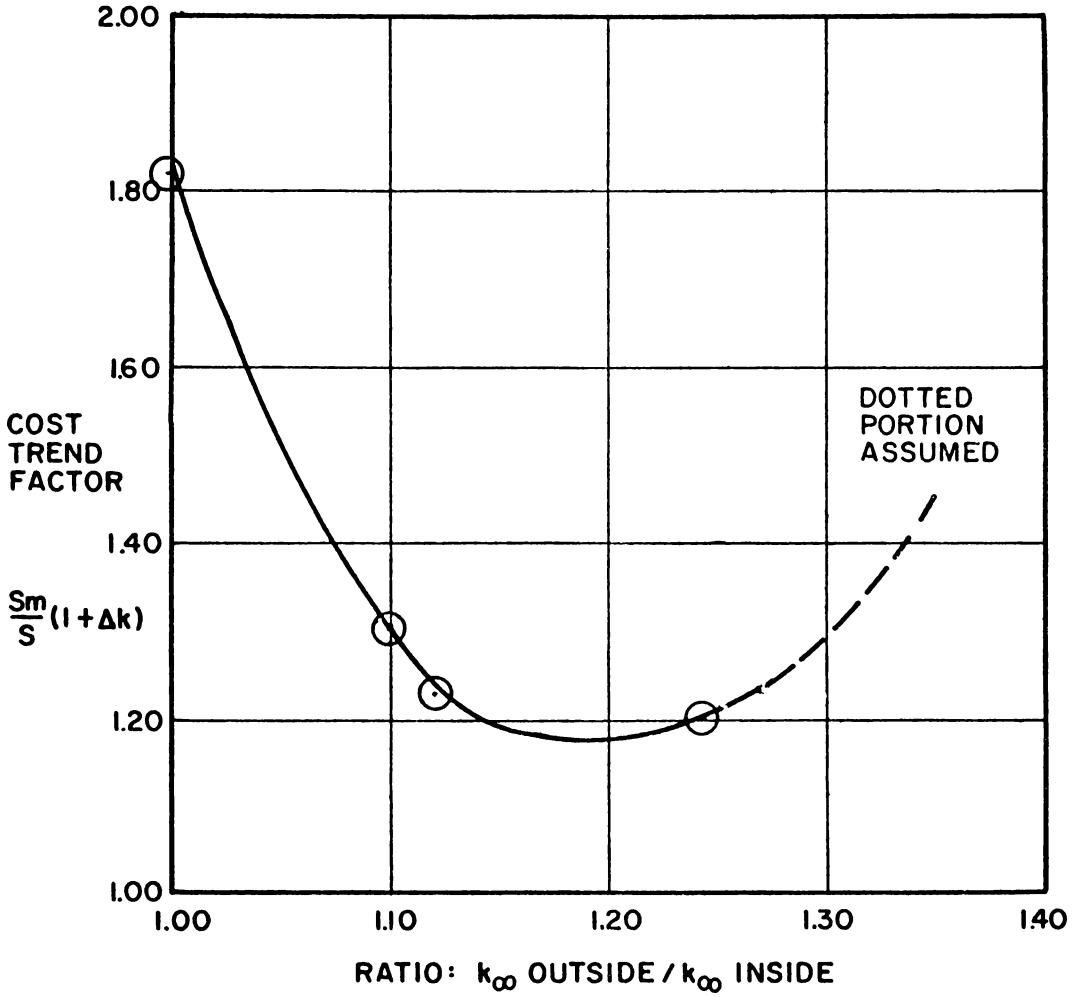

OPTIMUM SPATIAL REACTIVITY DISTRIBUTION

FIGURE 2.4

be able to achieve the same specific power density that fuels without erbium can attain.

The material cost of the erbium is about $50/lb. of natural erbium oxide. The amount of erbium oxide required would be about 200 to 400 lbs. per core load, which will amount to $10,000 to $20,000 per core load for the erbium. The additional costs of putting the erbium in the fuel was assumed to be negligible as is the material cost of the erbium oxide (.001 to .002 mills/kw-hr additional cost on the total plant basis).

2.1.4 Discussion of Results

2.1.4.1 General Nuclear Characteristics of Erbia Containing Fuel

In earlier studies of erbium burnable poison, it was generally concluded that erbium would contribute a very large negative reactivity effect due to increasing moderator temperature. However, subsequent analyses, incorporating a new analytical model derived by G. T. Petersen which took into account spatial effects in the thermal neutron energy group, showed that this large negative temperature effect is not present and for certain cases a small positive temperature effect is seen. This is very important from the standpoint of the amount of control that can be practicably accomplished with erbium for the cold (20°C) reactor conditions.

In Figures 2.1 and 2.2, the necessary typical control strengths required for a 3% shutdown margin are shown for the hot operating and cold flooded core conditions at beginning of life. Since beginning of life conditions do not represent the maximum reactivity available for some of the higher erbium content fuels

which actually undergo an increase in reactivity for a time, as exposure increases (see Figures 2.5, 2.6, and 2.7), the control strength required, if all of the fuel in the core were at the exposure giving a maximum reactivity, is shown in the figures as a dashed line. Since all of the fuel is at the same exposure only at the beginning of life, the dashed line represents an upper limit for these cases.

The maximum available control strength using "black" control rods for this reactor, in the cold, flooded condition, is probably on the order of 18% Δk. All the points in Figures 2.1 and 2.2 lying above this value in the cold flooded condition would not be physically realizable without some form of additional control such as "temporary" poison inserts.

The hot flooding reactivity change, hot to cold temperature swing, and cold unflooding reactivity change for beginning of life with all rods out are tabulated in Table 2.1. Table 2.2 lists the maximum hot flooding reactivity changes for several cases. These changes will occur for exposure conditions where reactivity is at its maximum. When reactivity is at its maximum, criticality will be achieved for the smallest possible core and thus, the leakage effects will be at their maximum, giving the maximum hot flooding reactivity changes. It must be pointed out here that the method of calculation used to obtain the maximum hot flooding reactivity changes, shown in Table 2.2, assumes the leakage characteristics of a core with "black" control rods in a just critical "ganged" pattern. If grey rods are used, these reactivity changes will be somewhat different.

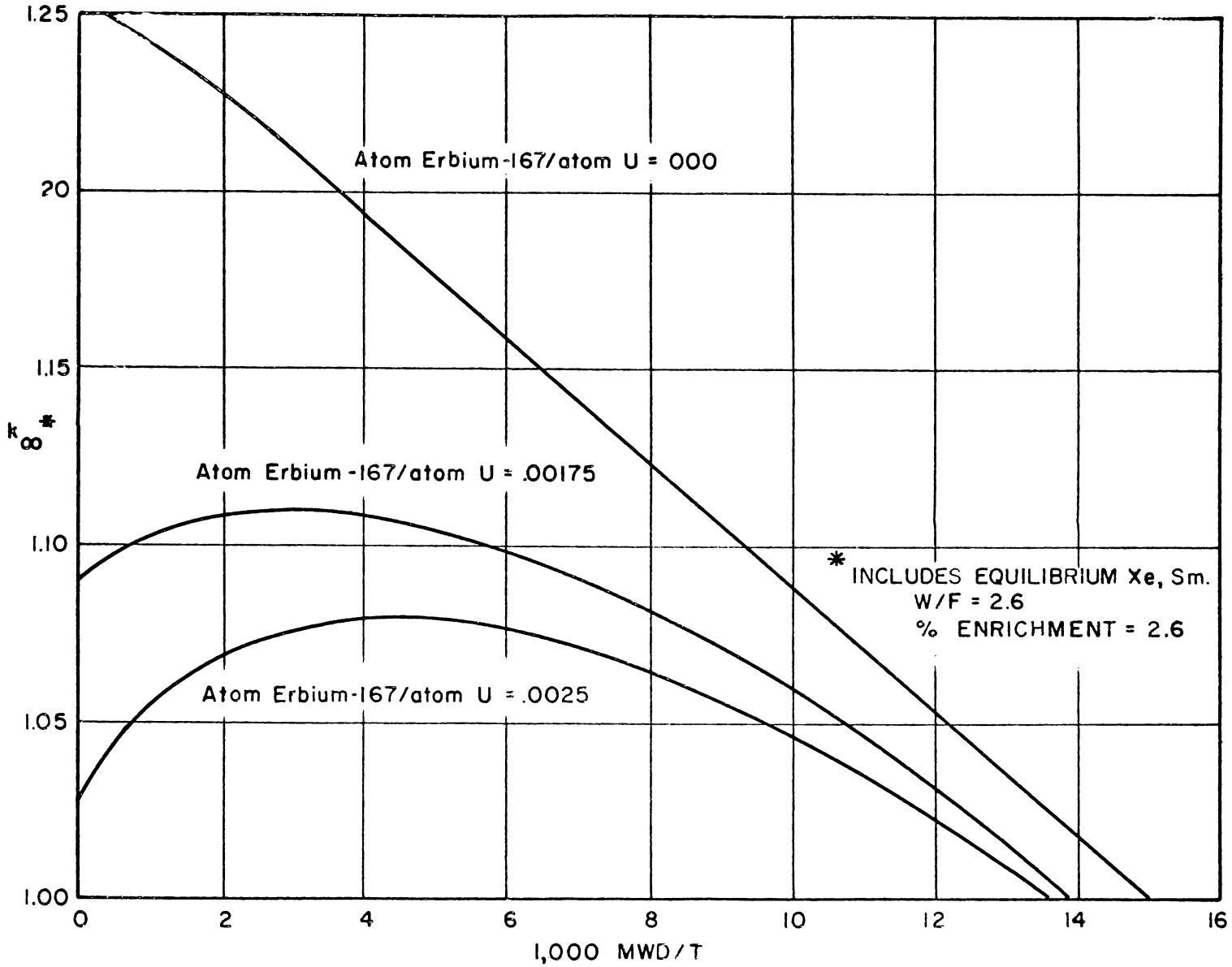

REACTIVITY VS. EXPOSURE ZERO-DIMENSIONAL BURNUP RESULTS

FIGURE 2.5

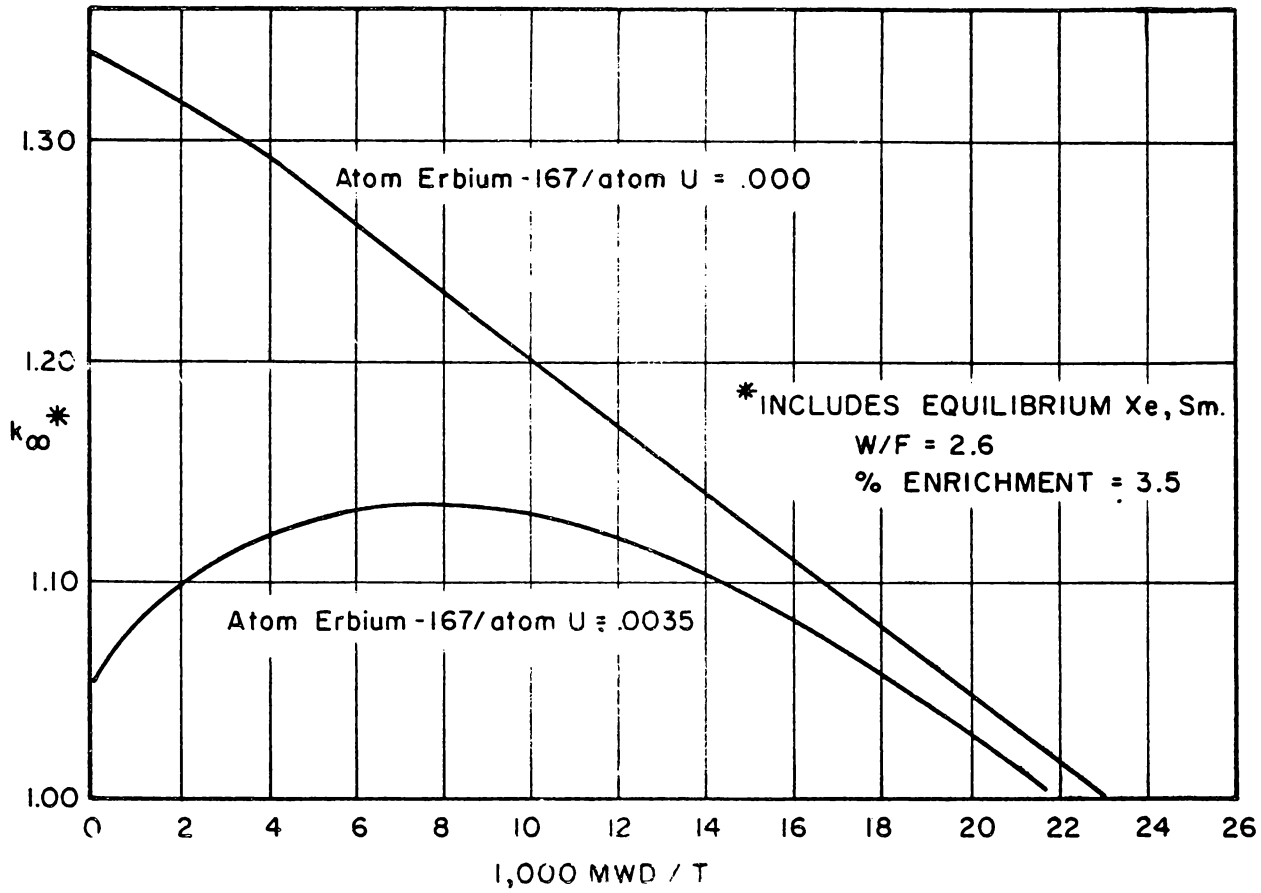

REACTIVITY VS. EXPOSURE ZERO-DIMENSIONAL BURNUP RESULTS

FIGURE 2.6

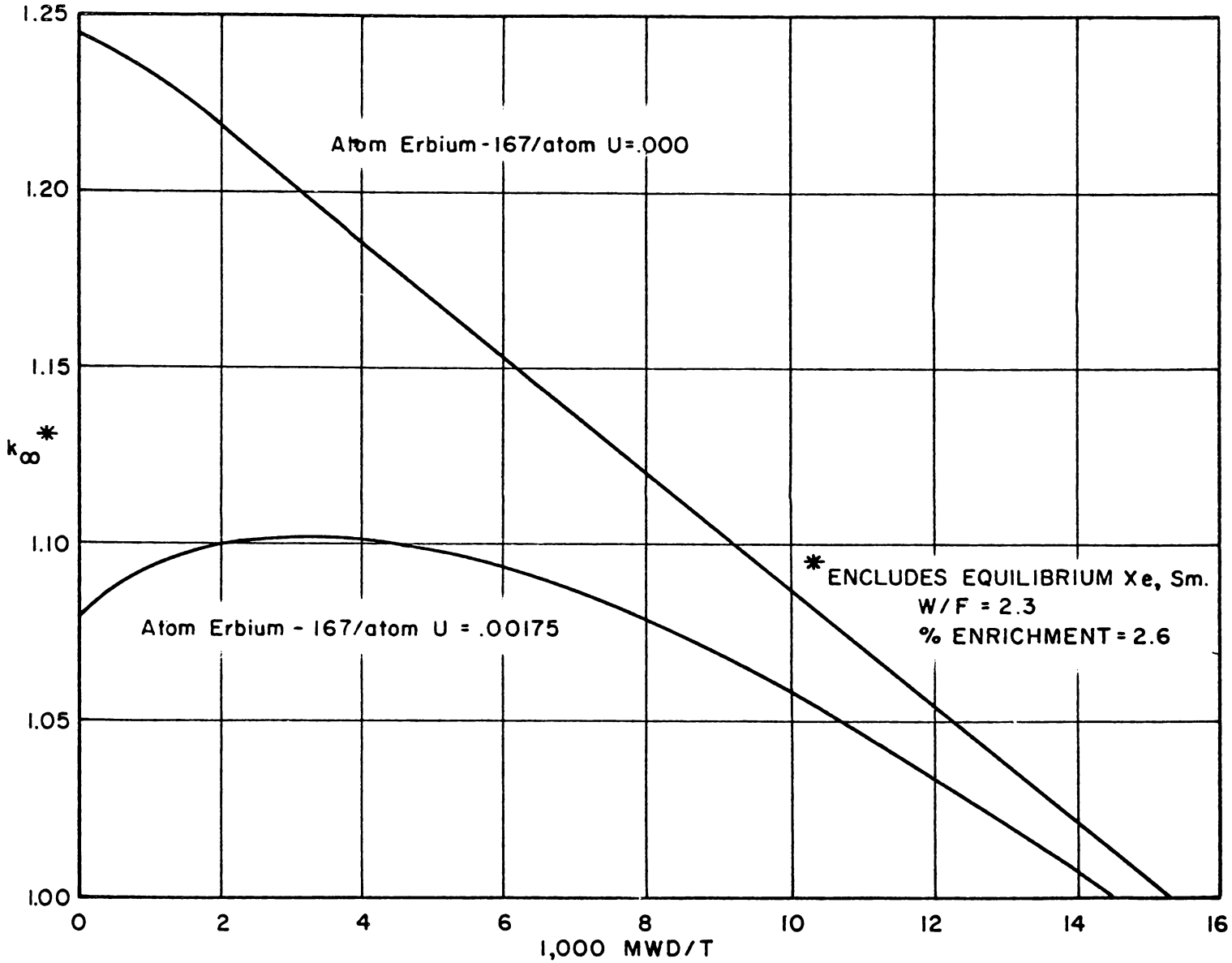

REACTIVITY VS. EXPOSURE ZERO DIMENSION BURNUP RESULTS

FIGURE 2.7

From Figures 2.1 and 2.2, it is evident that through the use of erbium one can utilize "grey" rods and still achieve an adequate shutdown margin. For reasonable amounts of erbium, 304 stainless or perhaps Inconel X control rods could be used. The combination of "grey" rods and relatively low worth fuel leads to a very desirable reduction in maximum control rod worths which reduces the severity of postulated rod ejection accidents. The low worth fuel will also lessen the magnitude of the calculated refueling accident. A series of one-dimensional control rod ejection problems was calculated. The results shown in Figure 2.3 are for a rod removed from the center of a just critical unrodded central portion of the core. The two main factors contributing to the differences shown in the figure are the rod "greyness" and the size of the uncontrolled fuel region required for criticality from which the rod is removed which affects the flux shape and thus the reactivity "importance" of the rod. The size of the central controlled fuel region that is replaced by uncontrolled fuel to simulate the rod ejection and the over-all size of the reactor are fixed from specifications in the reference design (300 MW(e) Separate Superheat Plant). This calculational model is somewhat crude but it is adequate to indicate the trends involved.

2.1.4.2 Economic Considerations

Once the over-all general design of a reactor has been chosen and discharge exposure requirements fixed, the economic picture for this reactor will depend mainly on two considerations. These are: The U-235 enrichment requirements in order to reach the given exposure, which will dominate the fuel costs; and the specific power density limitations, imposed by local and

and gross power peaking, which strongly influences capital costs.

The mode of refueling the reactor in an equilibrium condition, which is taken here to mean some sort of repeating pattern for replacing fuel, will determine to a large extent what the enrichment requirements and the gross radial power peaking factors are to be. This is true because at the time of refueling, fuel with various exposures and thus various reactive properties (k_∞) will be available and (unless limited to a single batch operation) one is faced with the problem of where to place these various fuels for optimum operation over the next cycle. If one chooses to place the most reactive fuel around the core periphery in order to flatten power, the expense of putting this fuel in a low statistical weight region is incurred, and thus a penalty is paid in the over-all core multiplication factor which amounts to an enrichment penalty. The problem of deciding how to balance these factors for the optimum situation is exceedingly complex.

A first cut at an "optimum" spatial distribution in reactivity was attempted and the results are tabulated in Table 2.3 and plotted in Figure 2.4. One-dimensional diffusion theory problems were calculated where fuels with various reactivities were loaded into three equal annular regions of the core. The cases having the same fuel in all regions (homogeneous, single batch) were taken to be the base point. As the power was flattened by shifting the U-235 inventory, the penalty in k_{eff} was noted and these two factors (radial peaking and Δk penalty) were assumed to have equal weighting in their influence on the economic picture. The assumption of equal weighting is recognized

as not being wholly correct but at least the trends can be seen.

The difficulty in choosing an optimum refueling mode is compounded for fuels containing significant amounts of erbium as the reactivity versus exposure no longer decreases linearly.

Several equilibrium cycle cases were calculated for fuel with and without erbium, for a multi-batch refueling mode with fuel shuffling, and for single batch reactor operation. The results are presented in Table 2.4, 2.5, and 2.6, and show the enrichment penalties incurred by erbium fuel along with the radial peaking factors. The single batch cores were divided into three equal regions and the burnup followed regionwise.

From Tables 2.4, 2.5, and 2.6, it can be seen that the erbium fuels entail a significant enrichment penalty along with poor power distributions. The enrichment penalty is due primarily to the residual erbium in the fuel at the end of the cycle. The relatively poor power distribution in the single batch cases for the erbium fuel compared to no erbium case was expected. The center region of the core without erbium burns out much more quickly and tends to flatten power due to the greater reactivity loss versus exposure for fuels without erbium. The poor power distribution for the multi-batch, shuffled erbia-containing fuels is not so much a characteristic inherent to erbia-containing fuels as it is an incompatibility of a three-batch system with these specific cases. Although fuel without erbium may lend itself more easily to obtaining an optimum configuration in a shuffled fuel pattern, this does not mean that erbia-containing fuels cannot

achieve the radial peaking factors of fuel without erbium. From Figure 2.4, it can be seen that a near optimum situation embraces quite a large range (1.10 to 1.30) of outside to inside reactivity ratios. This, coupled with the fact that erbium may allow the use of "grey" rods which can reduce the local peaking effects, provides some hope that an erbium core will have similar power peaking characteristics to a core without erbium.

The beginning of cycle reactivity for the equilibrium core without erbium, discharging fuel at 18,000 MWD/T (Table 2.5) when lowered to k_{eff} = 1.0 at end of life conditions, should be able to be controlled easily with black rods. However, some form of additional (temporary) poison will be required in the initial core prior to attainment of equilibrium. The cold shutdown margin will be limiting for the initial core without burnable poisons. This difficulty will not be encountered in the erbium fuel case.

In order to determine the erbium enrichment penalty in mills/kw-hr, a fuel cost analysis was done for the shuffled cases discharging fuel at 18,000 MWD/T. Only the depletion, reprocessing, and use charges will be significantly affected. The case containing erbium had the following excess cost over the case without erbium:

	Basis		
	SHR Only	Total Plant	
Depletion	0.0819	0.0205	mills/kw-hr
Reprocessing	0.0047	0.0017	mills/kw-hr
Use	0.0967	0.0242	mills/kw-hr
TOTALS	0.1830	0.0460	

The above costs assumed that the power rating or the specific power density is the same for both the cases with and without erbium. On the basis of a capital cost of $14,000 per cubic foot of additional core volume, it would take about a 20% increase in specific power density for cores with erbium over those without (discharging fuel at 18,000 MWD/T) to compensate for the enrichment penalty costs. Any decrease in power density entailed by erbium-containing cores over that of the no erbium cores would entail a capital cost penalty in addition to the enrichment or fuel cost penalty.

2.1.4.3 Methods of Analysis

The FORM (modified MUFT) computer code employing a Fourier transform method was used to determine the epithermal cross sections along with corrections made for the U-238 resonance absorption and fast fission.

A modification to the conventional boiling water reactor analysis procedure derived by G. T. Petersen was utilized in determining the thermal neutron cross sections. This modification was incorporated in order to account for spatial differences in the thermal neutron energy spectrum. The effect of the spectral shift is to harden the fuel spectrum and to soften the moderator spectrum relative to the usual zero-dimensional spectrum.

The modified calculational technique consisted of the following:

a. The fuel spectrum was calculated using the Wilkins heavy gas model allowing water only with one λ_s (scattering) of the outer fuel surface to be included in this calculation.

b. This balance of the water in the cell was then introduced

with softened cross sections. The amount of softening was determined by:

$$\text{Percent Softening} = 100\left\{1 - \left[\exp\left(-1.1\, t/\lambda_s\right)\right]\right\}$$

where t = thickness of water beyond λ_s (cm).

c. P-3 flux weighting of the cross sections was then employed to average the cross sections from the various materials and determine the thermal utilization for the cell.

The differences in the thermal cross sections for Erbium-167 and Uranium-235 obtained by the old and new methods are shown below for a cell W/F ratio of 2.6 and % enrichment = 4.5 with an erbium concentration of 0.0050 atom erbium-167/atom U.

	Spectral Shift Method of G. T. Petersen		Conventional Boiling Water Reactor Method	
	Hot 285°C	Cold 20°C	Hot 285°C	Cold 20°C
$\bar{\sigma}_{a_3}$ Erbium-167	1290.0	1478.2	1219.6	1134.1
$\bar{\sigma}_{a_3}$ Uranium-235	315.7	343.4	322.9	410.3
$\bar{\sigma}_{a_3}$ 1/v	.5046	.5429	.5152	.6376
"Effective" W/F Ratio	2.254	1.3027	2.6	2.6
"Effective" Hydrogen/ Uranium Ratio	4.8067	3.754	5.5446	7.493
$\bar{\sigma}_{a_3}$ Erbium-167/$\bar{\sigma}_{a_3}$ U-235 Ratio	4.086	4.305	3.777	2.764

These large changes in cross sections are brought about due to the fact that the Wilkins neutron flux shape is determined by ($\Sigma a/\xi\Sigma_s$). In the case of the conventional calculational model, the absorption cross section in the numerator increases more slowly in going from hot to cold moderator conditions than does the scattering cross section in the denominator due to the

large change in density and thus the atoms per cubic centimeter of the moderator. This causes ($\Sigma_a/\xi\Sigma_s$) in the hot condition to be greater than ($\Sigma_a/\xi\Sigma_s$) in the cold condition and since the Wilkins thermal neutron flux shape becomes flatter as the ratio ($\Sigma_a/\xi\Sigma_s$) increases, the hot case will have a flatter or broader flux spectrum than will the cold case. This will tend to produce more neutrons in the range of the erbium low lying resonances for the hot condition than in the cold. Also, there is a slight shift of the total flux to a higher energy at the higher moderator temperature.

In the "spectrum shifted" cases, the flux shape is reversed, the cold case having the flatter flux spectrum and thus more neutrons in the low lying resonance range. This is true for the following reasons: The Σ_s for the cell that appears in the ratio ($\Sigma_a/\xi\Sigma_s$) (cell) is principally determined by the moderator region; i.e.,

$$\Sigma_s(\text{cell}) = \Sigma_s(\text{mod}) \times \sqrt{F}(\text{mod})$$

The volume fraction of the moderator ($\sqrt{F}$ mod) is determined in the spectrum shifted cases, principally by λ_s(mod) which is just $1/\Sigma_s$(mod). Thus, Σ_s(cell) in the spectrum shifted cases remains relatively constant as moderator temperature changes. This means that the parameter determining the Wilkins flux shape ($\Sigma_a/\xi\Sigma_s$) depends principally on Σ_a which is greatest for the cold conditions and thus produces the flatter flux shape in the cold condition. This is opposite to the conditions found in the conventional calculational technique.

The flatter flux shape in the cold condition overrides the fact

that the total curve is shifted slightly to a lower energy in the cold condition relative to the hot condition, and therefore more neutrons are found in the erbium low lying resonance energy region in the cold condition than in the hot condition for the spectrum corrected cases.

The cross sections determined as described above were utilized in zero-dimensional burnup calculations to determine the changes undergone as a function of exposure. The burnup results were then used in one-dimensional diffusion theory problems to determine equilibrium core conditions, maximum rod worths, etc.

No attempt was made to incorporate lifetime effects on the neutron flux spectrum into the burnup calculations. As a result, the change in the erbium cross section due to self-shielding changes with burnup have not been accounted for and the calculated burnup rate for erbium is perhaps slightly lower than actual. However, there is an effect that reduces the effective erbium cross section which will tend to compensate for the increase due to lower self-shielding. This effect is due to the decrease with life of the over-all fuel absorption cross section and thus the softening of the thermal neutron spectrum which tends to remove neutrons from the low lying resonance energy region. The erbium burnup rate will affect the reactivity changes with life.

As the spectrum is softened with burnup, larger temperature reactivity changes would normally be expected due to erbium. However, the spectrum softening is primarily due to erbium depletion so the amount of erbium present to contribute to a larger temperature change is also decreasing and will tend to compensate for the spectrum change.

A measure of the spectrum changes with burnup can be seen in Table 2.7 where data for a case having a W/F ratio = 2.6, % enrichment = 4.5 and an

initial erbium content of 0.0050 atom erbium-167/atom U is presented. The large changes in temperature reactivity effect between the thermal spectrum spatially corrected Wilkins case and the uncorrected case come about due to a difference of 0.1015 in $(\Sigma_a/\xi \Sigma_s)$ changes. Even at 18,000 MWD/T, the change in $(\Sigma_a/\xi \Sigma_s)$ from beginning of life is only 0.039. This corresponds to an almost negligible amount of erbium in the core that can contribute to temperature effects.

Table 2.1

Reactivity Changes With Reactor Conditions

(Calculated for beginning of life with all rods out)

W/F	% Enrichment	Atom Erbium-167/Atom U	% $\Delta k/k$		
			Hot Flooding	Temperature Change	Cold Unflooding
2.6	2.6	.000	4.23	0.92	3.33
		.00175	4.45	1.17	3.44
		.0025	3.71	----	----
		.0035	3.00	1.08	3.51
2.6	4.5	.000	4.66	1.34	2.23
		.0035	3.49	0.72	3.79
		.0050	2.46	1.17	3.25
2.3	4.5	.000	6.10	2.45	1.80
		.0035	4.71	1.67	----
		.0050	3.87	0.92	1.73

NOTE:

1. Hot flood % $\Delta k/k$ $= \dfrac{k_{eff}\ (\text{hot flood}) - k_{eff}\ (\text{hot void})}{k_{eff}\ (\text{hot flood})} \times 100$

2. Cold unflood % $\Delta k/k$ $= \dfrac{k_{eff}(\text{cold void}) - k_{eff}(\text{cold flood})}{k_{eff}\ (\text{cold flood})} \times 100$

3. Temperature Change $\%\Delta k/k = \dfrac{k_{eff}(\text{cold void}) - k_{eff}(\text{hot void})}{k_{eff}\ (\text{hot void})} \times 100$

4. k_{eff}'s determined for full core geometric buckling.

Table 2.2

Maximum Hot Flooding Reactivity Changes

W/F	% Enrichment	Atom Erbium-167/Atom U	% $\Delta k/k$	Exposure E (MWD/T) At Which k Maximum Occurs	Critical B^2
2.6	2.6	.000	8.33	000	.003737
2.6	4.5	.000	11.34	000	.00618
2.6	4.5	.0035	7.92	8,000	.002326
2.6	4.5	.0050	7.66	12,000	.001026

NOTE:

1. $B^2 \text{ Crit} = \left(\frac{k_\infty (E) - 1}{M^2} \right)$ (hot void conditions)

2. $\% \Delta k/k = \left[\frac{k_\infty (E) \text{ (hot flooded)}}{1 + \beta^2_c \ M^2 \text{ (hot flooded)}} - 1 \right] \times 100$

Table 2.3

Optimum Spatial Reactivity Distribution

Ratio: $\frac{k_\infty \text{ Outside Region}}{k_\infty \text{ Inside Region}}$	Radial Peaking Factor $S^{max}/\bar{S}$	Δk_{eff} Penalty	Trend Factor* $S^{max}/\bar{S}(1 + \Delta k_{eff})$
1.0	1.83	0.00	1.83
1.106	1.302	0.004	1.31
1.123	1.198	0.028	1.23
1.242	1.158	0.047	1.21

* Higher factor has higher costs.

Table 2.4

Three-Batch, Out-In Shuffling Refueling

Mode Discharging Fuel at 12,000 MWD/T

W/F = 2.6 % Enrichment = 2.6

Atom Erbium-167/Atom U-235 = .000

	k_{eff}	Radial* Peaking Factor	k_∞ Distribution Regionwise		
			Inside	Middle	Outside
Beginning of Cycle	1.095*				
End of Cycle	1.032	1.18	1.08	1.16	1.23

Atom Erbium-167/Atom U-235 = .0025

	k_{eff}	Radial* Peaking Factor	Δk_{eff} Penalty	Corr. Enrich. Penalty	k_∞ Distribution Regionwise		
					In	Middle	Out
Beginning of Cycle	1.039**						
End of Cycle	0.976	1.43	0.056	0.5%	1.05	1.09	1.11

* Over-all peak to average source in fuel regions.

** Estimate.

Table 2.5

Three-Batch With Shuffling Refueling Mode

Discharging Fuel At 18,000 MWD/T

W/F = 2.6 % Enrichment = 3.5

Out-In Shuffling

Atom Erbium-167/Atom U = .000

	k_{eff}	Radial* Peaking Factor	k_∞ Distribution Regionwise		
			Inside	Middle	Outside
Beginning of Cycle	1.168	1.20	1.185	1.28	1.34
End of Cycle	1.080	1.18	1.08	1.185	1.28

Atom Erbium-167/Atom U = .0035

	k_{eff}	Radial* Peaking Factor	Δk_{eff} Penalty	Corr. Enrich. Penalty	k_∞ Distribution Regionwise		
					In	Middle	Out
Beginning of Cycle	1.060	2.13			1.13	1.105	1.055
End of Cycle	1.025	1.38	0.055	0.55%	1.05	1.13	1.105

Load Annular Region, Out-In Shuffling

Atom Erbium-167/Atom U = .0035

Beginning of Cycle	1.053	2.23			1.13	1.055	1.12
End of Cycle	1.026	1.34	0.054	0.54%	1.05	1.12	1.13

* Over-all peak to average source in fuel regions.

Table 2.6

Single-Batch Refueling Mode

W/F = 2.6 % Enrichment = 3.5

Atom Erbium-167/Atom U = .000

MWD/T Core Average Burnup	k_{eff}	Radial* Peaking	k_∞ Distribution Regionwise In	Middle	Out
000	1.27	1.85	1.34	1.34	1.34
6,000	1.17	1.44	1.21	1.27	1.31
12,000	1.07	1.17	1.09	1.17	1.24
18,000	0.985	1.18	0.99	1.07	1.16

Atom Erbium-167/Atom U = .0035

000	0.99	1.85	1.055	1.055	1.055
6,000	1.066	1.89	1.13	1.13	1.11
12,000	1.008	1.29	1.05	1.12	1.13

	Δk	% Enrichment
Erbium Penalty at 12,000	0.07	0.7%

* Over-all peak to average source in fuel regions.

Table 2.7

Thermal Spectrum Changes With Burnup

Burnup Results			Initial Core	Corrected[1] Wilkins		Uncorrected Wilkins	
MWD/T	$\Delta(\Sigma_a/\xi\Sigma_s)$[2]	Atom Erbium-167 / Atom U	$\Sigma_a/\xi\Sigma_s$ =	Hot .193	Cold .278	Hot .171	Cold .154
0.0	0.0	0.0050	$\Delta(\Sigma_a/\xi\Sigma_s)$[5] =	+0.085		-0.0165	
5,000[3]	0.015	0.0027	Temperature Change[6] =	1.17% $\Delta k/k$		8.75% $\Delta k/k$	
11,000[4]	0.029	0.0012					
18,000	0.039	0.00045					

NOTE:

(1) Corrected for spatial spectrum effects.

(2) $\Delta(\Sigma_a/\xi\Sigma_s) = \left[\Sigma_a/\xi\Sigma_s\ (0.0) - \Sigma/\xi\Sigma_s\ (\text{MWD/T})\right]$

(3) Beginning of equilibrium cycle core average exposure (3 batch).

(4) End of equilibrium cycle core average exposure (3 batch).

(5) $\Delta(\Sigma_a/\xi\Sigma_s) = \Sigma_a/\xi\Sigma_s$ (cold) - $\Sigma_a/\xi\Sigma_s$ (hot).

(6) Temperature Change = k_{eff} (cold) - k_{eff} (hot)/k_{eff} (hot) x 100.

2.2 Control and Safety System for Separate Superheat Reactor

2.2.1 Introduction

The safety and control problems of a nuclear power plant producing superheated steam have been studied. In the plant studied, a forced circulation, single cycle boiling water reactor (BWR) and a separate superheating reactor (SSH) combine to deliver 2.6×10^6 lb/hr of steam at 900°F and 965 psia to a tandem compound double flow turbine-generator set. The net electrical output is approximately 300 MW. Design of the containment for the nuclear system is based on the pressure suppression concept. The reactors are contained in individual drywells with provision for venting of those drywells to a water pool in the event of a system rupture.

An analog computer was used to study the dynamics of the two-reactor system. Both reactors and the connecting steam piping were simulated and the following control and safety problems were studied:

A. Normal plant power, pressure and temperature control

*B. Turbine bypass valve control

C. Emergency steam dump and emergency condenser operation

*D. Steam safety valve operation

* Denotes subjects briefly reported in Seventh Quarterly Progress Report, GEAP-3724

In addition, a digital computer program was used to study the superheater hot channel behavior for certain loss of steam flow transients. The hot channel maximum clad temperature at rated conditions is 1250°F, and the hot channel exit steam temperature is 1050°F.

As a result of these studies, a proposed control and safety system has been established and is described below. This report does not include evaluation of reactivity accidents (these have been studied earlier and reported in the Sixth Quarterly Progress Report, GEAP-3686), but is concerned primarily with the effects and control of steam flow variations.

2.2.2 General Criteria

The general criteria used in evaluating the control and safety systems are as follows:

2.2.2.1 Normal Control System

1. Change load at any rate up to ± 3%/minute and hold steam temperature change to ± 25°F.
2. Take sudden load change of ± 10% and return steam temperature to ± 50°F within 1.0 minute.

2.2.2.2 Bypass Valve Control

1. The bypass valve is pressure controlled and on a turbine governor load rejection (full or partial rejection from any load level). It must act to prevent:
   a. High flux scram
   b. High pressure scram
   c. SSH hot spot clad temperatures in excess of 1350°F. A 150°F margin below 1500°F is set to allow failure of the bypass valve to be detected and consequent opening of the emergency dump valves to limit SSH hot spot clad temperature to 1500°F.
2. Closure of the turbine stop valve will cause a scram,

but the bypass must open to provide cooling of the SSH fuel so as to limit the SSH hot spot clad temperature to 1350°F.

2.2.2.3 Emergency Steam Dump and Emergency Condenser Control

1. Provide an emergency heat sink in the event of loss of the main turbine condenser. Typical control requirements are:
   a. Sense failure of the bypass valve on load rejection or other abnormal high steam temperature condition and operate to limit SSH clad temperature to 1500°F.
   b. Sense failure of bypass valve on stop valve closure and operate to limit SSH clad temperatures to 1500°F.
2. Operation of the steam dump causes reactor scram, if one has not already occurred. The steam dump valves will discharge a pre-programmed steam pulse to the pressure suppression pool. After the steam dump valves close, the emergency condenser must supply a heat sink sufficient to limit SSH clad temperatures to 1500°F considering decay heat after scram and closure of dump valves.

2.2.2.4 Safety Valves

The basis for determination of safety valve requirements is:

1. The safety valves must act to limit the excursion resulting from closure of the turbine stop valve with failure of all bypass valve and safety system actions.
2. The resulting system pressure rise should not exceed 300 psia.

2.2.3 Conclusions

The conclusions take the form of certain general statements which can be made about the system transient performance, plus specific

proposals for the control and safety system design. The general conclusions are given here, while the specific proposals are included in later sections of this report.

2.2.3.1 The BWR-SSH system can be manually controlled to meet both turbine and utility requirements in the 25-100% power range. The control rods are manually positioned while the turbine control and bypass valves automatically control system pressure.

2.2.3.2 The SSH can use the locking piston drive (3 to 4 inch steps worth 5 to 10 cents per step) and maintain $\pm$ 10 to $\pm$ 20^{o}F temperature control above 25% steam flow. This controlability is due to the Doppler and moderator void reactivity effects in the SSH.

2.2.3.3 An automatic control for pressure and temperature can be designed to meet both turbine and utility requirements in the 25-100% power range.

2.2.3.4 Commercially available steam bypass valves can be used to protect the system against sudden loss of steam flow due to turbine load rejection. Superheater hot spot clad temperature rise can be limited to 100 - 150^{o}F on a turbine stop valve closure. The bypass valve requirement is: 120% capacity with 0.35 to 0.5 second or less opening time (including control system response). The bypass valve speed is essentially equal to the stop valve speed, and is set such that the safety system will not operate on full load rejection.

2.2.3.5 An emergency cooling system can be designed to protect against loss of the main turbine condenser heat sink (e.g., closure

of isolation valves, rupture of main condenser, or failure of the bypass valve.) Superheater hot spot clad temperature rise can be limited to 200-250°F on a turbine stop valve closure and simultaneous failure of the turbine bypass valves. The steam dump valves discharge to the pressure suppression pool, and the flow capacity requirement is: 60-70% capacity for 10-20 seconds with an 0.3 second opening time. By using electric pilot type valves, the steam dump valves may be integrated with the steam safety valves at the SSH exit. A 6% emergency condenser is satisfactory following the emergency dump operation.

2.2.3.6 Steam safety valves can be set to protect both vessels against overpressure; the required capacity is approximately 240% steam flow. Safety valves are placed at the SSH steam exit (100% including 60% steam dump valves) and on the BWR vessel (140%). In the event that no other safety devices (including reactor scram) operate on a full load rejection incident, the safety valves at the SSH exit will open first to protect the superheater fuel. If pressure continues to rise, the BWR safety valves will open. On this incident, some central fuel melting will occur in the BWR hot channel, and some fuel and clad melting will occur in the SSH hot channel. However, the average channels will not experience excessively high temperatures.

2.2.4 Summary of Normal BWR-SSH Control System

This section deals with the normal control of power, pressure and temperature. While a completely automatic system could be built, the proposed system incorporates manual control of plant power and temperature with automatic pressure control. The proposed control system is described in Case I, while the automatic controls are described in Cases II and III.

2.2.4.1 Case I -Proposed Control System (See Figure 2.8)

A. Pressure Regulator (Automatic)

1. Controlled Variable - SSH vessel pressure and SSH exit steam pressure. Use vessel pressure and pressure rate as control signals. Use SSH exit steam pressure rate to obtain fast transient indication of flow change.
2. Control Means - turbine control valve.
3. Controller Parameters (approximate numerical values)

   Pressure proportion gain - 20 to 50 psi/100% flow

   Pressure rate gain - 0 to 10% flow/psi/sec

   Over-all effective time constant of the control system - approximately 1.0 second.

$$\text{Turbine Control Valve Position} = \left[K_1 P_v + \frac{K_2 S P_v}{(\tau_2 S + 1)} + \frac{K_3 S P_{exit}}{(\tau_3 S + 1)} \right] \frac{1}{(\tau_1 S + 1)}$$

Where: S = LaPlace transform variable

$\tau_1 \approx$ 1.0 second

P_v = SSH vessel pressure

P_{exit} = SSH exit steam line pressure

K_1, K_2, K_3 = controller gains

τ_2, τ_3 = derivative signal time constants

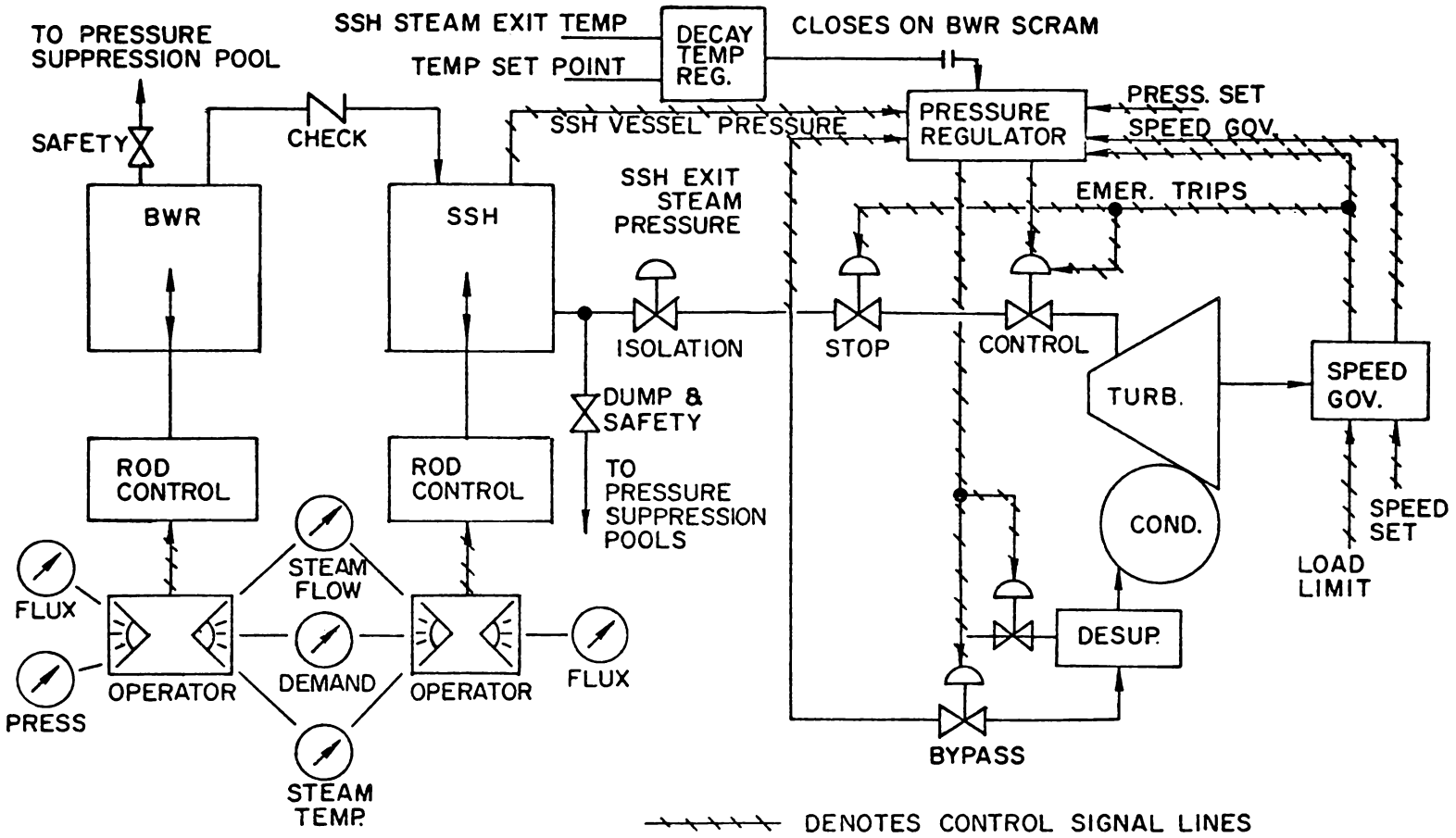

CONTROL SYSTEM SCHEMATIC FOR SEPARATE SUPERHEAT PLANT
NORMAL PRESSURE AND TEMPERATURE CONTROL

FIGURE 2.8

B. Plant Power Control

1. Control Means - operator movement of BWR control rods
2. Rod Reactivity Step (Average) - 10¢ (approx. 2.5% power)
3. Rod Reactivity Rate (Average) - 10¢/sec

C. Steam Temperature Control - SSH at power only when steam flow is 25% or greater

1. Controlled Variable - SSH outlet steam temperature
2. Control Means - operator movement of SSH control rods
3. Rod Reactivity Step (Average) - 5¢ for 10°F temp. steps
4. Rod Reactivity Rate (Average) - 2¢/sec
5. Temperature Sensor Time Constant - 2-4 seconds or less in the range 25-100% steam flow.

In addition, two variations of automatic control were briefly studied. They are described below.

2.2.4.2 Case II - Automatic Steam Temperature Control

A. Retain Pressure and Power Control Features Described in I-A and B

B. Steam Temperature Control

1. Controlled Variable - SSH outlet steam temperature
2. Control Means - SSH control rod position control
3. Controller Parameters

Temperature proportional gain - 10¢/25°F

Temperature integral gain 2¢/25°F-sec

Temperature rate gain - depends on temperature sensor time constant and flow change rate, not needed for present conditions

4. Temperature Sensor Time Constant - 1 second or less

5. Rod Reactivity Rate (Average) - 2¢/sec

6. Control Rod Position Control Time Constant - 1 second

2.2.4.3 Case III Automatic Plant Control

A. Pressure Regulator

1. Controlled Variable - BWR vessel pressure

2. Control Means - BWR control rods

3. Controller Parameters

Pressure proportional gain - 10¢/psi

Pressure rate gain - 10¢/psi/sec

B. Plant Power Control

1. Controlled Variable - turbine speed (load)

2. Control Means - turbine control valve

C. Steam Temperature Control

1. Controlled Variable - SSH outlet steam temperature

2. Control Means - SSH control rods

3. Controller and Temperature Sensor Parameters

same as Case II-B

Case III above depends on the ability of the plant to transiently supply a sudden demand from the stored energy in steam and saturated water. In the case of a plant with a relatively small amount of energy storage in steam and saturated water, it may be necessary to alter III above so that pressure is controlled by the turbine control valve, and a demand signal acts on the BWR control rods. This alternative was not studied.

All of these systems will meet the requirements specified in the ground rules set forth in the Introduction to the report; namely:

1. Change load at any rate up to ± 3%/min and hold steam temperature change to ± 25°F.
2. Take sudden load change of ± 10% and return steam temperature to ± 50°F within one minute.

The ability of the SSH control rods to regulate SSH steam and clad temperatures is limited on decreasing steam flow transients because of the effect of stored heat in the fuel and variation of surface heat transfer coefficient with steam flow. In general, the studies have shown that a sudden 50% decrease in steam flow will result in SSH clad temperatures in excess of 1500°F regardless of how rapidly the SSH power can be reduced after the change in steam flow. Use of steam flow control to regulate SSH temperatures was studied but not considered practicable as normal operating control. Steam temperature may be used in the turbine bypass and emergency steam dump control as will be discussed later.

The low flow limit of 25% for normal operations was set because of the effects of steam flow and SSH control rod reactivity step changes on SSH clad temperature.

An interlocking system will be necessary to bypass various safety and control system functions during different phases of reactor operation. The proposed operating modes are:

1. Unload-Load Fuel
2. Start-Up BWR
3. Power Operation - BWR
4. Start-Up SSH (At 25% steam flow)
5. Power Operation - SSH

In addition, the pressure regulating system will have several

operating modes:

1. Manual (Bypass and Turbine Control Valves)
2. Bypass Operation (Turbine Control Valves on Manual)
3. Turbine Operation (Bypass Valve controlled by tip-over pressure regulator)

2.2.5 Summary of the Bypass Valve Control

The particular set of numbers used in this study show that a bypass valve control which meets ground rule 1a (Section 2.2.2.3), will also meet 1b and 1c, for the case of 100% load rejection. In fact, depending on the initial pressure rate and the effect on reactivity, it may be difficult to meet 1a without use of a filter in the flux scram circuit to allow a sharp flux peak in excess of the steady state scram level. This is typical of advanced BWR designs in which water and steam volumes in the reactor vessel have been reduced. However, conditions arise, when operating at power levels below 100%, where satisfying 1a and 1b does not automatically satisfy 1c.

Rather than try to obtain bypass operation by detecting steam temperature or steam flow, the system proposed here relies on simultaneous actuation of the bypass and control valves (and/or stop valves). It is believed that this system causes the least steam flow distrubance for the cases of control valve closure and stop valve closure from any power level. The section of this report on the steam dump and emergency condenser operation will deal with detecting failure of the bypass valve and the resulting temperature transient.

2.2.5.1 Proposed Bypass Valve Control System (See Figure 2.9)

1. Bypass valve speed - 200%/sec. (Full stroke in 0.35 to 0.5 sec. or less on stop valve trip, including control response time, should be able to open almost as fast as the stop valve closes.)

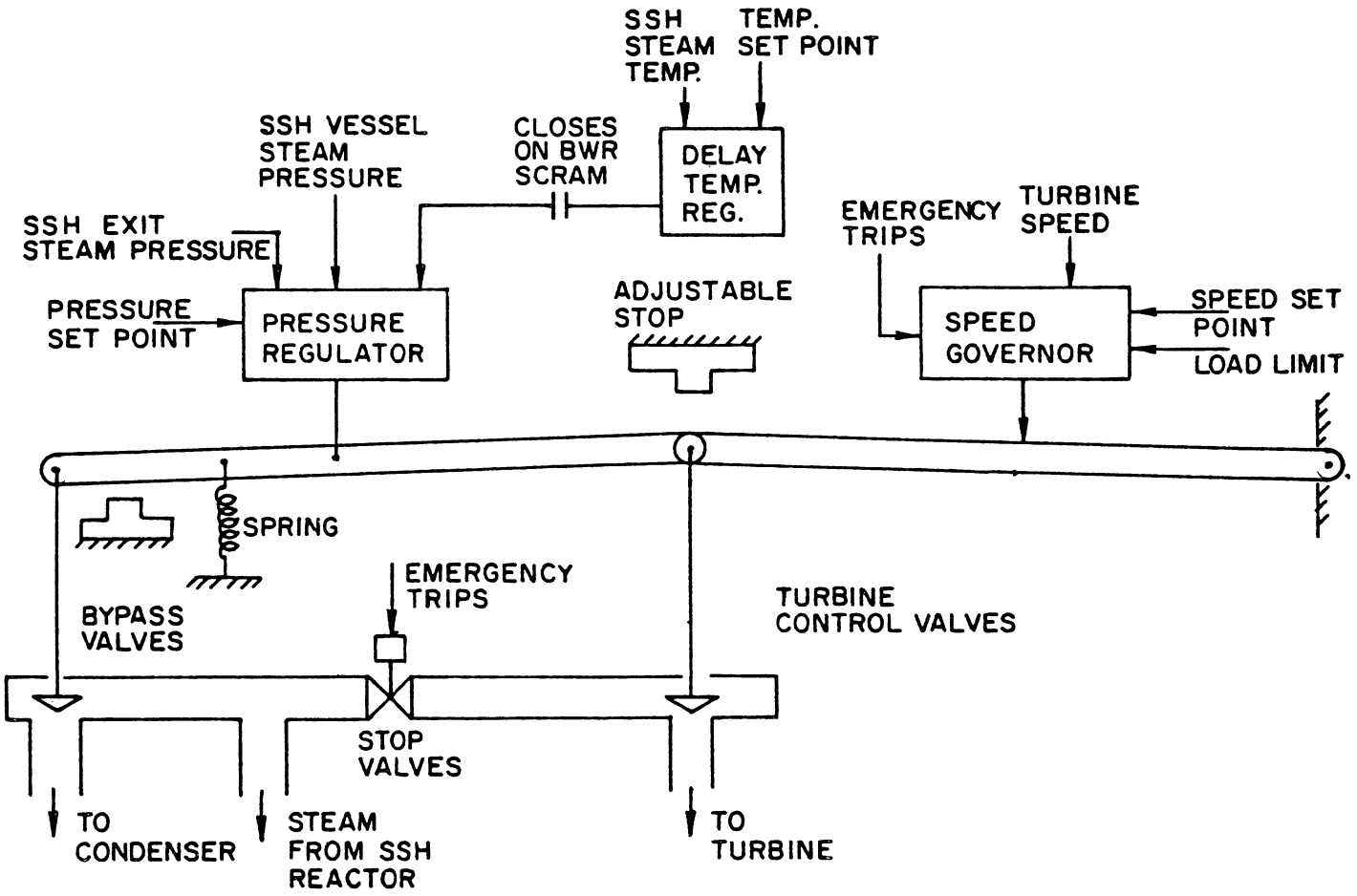

PRESSURE REGULATOR SCHEMATIC

FIGURE 2.9

2. Bypass valve capacity - 120% (So as to insure adequate control margin on a 100% load rejection)

3. Controller Action:

   The speed governor opens the bypass valve by approximately the same amount as it closes the control valve. The pressure regulator then acts on the bypass valve to maintain system pressure. Time response of control elements are identical for bypass valve and control valve. Use of the "tip-over" pressure regulator allows holding essentially the same steady state pressure before and after a load rejection.

4. For the case of turbine control valve closure, the maximum tolerable steam flow disturbance is:

   a. Transient drop in steam flow equal to or less than 25% of initial steam flow.

Initial Flow	Maximum Flow Change	Minimum Transient Flow
100%	25%	75%
50%	12.5%	37.5%
25%	6%	19%

   b. Initial integrated flow mismatch equal to or less than 0.4 full flow second. The illustration shows the 100% load rejection case.

100%

75% Area A 0.4 Full Flow Second

Time

5. After scram, the pressure regulator will throttle steam flow to maintain pressure. Energy storage in system steam and saturated liquid, together with droop of pressure regulator, is sufficient to supply cooling flow to SSH fuel. Heat losses in the BWR and piping may equal or exceed decay heat so that normal pressure

regulator action will not hold SSH clad temperatures. Consequently, a steam temperature signal is added to the pressure controller whenever a BWR scram occurs. This signal serves to increase steam flow if steam temperature rises. A 50 psi pressure regulation over the full load range will help to provide adequate cooling of the SSH fuel after scram. Thus, the bypass valve control after scram allows pressure to drop as steam flow drops so as to maintain adequate cooling of the SSH fuel.

6. The emergency speed governor closes the turbine stop valves and control valves, and simultaneously opens the bypass valves through the "tip-over" pressure regulator. Initiation of stop valve closure scrams both reactors. Ideally, the bypass valve response should be matched to the stop valve response, so that failure of the bypass can be detected and the emergency steam dump opened to limit clad temperature to 1500°F. The maximum tolerable steam flow disturbance for the case of stop valve closure is:

   a. Transient drop in steam flow equal to or less than 50% of the initial steam flow.

   b. Integrated flow mismatch equal to or less than 0.2 full flow second. The illustration shows the 100% load rejection case:

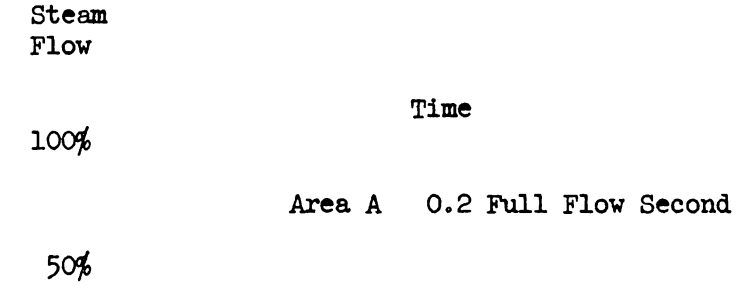

Discussions with potential bypass valve vendors, and familiarity with equipment being supplied to the Pathfinder and BONUS superheat reactor plants indicates that a bypass valve such as described above can be supplied. The control-actuator system would be electro-hydraulic.

A computer analysis of the average and hot channel temperature transients following a stop valve closure and bypass valve action gave the following results:

Stop Valve Closing Time	Bypass Opening Time	(Analog Comp) Avg. Clad Temp. Rise	(Dig Comp) Max. Clad Temp Rise	(Analog Comp) Avg. Exit Steam Temp. Rise	(Dig Comp) Max. Exit Steam Temp. Rise
0.2 sec	0.5 sec	50°F	76°F	35°F	65°F

The clad thickness for the above case is 28 mils outer clad, and 20 mils inner clad. If the clad thickness is changed to 12 mils and 10 mils respectively, the hot channel transient peaks are:

Max Clad Temp Rise = 114°F

Max Exit Steam Temp Rise = 96°F (Digital Computer results)

The increase in the transient temperature rise is caused by the reduction in heat capacity for the thinner clad.

With the stop valve flow versus time characteristic shown in Figure 2.10, it appears that the bypass valve control can be designed to give a transient flow increase on stop valve closure. Thus, the thinner clad could be used and the 1350°F temperature limit maintained.

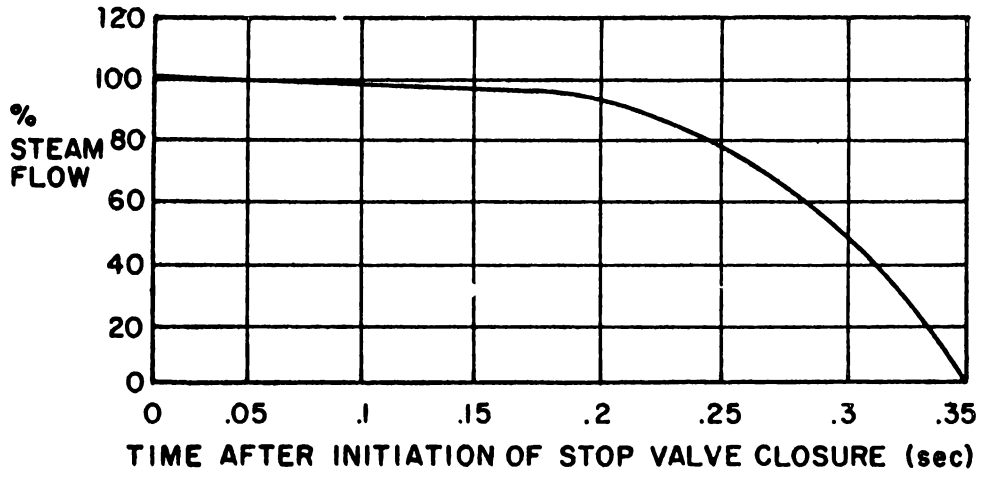

TURBINE STOP VALVE FLOW VERSUS TIME CHARACTERISTIC

FIGURE 2.10

2.2.6 Summary of the Emergency Steam Dump and Emergency Condenser Control

The emergency steam dump acts to provide an emergency heat sink of limited capacity in the event the main turbine condenser is lost. It is proposed to provide steam dump valves of the electric pilot type which will open on high pressure as well as loss of steam flow. The proposed system is outlined below. The emergency dump valves will discharge to the pressure suppression pool.

1. Total steam dump and relief valve capacity at the SSH exit: 100% steam flow.
2. Steam dump valves:
   a. Pressure actuated valves - set to lift at + 150 psi pressure rise.
   b. 40% capacity
   c. Open in 0.3 second.
4. High steam temperature protection - steam dump valve control
   a. Open if stop valves are closed and bypass valves are not at least 25% open.
   b. Open when the following combination of neutron flux, steam temperature and steam flow equals or exceeds a pre-set value:

$$\text{Signal} = \frac{K_1 N}{\tau_1 S + 1} - \frac{K_2 F}{\tau_2 S + 1} + \frac{K_3 \Delta T}{\tau_3 S + 1}$$

Where: N = % Neutron flux

S = LaPlace Transform Variable

F = % Steam flow

ΔT = SSH exit steam temperature deviation from set point

Gains	Time Constants
$K \lesssim 1.0$	$\gamma 1 \lesssim 7.5$ sec.
$K \lesssim 1.0$	$\gamma 2 \lesssim 0.5$ sec.
$K \lesssim 0.005$	$\gamma 3 \lesssim 2.0$ sec.

The purpose of this signal is to indicate a condition which could result in excessively high SSH clad temperatures. The signal causes a reactor scram at a lower value than that required to open the dump valves:

Scram at Signal = 0.3

Open Dump at Signal = 0.5

c. The steam dump valve control would be pre-programmed to pass 60% flow for 10 to 20 seconds (adjustable) and then close.

5. An emergency condenser of 6% steam flow capacity would be actuated when the dump is tripped. It must be operating at full capacity by the time the dump valves re-close to dissipate the decay heat after scram. The maximum superheated steam temperature which the emergency condenser would see would be 100°F over the normal operating temperature.

6. Since the emergency steam dump is a vital operation and also should not operate unnecessarily, it is proposed to use highly reliable components in a dual channel trip system. The de-energization of both of these channels (by the flux-flow-temperature control) is required to open the dump valves. Simultaneous failures in both channels would open the dump, while a failure in one channel would be annunciated.

A computer analysis of the average and hot channel temperature transients was made for the case of a stop valve closure, bypass valve failure, and subsequent dump valve operation. The results are:

top Valve Closure	Dump Valve Opening	(Analog Comp) Avg. Clad Temp. Rise	(Digital Comp) Max. Clad Temp. Rise	(Analog Comp) Avg. Exit Steam Temp Rise	(Digital Comp) Max. Exit Sm. Tmp Rise
0.2 sec.	1.0 sec	1.40	300°F	115	250°F

The clad thickness for the above case is 28 mils outer clad, and 20 mils inner clad. If the clad thickness is changed to 12 mils and 10 mils, respectively, the hot channel transient temperature peaks are:

Max. Clad Temp. Rise = 420°F

Max. Exit Steam Temp. Rise = 355°F

It is evident that the dump valve action will have to be faster than given in Section 2.2.6 if we are to hold the thinner clad temperature to 1500° starting with a 1250°F steady state maximum clad temperature.

With the dump valve trip system described here, the dumps would be opened when the stop valve reached the closed position and the bypass had failed to open beyond 25%. The stop valve flow vs. time characteristic (see Figure 2.10) is such that the flux-flow-temperature signal would not have responded by the time the stop valve is closed.

2.2.7 Summary of Safety Valve Requirements

The safety valves must act to protect the reactor vessels against high steam pressure. Since a rise in pressure causes a rise in power in a BWR, the required safety valve capacity is in excess of 100% steam flow. While the primary concern is to protect the vessels, we also wish to protect the SSH fuel as much as possible. Consequently, part of the safety valve capacity is placed at the SSH exit and set to lift at a pressure rise of +150 psi. The rest of the capacity

is placed on the BWR vessel and set to lift at a higher pressure. The valves discharge to the pressure suppression pool. The proposed system is given below:

SSH Exit Safety Capacity - 100%

(Composed of 70% electric pilot type valves-dual purpose dump/safety valves; and 30% safety valves)

SSH Exit Valve Lifting Pressure - +150 psia

SSH Exit Valves fully open at - +200 psia

BWR Safety Capacity - 140%

BWR Valves Lifting Pressure - +200 psia

BWR Valves fully open at - +250 psia

The resulting system pressure rise will not exceed 300 psia over the normal operating pressure.

The required safety valve capacity is a complex function of the BWR design factors, in particular the following:

1) Initial system pressure rate of rise on load rejection.
2) Pressure effects on BWR void reactivity.
3) Safety valve lifting pressure and operating range.

As the safety valve requirements are set by the BWR design, the recommended safety valve requirements will change as the BWR design changes.

It should be noted that the safety valves limit the nuclear power and pressure excursion, but they do not prevent SSH fuel clad or BWR central fuel melting.

2.2.8 Summary Of The Reactor Safety System Functions

Table 2.8 shows a functional listing of the hazardous conditions which are sensed to cause safety system action. For the purpose of this

study, the safety system is defined to include the following actions:

1. Reactor Scram (BWR & SSH)
2. Emergency Steam Dump
3. Emergency Condenser
4. Isolation Valves
5. Safety Valves

Other safety devices, such as core spray and liquid poison, are generally manually controlled and are not included in this study.

Table 2.9 shows a summary of the protection against various loss of steam flow incidents together with the back-up protection. Local plugging of fuel elements is not included in this tabulation, since it does not seem that any automatic control action could prevent local clad melting in this case. Steam temperature and flow monitoring of fuel assemblies could be used to actuate warning signals. Also, radiation monitoring of the exit steam could be used to effect plant shutdown in the event of loss of clad integrity.

Table 2.10 shows a summary of the overpressure protection schedule. In this schedule, it is assumed that a 50 psi regulation is used in the pressure control system (50 psi change-over full load range) and that there is a 50 psi drop through the SSH at full steam flow. "Zero" pressure is taken as the normal pressure at 100% load. A line drop of 20 psi is assumed between the BWR and SSH at full load.

It is evident that a scram in the BWR should cause a scram in the SSH. Should a scram occur in the SSH the steam temperature would drop and the turbine would have to be isolated to protect against thermal transients. This would require the bypass valves to open, passing steam to the main condenser. The SSH would then be rapidly cooled

to saturated steam temperature. Without a detailed study of the thermal transient effects in the SSH, it would seem desirable to limit the rate of cooling in the SSH. Thus, the following sequence is established for all scrams:

1. Scram of BWR causes scram of SSH, and vice-versa.
2. Scram causes closure of turbine control valve. Bypass valve will open due to action of pressure regulator.
3. Bypass valve will act to maintain steam flow such that the SSH exit steam temperature does not decrease too rapidly.

The scram speed for the SSH is not required to be any faster than that for a BWR. A brief examination of the reactivity accidents indicate that the fuel Doppler reactivity effect is the important limiting mechanism for the rapid reactivity excursions. The Doppler effect acts to sharply decrease the rate of rise of fuel temperature before scram can occur. The scram acts to prevent temperatures from rising beyond the initial limit provided by the Doppler effect. For slower reactivity excursions, the scram may act before the limiting Doppler effect. The SSH steam flow conditions limit the reactivity excursions which can be tolerated without SSH fuel damage. By proper SSH design, these reactivity limitations can be built into the reactor for all accidents except those types that also cause fuel damage in a BWR. An increase in scram speed beyond that which is reasonably achievable with present designs would be necessary in both the BWR and SSH to protect against fuel damage on the fast reactivity excursions. A typical scram characteristic for the locking piston drive is given below. The time between the scram trip signal and start of rod motion is about 0.2 second.

Time after Start of Rod Motion	% Travel
0.0 sec	0
0.5 sec	3
0.6 sec	10
1.0 sec	50
2.5 sec	70
3.0 sec	100

In general, approximately -$1.00 should be inserted in the first 0.5 second of rod motion.

The case of a break in the pipe connecting the BWR and SSH has not been analyzed in this report. It is evident that the flux-flow-temperature signal would cause scram and open the emergency steam dump valves. A check valve built into the SSH vessel steam inlet nozzle would close to stop steam flow from the SSH vessel to the break. The SSH vessel water would then flash and provide coolant flow through the SSH core to the pressure suppression pool and emergency condenser. The initial SSH fuel temperature transient is dependent on the action of the check valve to limit flow out of the SSH vessel to the pipe break.

TABLE 2.8

SAFETY SYSTEM FUNCTIONS

	Level	Scram	Open Dump Valves to Pressure Suppression Pool	Open Emergency Condenser	Close Isolation Valves
Short Reactor Period, BWR	10 sec	X			
Short Reactor Period, SSH	10 sec	X			
High Neutron Flux, BWR	1.25	X			
High Neutron Flux, SSH	1.25	X			
High Vessel Pressure, BWR	50 psi	X	X	X	X
High Vessel Pressure, SSH	50 psi	X	X	X	X
High Dry Well Pressure, BWR		X	X	X	X
High Dry Well Pressure, SSH		X	X	X	X
Low Water Level, BWR		X	X	X	X
Low Water Level, SSH		X	X	X	X
High Water Level, BWR (1)		X			
High Water Level, SSH (1)		X			
High Water Level in Scram Dump Tank		X			
Low Condenser Vacuum (1)		X			
Closure of Isolation Valves		X	X	X	
Loss of Auxiliary AC Power		X	X	X	X
Closure of Stop Valves (1), (2)		X			
Low Steam Flow (1)	25%	X			
Flux-Flow-Temperature	0.3	X			
Flux-Flow-Temperature	0.5	X	X	X	
Stop Valve Closed and Bypass Valve Less than 25% Open		X	X	X	
Manual Action		X	X	X	X
Emergency Cump Valve Open		X			
Low Vessel Pressure, BWR (1)		X	X	X	X
Low Vessel Pressure, SSH (1)		X	X	X	X
Turbine Control Valves and Bypass Valves Closed (1)		X			
Seismic Distrubance					

Notes: (1) Function bypassed during re-fueling and start-up.

(2) Function bypassed when in "Bypass Operation" mode.

TABLE 2.9

LOSS OF STEAM FLOW - SSH PROTECTION

Incident	First Line Defense	Back-Up	Others in Approximate Order of Occurrence			
Control Valve Closure	Bypass valve. (1350°F max clad temperature	Scram & steam dump on flux-flow temp. trip signal (1500°F max. clad temp.). Scram & trip steam dump on detection of bypass failure by limit switch logic.	High flux scram (Over 1500°F depending on flux transient)		High pressure scram & open steam dump & SSH emergency condenser (over 1500°F depending on pressure transient.	Safety Valves. (Part of core melts)
Scram BWR	Simultaneous SSH scram (1350°F max. clad temp.)	Flux-flow-temp. scram & dump (1500°F max. temp.	Operator action			
Isolation Valve Closure	Scram BWR & SSH & open SSH emergency condenser. (1350°F max. clad temp.)	Flux-flow temp. scram & dump (1500°F max. clad temp.	High flux scram	Operator Action	High pressure scram & open SSH emergency condenser.	Safety valves
Loss of Main Condenser Vacuum (closure of stop valve & eventual closure of bypass valve)	Scram on condenser pressure limit which closes stop valve (1350°F max. clad temp. if bypass valve is allowed to open)	Flux-flow-temp. scram & dump (1500°F max. clad temp.	High flux scram		High pressure scram	Safety Valves
Break in Pipe between SSH & BWR	Scram & open dump valves on flux-flow-temp. trip signal. Check valve built into SSH vessel inlet nozzle would close to seal SSH vessel on upstream side.	Scram on high dry well pressure.	Operator Action	Low Pressure	Low water level scram	

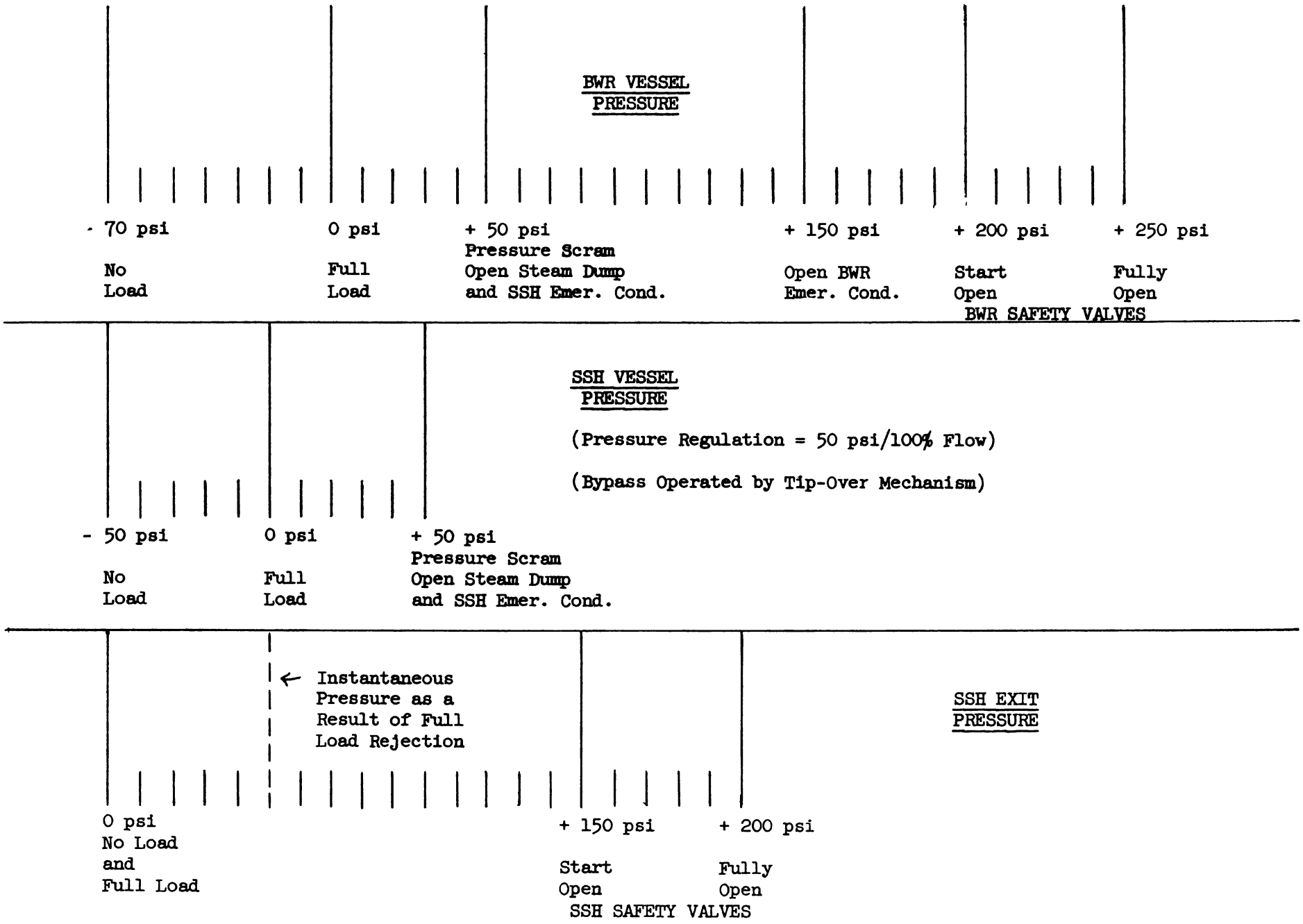

OVER PRESSURE PROTECTION SCHEDULE

TABLE 2.10

3.0 TASK B - FUEL TECHNOLOGY

3.1 Fuel Irradiation in SADE

3.1.1 SH-4 - The fuel element was inserted in the loop June 2 and VBWR power level was 14-30 MWT for a total of 4 days during June. The number of significant cycles from power levels of 0 to 15 MWT or above was 6. Maximum fuel clad temperature was 900°F at an exit steam of 720°F for about 48 hours.

3.1.2 SH-4B - The SH-4B fuel element is a .028" stainless steel clad, annular fuel element fabricated with 4.5% enriched UO_2 pellets. The fuel element dimensions are 1-1/4" O.D. x 3/4" I.D. x 36" active length. The design conditions for this element are 925°F exit at 1032 lb/hr, 100 KW(t) with maximum clad temperature of 1200°F. On May 24, 1961, the fuel element was removed from the SADE facility because of activity measurements which indicated a fuel defect. The fuel element was stored in the fuel storage pit at VBWR awaiting VBWR shutdown to permit removal of the fuel and cask through the VBWR containment air lock. During this period, the existence of a defect was confirmed by measurements of iodine in the water from the hermetically sealed can containing the fuel element. The fuel element was visually inspected in the Radioactive Materials Laboratory at which time, the defects were located. Two leaks were found. The first leak is a small line crack, located at the transition between active fuel pellets and inert zirconia pellets near the mid-plane spacers. The second defect is about 2" below the radial spacer pieces and is over active fuel pellets.

The irradiation history for SH-4B was as follows:

FIRST CYCLE (JAN. 15 to JAN. 29, 1961)

Approximate Steam Exit Temperature	Approximate Clad Temperature	Hours
600-650°F	800°F	140 hours
700°F	850°F	100 hours
740°F	910°F	72 hours

SECOND CYCLE (APRIL 24 to MAY 23, 1961)

Approximate Steam Exit Temperature	Approximate Clad Temperature	Hours
600-675°F	825°F	150 hours
700-800°F	1000°F	75 hours
850-900°F	1150°F	80 hours

The following summarizes Radioactive Material Laboratory observations. Photographic results of the SH-4B post-irradiation examination are shown in Figures 3.1 to 3.4.

1. Two cracks, each approximately 3/4 to 1" long were found, located on the outside clad. One of the cracks is transverse and the other longitudinal to the axis of the fuel element.
2. Both defects are located on the outer clad (the large diameter) at the high heat flux region (middle section of the fuel element).
3. Leak checking revealed no clad defects in the inside clad of the annular fuel element.
4. One of the cracks (transverse) was found to emanate from the weld of the mid-spacer tab. The weld penetration through the clad was confirmed by visual examination of the underside of the clad section.
5. Although residual stresses were found to be low upon longitudinal sectioning and measurement, these were concentrated near the mid-plane spacer tabs where one of the defects was located.

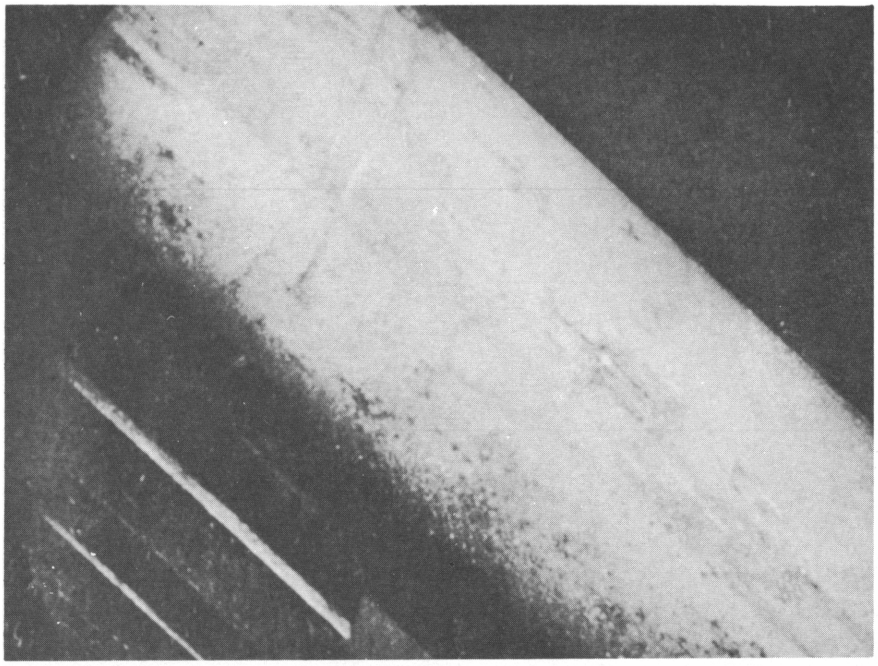

FIGURE 3.1
CLAD DEFECT FOUND IN SH-4B,
2" BELOW THE MID-SPACER

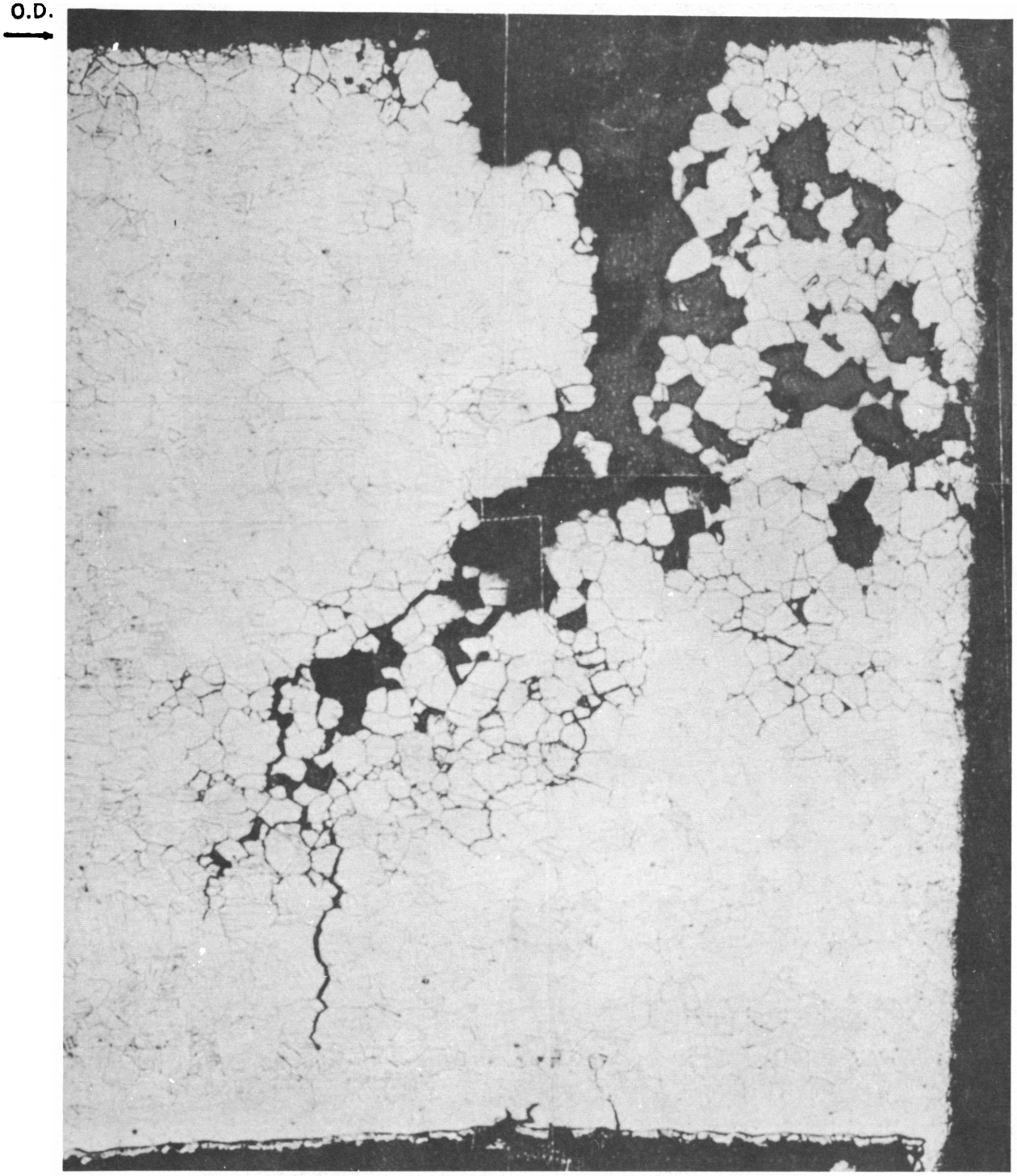

FIGURE 3.2
TYPICAL DETAILS OF CLADDING CRACK FOUND AT
THE OUTER ANNULAR TUBING SH-4B NEAR THE MID-SPACER

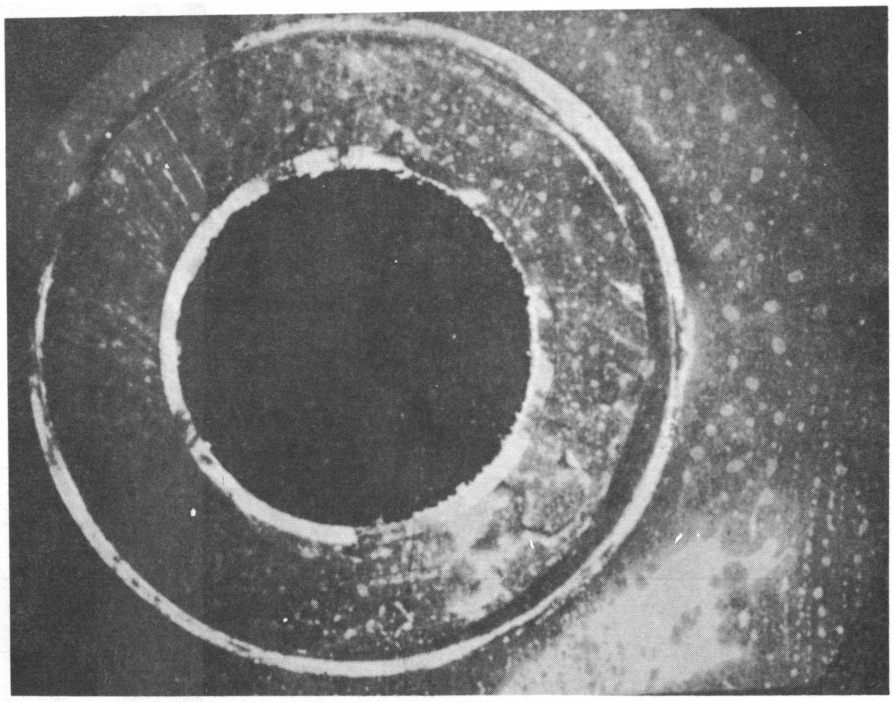

FIGURE 3.3
CROSS SECTION OF SH-4B SHOWING THE OUTSIDE CLAD COLLAPSED UNIFORMLY AROUND THE UO_2 WHICH SUPPORTS IT

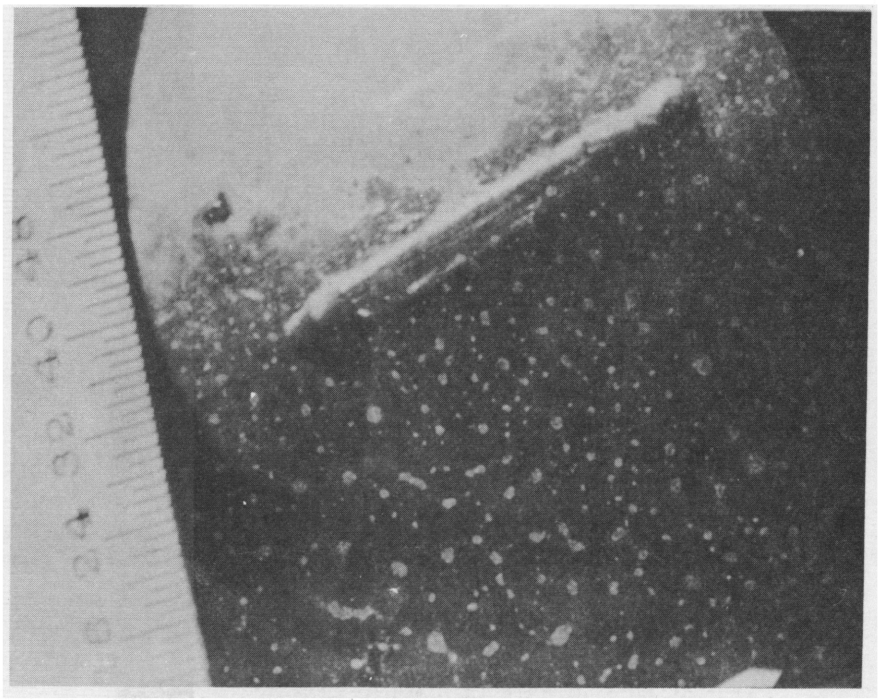

FIGURE 3.4
WATER DROPLETS, AT THE CLAD DEFECT, MID-SPACER NEAR THE ZrO_2 - UO_2 BOUNDARY

6. The second defect, on preliminary observations, appears to contain an "active core" suggesting the presence of a clad inclusion. Further metallographic work is now being done.
7. There is some evidence that UO_2 under the second defect may be oxidized. If this is confirmed upon further detailed examination, it may suggest that one or both defects existed prior to the reactor shutdown, and that one may have influenced the other.
8. Data available in regard to chemical condition of the reactor water and crud deposited on the fuel element are now being analyzed, to ascertain whether any impurities have influenced the performance of SH-4B.

3.1.2.1 Details of SH-4B

The fuel element was removed to Radioactive Materials Laboratory, and upon visual examination it was discovered that there were two cracks on the outer clad, both at the high heat flux area, near the middle spacer.

Visual and dimensional examination shows decrease in outside diameter and a uniform collapse of the clad over the pellets, of about 0.012" maximum. The inside diameter remained unchanged.

Bow measurements show a maximum of 0.080" in one direction, but the data has not been satisfactorily analyzed, and this measurement must be regarded as preliminary.

Length measurements indicate no plastic deformation of the clad in the axial direction. The measurements, taken at four points around the circumference between the weld shoulders show no change, with an accuracy of $\pm$ .005".

Sectioning of the gum drop monitor shows that the fuel pellet column contracted by about 0.100" during operation with respect to the clad. This information is valuable in designing the plenum support for subsequent fuel assemblies.

Fuel clad sectioning at the longitudinal crack found at 2" below the middle spacer shows severe intergranular attack of the metal matrix. Carbide precipitation is evident, both in grain boundaries and slip planes of the grains.

Several micro-cracks were also found, emanating from the clad outside diameter near (distance of 1/2" to 3/4") the large crack. In all of these cases, the attack is intergranular. It is to be noted that because the clad temperature was operated at 1100°F, carbide precipitation at the grain boundaries is to be expected.

The sectioning of the second crack, which is located near the weld of the spacer fins, shows similar details as the crack found 2" below the spacer. In addition to these two large, visually detectable defects, metallographic examination shows cracks near the root of spacer welds, but these cracks are transgranular in character. These micro-cracks are located in the base metal, but at the point corresponding to ZrO_2 inert pellet regions, where the clad temperature was relatively low during reactor operation. Although some carbide precipitation is visible, it is estimated to be significantly less than that observed in other regions. Analytical work is continuing to determine the clad temperature in the region where the trans-granular cracks were observed.

The UO_2 near the clad defect located below the spacer shows considerable amount of oxidation and some recrystallization. Because there is a visible corrosion attack at the clad interior, and because this attack diminishes with distance away from the large crack, it is certain that the clad defect existed during irradiation at high power in VBWR. Stack activity data during this run are now being analyzed.

Microstructure examination at the end plug welds revealed no defects.

The irradiation of SH-4B took place during a period when there was an anoralous condition in the reactor water chemistry. Specifically, the chloride content increased to as high as 3 ppm for a few hours. Although the chloride and oxygen concentrations in the water phase are not important at the observed levels, these conditions are extremely important under superheat service. The unusually high water carryover in steam coolant, possible water leakage in the SADE, the high stresses that exist in SH-4B, and the inherently high oxygen level in SADE loop may have been instrumental in causing clad failure, in addition to the presence of chloride ion contamination.

From experiments reported in the literature, and the observations available thus far from SH-4B, clad failure through a stress corrosion cracking mechanism is certainly possible.

Important knowledge gained from SH-4B irradiation is as follows:

1. Fuel element clad thickness of 0.028" constitutes a pellet supported clad design for the geometry tested.

2. The UO_2 load, as a whole, does not expand to fill the upper plenum area, instead it was found to contract or settle.
3. End plug design and welding of this type is satisfactory.
4. Collapsing of the clad over the pellets is uniform, without wrinkling.
5. ZrO_2 inert pellet, which was omitted in the SADE V and ESH-1 designs before information from SH-4B was available, is not necessary.
6. Fin (spacer) welding on clad must be either omitted or better welding methods be developed. (Magnetic force welding appears to be satisfactory from the control of penetration and strength standpoints).
7. Water chemistry control is a very important operating factor, with respect to fuel element clad integrity. An upper limit may have been established as a result of the SH-4B experience. Data are not as yet complete in this respect.

3.2 FABRICATION DEVELOPMENT

3.2.1 Fuel Fabrication

Critical Fuel - Twenty special annular fuel elements for the Phase II Physics Experiments were completed. The design incorporated both welded and mechanical sealed joints which will allow the fuel column to be disassembled at various stages of the experiment. The drawing for this "as build" fuel element is shown in Figure 3.5.

SH-5 - This .016" clad annular fuel element was completed. The element design included a double spring supported plenum. During a 1300 psi pressure test, a small axial wrinkle occurred

TITLE FUEL ELEMENT (SPECIAL)

FIRST MADE FOR AEC 3H CRITICAL X

P.L. ISSUED

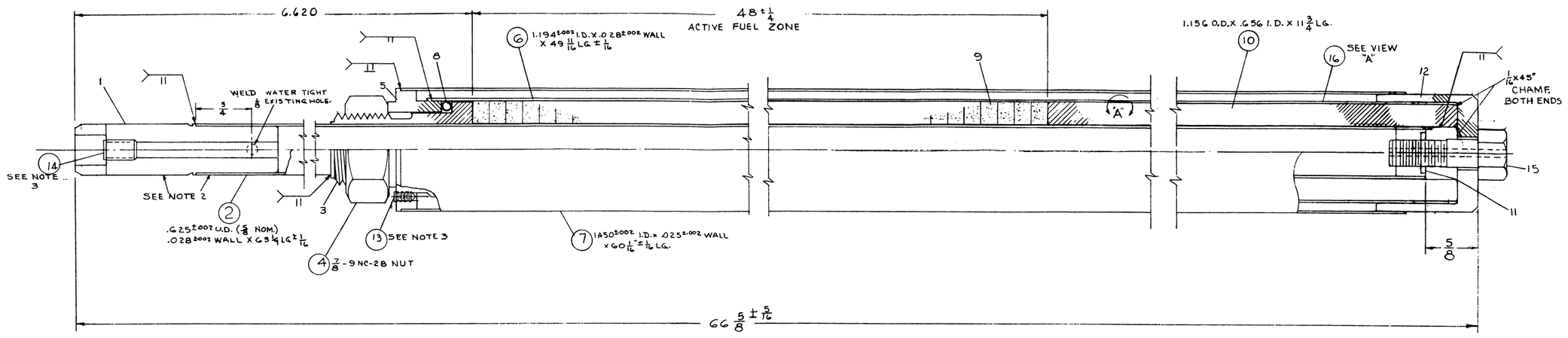

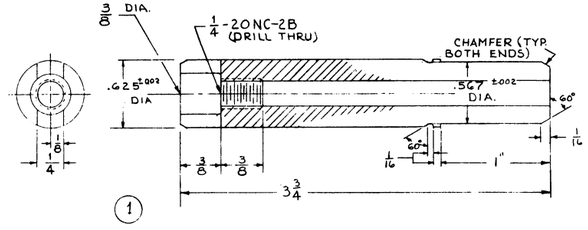

(1)

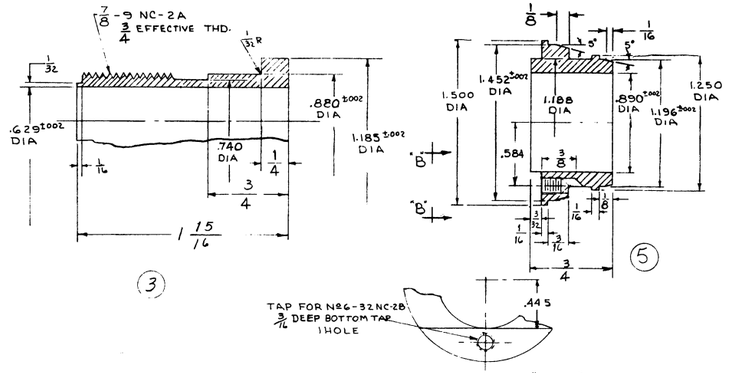

(3) (5)

SECTION "B-B"

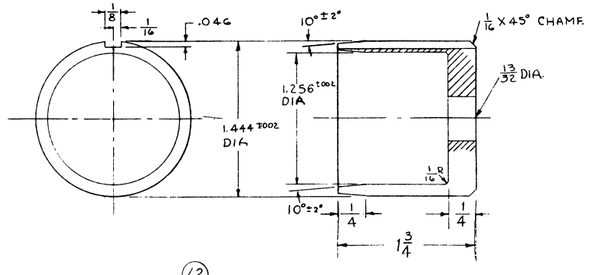

(12)

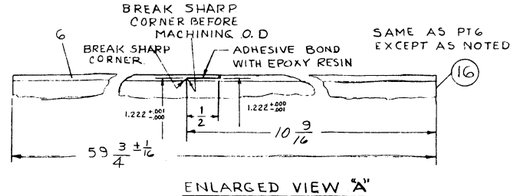

ENLARGED VIEW "A"

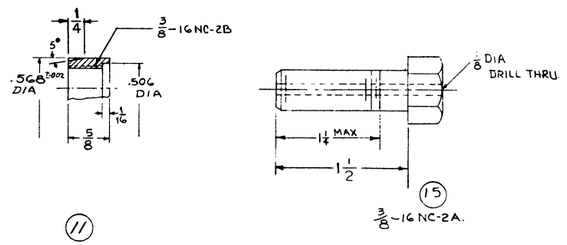

(11) (15)

NOTES:-

1- LEAK TEST ASM. PER ENGR. INSTRUCTIONS.

2- MARK WITH 6 DIGIT NUMBER OF THE FORM 340XXX EITHER SURFACE INDICATED BY ARROWS.

3 COAT THREADS WITH G.E. RED GLYPTAL. FOR SEAL.

AS BUILT

FIGURE 3.5

over the plenum area. Neither the cause of this wrinkle nor its effect on the fuel element performance have been determined. An identical plenum has been cycled in the high temperature autoclave to 1500 psi at 1200°F without any evidence of wrinkling or collapse. Further tests will be conducted on SH-5 in the corrosion loop.

NUSU Pellets - Pellets for one SADE type element were completed. Quality of the pellets was generally considered below average, the main causes being porosity and axial cracks. However, pellets were believed to be adequate for a test of the SADE type. Zirconium oxide pellets were also made for the NUSU element although a recommendation was made against its use in fuel elements, based on SH-4B experience.

Miscellaneous Specimens - Additional specimens were completed for Trail Cable, clad cycling, plenum support, thermal shock and corrosion tests.

3.2.2 Fuel Fabrication Development

Spacer Fabrication - Three methods of spacing fuel elements in process tubes are currently being investigated. They are shown in Figure 3.6. The first, spiral wrapped wires welded only to the end plugs are simplest to fabricate, but must be demonstrated to be satisfactory from standpoints of heat transfer, crevise corrosion and fretting corrosion. Integral spiral finned tubes can be fabricated and offer a possible solution to the spacer problem if the wire spacers should prove unacceptable. Intermittant fin spacers offer the same advantages as the integral spiral fin but will possibly cause higher stress

FUEL ELEMENT SPACING CONCEPTS

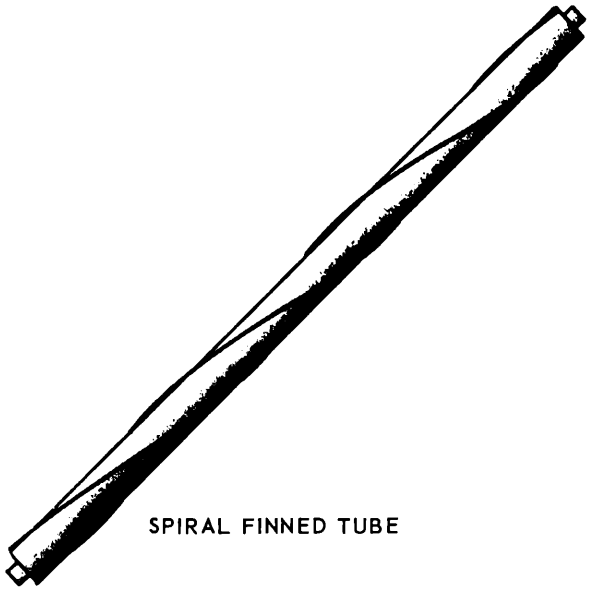

SPIRAL FINNED TUBE

SPIRAL WIRE FINS
END WELD ATTACHMENT

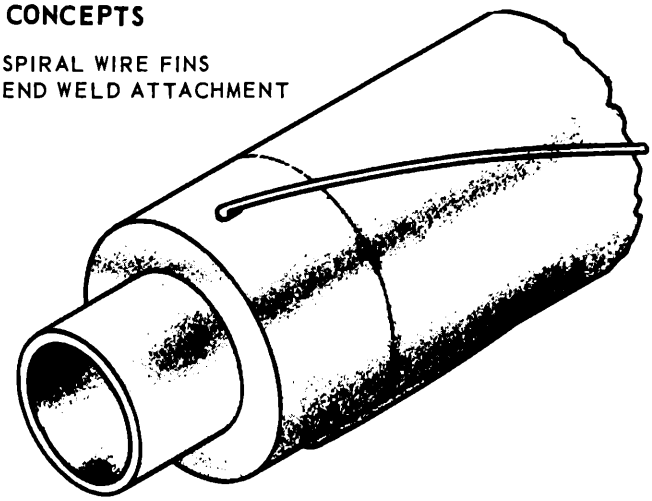

INTEGRAL SPIRAL FINS

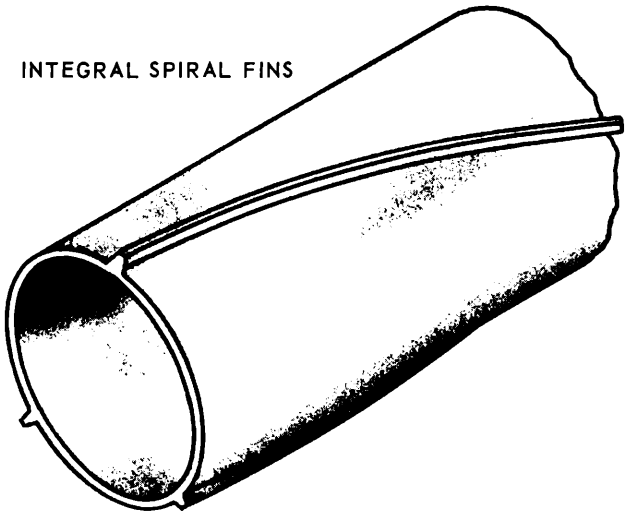

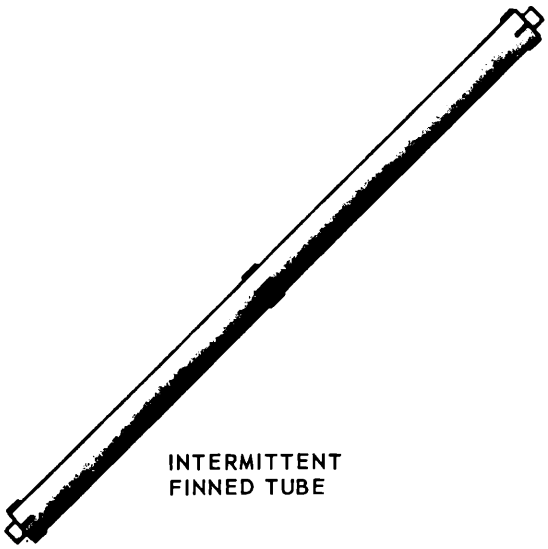

INTERMITTENT
FINNED TUBE

FIN SPACER

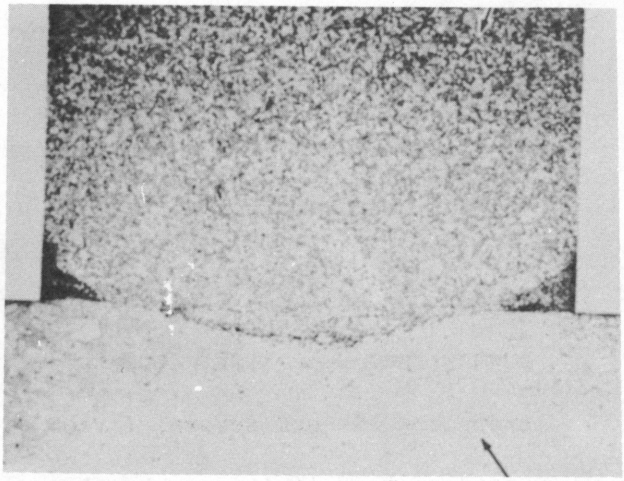

CLADDING

MAGNETIC FORCE WELDED FIN

MAG 75 X

FIGURE 3.6

concentrations over the fuel column. Magnetic force welding is being investigated as a means of attaching fins to thin wall cladding with minimum damage to the cladding material.

Plenum Support - Support of the plenum area in superheat fuel elements fabricated with non-freestanding clad is still a major problem. SH-5A, the next .016" clad element, will be fabricated with the plenum support shown in Figure 3.7. This type plenum support provides reinforcing sleeves on both the internal and external cladding tubes, pellet settling is accommodated by a spring loaded support plug following the pellet column down the tube. This plug limits the extent of clad radial depression which can be caused by external pressure; the rounded edges on the plug and sleeves control the curvature of the cladding into the depression. Powder elements will include a reinforced section at the top of the powder column as shown in Figure 3.8. Sleeve inserts will prevent cladding collapse in the event of a settling of the powder column.

Pellet Fabrication - A method for diamond grinding the internal diameters of pellets has been developed. The method represents a savings of over 90% in direct labor costs for this operation and the resulting product can be held to closer tolerances.

Powder Compaction - Preliminary work on the fabrication of powder fuel superheat elements was initiated. Two Trail Cable type capsules and several larger specimens were fabricated. Based on this limited work, it would appear that 85% of theoretical density can be achieved by vibratory compaction of a graded arc-fused powder and the density can be increased another 1 or 2% by swaging in nylon dies.

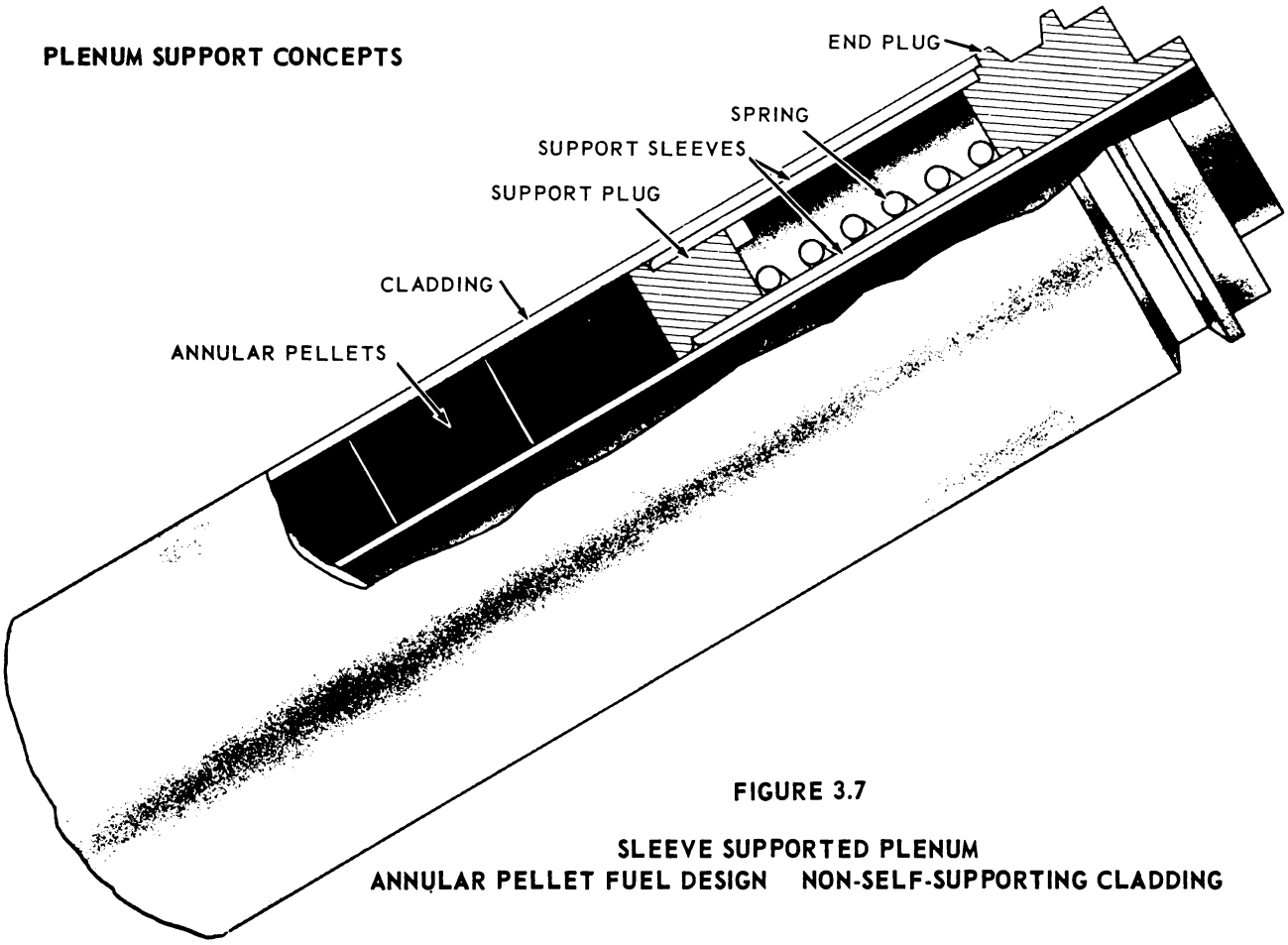

FIGURE 3.7

SLEEVE SUPPORTED PLENUM
ANNULAR PELLET FUEL DESIGN NON-SELF-SUPPORTING CLADDING

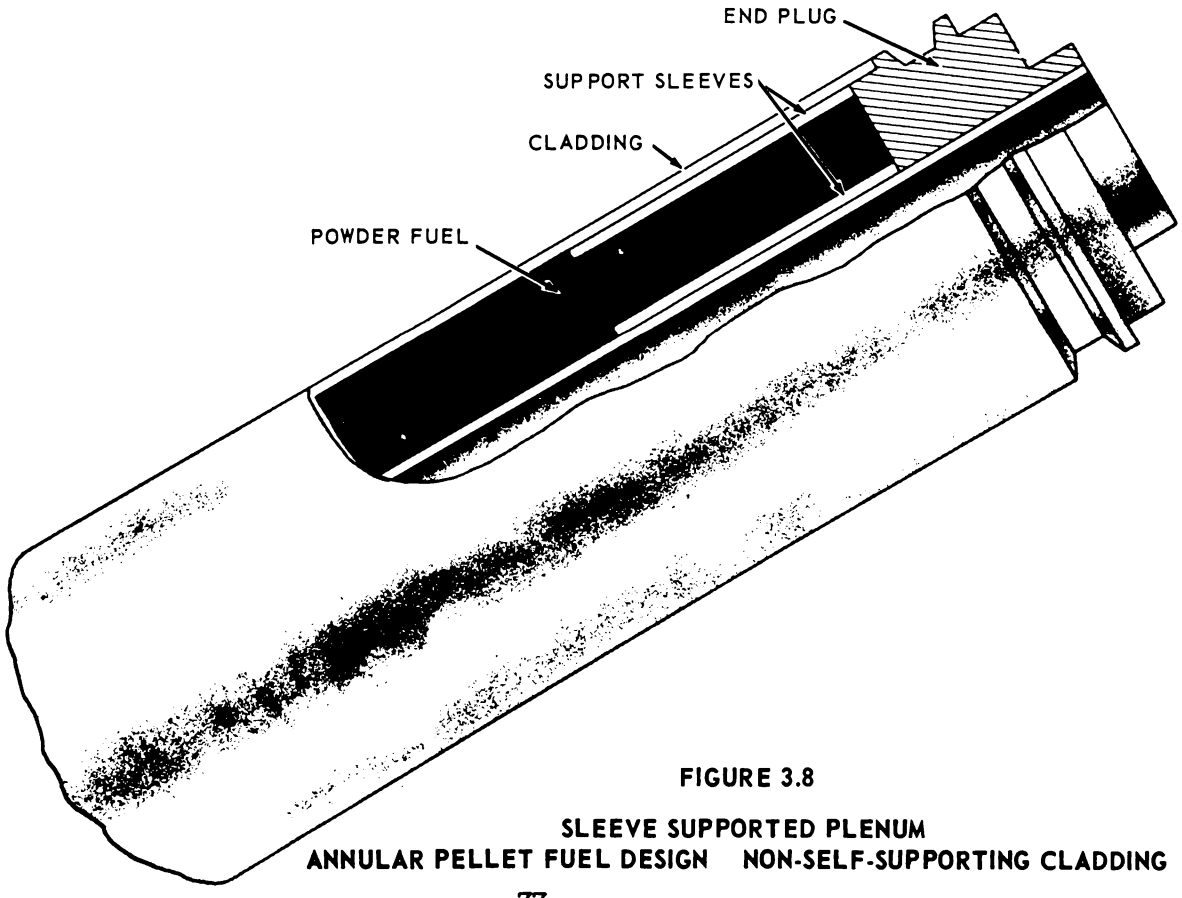

FIGURE 3.8

SLEEVE SUPPORTED PLENUM
ANNULAR PELLET FUEL DESIGN NON-SELF-SUPPORTING CLADDING

Inspection - Permanent records of ultrasonic cladding checks are now being made on an oscillograph recorder. Further work is being done to determine the feasibility of using ultrasonic techniques for the detection of stress corrosion cracking during post-irradiation examinations. The oscillograph traces will allow an accurate comparison or pre- and post-irradiation inspections. The first permanent ultrasonic record was made for the SH-5 assembly, showing no damage of the clad resulted from the swaging operation.

3.3 Superheat Fuel Element Bowing Tests

The objective of this experiment was to investigate the bowing characteristics of an annular fuel element due to circumferential thermal gradients that may exist during reactor service. The scope of the test included the magnitude of bowing as well as the forces involved to restore straightness under simulated thermal gradients. A quantitative understanding of these areas will facilitate the design of spacer configurations in superheat fuel.

During the experiment, the element, SADE IV-A, was supported at each end of the active fuel section by V-blocks. A thermocoax heating wire was used as a variable heat source to half of the clad circumference. Chromel-alumel thermocouples were intermittently spaced along the length of the element to record the temperature distribution.

As a result of this investigation, a relationship was obtained between circumferential temperature variation of the clad and bowing of the fuel element with its accompanying forces required to offset bowing. The experimental data were plotted in Figures 3.9 and 3.10 and a linear relationship was obtained in the range and temperature levels studied. A force of 0.2 $\pm$ 0.01 kilograms was required to

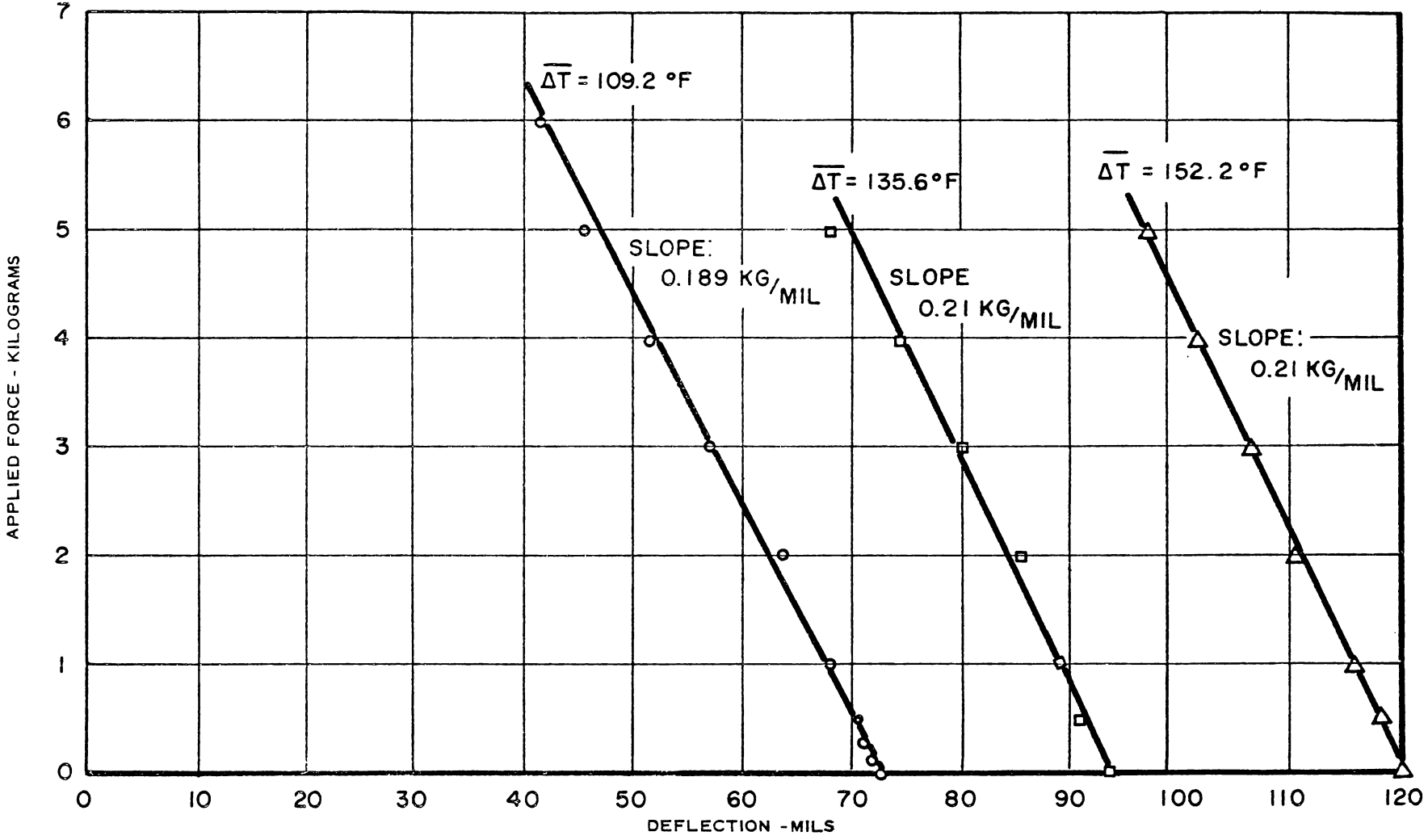

FIGURE 3.9

RESTRAINING FORCE VS. DEFLECTION

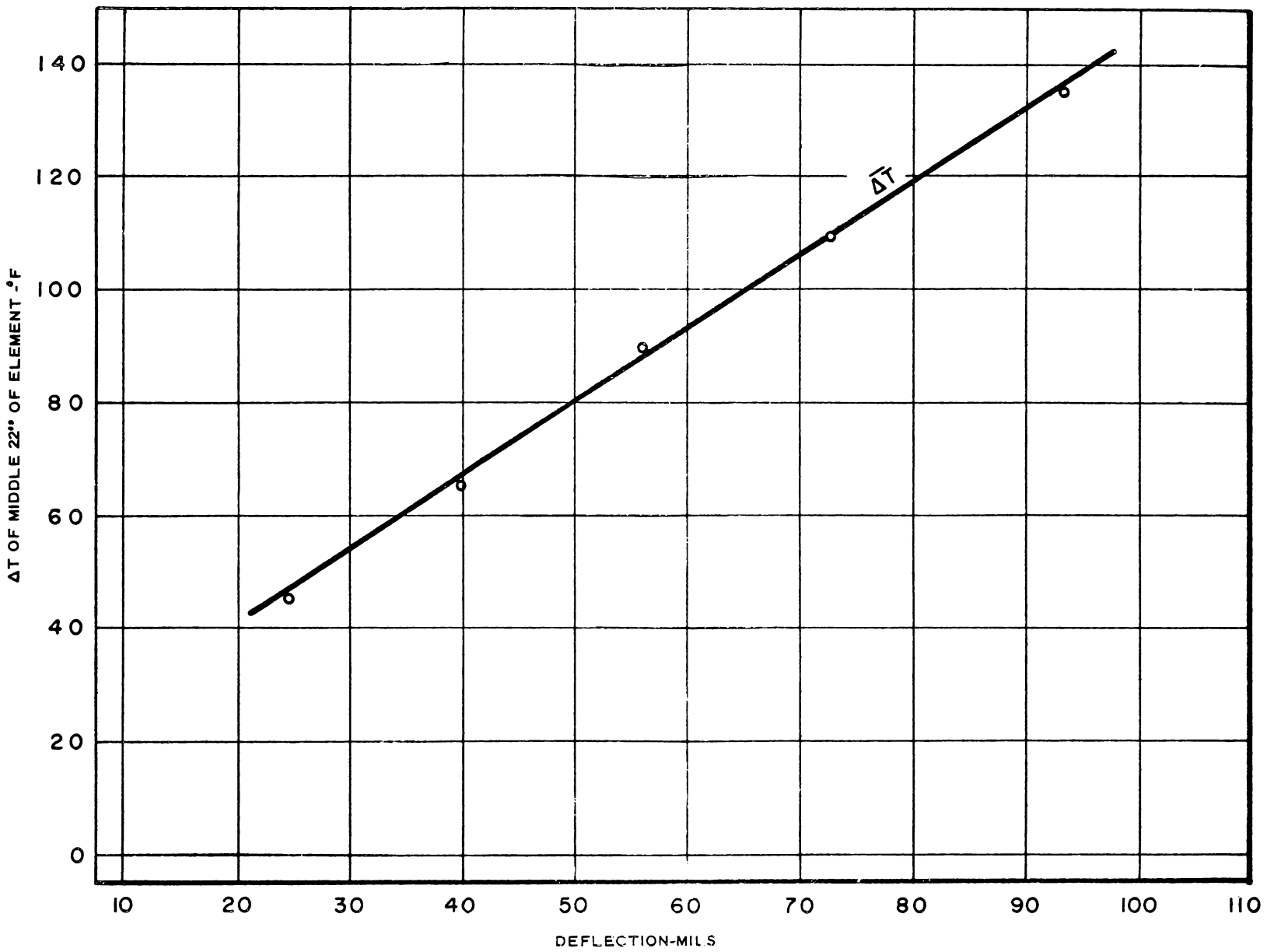

FIGURE 3.10
ΔT VS. DEFLECTION

decrease the bowing deflection a distance of 1 mil. This force is independent of the temperature level in the ranges studied and circumferential variation.

During reactor exposure, it is anticipated that radial temperature variations will occur due to coolant flow irregularities or neutron flux variations across the fuel cross-sectional area. These variations will range from 50°F to 150°F depending on position in the reactor. Therefore, in the extreme case a bowing deflection of 0.120" can be expected. A movement of this magnitude in a superheat process tube can be important with respect to flow areas and heat transfer characteristics. The force exerted by a spacer in the center of the fuel element can be estimated at 53 pounds.

3.4 Trail Cable Irradiation Experiments

3.4.1 Summary

The experimental results and data analysis for the 36 pellet-filled annular capsules have been incorporated in a topical report, GEAP-3739, "Plastic Strain In Thin Fuel Element Cladding Due to UO_2 Thermal Expansion."

The summary and conclusions of the above report are recorded below.

3.4.2 Summary Of Work Reported In GEAP-3739, "Plastic Strain In Thin Fuel Element Cladding Due To UO_2 Thermal Expansion"

A total of 36 fuel bearing capsules have been irradiated and examined to date in the program with the following generalized results:

1. The diameter of the capsule external cladding increased

significantly as a result of irradiation for almost every capsule.

2. The over-all length of the capsules increased with only one or two exceptions and the length increase was found to vary in a consistent pattern around the periphery of the capsule.
3. No significant change was observed in the diameter of capsule internal cladding with one possible exception.

Analysis of the external cladding dimensional changes has shown the magnitude of the change to be a function of the restraining forces imposed on the UO_2 by the clad as well as a function of the capsule heat generation and the initial pellet-cladding gap. These functional relationships are stated in general terms as follows:

1. The diameter change, or growth, decreases with increased cladding strength.
2. The diameter change increases essentially linearly with increasing capsule heat generation.
3. The diameter change decreases somewhat with increased initial pellet-cladding gaps. However, the UO_2 appears to thermally expand sufficiently to close any of the initial gaps within the range studied - 0 to 11 mils - and produce clad growth.
4. For the particular capsule configuration and operating conditions employed in these tests, the maximum expected outside diameter increase is approximately 10 mils, equivalent to 0.8% total strain.

The plastic straining of the cladding observed as the result of

a single cycle of irradiation in these tests will probably be cyclic with changes in power generation when the cladding is non-freestanding under the existing external pressure. It was experimentally determined that the UO_2 shrinks back to approximately its original dimensions when power generation ceases.

Analysis of the observed capsule length changes has not been completed. The changes in length appear to be the result of action of the pellets against the adjacent cladding rather than direct axial expansion since changes in the initial axial gap did not significantly affect the increase in length. The length increases varied sinusoidally around capsule periphery, indicating that the relatively heavy end plugs were tilting with respect to each other, probably as a result of circumferentially non-uniform heat generation within the capsule.

Relatively large amounts of gas - 6×10^{-2} cc/gm - were found to evolve during irradiation from the conventionally processed, sintered UO_2 pellets used in the initial capsules. By modifying the capsule design, and improving the capsule fabrication procedure, the magnitude of the gas evolved in subsequent capsules was reduced significantly and internal gas pressure eliminated as a possible contributor to the observed cladding growths. Comparison of subsequent growth results with those obtained previously indicated several cases where internal gas pressure was a factor. These capsules were not considered in data analyses or in forming the experimental conclusions.

No difference was observed within the experimental error between

swaged and unswaged capsules in producing outside cladding growth other than that attributable to generally smaller initial gaps present in swaged capsules.

New equipment was designed and built and a completely new irradiation technique developed to permit the rapid conduct of these capsule irradiations in the GETR Trail Cable Facility and the post-irradiation dimensional measurements in the GETR canal.

3.4.3 Conclusions Of Results Given In GEAP-3739

Both circumferential and axial plastic strains were produced in thin fuel element cladding as a result of UO_2 thermal expansion during irradiation. Evidence was obtained that the circumferential cladding plastic strain will be cyclic with changes in the fuel element power when the cladding is non-self supporting under the external pressure environment.

Calculations have been made to indicate the life to failure from plastic strain cycling of a fuel element cladding experiencing circumferential strains of the order observed in these tests. Using the Coffin relation and available property data on 304 stainless steel at approximately 1200°F, the results predict a life in excess of 1000 complete strain cycles. This compares with a maximum of 500 full power cycles expected during actual superheat fuel element life. The quantitative significance of the above result is severely limited by at least the following qualifications:

1. The circumferential strain may not be the most severe repetitive clad strain.
2. The magnitude of the plastic strain observed in these

room temperature tests may become appreciably larger at superheat operating temperatures.

3. The strain cycle behavior of 304 stainless steel may be unfavorably altered by environmental factors such as irradiation, steam corrosion, low frequency cycling, etc.

The above result can, at most, only be considered encouraging; a definite conclusion concerning the strain cycle life limitation must await more extensive evaluation of the behavior of 304 stainless steel followed by actual operation of prototype superheat elements for a total number of cycles in excess of that expected during the fuel element life. The maximum number of power cycles experienced by one of the SADE loop test elements to date is 55.

The consequences of the observed axial cladding strain cannot be evaluated because it is uncertain whether the strain is localized or uniform along the clad length and because it is not known if the strain will be cyclic. If both cyclic and highly localized, the axial strain could be more significant as a failure mechanism than the circumferential. The axial strain observed in full length SADE elements has been of the same order as observed in these capsule tests.

Significant quantities of gas were found to be evolved from conventionally fabricated UO_2 sintered pellets. Gas, in this amount, has serious consequences with regard to the long-term pressure buildup within the element. Inclusion of an evacuation and heating step in the capsule fabrication procedure affected a sevenfold reduction in the gas evolved during irradiation.

Both the pellet gas release described above and the fact of UO_2 thermal expansion itself, separately and together, have important implications with respect to the internal heat transfer characteristics of the annular element. Future calculations should be modified to account for the considerably improved heat transfer path to the outsdie surface due to high UO_2 clad interference pressures and the poorer heat transfer path to the inside surface due to both a larger gap and lower gas conductivity. This effect has been partially evaluated for the purpose of analyzing the capsule growth data. A significant shift may result in the heat flow split between inner and outer clads.

3.4.4 Additional Trail Cable Irradiations

Two powder-filled annular capsules were fabricated and irradiated during the quarter. They were designated TR-23 and TR-24. TR-23 used 28 mil wall 304 stainless steel for cladding, and TR-24 used 16 mil 304. Both capsules had an outside clad O.D. of 1.25", an inside clad O.D. of 0.75", an over-all length of 5.85", and an active fuel length of 4.5". Fuel was 3.5% enriched arc-fused UO_2 powder, vibratory compacted to 83% of theoretical UO_2 crystalline density. The density was increased to 84% or greater by swaging. Before the final end plug weld the capsules were heated to 800°F and then evacuated and backfilled with Helium 6 times. This was to reduce the residual amount of gas in the 45 fabricated fuel elements.

TR-23 was irradiated once, at an average heat flux of 311,000 Btu/hr-ft^2. Its average diameter growth was 0.6 mil.

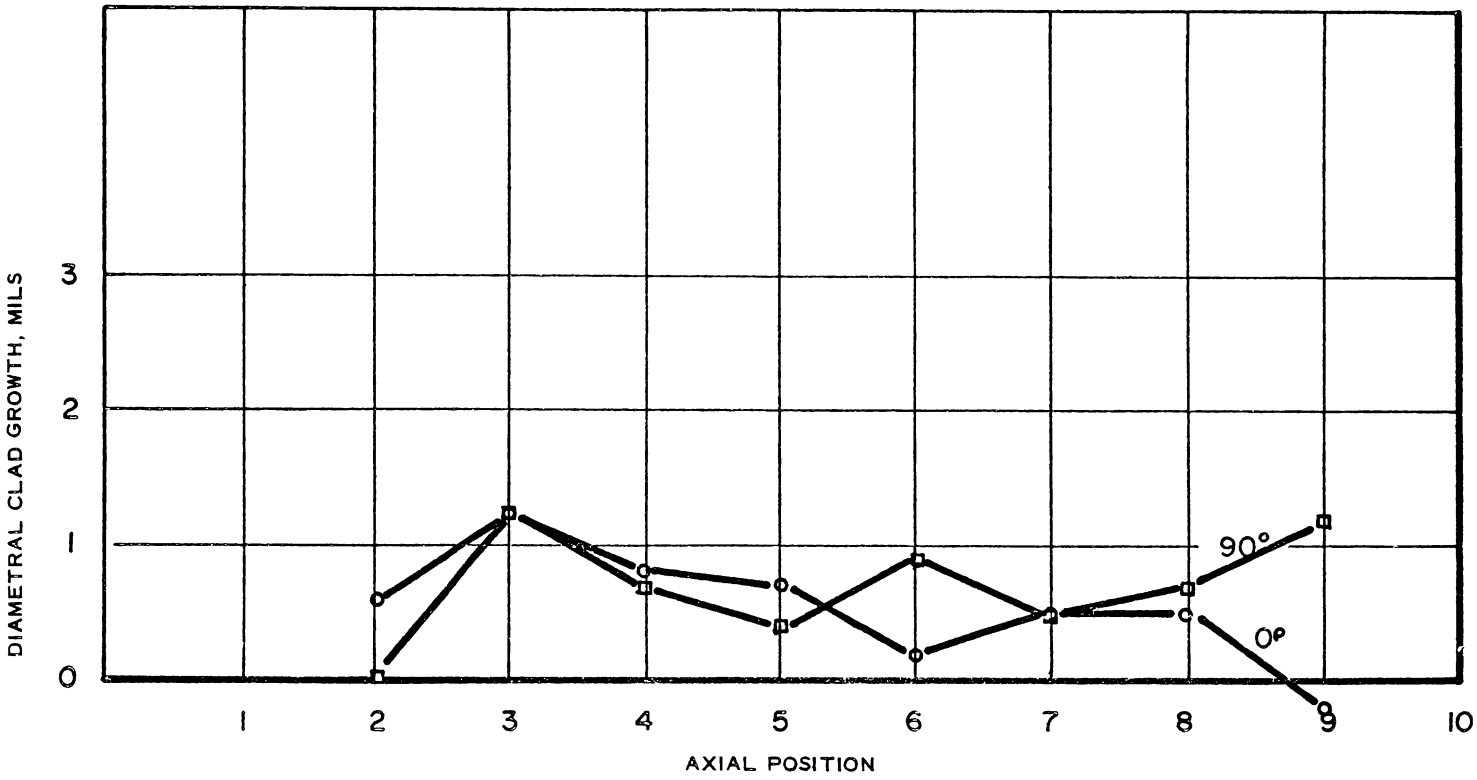

FIGURE 3.11

DIAMETER CHANGE VS. AXIAL POSITION, TR-23, 28 MIL WALL 6-13-61

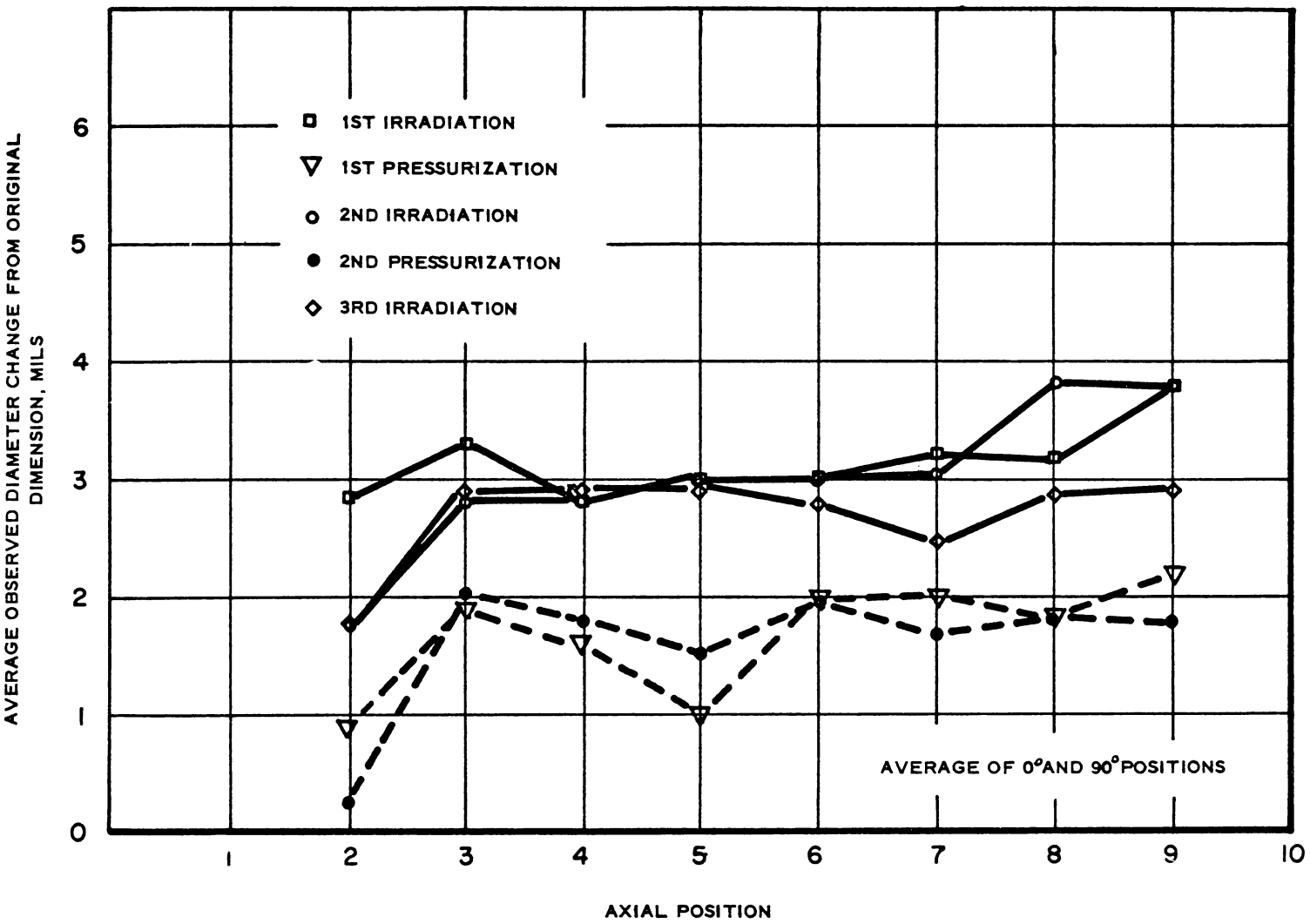
1ST IRRADIATION
1ST PRESSURIZATION
2ND IRRADIATION
2ND PRESSURIZATION
3RD IRRADIATION
AVERAGE OF 0° AND 90° POSITIONS
AVERAGE OBSERVED DIAMETER CHANGE FROM ORIGINAL DIMENSION, MILS
AXIAL POSITION
0
1
2
3
4
5
6
7
8
9
10

Figure 3.11 shows diameter change of TR-23 versus axial position. TR-24 was irradiated three times and was hydraulically pressurized (3500 to 4000 psi), after each of the first two irradiations. Figure 3.12 shows each diameter change of TR-24 versus axial position. The first irradiation of TR-24 was at an average heat flux of 293,000 Btu/hr-ft^2, and resulted in an average clad O.D. increase of 3.2 mils. The next two irradiations also caused the O.D. to increase to about the same value above the pre-irradiation average diameter. Each pressurization of TR-24 reduced the O.D. to about 1.6 mils above the pre-irradiation average. Taking the elastic spring-back of about 1.5 mils into account, the pressurization results for TR-24 indicate that the UO_2 powder recedes back to, or close to, its pre-irradiation diameter.

The pressurization results also indicate that if powder-filled annular fuel elements are jacketed with non-freestanding clad, then plastic strain cycling of the clad can be expected under reactor power cycling and reactor pressure. This is not different than the results found for the sintered pellet-filled fuel specimens.

Fabrication of the six pellet-filled rod capsules was completed. Their designations were D-1 through D-6. All six were constructed with 11 mil clad of 304 stainless steel. Clad O.D. was 0.485" (nominal). Pellet-to-clad diametral gap was 9 mils for D-3 and D-4, while the gap for D-2 and D-6 was 4 mils. D-1 and D-5 were swaged with presumably zero initial gap. Over-all capsule length was 6.5", and fuel length was 5". The fuel was 3.5% enriched UO_2 powder, pressed and sintered

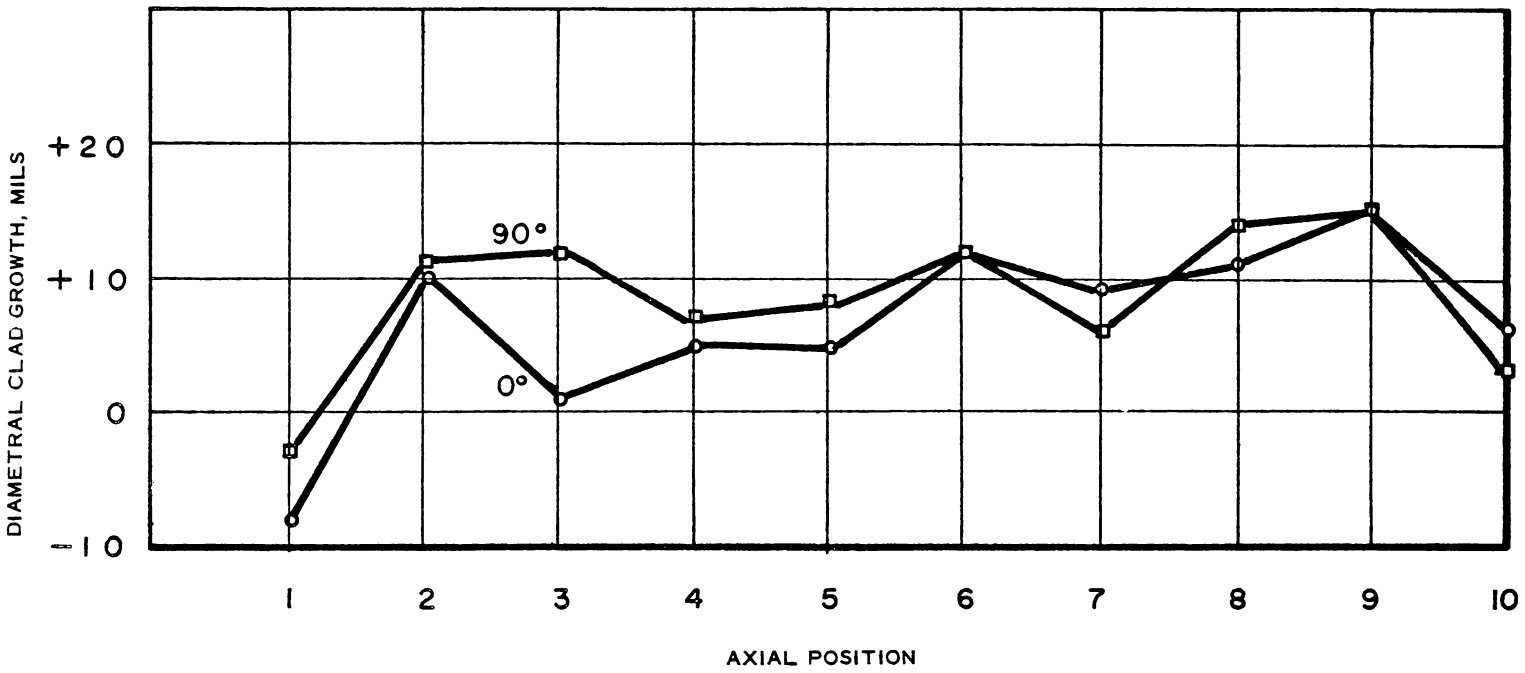

FIGURE 3.13
DIAMETER CHANGE VS. AXIAL POSITION ROD D-1
11 MILL WALL, SWAGED 6-20-61

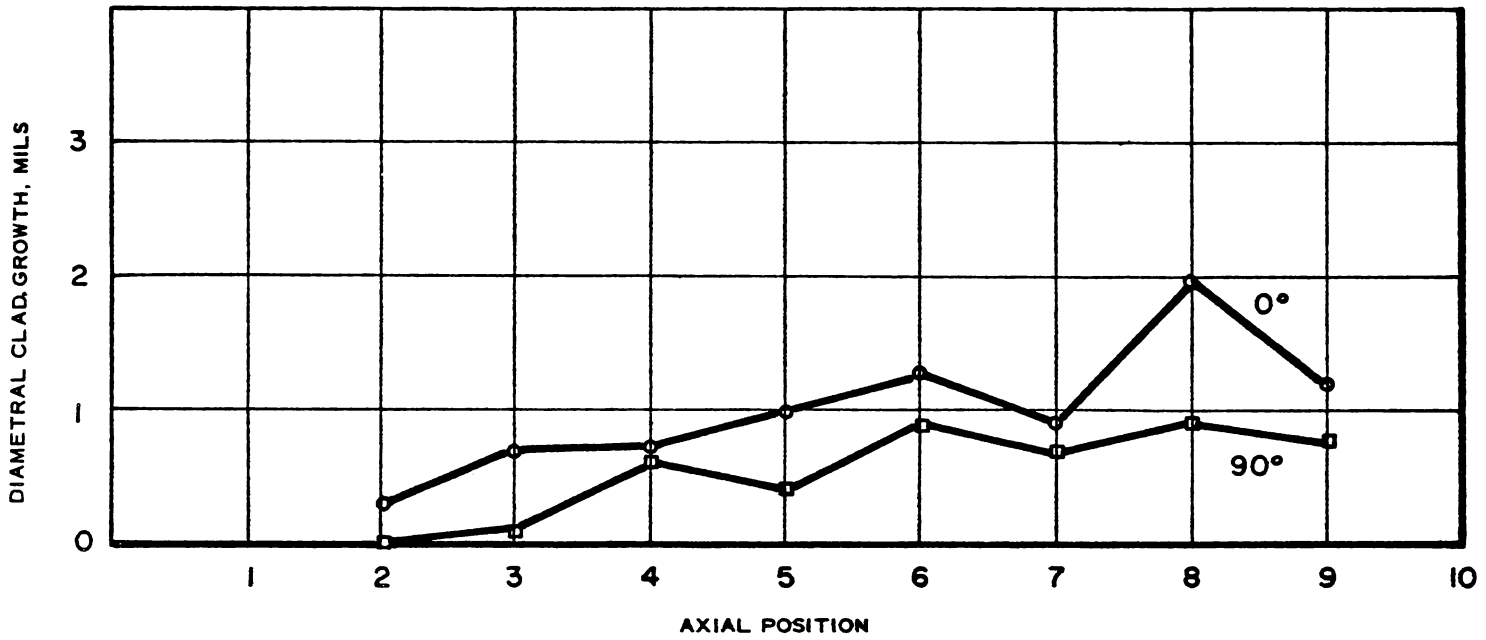

FIGURE 3.14
DIAMETER CHANGE VS. AXIAL POSITION ROD D-2,
11 MIL WALL, 4 MIL GAP 6-29-61

into pellets having density greater than 95% of theoretical.

Fabrication procedure included 6 cycles of evaluating and backfilling with helium while each capsule was at 800°F.

The six rods were irradiated in groups of three. The first group consisted of D-1, D-2 and D-3. The second group consisted of D-4, D-5 and D-6. Average heat fluxes were 390,000 Btu/hr-ft^2 for the first group and 280,000 Btu/hr-ft^2 for the second.

The swaged rods and the rods with the 4 mil gap had average diametral growths in the 0.4 mil to 1.0 mil range. No diametral growth was observed in the case of the two rods with the 9 mil gap. Figures 3.13 and 3.14 show the diameter increase as a function of axial position for D-1 and D-2.

Three of the four rods having diametral gaps had exhibited axial growth of 17 to 23 mils, while the other rod grew 2.5 mils axially. Post-irradiation length measurements were repeated several days later and all checked within 1.1 mil of the earlier post-irradiation measurements.

Two of the previously irradiated pellet-filled annular capsules were pressurized and re-irradiated with results similar to what had been obtained before. Clad diametral shrinkage occurred during pressurization, and diametral growth occurred during the second irradiation. These results give added support to the previous conclusion that clad plastic strain cycling can be expected for pellet-filled annular capsules using non-freestanding clad.

3.5 Process Tube Development

3.5.1 Zirconium Process Tube - CL-I Loop Tests

Two zircaloy-2 simulated process tubes with stainless steel thermal liners were exposed for 1000 hours each in the dynamic superheat loop. Test conditions were as follows:

Steam flow: 500 lbs/hr
Steam velocity: 110 ft/sec
Inlet temperature: 725°F
Outlet temperature: 695°F

The stainless steel liners differed in wall-thickness and design; one was a .028" wall tube with four small vent holes at top and bottom only, while the other had a .010" wall (with stiffening "ribs" at 2" intervals) and vent holes along its entire length. The insulation gap (space between liner O.D. and process tube I.D.) was .015" for the .028" wall liner and .030" for the .010" wall liner, but the same temperature drop occurred in both tests. It is believed that the steam turbulence caused by the greater number of vent holes in the .010" liner minimized the insulating effects of its associated wider thermal gap. The I.D. of both zircaloy-2 tubes gained weight which is comparable to those obtained from static autoclaving in the 500-600°F range:

Tube #3 (.010" wall liner): 10.5 mg/dm^2
Tube #4 (.028" wall liner): 11.9 mg/dm^2

Hydrogen pickup and/or redistribution was not measurable, but an increase in oxygen concentration (500 ppm) was noted in the upper portion of the tube. Physical tests on sections of the process tube (burst and tensile tests) showed results not appreciably different than those on the as-received material.

A detailed summation of this data will be presented in a topical report now being prepared.

3.5.2 Stainless Steel Annular Process Tube

At-temperature differential pressure tests on a configuration utilizing flame-sprayed oxide on the inner clad showed it to be unsatisfactory for pressures in the range of 250 psi. Two other low-cross-section clad strengthening mechanisms were investigated and one of them exhibited exceptional promise. This concept relies on thin (1/32" axial) stainless steel rings attached to the inner clad at 1 inch intervals. A small radial gap is left between the stiffening ring O.D. and the outer clad to allow vibratory compaction of Al_2O_3 powder in the annulus. The ring material adds the equivalent of about 2 mils SST wall thickness to the configuration. A 30" prototype of this design withstood an at-temperature (650°F) differential pressure of 250 psi for one half hour with no deformation of the tube I.D. dimensions. Fabrication details were as follows:

Outer clad: 1.650" O.D. x .007" wall 304 SST
Inner clad: 1.400" I.D. x .010" wall 304 SST
Annulus material: Al_2O_3 powder compacted to 77% of TD
Ring attachment: Induction brazing

The stiffening rings were brazed in place because this was the most convenient method, but work has been done on alternative attachment methods. Two of these ring-stiffened annular tubes will be tested in the ESH-2 fuel assembly.

TASK C - MATERIALS DEVELOPMENT

4.1 Materials Specification For Stainless Steel Superheat Cladding

A specification to order stainless steel tubing for nuclear superheat fuel element cladding has been written. This specification was written using knowledge of superheat fuel element cladding that is currently available. The specification will be revised as further information concerning superheat fuel cladding becomes available.

The following sub-tasks are being pursued to obtain further information of the physical and mechanical properties of stainless steel tubing for use as nuclear superheat fuel element cladding.

4.1.1 Acceptable Cladding Defect Levels

The effect of defects on the mechanical strength of stainless steel tubing, used for superheat fuel element cladding, is being determined. At the present, fifty Type 304 stainless steel tubing specimens have been burst at 1250°F. A standard ultimate hoop strength has been determined from the 1250°F burst tests of a statistical sample. A comparison of the ultimate hoop stress obtained from burst specimens having precision spark-eroded defects to 10%, 20%, and 30% of the wall thickness have produced the following results:

Wall Thickness Defect Level on O.D.	Failed At Defect	Percent Decrease In Ultimate Hoop Strength
30%	yes	30%
20%	yes no	4%
10%	no	0%

The preliminary test results above indicate tubing defects that are less than 10% of the wall thickness have no effect on the mechanical strength of the tubing and are therefore considered to be acceptable. However, further burst tests are being performed on specimens having 10% and 20%

defects to substantiate these preliminary data.

Records of non-destructive testing examinations of tubing used for fuel cladding at APED are being reviewed. Information concerning dimensional and ultrasonic/eddy current tolerance and defect level versus percent rejects will be made available within the next report period.

4.1.2 Materials Purchased

The stainless steel tubing tabulated below has been purchased for developing non-destructive testing techniques, establishing rejection criteria based on non-destructive and destructive tests, and for building prototype nuclear superheat fuel elements.

Material	Condition	Geometry	Amount
316L	annealed	0.750 x .028	54 feet
316L	annealed	0.750 x .016	48 feet
316L	annealed	0.625 x .028	54 feet
304L	annealed	0.750 x .016	54 feet
304L	annealed	0.750 x .028	54 feet
304L	annealed	0.625 x .028	42 feet
316L	annealed	1.250 x .016	50 feet
316	annealed	1.250 x .028	50 feet
304	annealed	1.250 x .028	53 feet
304	annealed	0.750 x .016	100 feet
304	annealed	1.250 x .016	190 feet
304	annealed	1.250 x .028	120 feet
304	annealed	0.750 x .010	72 feet
316	annealed	0.750 x .035	50 feet
316L	annealed	0.750 x .049	50 feet
347	annealed	0.750 x .028	50 feet
304	annealed	0.750 x .016	50 feet
304	annealed	0.625 x .028	50 feet
304	annealed	0.750 x .028	50 feet

4.1.3 Superheat Autoclave

The superheat pressure vessel furnace has been rebuilt and packed with microquartz insulation by the furnace manufacturer. The furnace has been re-installed in the pressure vessel and thermal cycling of prototype nuclear superheat fuel elements under pressure has been resumed.

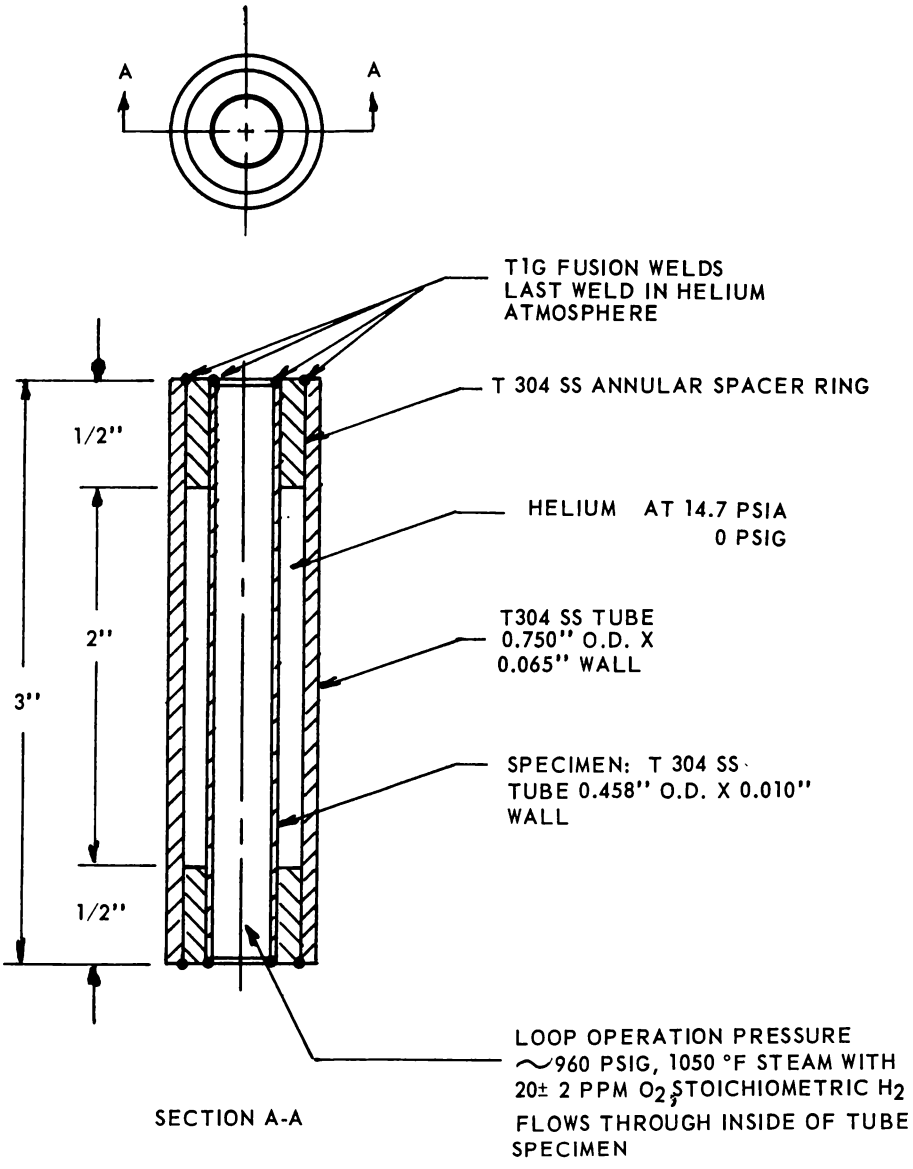

FIGURE 4.1
TUBING STRESS FIXTURE

4.1.4 Stress Corrosion Susceptibility, Under Dynamic Conditions (Out of Reactor Superheat Loop)

A preliminary investigation of the stress corrosion susceptibility of annealed and coldworked Type 304 stainless steel tubing in oxygen and hydrogen bearing, 1050°F steam has been initiated and is in progress. A description of the investigation, together with the results of the past 1,000 hour exposure examination follows:

4.1.4.1 Test Materials

The test specimens were prepared from tubing having the following geometry, chemical composition, and coldwork conditions:

AISI Type 304 stainless steel tubing, 3" long by 0.458" O.D. by 0.010" wall thickness.

Chemical Composition

18.26% Cr	0.011% S
9.11% Ni	0.016% P
1.11% Mn	0.05% C
0.50% Si	Balance Fe

Number of Specimens	Condition	0.2% Yield Strength
4	Annealed & pickled	40,000 psi
4	10% cold work	92,000 psi
4	20% cold work	117,000 psi

4.1.4.2 Applied Stress

A constant stress was applied to the tubing specimens by using the stress fixture illustrated and noted in Figure 4.1. For this investigation, the stress was equal to 100%, 90%, and 80% of the applied stress in the coldworked specimens, respectively. The

1,000 hour examination showed the annealed specimen had yielded slightly at the junction of the tubing specimen with the annular support ring, thereby illustrating the levels of stress that can be imposed by this stress fixture.

With reference to Figure 4.1, the corrosion loop operating pressure imposes a constant maximum stress on the tubing specimen which is expressed by:

$$c = P \frac{R}{t}$$

where c is the circumferential stress on the tube specimens.

P equals 960 psig in the section used.
P is the corrosion loop operating pressure.

R is the mean radius of the tube specimen.

t is the tube wall thickness.

An analytical stress analysis in conjunction with experimental residual stress measurements showed the stress computed from the above expression to be the maximum principal stress imposed on the tubing specimen. The stress on the specimens was computed to be 21,000 psi tension.

4.1.4.3 Stress Corrosion Environment

The corrosion environment of the specimen was maintained at:

1050°F superheated steam with
17-18 ppm oxygen
2.5 ppm hydrogen
from water having less than 0.03 ppm chloride ion.

The above corrosion environment was maintained in the superheat section of the corrosion loop by methods and techniques developed at APED. The test conditions are now being modified to purposely increase the chloride concentration

to 1.5 ppm in CL-1 loop. This is being done to examine extreme or limiting cases of chloride stress corrosion cracking in superheat media, and to duplicate the conditions that lead to SH-4B fuel element failure in VBWR.

4.1.4.4 Results

A thorough examination of the stress corrosion specimens after a 1,000 hour exposure period showed no indications of stress corrosion failures. One specimen each of the annealed, 10% and 20% coldworked specimens were sectioned for microscopic examination. The remaining specimens were returned to the corrosion loop to obtain longer exposure time. A discussion of the microstructural examination follows:

Figures 4.2, 4.4 and 4.6 show the scale formed on the exposed surface of the annealed, 10% and 20% coldworked specimens, respectively. The specimen surfaces have a "wrinkled" appearance in the microphotographs taken at a magnification of 15X. The size of the areas delineated by the wrinkles appear to be in direct proportion to the grain size of the specimens, thereby indicating preferential corrosion has taken place. Figures 4.3, 4.5 and 4.7 are micrographs of the specimen cross sections paralleled to the maximum principal stress. The microstructure shows extensive carbide precipitation at the grain and twin boundaries, and also at slip bands in the coldworked specimens. In some crystals, the corrosive attack has produced scale up to 0.001" in thickness in 1,000 hours of exposure. The unetched cross section of the specimens parallel to the maximum principal stress are shown in Figures 4.8, 4.9, and 4.10. A scale has been imposed on

FIGURE 4.2

SURFACE SCALE FORMED ON ANNEALED TYPE 304 STAINLESS STEEL SPECIMEN, X 15

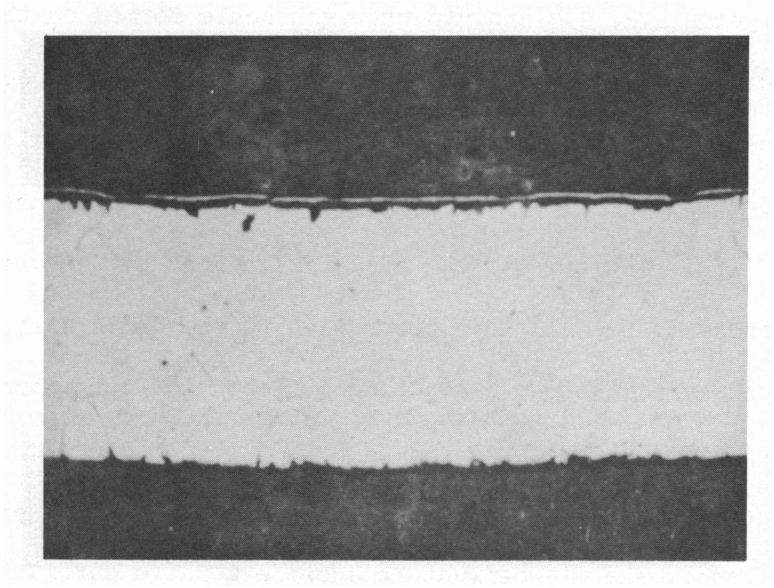

FIGURE 4.3

TRANSVERSE SECTION OF ANNEALED SPECIMEN PARALLEL TO PRINCIPAL STRESS, X 150 10% OXALIC ELECTROLYTIC ETCH. NOTE PHASE FORMED ON EXPOSED SURFACE.

FIGURE 4.4

SURFACE SCALE FORMED ON 10% COLD WORKED, TYPE 304 STAINLESS STEEL, SPECIMEN X 15

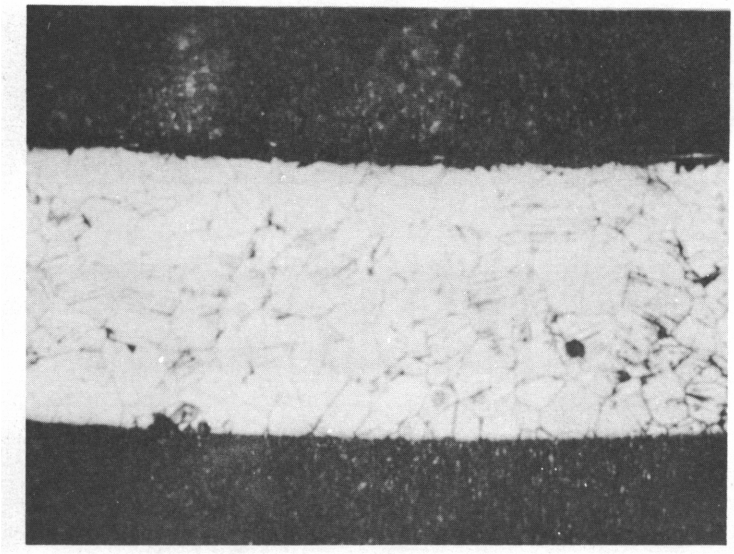

FIGURE 4.5

TRANSVERSE SECTION OF 10% COLD WORKED SPECIMEN PARALLEL TO PRINCIPAL STRESS, X 150 10% OXALIC ELECTROLYTIC ETCH. NOTE GRAINS SHOWING PREFERENTIAL ATTACK

FIGURE 4.6
SURFACE SCALE FORMED ON 20% COLD WORKED, TYPE 304 STAINLESS STEEL SPECIMEN, X 15

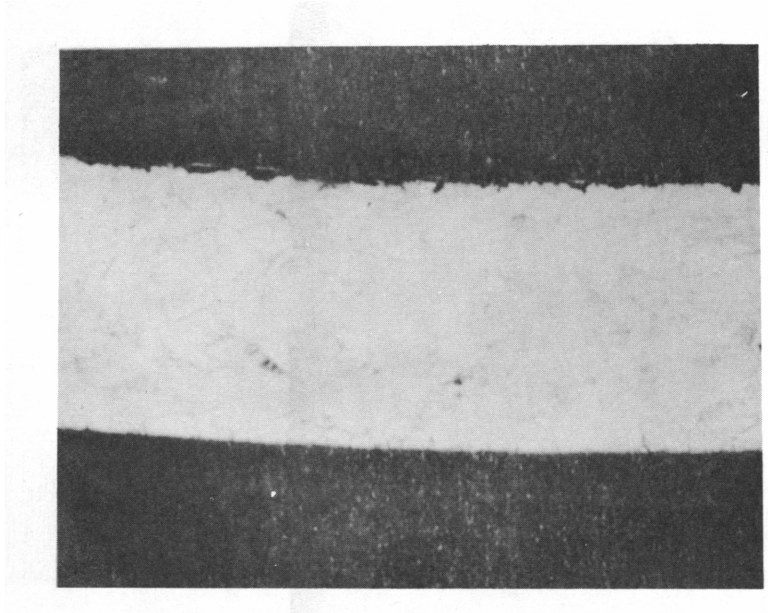

FIGURE 4.7
TRANSVERSE SECTION OF 20% COLD WORKED SPECIMEN PARALLEL TO PRINCIPAL STRESS, X 150. 10% OXALIC ELECTROLYTIC ETCH. NOTE GRAINS SHOWING PREFERENTIAL ATTACK AND PHASE FORMED ABOVE THEM

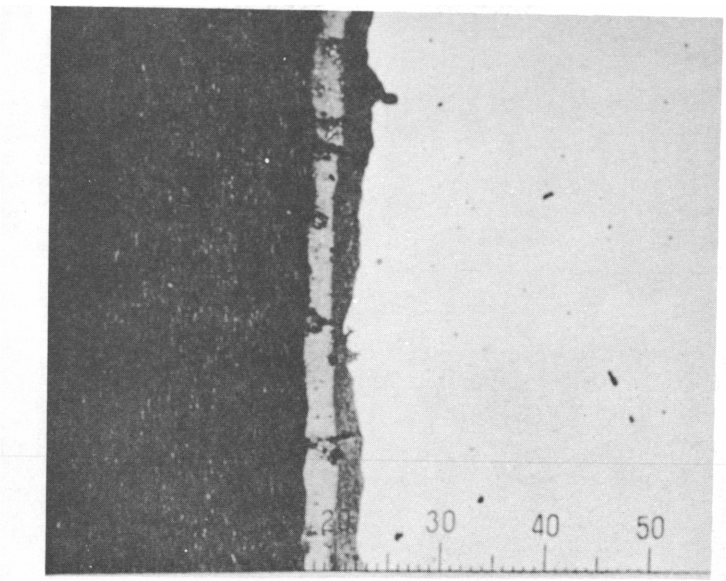

FIGURE 4.8
BAKELITE/SCALE/SPECIMEN TRANSVERSE SECTION, SHOWING SCALE FORMED ON ANNEALED TYPE 304 STAINLESS STEEL SPECIMEN. UNETCHED, X 400,0.0001 INCH PER DIV.

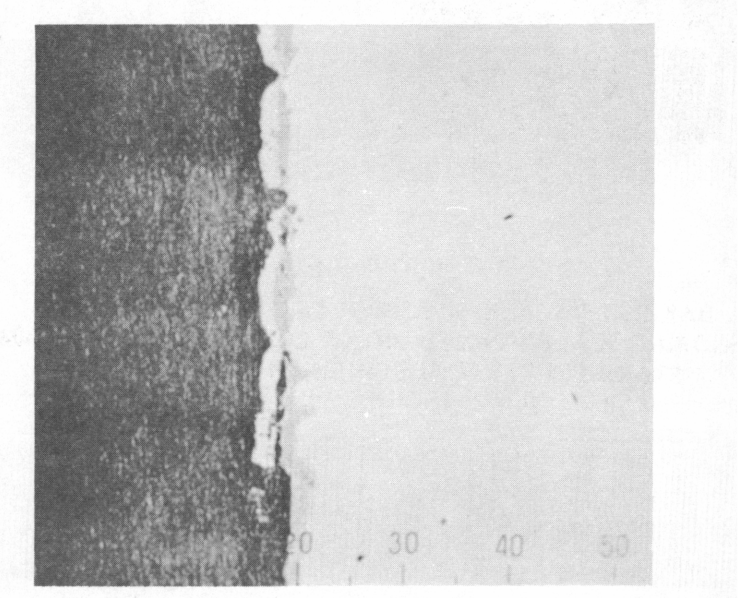

FIGURE 4.9
BAKELITE/SCALE/SPECIMEN TRANSVERSE SECTION SHOWING SCALE FORMED ON 10% COLD WORKED TYPE 304 STAINLESS STEEL SPECIMEN, X 400, 0.0001 INCH PER DIVISION UNETCHED

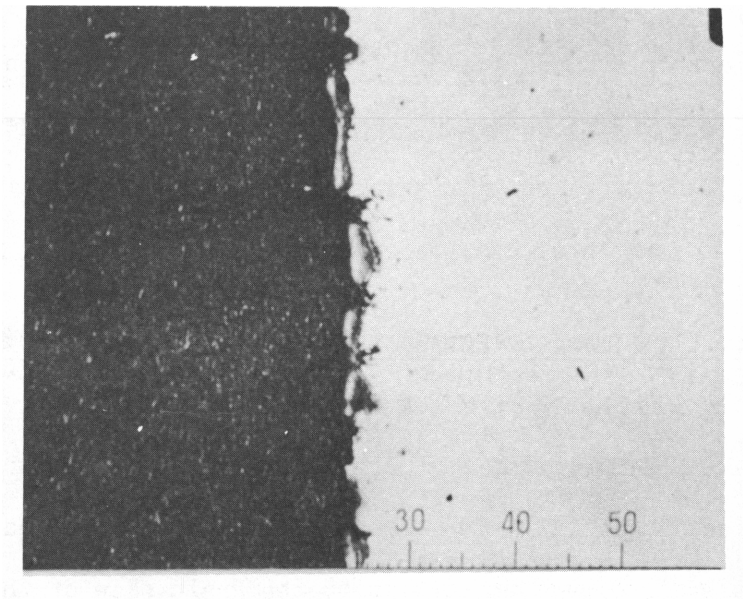

FIGURE 4.10

BAKELITE/SCALE/SPECIMEN TRANSVERSE SECTION SHOWING SCALE FORMED ON 20% COLDWORKED TYPE 304 STAINLESS STEEL SPECIMEN, UNETCHED, X 400, 0.0001 INCH PER DIVISION

to 1.5 ppm in CL-1 loop. This is being done to examine extreme or limiting cases of chloride stress corrosion cracking in superheat media and to duplicate the conditions that lead to SH-4B fuel element failure in VBWR.

4.1.4.4 Results

A thorough examination of the stress corrosion specimens after a 1,000 hour exposure period showed no indications of stress corrosion failures. One specimen each of the annealed, 10% and 20% coldworked specimens were returned to the corrosion loop to obtain longer exposure time. A discussion of the microstructural examination follows:

Figures 4.2, 4.4, and 4.6 show the scale formed on the exposed surface of the annealed, 10% and 20% coldworked specimens, respectively. The specimen surfaces have a "wrinkled" appearance in the macrophotographs taken at a magnification of 15X. The size of the areas delineated by the wrinkles appear to be in direct proportion to the grain size of the specimens, thereby indicating preferential corrosion has taken place. Figures 4.3, 4.5, and 4.7 are micrographs of the specimen cross sections paralleled to the maximum principal stress. The microstructure shows extensive carbide precipitation at the grain and twin boundaries, and also at slip bands in the coldworked specimens. In some crystals, the corrosive attach has produced scale up to 0.001" in thickness in 1,000 hours of exposure. The unetched cross section of the specimens parallel to the maximum principal stress are shown in Figures 4.8, 4.9, and 4.10. A scale has been imposed

on the micrograph negative to show the depth of the two phase corrosion product. The micrographs were taken of the specimens in the unetched condition to show that the scale formed was composed of two phases. The outer phase of the scale has a metallic luster in contrast to the intermediate phase which has a non-metallic, mottled, green-blue hue typical of the oxides of chrome and iron.

Methods of analysis of the scale are being reviewed in order to make identification of the major corrosion product formed.

4.1.4.5 Summary of Work on Stress Corrosion Investigation

No indications of stress corrosion cracking failures have been observed after 1,000 hours of exposure of stressed Type 304 stainless steel tubing in the annealed, 10% and 20% coldworked condition.

However, the general corrosion rate is greater than observed for standard corrosion coupons in the same environment. Perhaps the increased corrosion rate may be due to the specimens being in a relatively high state of tensile stress. The specimens will be thoroughly examined at the 1700 hour exposure level.

The chemistry conditions in CL-1 loop are now being revised to increase the chloride content in the water, to simulate secure reactor chemistry conditions similar to those that existed in VBWR when SH-4B assembly was irradiated and which resulted in a clad failure.

4.1.5 Ultrasonic Techniques for Tubing Inspection

A non-destructive ultrasonic technique has been developed which permits tubing inspections to detect cracks caused by stress corrosion. The objective is to detect and define cracks that may be as small as 10% of the tube wall thickness. This technique may be perfected to the point where it can be used in in-cell (Radioactive Materials Laboratory) inspections during interim fuel element observations.

Stress corrosion cracks of varying magnitude were made in Type 304 stainless steel tubing. These samples were then ultrasonically tested to determine the depth of the cracks. Records were obtained from an oscillograph recorder for accurate measurement and for a permanent record.

Cladding samples (Type 304 SS, 0.458" O.D. x 0.010" wall, 6" lengths of varying coldwork levels - 50%, 40%, 30%, 20% and 10%) were exposed to a boiling solution of saturated $MgCl_2$ to obtain stress corrosion cracks. To determine the duration of boiling necessary, 15 samples (3/4" lengths) were boiled and observed until cracking was seen to follow a pattern - with the solution boiling at 287°F ($\pm$ 2°) cracks were first noticed in the 50% cold work material after 15 min. (40%, after 30 min.; 30%, 60 min.; 20%, 120 min.; 10%, 160 min.). The 6" length tubes were then cracked according to the pattern; the cracks were first observed by use of a 50X microscope and then investigated by ultrasonic methods. Calibration is now in progress to obtain a relationship between size of cracks and oscilloscope signal. Using a standard discontinuity, the depth of which was shown to be 1.6 mils (measured with the 50X microscope), depths of cracks (indicated by deflections of the recorder) were recorded between 37% and 430% of the standard.

4.2 Strain Cycle Tests

4.2.1 Summary

Difficulties in procurement of equipment for the in-reactor strain cycle tests have forced a delay in this program. An alternate equipment design for the in-reactor apparatus was completed June 30. The alternate mechanical cycling concept is based on the use of mandrel, with heat supplied from gamma heating in the reactor.

Sealol Corporation, Connecticut, bellows subcontractor, has encountered difficulty in the welding process. A prototype bellows was completed by Sealol, but under testing against specifications provided by General Electric, the bellows failed. Test included static pressure of 2250 psig and cycling at 1500 psig. Static test was successful but failure occurred at 1300 psig on the cycling portion.

A successful weld has been made on the outer diameter edges of the Inconel "X" plates making up the bellows, but welding at the inner diameter of the plates has not been satisfactory. It is reported that aluminum oxide at the interface results in a weak spot in the weld. Sealol is continuing effort to develop a successful technique.

Work has continued on the two control panels which are now 75% complete. Panels include temperature measuring devices, heater power control measurements and pressurization system.

It is believed that most of the materials on hand or on order will be useable on the alternate scheme, and that the control panel will readily be adapted to the new capsule design.

Concept design for the mandrel activating device was completed in June. Detail design on the new capsule, which initially will not include a heater, is 10% complete. Detail design of the new bench test apparatus is 100% complete. The alternate design will allow a specimen outside diameter of 1-1/4".

5.0 TASK D - EXPERIMENTAL PHYSICS

5.1 Summary

All experimental measurements (Phase I and II of the program) are now complete. Data reduction and the final detailed report covering this work will be completed later in the year. Phase I of the program which was completed last quarter included measurements of critical size, $\left(\frac{\partial \rho}{\partial H}\right)$, temperature coefficients, void coefficients, and flux distributions. Phase II which was completed this quarter included measurements of thermal utilization and conversion ratio.

5.2 Phase II Experimental Results

Thermal utilization has been measured for four superheat fuel configurations utilizing copper foils. Foils were placed within fuel element, in each water region, and on both sides of each SS-304 tube. The measured thermal utilizations are given in Table 5.1.

Table 5.1

Fuel Configuration		
Element Pitch Inches	Flooding	Measured Thermal Utilization
1.800	V-V	0.763 ± 0.015
2.000	V-V	0.716 ± 0.015
1.800	F-F	0.714 ± 0.015
2.000	F-F	0.667 ± 0.015

The conversion ratio has also been measured in these four fuel configurations. A new method for measuring the conversion ratio was used[1]. The conversion ratio C is obtained from the parameter C^1 which is experimentally determined.

$$C^1 = N_{n_p}/N_5 = C\,(1 + \alpha)$$

(1) H. M. Antunez "Method for Measurement of Conversion Ratio (And Resonance Escape Probability)." Trans. Am. Nuclear Soc. 4 No. 2 (1961)

Where N_{n_p} is the number of N_p^{239} atoms produced, and N is the number of U^{235} fission which occurred in an irradiated fuel sample; and where $(1 + \alpha)$ is the ratio of the volume and energy weighted average of the absorption cross section of U^{235} in the fuel sample. C^1 measured by counting solutions of irradiated fuel samples. The experimental results are given in Table 5.2.

Table 5.2

Fuel Configuration

Element Pitch Inches	Flooding	Measured C^1	Proposed $(1 + \alpha)$	C
1.800	V-V	0.399 ± 0.013*	1.213	0.329
2.000	V-V	0.361 ± 0.007	1.204	0.300
1.800	F-F	0.332 ± 0.005	1.204	0.276
2.000	F-F	0.309 ± 0.004	1.199	0.257

* 95 per cent confidence limit

5.3 Comparison of Experimental Measurements to Theory

As reported last quarter, a comparison of the experimental measurements and the predictions based on a standard analytic model has indicated significant discrepancies. The prime source of these discrepancies has been postulated to be the omission of the spatial variation in thermal spectrum in the calculations. Its presence would be expected to cause appreciable error in thermal utilization calculations based on a zero-dimensional spectrum when several mean free paths of water are present between fuel surfaces. Both experimental and analytic confirmation of this postulation has now been obtained.

The standard analytic model used to determine the relative neutron capture rate in the fuel and moderator (thermal utilization) consists of the Wilkins zero-dimensional spectrum weighted cross sections for the smeared fuel cell media and P-3 flux weighting of the cross sections for the geometric flux

depression. This technique has demonstrated reasonable accuracy ($\pm$ 1/2% $\Delta f/f$) for typical boiling water lattices. However, one would expect that when the fuel cell dimensions increase to several mean free paths that a significant spectral shift would occur between the moderator and fuel regions. In comparison, the superheat lattices have over 4 λ_s of water between fuel surfaces when the fuel element is flooded, while a typical boiling water reactor lattice (water to fuel volume ratio of 2) has about 1.2 λ_s of water between fuel surfaces. The effect of the spectral shift is to harden the fuel spectrum and to soften the moderator spectrum relative to the zero-dimensional spectrum calculated for the fuel cell. This effect will therefore lower the magnitude of the calculated thermal utilization for any given case.

The spectrum shift has been determined analytically through use of the SLO P-1 code[2]. SLO P-1 is a multi-thermal group code which allows scattering from each group to all other groups and solves the neutron transport equation by the P-1 approximation. The SLO P-1 calculations were performed for each of the cases for which thermal utilization was measured. Thermal utilization has been measured for uniform arrays of superheat fuel at the element pitches of 1.800 and 2.000 inches for both the flooded and unflooded configurations. These measurements were made with 1/v foil activation. Table 5.3 compares the analytic and measured thermal utilization.

Although the SLO P-1 code is very useful for demonstrating the spectrum shift and for obtaining a quantitative prediction of its magnitude, its use in routine design calculations is greatly limited by the cost per problem. A typical SLO P-1 problem required 45 minutes of 704 computation time. For

(2) H. Bohl, E. M. Gelbard, P. Buerger, and G. Culpepper, "SLO P-1 - A Thermal Multigroup Program for the IBM-704" WAPD-TM-188, (October, 1960).

Table 5.3

Thermal Utilization in Superheat Lattices

Fuel Configuration			Theoretical f		
Element Pitch (inches)	Flooding	Measured f	SLO P-1	Semi-Empirical "Patch"	Zero-Dimensional Spectrum
1.800	V-V	0.763 ± .015	0.760	0.759	0.769
2.000	V-V	0.716 ± .015	0.713	0.705	0.731
1.800	F-F	0.714 ± .015	0.717	0.719	0.737
2.000	F-F	0.667 ± .015	0.671	0.666	0.696

this reason a semi-empirical "patch" has been developed which gives reasonable agreement with the experiments and with the more exact SLO P-1 calculation. The analytic values listed in Table 5.3 under the heading "Patch" were determined by this technique.

The semi-empirical technique involved the following steps. An amount of water within λ_s of the outer fuel surface was included with the fuel, clad, and process tube to determine a zero-dimensional spectrum for these materials. Then the water beyond λ_s was introduced with partially "softened" parameters. The percent of softening was determined by the following relation:

$$\text{Percent Softening} = 100\left\{1 - \left[\exp(-C_o\, t/\lambda_s)\right]\right\}$$

where: C_o = empirical constant $\cong$ 1.1

t = thickness of water beyond λ_s from the outer fuel surface

This relation has reasonable limits. As a large amount of water is added, softening becomes complete and for small amounts of water there is very little softening. The completely soft parameters are determined for an equilibrium water spectrum at the temperature of the moderator. The constant

C_o was initially chosen to yield reactivity and coefficient agreement for the Phase I measurements at 1.1 and it now appears that this was an excellent choice for this fuel element since the "Patch" values agree well with experiment and the more exact SLO P-1 calculations. It must be emphasized that this semi-empirical technique is not necessarily valid outside the range for which SLO P-1 calculations and experiments have been used to check it out and that additional SLO P-1 problems would be required for another fuel geometry.

A few of the Phase I parameters have been recalculated utilizing the patch described above. Table 5.4 indicates the improvement in the experiment-theory correlation.

Table 5.4

Experiment-Theory Comparisons

Parameter	Case	Experiment	Theory	
			Old Model	Revised Model
Multiplication	1.800 inch Pitch			
	Unflooded	1.000	1.022	1.001
	Flooded	1.000	1.037	1.000
	2.000 inch Pitch			
	Flooded	1.000	1.050	0.999
Temperature Coefficient	1.800 inch Pitch			
	Unflooded	$+3 \times 10^{-5}$ $\Delta k/^oC$	-1×10^{-5} $\Delta k/^oC$	$+4 \times 10^{-5}$ $\Delta k/^oC$
Void Coefficient	1.800 inch Pitch			
	Unflooded	-1.2×10^{-3} $\Delta k/\%$ Void	-2.7×10^{-3} $\Delta k/\%$ Void	-1.9×10^{-3} $\Delta k/\%$ Void

It can be seen that the coefficients as well as the over-all reactivity are

now in excellent agreement with experiment.

In addition to the measurements and more exact analysis of thermal utilization, the resonance capture by U-238 has received careful attention. Monte Carlo calculations utilizing Richtmyer's NYU-REP[3] code have been performed for three configurations of the superheat fuel. The resulting resonance escape probabilities are compared to the predictions based on the standard technique (Hellstrand's $\sqrt{S/M}$ dependence of the effective resonance integral[4]) in Table 5.5

Table 5.5

Case		Resonance Escape	
Element Pitch (inches)	Flooding	Monte Carlo (REP)	Hellstrand
1.800	Unflooded	0.862 ± .002*	0.863
1.800	Flooded	0.894 ± .002	0.891
2.000	Flooded	0.921 ± .002	0.922

* The probable error due to Monte Carlo sampling only. The uncertainty in the unresolved resonance contribution will increase the over-all uncertainty to as much as ± .01 in resonance escape.

It can be seen that the agreement between Monte Carlo and Hellstrand's technique is excellent in all cases. Although it is recognized that uncertainties in the unresolved resonance contribution may introduce as much as

(3) Richtmyer, R. D., et al, "The Monte Carlo Calculation of Resonance Capture in Reactor Lattices" Proc. of the Second Geneva Conference, United Nations, New York, Vol. 8, (1958)

(4) Hellstrand, E., "Resonance Integral for U Metal Rods" J. Applied Physics, 28, 1493, (1957)

1% uncertainty in the calculated resonance escape, it is now felt that resonance escape is not a major cause of uncertainty in these superheat lattices.

In addition to the Monte Carlo support of the resonance escape as calculated by Hellstrand's $\sqrt{S/M}$ dependence of the effective resonance integral, experimental conversion ratio measurements made at the Vallecitos Critical Experiment Facility indicate that the deviation between experiment and theory is quite small for the four cases investigated. Three analytic techniques were used to calculate the conversion ratio. The first utilized the standard BWR calculational scheme (MUFT-HELLSTRAND-WILKINS). The second used the Monte Carlo results for U-238 resonance capture (MUFT-NYU-REP-WILKINS) and the third included the thermal spectrum shift as determined by SLO P-1 (MUFT-NYU-REP-SLO P-1). Table 5.6 provides a comparison of the measured conversion ratio to the predictions of the alternate calculational schemes.

Table 5.6

Conversion Ratio Comparison

Fuel Configuration			Calculated Conversion Ratio		
Element Pitch	Flooding	Measured CR*	Scheme 1	Scheme 2	Scheme 3
1.80	Unflooded	.329 ± .011	0.341	0.343	0.347
2.00	Unflooded	.276 ± .004	0.269	0.271	0.275
1.80	Flooded	.300 ± .006	0.303	0.294	0.310
2.00	Flooded	.257 ± .004	0.259	0.256	0.265

* 95 per cent confidence limit

Scheme 1 = MUFT-HELLSTRAND-WILKINS

2 = MUFT-(NYU-REP)-WILKINS

3 = MUFT-(NYU-REP)-(SLO P-1)

It can be seen that all three schemes give good agreement with the measured conversion ratio. The good agreement between schemes 1 and 2 lends support to Hellstrand's resonance integral formulation. The agreement between schemes 2 and 3 is due to the very weak dependence of the conversion ratio on thermal spectrum shifts rather than to the absence of such a shift.

With the agreement between the more exact calculations and experiments for thermal utilization and conversion ratio, it is felt that the physics of uniform arrays of annular superheat elements is on a firm base. This conclusion is further substantiated by the agreement between the modified predictions of criticality and reactivity coefficients and the experimental determinations for uniform arrays.

5.4 VESR Preliminary Critical

Pre-analysis of the VESR Preliminary Critical measurements has been completed. Parameters included in the pre-analysis are critical size, multiplication of the full core for various controls distribution, flooding effects, temperature effects, void coefficients, fuel element worth and power distributions.

Initial criticality was attained on June 28 with a core loading of 23 1/3 bundles at 79°C. The predicted loading for a fully reflected core of unflooded elements at 20°C was between 19 and 20 bundles. Extrapolation of the measured critical size to 20°C yields an approximate value of 27 bundles.

This size would indicate a reactivity over-prediction of 2% $\Delta k/k$. However, a numerical error in the value of ν for U-235 used has been determined which lowers the discrepancy to 1% $\Delta k/k$. Preliminary temperature and void coefficient measurements indicate excellent agreement with the predicted values.

6.0 TASK E - COOLANT CHEMISTRY

6.1 Out-Of-Pile Superheated Steam Corrosion Loop

6.1.1 Materials Evaluation

Exposures for 500-hr, 1000-hr and 2465-hr under dynamic heat transfer conditions with controlled superheat environment have been completed on Type 304 stainless steel. The following corrosion data are available to date:

Calculated Metal Temperature °F	Run No.	Time of Test, hrs.	Total Corrosion mg/dm^2	mils	Metal-to-System Loss, mg/dm^2
900 - 1100	41-42*	950	143	0.07	9
	43-45	2465	103	0.05	-83*
1100 - 1300	41-42**	950	452	0.23	120
	46	1000	284	0.14	87
	43-45	2465	354	0.18	74

* Represents a weight gain from deposition
** Reported in previous quarterly report - GEAP-3724

A comparison of run 41-42 and run 46, both approximately 1000-hour exposures, indicated a large difference in corrosion rates. It was established that nine interruptions occurred during 950 hours of exposure in runs 41-42 as compared to only two interruptions during the 1000 hours of run 46. Although these data indicate a definite sensitivity of corrosion rate to shutdowns and startups during exposure, this sensitivity may exist primarily during the time before the scale has reached equilibrium with the environment.

The specimen with a temperature range of 1100°F - 1300°F has a .002" structure "layer" associated with the decarburization at the 1300° end after 1000 hours and .004" to .005" after 2465 hours of exposure. The chemical composition of this layer is being determined.

The corrosion and metallurgical evaluations will be completed and a topical report issued during the next Quarter.

6.1.2 Environment Evaluation

This study of recombination across the superheat heaters as a function of temperature was completed. Both the thallium columns and the gas stripper and gas chromatograph system were utilized for the test.

The data are being evaluated and will be included in a topical report.

6.2 SADE In-Pile Evaluations

6.2.1 Introduction

Irradiation of SH-4B extended intermittently from January 15 to May 24. Chemical measurements during the period were minimal because of interference from reactor operational problems, but were adequate to provide considerable information relative to the development of the defect.

6.2.2 Fission Product Release

Samples of steam entering and leaving the SADE loop during the week of January 15 and on May 5 indicated SH-4B was not releasing significant quantities of iodine or fission gases at those times. On May 24, samples of condensate from entering and leaving steam showed gross quantities of radioiodine apparently from SH-4B. Further measurements of I-132 while the element was in the VBWR pool confirmed the existence of a cladding defect.

The development of the defect cannot be completely reconstructed because of the absence of intervening SADE samples, difficulties with the SADE off-gas monitor, and the presence of other intentionally defected fuel in the VBWR core. The best evidence of the fuel's behavior between May 5 and May 24 is provided by the reactor off-gas

and stack radiation monitors. Data from these sources are given in Figures 6.1 to 6.4. The stack monitor senses fission gases from all sources in the VBWR, including the SADE fuel, whereas the off-gas monitor senses fission gases from all sources except SADE. The off-gas monitor also detects short-lived gases which decay prior to reaching the stack monitor.

In Figure 6.1, spikes in the radiation readings during power changes are characteristic of operation with defective fuel and occur throughout the period because of the other defected fuel in the VBWR core. During the period May 7 to 10, observation of fission gas release was obscured by the presence of unusual air-borne Na-24 activity. The problem was eliminated when demineralizer resins were replaced on May 9 and 10. Spikes on the stack monitor during power changes and the general radiation level during steady power operation appear to be higher during the period May 11 to 24 than before May 6 and after May 25. These observations are interpreted as indicating release of fission gases from SH-4B during the May 11 to 24 period. The severity of the spiking on May 24 as compared to that on preceeding days indicates a significant change in the rate of release at that time. The reactor did not operate from May 14 to May 17.

The release rate of six major fission gases from the VBWR during steady power operation on May 19 to 22 is estimated at about 1000 c/sec on the basis of the stack monitor measurements. A significant portion of this release is probably attributable to SH-4B. On May 24 the initial release rate from SH-4B was apparently several thousand c/sec while the reactor was operating at about 150 KW(t). With continued operation, the release rate decreased and the reactor power was raised as high as 1.5 MW(t) before being shut down. A transition from air cooling to steam cooling

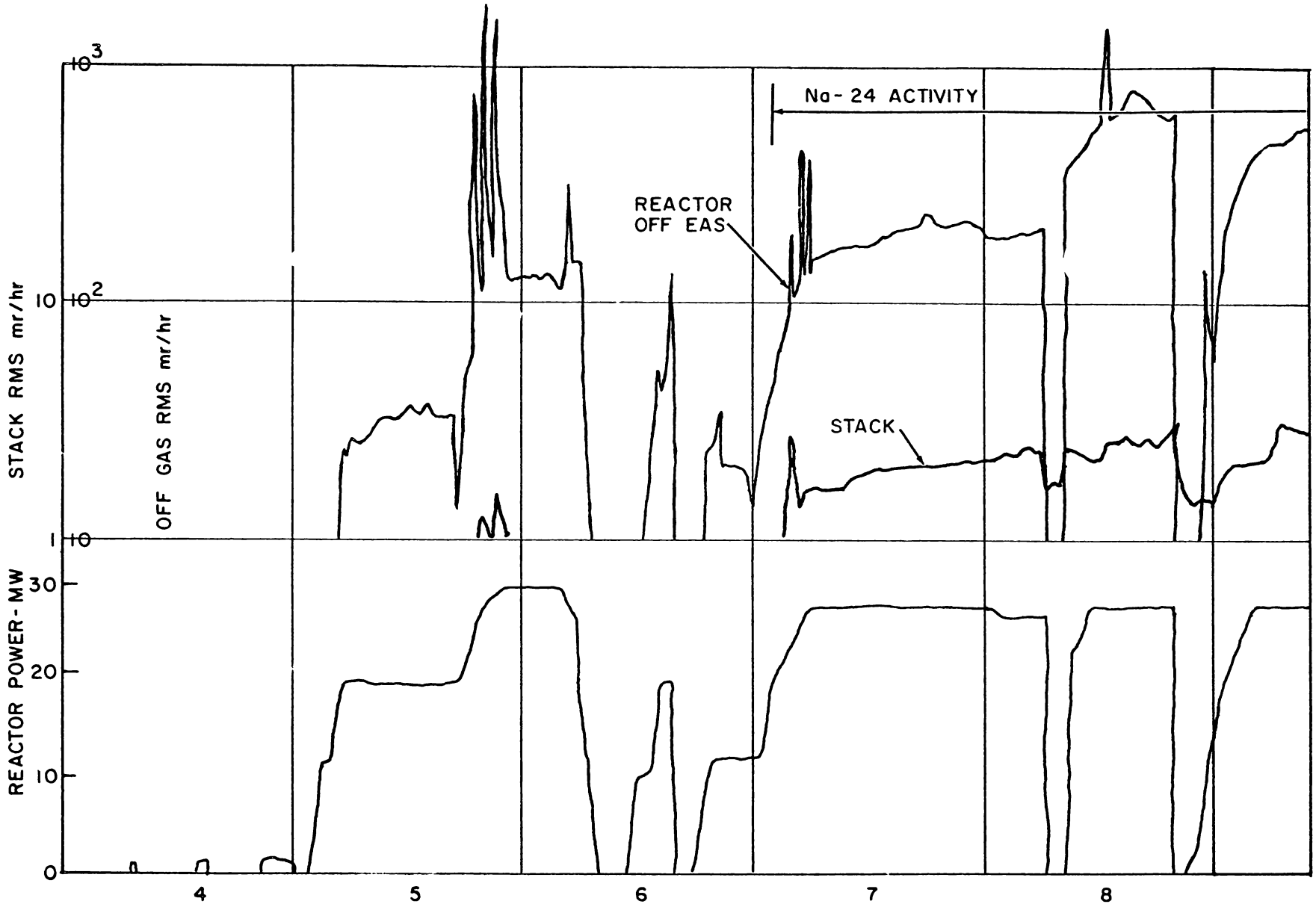
STACK RMS mr/hr
OFF GAS RMS mr/hr
10^3
10^2
10
1
Na-24 ACTIVITY
REACTOR OFF EAS
STACK
REACTOR POWER-MW
30
20
10
0
4
5
6
7
8
MAY 1961

FIGURE 6.1

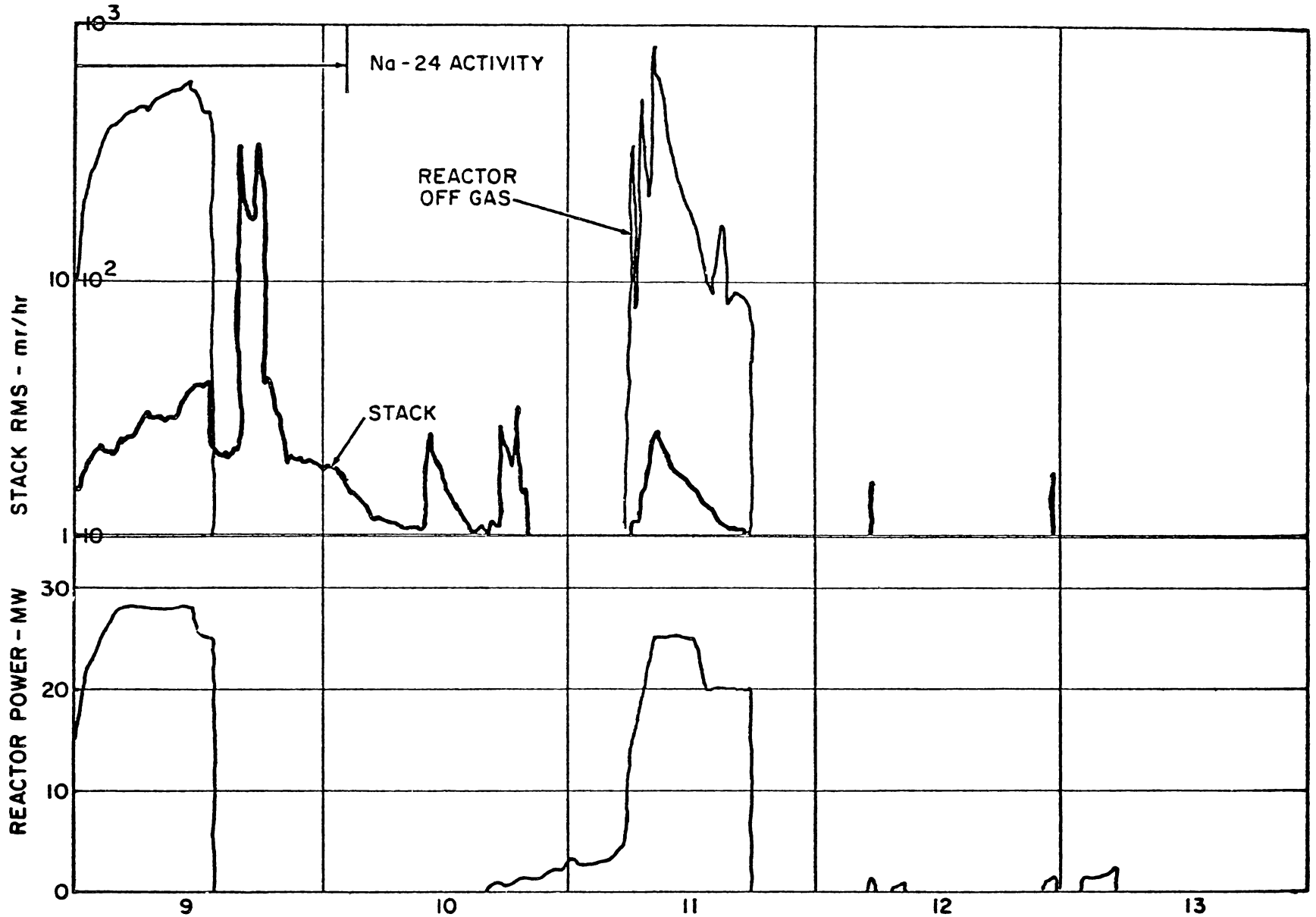
10^3
Na - 24 ACTIVITY
REACTOR
OFF GAS
10^2
10
STACK
1
STACK RMS - mr/hr
30
20
10
0
REACTOR POWER - MW
9
10
11
12
13
MAY 1961

FIGURE 6.2

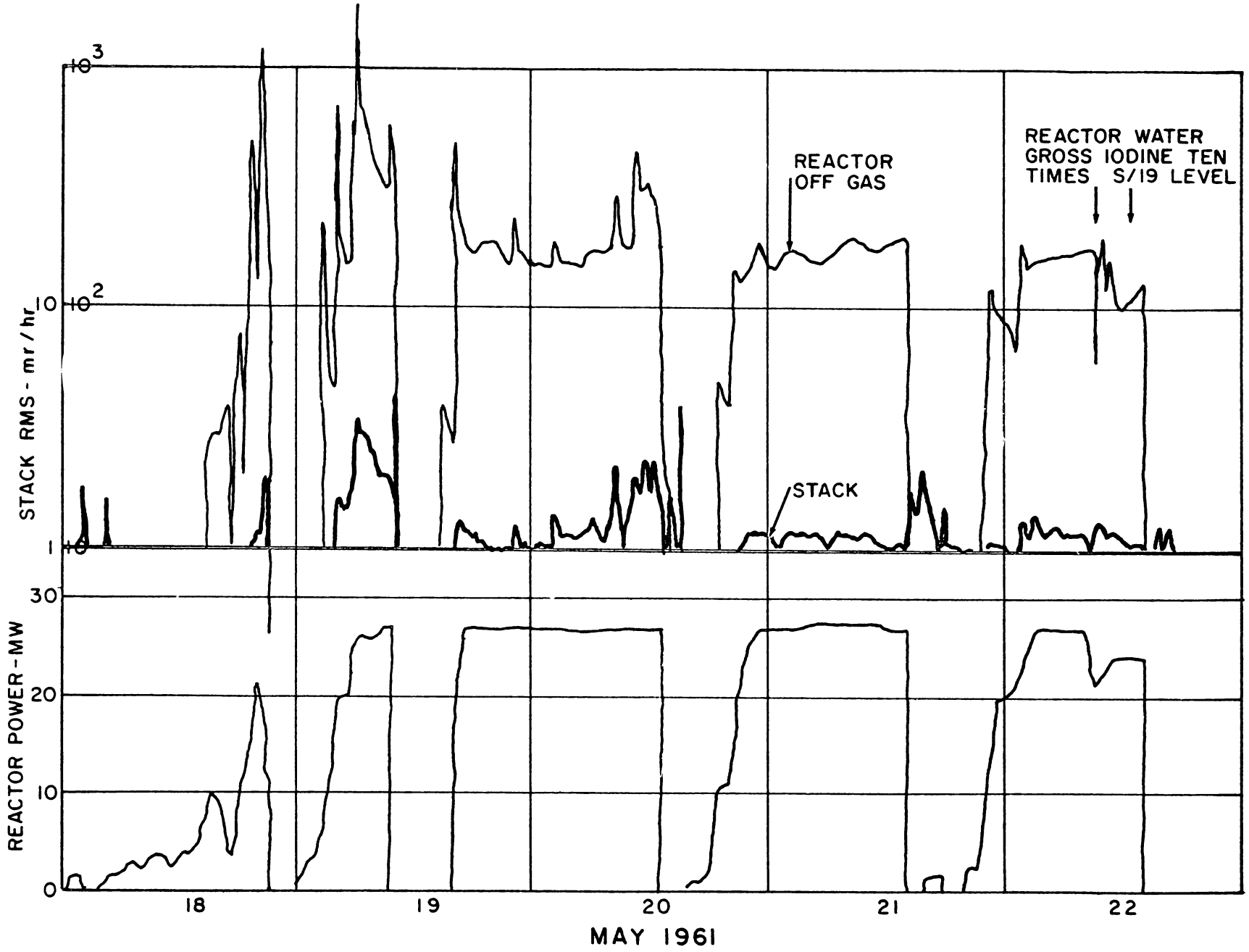
STACK RMS - mr / hr
10^3
10^2
10
1
REACTOR OFF GAS
REACTOR WATER GROSS IODINE TEN TIMES S/19 LEVEL
STACK
REACTOR POWER - MW
30
20
10
0
18
19
20
21
22
MAY 1961

FIGURE 6.3

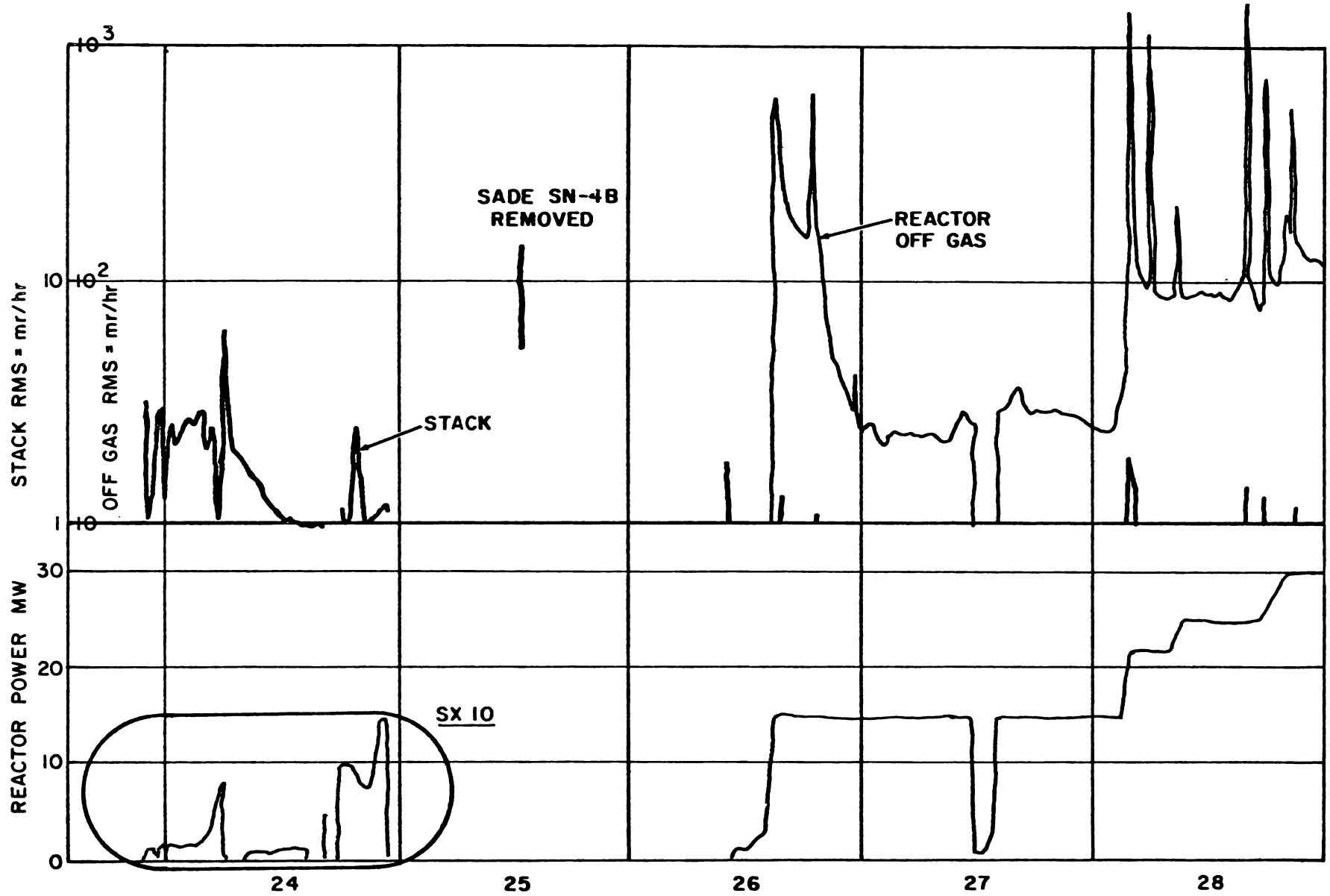
STACK RMS = mr/hr
OFF GAS RMS = mr/hr
10^3
10^2
10
1
SADE SN-4B
REMOVED
REACTOR
OFF GAS
STACK
REACTOR POWER MW
30
20
10
0
SX 10
24
25
26
27
28
MAY 1961

FIGURE 6.4

could not be made on May 24 until after the scram at 1615.

Radioiodine concentrations in reactor water also indicated release of fission products from SH-4B prior to May 24. Radioiodine from the SADE loop is returned to the reactor in the condensate via the reactor feedwater. Reactor water iodine concentrations increased more than ten-fold between May 19 and May 22, but the previous levels were re-established during high power operation following the removal of SH-4B. These increases in iodine concentrations correspond to release rates of 0.3 and 1.4 μc/sec of I-131 and I-133 respectively at a reactor power of about 25 MW(t). On May 24, two samples of SADE condensate and reactor water samples all indicated release rates of about 0.5 μc/sec for I-131 and I-133 during very low power operation. This relatively slow release of iodine compared to fission gases is consistent with previous VBWR experience with leaker type defects.

6.2.3 Reactor Coolant Conditions

During normal operation, the SADE fuel is cooled by saturated steam from the VBWR, and during startup of the reactor, before steam is formed, the SADE fuel is cooled with air. During the irradiation of SH-4B, the fuel was also exposed to reactor water to an unknown extent as a result of leakage through the fuel flange located just above the reactor core and by carryover with the steam during high power or transient periods.

Although the reactor water normally contains very low concentrations of impurities, for one period during the SH-4B irradiation, shown in Figure 6.5, it contained higher impurity concentrations. The rises in sodium and chloride concentrations were caused by depletion of the reactor cleanup demineralizers, but the source of ionic impurities which caused the depletion is uncertain. Because of their significance in stress corrosion cracking, reactor water chloride analyses for the

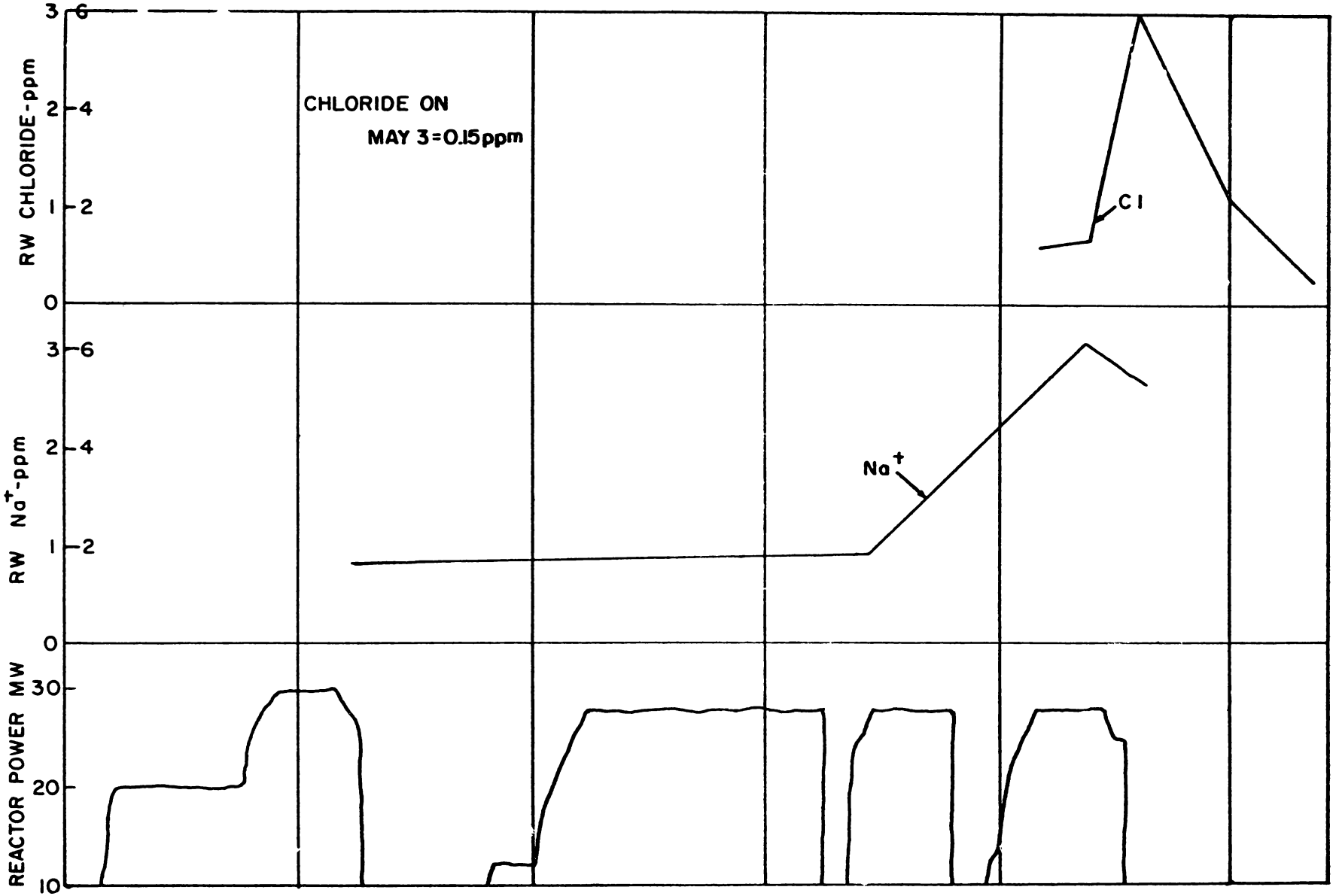
RW CHLORIDE-ppm
3
6
2
4
1
2
0
CHLORIDE ON
MAY 3=0.15ppm
Cl
RW Na+-ppm
3
6
2
4
1
2
0
Na+
REACTOR POWER MW
30
20
10
5
6
7
8
9
MAY 1961

FIGURE 6.5

complete irradiation period are given in Table 6.1.

Table 6.1

REACTOR WATER ANALYSES

Date	Time	Chloride ppm	Sodium ppm
Jan. 25		0.12	
May 3	1030	0.15	
6	0545		1.61
8	1045		1.75
9	0918	0.67	6.04
	1430	Ca 3.0	5.33
	2315	1.2	
10	0830	0.27	
	1300	0.073	
11	0840	0.26	
	1130		0.75
18	1015	0.04	
19	0835	0.089	
22	1015	0.028	
VBWR Pool			
May 26	1315	1.8	
SADE Condensate			
May 9	1430	0.15	0.19

During the January irradiation period the reactor water conductivity was consistently low, approximately one μmho/cm, and one chloride analysis indicated only 0.12 ppm. The next period of significant irradiation began on May 5 and continued through May 11. During this period the fuel could have been exposed to water containing up to three ppm of chloride. Note that the highest chloride concentration in the reactor water was detected on May 9 after shutdown of the reactor. A sample of condensate taken from the SADE loop at the same time (an hour and a half after shutdown) analyzed 0.15 ppm chloride. The reactor water chloride concentration decreased to less than 0.1 ppm within twenty-four hours after the observed peak when the demineralizer resins were replaced. The concentration was 0.26 ppm during the short irradiation on May 11 but was probably less than 0.1 ppm during the remainder of the irradiation period from May 18 to May 24.

6.2.4 Deposition

Coupons inserted in the SADE effluent steam line during the middle of April were examined after the May 24 shutdown. The coupons were found to be highly contaminated -- primarily with radioiodines. The surface dose rate was 800 mrems/hr (total) including about 5 mr/hr (gamma). The deposits were analyzed by measuring the radioactive decay of specific peaks on a gamma ray spectrometer. The results are given in Table 6.2. With the exception of the leaded bronze sample, the contamination levels of the various samples tested were not grossly different from each other. The leaded bronze appeared to exhibit a particular affinity for iodine, but not for tellurium or molybdenum.

Table 6.2

DEPOSITION ON COUPONS

Material	Previous Exposure - Hours	$\mu c/cm^2$ at reactor shutdown			
		I-131	I-133	Te-132	Mo-99
Leaded Bronze	818	4.40	1.31	0.016	0.1
Cr-Mo Steal	818	0.130	0.095	0.024	0.067
Carbon Steel	818	0.175	0.121	0.020	0.060
Carbon Steel *	818	1.12	0.48	0.015	0.060
Inconel-X	818	0.064	0.050	0.041	0.078
T1 Low Alloy Steel	818	0.063	0.050	0.017	0.036
502 SS	818	0.092	0.065	0.022	0.044
410 SS	818	0.067	0.050	0.017	0.037
430 SS	818	0.077	0.052	0.014	0.027
304 SS	818	0.117	0.120	0.023	0.037
347 SS	818	0.059	0.034	0.030	0.045
304 SS	0	0.058	0.031	0.046	0.053

* Possibly contaminated from leaded bronze sample.

Longer-lived corrosion product nuclides, such as Co-60 and Co-58, were completely overshadowed by the short-lived nuclides measured. The relative amounts of I-131 and I-133 indicate the major deposition occurred during the last day of operation. Continued operation with this order of fission product release would probably produce contamination levels an order of magnitude higher. One-third of the iodine activity was removed from one of the stainless steel coupons by rinsing in water for a few minutes, and half of the remainder was removed by soaking in water for sixteen hours.

The results of a radiation survey performed on June 3, nine days after SADE shutdown, are given in Table 6.3. The levels are somewhat higher than those measured on the coupons, probably because of inadequate area correction for the coupon measurements. The high total dose rates near the bottom of FCV 1101 and FCV 1103 indicate significant external contamination whereas the deposits in other locations are internal.

Table 6.3

RADIATION SURVEY

0345 June 3, 1961

Location	Total mrems/hr	Gamma mr/hr	
General background	3 to 5	3 to 5	Field
Steam line to SADE	5	5	2"
FCV 1103 bottom	560	20	Surface
FCV 1101 bottom	3200	20	Surface
Desuperheater	10	10	2"
Condenser	18	18	2"
Vent Condenser	15	15	2"
After cooler	25	25	2"
CV 1101	17	17	2"
Tee by RV 1104	30	30	2"

7.0 TASK F - HEAT TRANSFER

7.1 Task F-1, "Once-Through" Superheat

A topical report, GEAP-3703, "Heat Transfer Coefficients with Annular Flow During 'Once-Through' Boiling of Water to 100% Quality at 800, 1100, and 1400 psi," was completed and issued.

7.2 Task F-2, Heat Transfer to Superheated Steam

The first two months were used in completing the assembly and hydro testing of the components.

No results were obtained from two annular flow assemblies. The first caused thermocouple shorting due to a leaky heater rod joint, and the second assembly failed due to shorting of the heater rod.

Two assemblies, with steam flow inside a 0.370" I.D. circular tube were tried. An open circuit developed in the first due to failure of a brazed joint. Three data runs were obtained in June with the second assembly with approximate conditions as shown below.

Run No.	Pressure	W-lb/sec	G-lb/hr-ft^2 x 10^6	Δt superheat ^oF
2	830	0.28	1.35	125
3	1060	0.29	1.35	150
4	890	0.18	0.90	200

Pressure control was poor ($\pm$ 20 psi) due to a blocked condensate line which has been corrected.

Data is under reduction to establish correlation with other published data.

8.0 TASK G - MECHANICAL DEVELOPMENT

8.1 Steam Separator Development

8.1.1 Introduction

All steam separation development during the report period was applied to the radial vane type primary separator. Air-water and steam-water tests demonstrated significantly greater capacity than previously obtained. This type separator appears to be extremely promising for reactor use.

8.1.2 Summary and Conclusions

A full circle radial vane and a two-vane radial separator model were tested using air-water and 1000 psig saturated steam-water mixtures.

The most significant test results were:

8.1.2.1 Capacity has been demonstrated by tests of a 2-vane radial separator model to be about 5 times that of free surface separation over an area equal to that occupied by the separator.

8.1.2.2 At about 20,000 ft^3/hr of 1000 psig saturated steam-water flow a full circle of radial vanes was found to operate with moisture carry-over and vapor carry-under of 6% and 0.2% by weight respectively. This was sufficiently low to satisfy reactor operating requirements. Carry-over was limiting in this model.

8.1.2.3 Better performance can be obtained with a vane radius of 4 inches than with one of 8 inches.

8.1.2.4 Carry-under and pressure drop characteristics of the full circle radial vane separator showed good correspondences between air-water and steam-water tests.

8.1.2.5 Satisfactory steam separation can be obtained with relatively low separator pressure drop.

8.1.2.6 The radial vane separator acts essentially as a constant volume flow device.

8.1.2.7 Annulus thickness between vane discharge and downcomer shroud is important assuring satisfactory downcomer flow characteristics.

Tests were performed on small scale models with no secondary scrubbers, deflectors or other devices to improve carry-over characteristics.

8.1.3 Discussion

8.1.3.1 General

Work previously performed indicated radial vane type separators showed promise for nuclear reactor application. Subsequent work in air-water testing for flow configuration indicated good results could be expected from 1/4 to 1/2 inch wide nozzles and 4 inch to 6 inch radii vanes. A 2-vane radial separator utilizing a 1/4 inch wide x 18 inch long nozzle and 4 inch radius vanes was constructed for tests to determine carry-over limitations.

Carry-under characteristics were obtained by testing a model of a full circle of radial vanes small enough to simulate reactor flow characteristics within the capacities of the test loops. A full circle radial vane assembly was constructed and tested in air-water with good carry-under results. Steam-water tests subsequently showed carry-under to be generally below 0.3% vapor by weight, and decreasing with increasing flow rates.

Vane spacing has a significant effect on the number of vanes that can be used in a given size assembly. In order to determine the effect vane spacing has on separator carry-over, the 2-vane radial separator was assembled with one fixed and one moveable 4-inch radius vane and tested in the air-water and steam-water loops. Good results were observed with spacing of one inch on center-lines of the arcs. Spacing greater than 1 inch had insignificant effect on exit quality.

In summary, the full circle radial vane separator consisting of 30 two-inch radius vanes and 3/16 inch wide by 6 inch high nozzles gave satisfactory steam-water separating characteristics for total volume flows of about 20,000 ft^3/hr. Satisfactory carry-over was obtained with two 4 inch radius vanes on 1 inch spacing and a 1/4 inch wide by 18 inch high nozzle with about 8,100 ft^3/hr saturated steam-water mixture at 1000 psig.

Measured nozzle pressure drops in tests conducted with the 2-vane radial separator were slightly greater than those calculated for abrupt constriction of rectangular ducts in two-phase saturated steam-water flow at 1000 psig. With low pressure drops (in the range of 1 to 3 inches Hg.) the full circle radial vane separator gave good steam separation results. The nozzle configurations of these two models were of different designs, with the full circle radial vane nozzles exhibiting the characteristics of an orifice.

As an example, pressure drop for the full circle radial vane separator was about 2.6 psi at 400,000 lb/hr water flow with

6% inlet quality, and pressure drop for the 2-vane separator was about 13 psi for 120,000 lb/hr water with 16,000 lb/hr steam.

8.1.3.2 Equipment Description

8.1.3.2.1 Full Circle Radial Vane Separator

A sketch of the separator assembly is shown in Figure 8.1, "Full Circle Radial Vane Separator Arrangement". Thirty vanes with 2 inch radius arcs of 135 degree arc length and 18 inches in height are assembled on equal spacing around a 7 1/2 inch O.D. x 6 3/4 inch I.D. plenum. Inlet nozzles were formed with 3/16" wide x 1/2" long x 6" high dimensions preceded by 1/2 inch radius round edge entrances. The trailing edge of the vanes discharged into a downcomer 2 inches wide made by a cylindrical shroud surrounding the vanes and extending one inch above and 5 1/2 inches below the vanes.

Free surface separation area was restricted by a sleeve extending from the top of the shroud to the separator base plate. The gap between the sleeve and shroud was approximately 1 inch. Side and top views of the separator assembly are shown in Figure 8.2.

Conductivity elements measured steam samples supplied through four equally spaced open end horizontal tubes located 6 inches above the separator vanes and from one sample ring located 12 inches above the vanes. Comparison of conductivity of samples versus re-

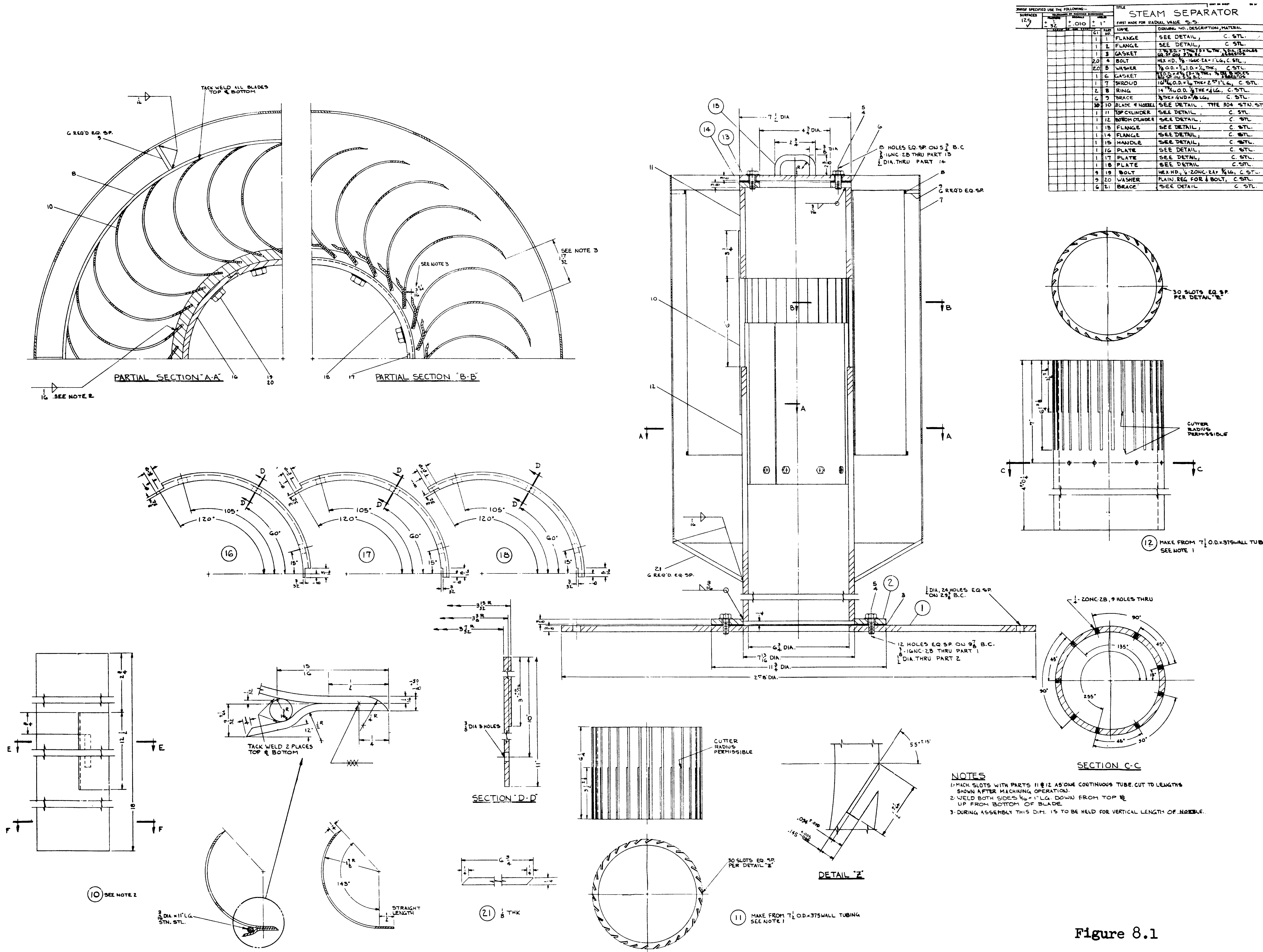
STEAM SEPARATOR
FIRST MADE FOR RADIAL VANE S.S.
SURFACES 125
± 1/32
± .010
± 1°
PART NO. | NAME | DRAWING NO., DESCRIPTION, MATERIAL
1 | 1 | FLANGE | SEE DETAIL, C. STL.
1 | 2 | FLANGE | SEE DETAIL, C. STL.
1 | 3 | GASKET | ASBESTOS
20 | 4 | BOLT | HEX. HD., 5/8-16UNC-2A × 1" LG., C. STL.
20 | 5 | WASHER | C. STL.
1 | 6 | GASKET | ASBESTOS
1 | 7 | SHROUD | C. STL.
2 | 8 | RING | C. STL.
6 | 9 | BRACE | C. STL.
30 | 10 | BLADE & NOZZEL | SEE DETAIL, TYPE 304 STN. STL.
1 | 11 | TOP CYLINDER | SEE DETAIL, C. STL.
1 | 12 | BOTOM CYLINDER | SEE DETAIL, C. STL
1 | 13 | FLANGE | SEE DETAIL, C. STL.
1 | 14 | FLANGE | SEE DETAIL, C. STL.
1 | 15 | HANDLE | SEE DETAIL, C. STL.
1 | 16 | PLATE | SEE DETAIL, C. STL.
1 | 17 | PLATE | SEE DETAIL, C. STL.
1 | 18 | PLATE | SEE DETAIL C. STL.
9 | 19 | BOLT | HEX. HD., 1/4-20NC-2A × 3/4 LG., C. STL.
9 | 20 | WASHER | PLAIN, REG. FOR 1/4 BOLT, C. STL.
6 | 21 | BRACE | SEE DETAIL C. STL.
PARTIAL SECTION "A-A"
PARTIAL SECTION "B-B"
TACK WELD ALL BLADES TOP & BOTTOM
SEE NOTE 2
SEE NOTE 3
SECTION "D-D"
SECTION "E-E"
SECTION "F-F"
SECTION C-C
DETAIL "Z"
30 SLOTS EQ. SP. PER DETAIL "Z"
CUTTER RADIUS PERMISSIBLE
TACK WELD 2 PLACES TOP & BOTTOM
(12) MAKE FROM 7 1/2 O.D. × .375 WALL TUBING SEE NOTE 1
(11) MAKE FROM 7 1/2 O.D. × .375 WALL TUBING SEE NOTE 1
(10) SEE NOTE 2
(21) 1/8 THK
NOTES
1- MACH. SLOTS WITH PARTS 11 & 12 AS ONE CONTINUOUS TUBE. CUT TO LENGTHS SHOWN AFTER MACHINING OPERATION.
2- WELD BOTH SIDES 1/16 × 1" LG. DOWN FROM TOP & UP FROM BOTTOM OF BLADE.
3- DURING ASSEMBLY THIS DIM. IS TO BE HELD FOR VERTICAL LENGTH OF NOZZLE.

Figure 8.1

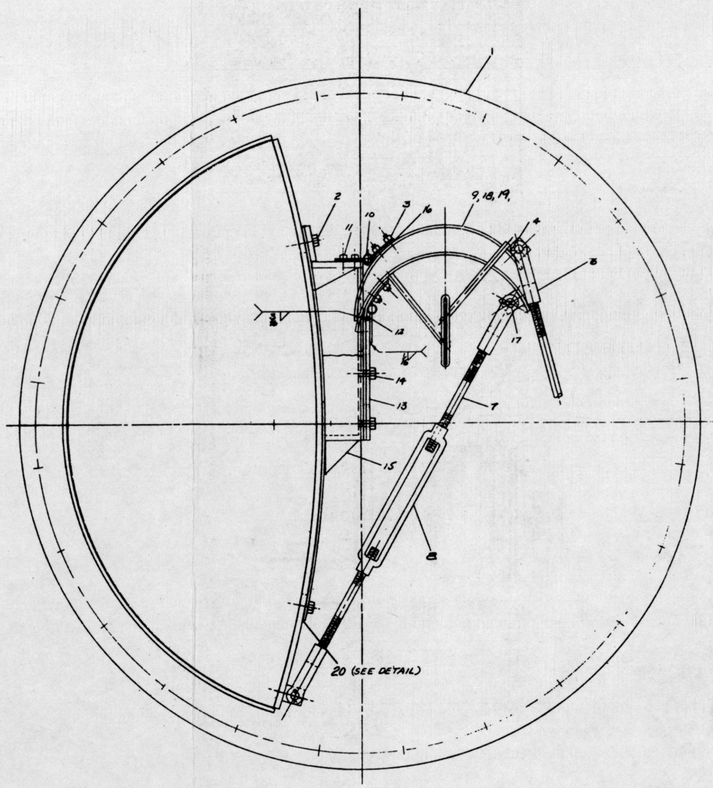

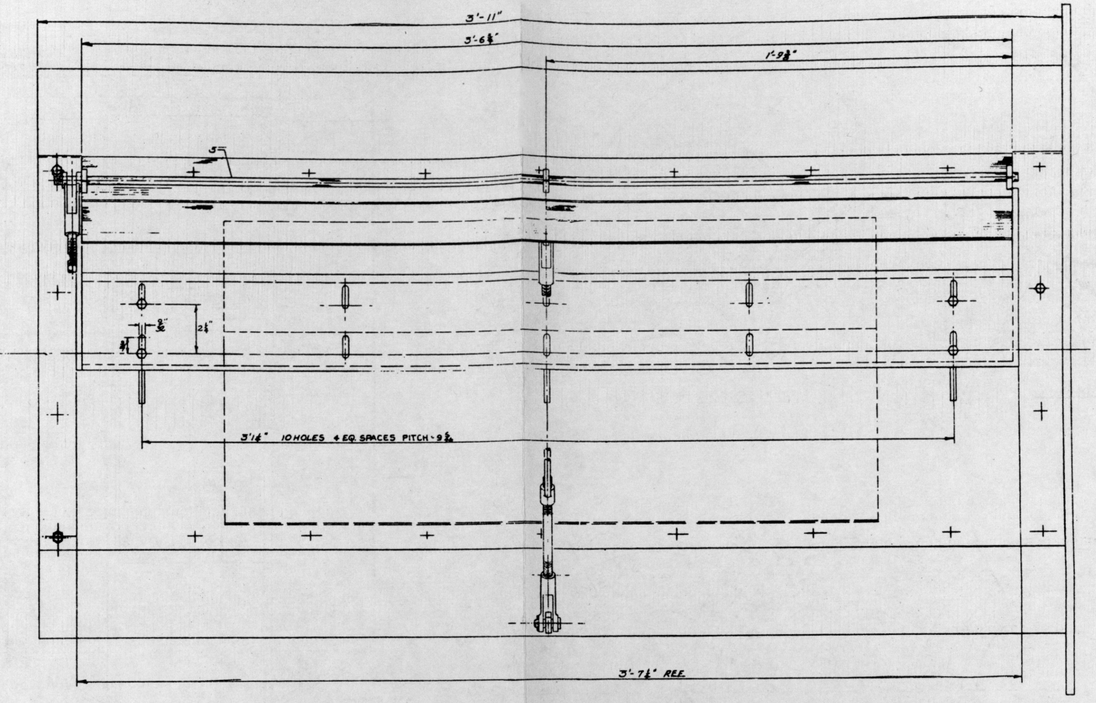

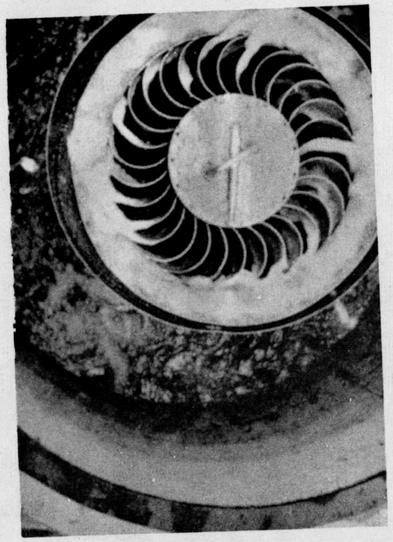

AIR-WATER LOOP OPERATION

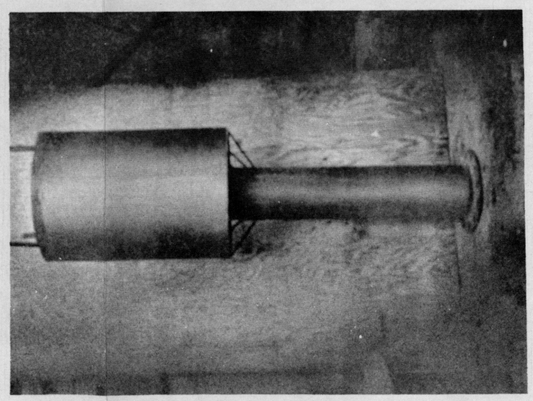

8.2b SIDE VIEW

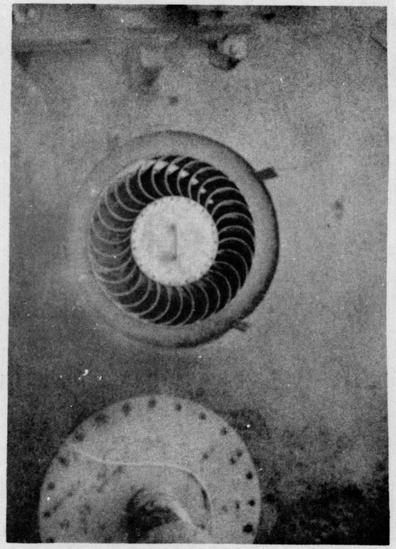

8.2 TOP VIEW

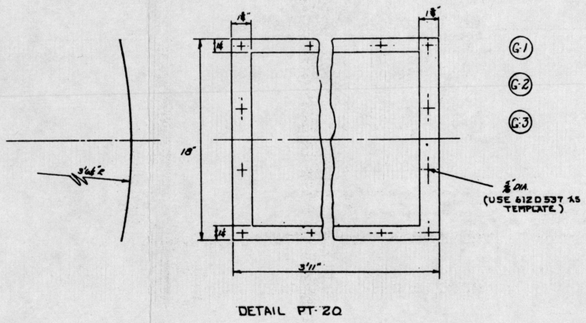

Figure 8.2

FULL CIRCLE RADIAL VANE SEPARATOR

circulation water provided the means for determining percentage moisture by weight carried over by the steam.

A pressure tap on the side of the plenum and an open end tube outside the plenum and at the same level as the pressure tap were connected to a mercury manometer to obtain nozzle pressure drops.

Flow rates of steam and water were obtained from orifices and mercury manometers.

Carry-under data was obtained by pump power and head measurements compared with curves of pump operating characteristics vs per cent by weight vapor carry-under.

8.1.3.2.2 2-Vane Radial Separator (Figure 8.3)

Two four inch radius x 32 inches high x 135 degree arc length vanes, one of which was fixed to the plenum and the other adjustable, were used to investigate vane spacing effect on carryover. A 1/4 inch wide x 1 inch long x 18 inch high nozzle with 1/4 inch radius rounded entrances directed mixture flow from the plenum onto the fixed vane. Fig. 8.4 shows the assembly top and side views and flow configuration during operation in the air water loop.

The adjustable vane was supported by brackets and rollers moving along two shafts attached to the plenum. Motion was along a horizontal

MOSS LANDING STEAM SEPARATION
TEST VESSEL

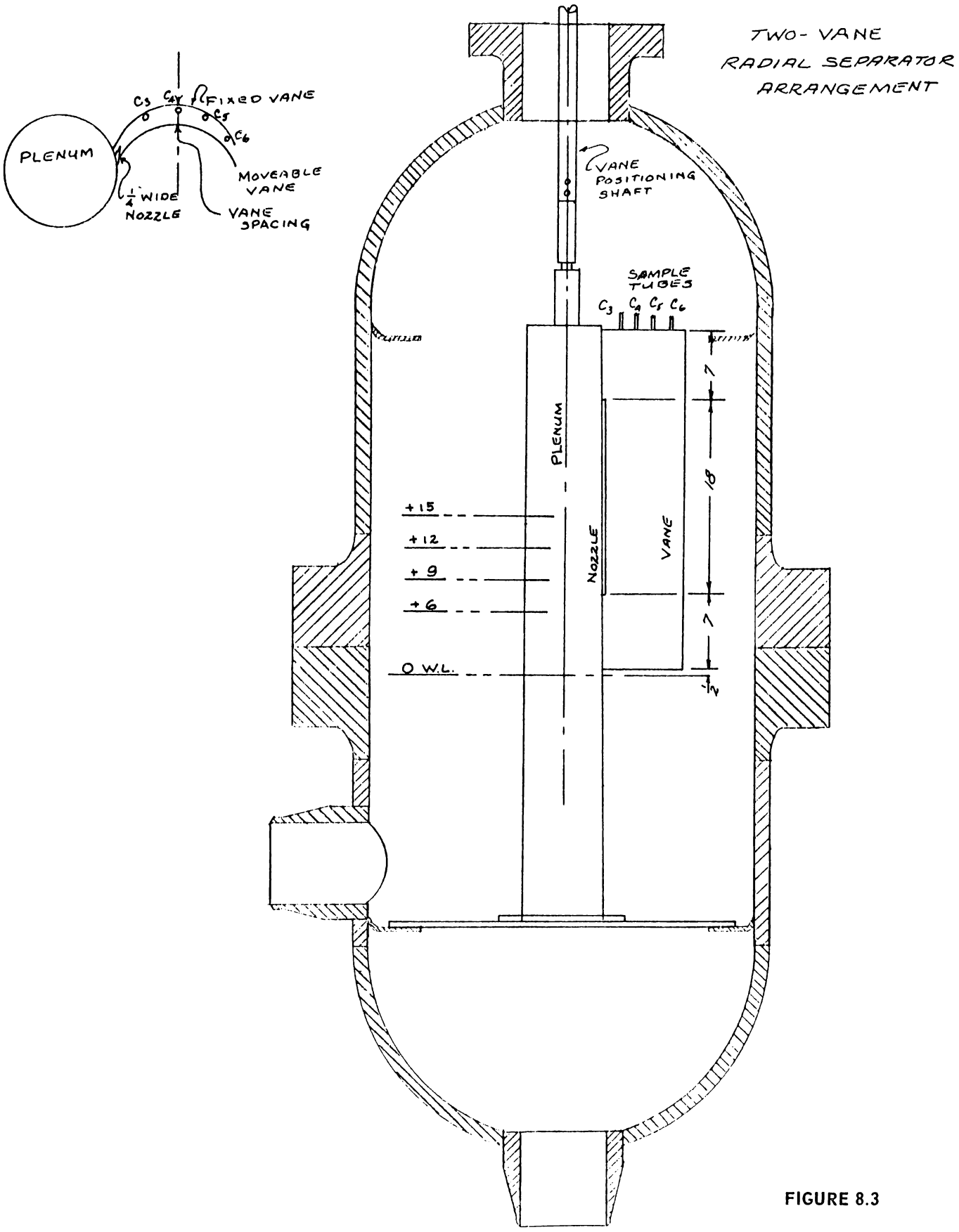

FIGURE 8.3

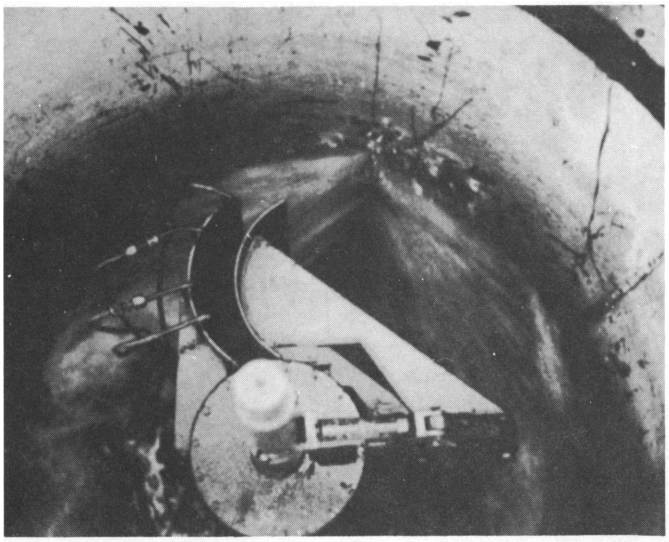

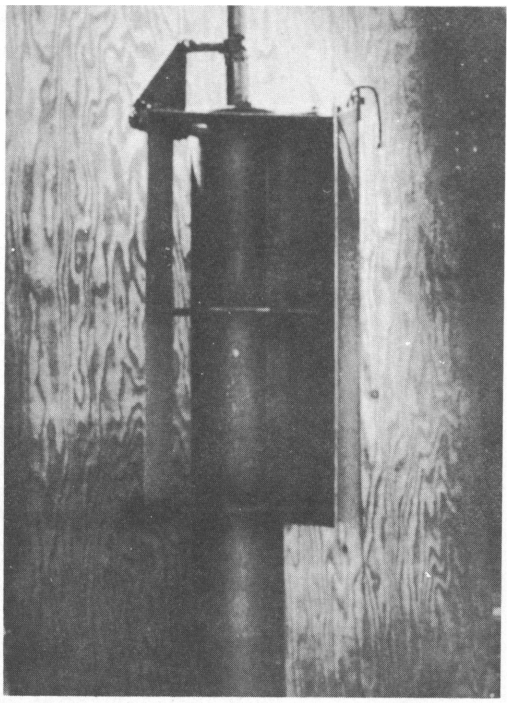

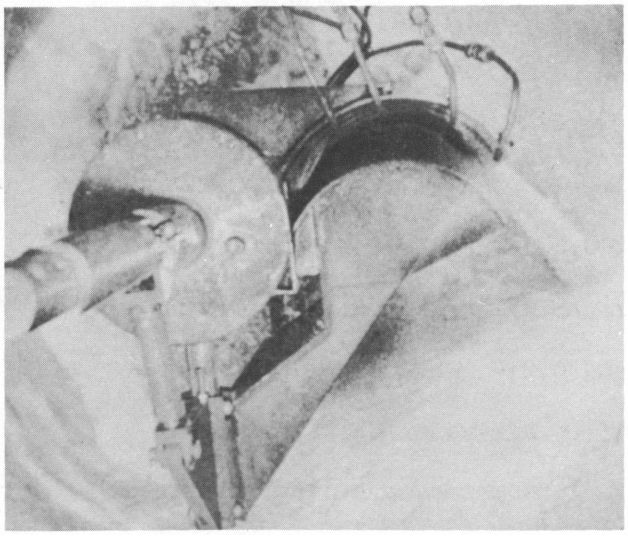

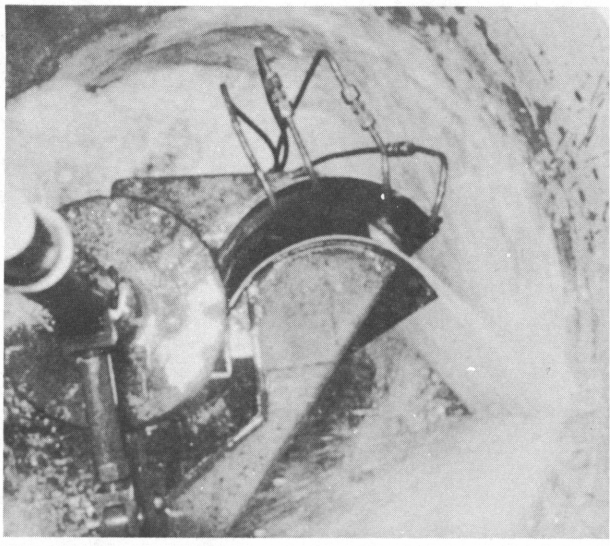

Figure 8.4
2-VANE RADIAL SEPARATOR

line between the vertical centerlines of the arcs of the two vanes and was provided by a shaft and connecting rod, the shaft penetrating the top nozzle of the vessel through shaft packing. Movement was limited to vane spacings of 1 to 2 1/4 inches.

Essentially the same instrumentation was used for tests of the 2-vane assembly as for the full circle radial vane separator. The exception was that four sample tubes with open ends directed downward and located just at the top and between the vanes were used for extracting samples from steam flowing vertically between vanes. Figure 8.5 is a sketch showing a top view of the 2-vane arrangement and sample tube locations.

8.1.4. Test Results

8.1.4.1 Full Circle Radial Vane

Data plots are shown in Figures 8.6 and 8.7. As shown by carry-under data, successful operation can be obtained with water flow rates of 300,000 to 400,000 lb/hr and steam flow up to 36,000 lb/hr where per cent vapor by weight in downcomer flow ranges between 0.10 and 0.27. This corresponded with carry-under data obtained from air-water tests for equal volume flow rates. Mixture flow rates were not limited by carry-under.

Carry-over was limited to about 20,000 ft^3/hr with moisture content not exceeding 6% by weight, as shown in Figure 8.8.

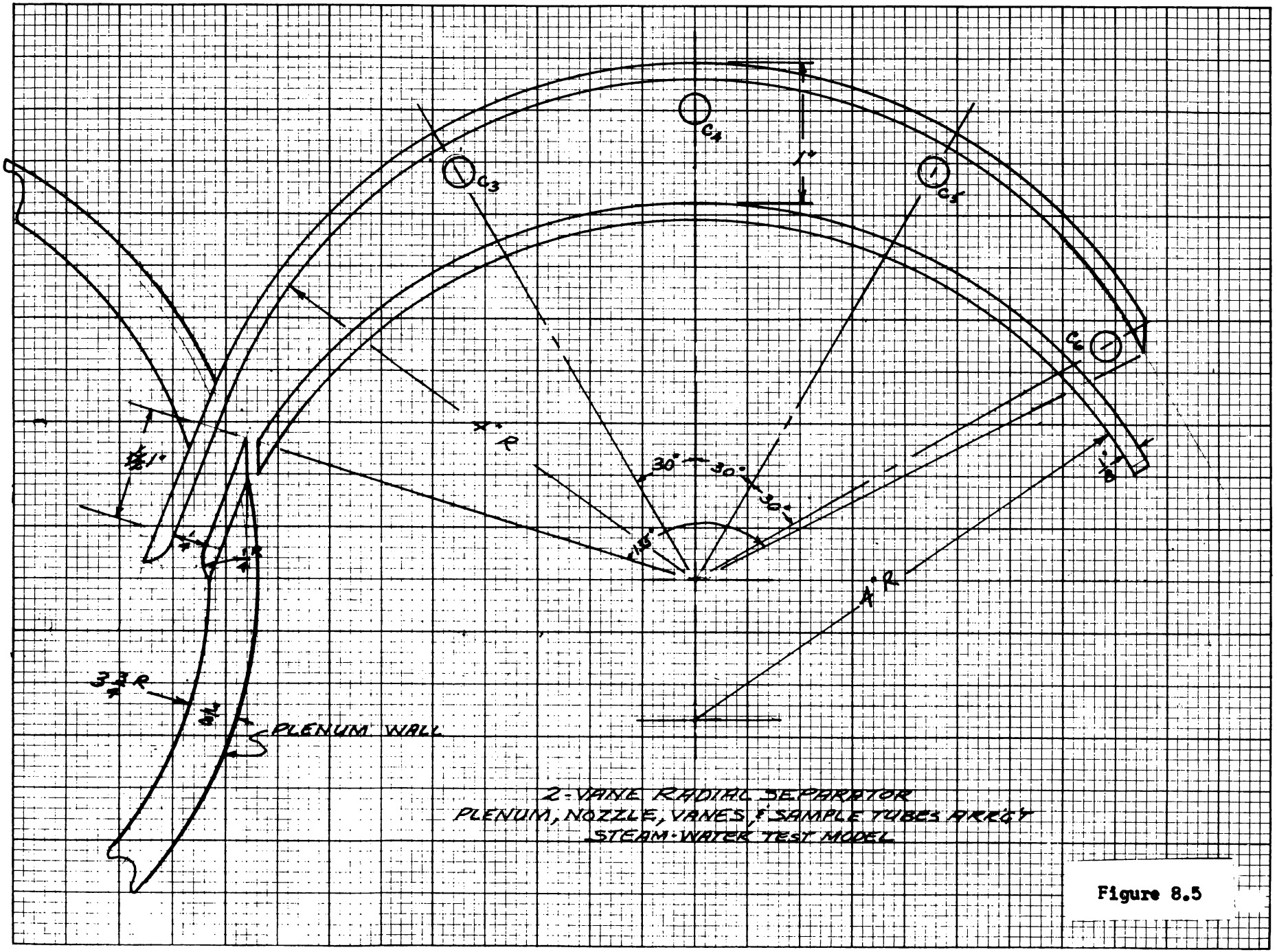

2-VANE RADIAL SEPARATOR
PLENUM, NOZZLE, VANES, & SAMPLE TUBES ARRAY
STEAM-WATER TEST MODEL

Figure 8.5

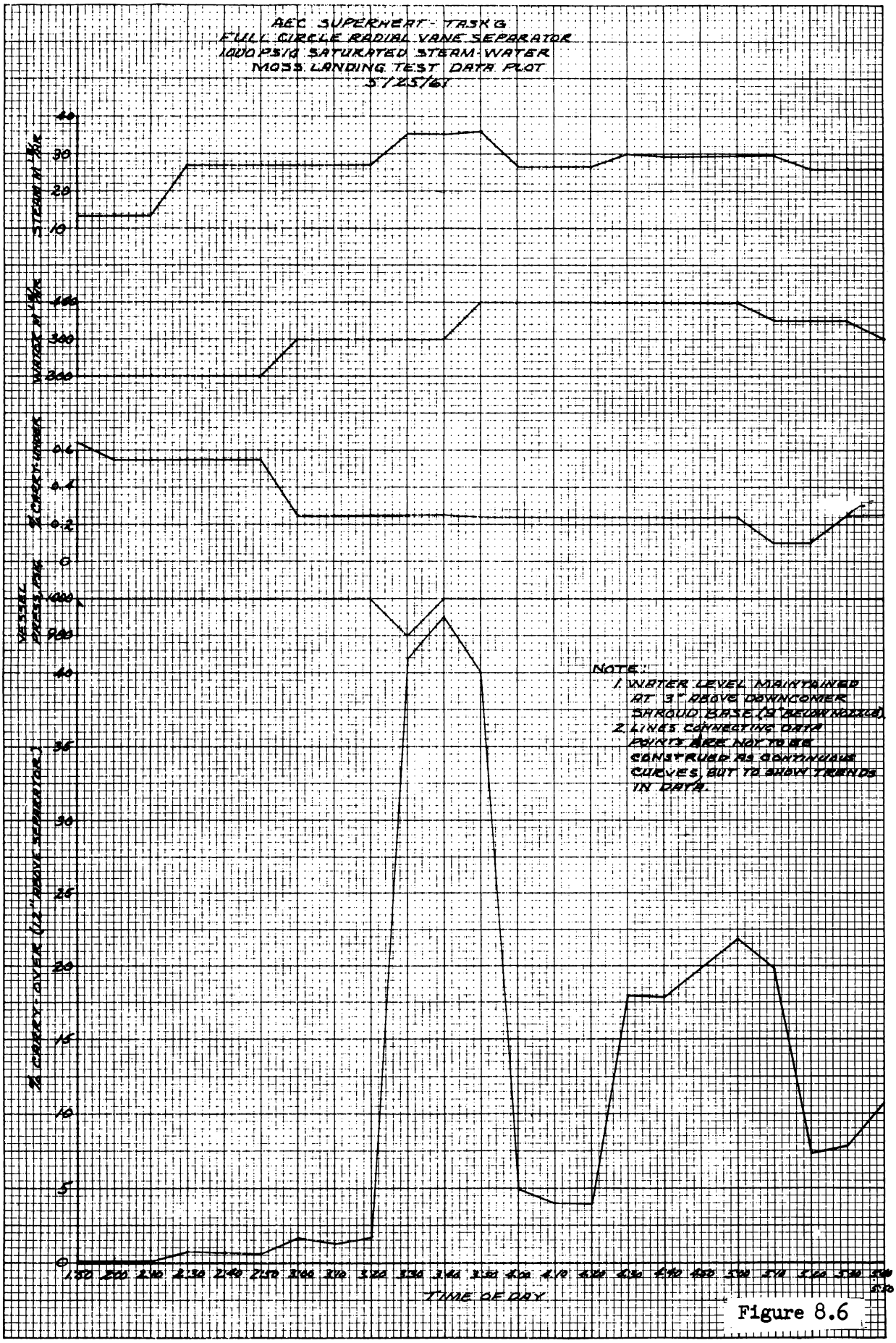
AEC SUPERHEAT - TASK G
FULL CIRCLE RADIAL VANE SEPARATOR
1000 PSIG SATURATED STEAM-WATER
MOSS LANDING TEST DATA PLOT
5/25/61
STEAM M lb/hr
WATER M lb/hr
% CARRY-UNDER
VESSEL PRESS. PSIG
% CARRY-OVER (12" ABOVE SEPARATOR)
TIME OF DAY
NOTE:
1. WATER LEVEL MAINTAINED AT 3" ABOVE DOWNCOMER SHROUD BASE (3" BELOW NOZZLE).
2. LINES CONNECTING DATA POINTS ARE NOT TO BE CONSTRUED AS CONTINUOUS CURVES, BUT TO SHOW TRENDS IN DATA.

Figure 8.6

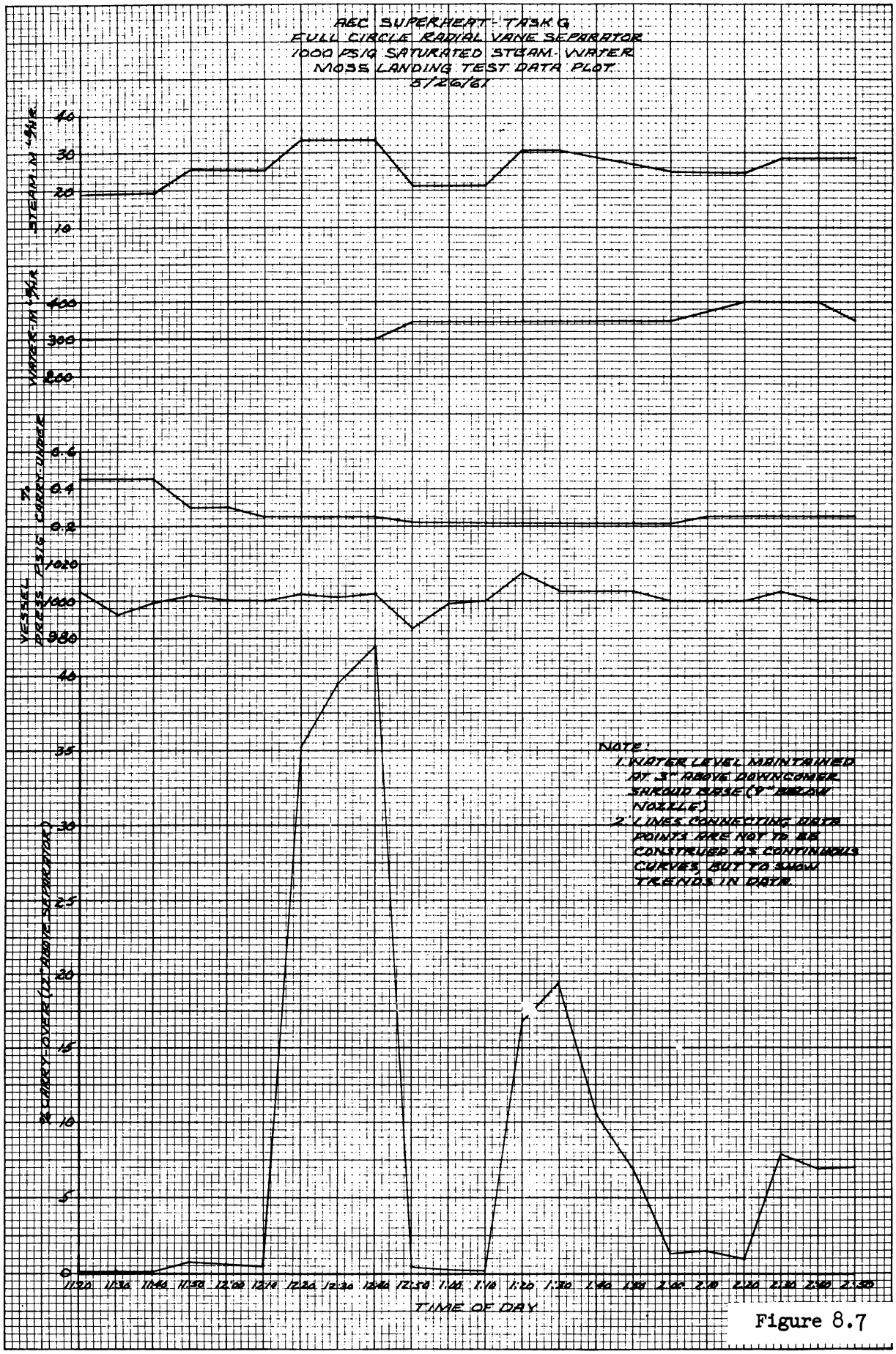
AEC SUPERHEAT - TASK G
FULL CIRCLE RADIAL VANE SEPARATOR
1000 PSIG SATURATED STEAM-WATER
MOSS LANDING TEST DATA PLOT
5/26/61
STEAM IN #/HR
WATER IN #/HR
% CARRY-UNDER
VESSEL PRESS PSIG
% CARRY-OVER (OF TOTAL STEAM FLOW)
NOTE:
1. WATER LEVEL MAINTAINED AT 3" ABOVE DOWNCOMER SHROUD BASE (7" BELOW NOZZLE).
2. LINES CONNECTING DATA POINTS ARE NOT TO BE CONSTRUED AS CONTINUOUS CURVES, BUT TO SHOW TRENDS IN DATA.
TIME OF DAY

Figure 8.7

Carry-over measurements were made from the sample ring located 12 inches above the top of the vanes. The other sample tubes received a good deal of moisture from splash, which could be eliminated by deflection or other devices, and are considered not to give reliable carry-over samples. Pressure drop measurements are shown in data sheets, Figs. 8.9 through 8.12.

During air-water tests it was observed that a portion of the nozzle length preceeding the 3/16 inch wide constriction was open to the outside of the plenum resulting in vertical jets of water at these points. No changes were made in the nozzle for succeeding tests. It is presumed that carry-over limitations could be expanded if the nozzles were completely housed inside the plenum.

8.1.4.2 2-Vane Radial Separator

Figures 8.13 to 8.19 are data plots of 2-vane radial separator tests performed with 1000 psig saturated steam-water mixtures. Although there is some variation in data points, reliably satisfactory exit steam quality (less than 6% by weight exit moisture) was obtained from all four sample tubes with a water flow of about 120,000 lb/hr, and steam flow of about 16,000 lb/hr. as shown in Figure 8.19. During tests performed on 6/16/61, the sample rates were increased, relative to previous testing, to give more nearly isokinetic samples and steam leaving velocities. It is expected that this change is responsible for the better data obtained on this run than obtained previously.

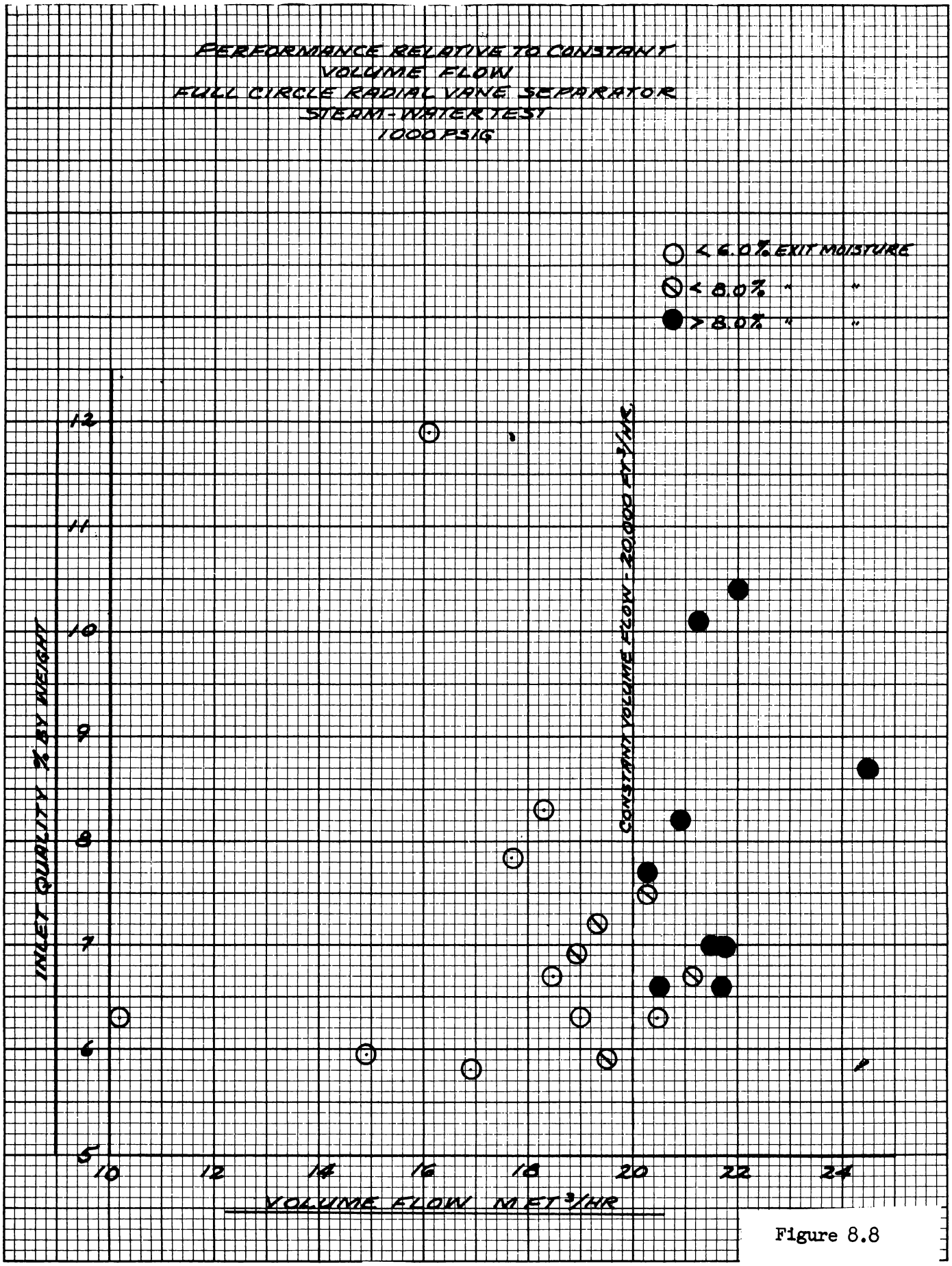
PERFORMANCE RELATIVE TO CONSTANT VOLUME FLOW
FULL CIRCLE RADIAL VANE SEPARATOR
STEAM-WATER TEST
1000 PSIG
< 6.0% EXIT MOISTURE
< 8.0% " "
> 8.0% " "
INLET QUALITY % BY WEIGHT
CONSTANT VOLUME FLOW - 20000 FT³/HR.
VOLUME FLOW M FT³/HR
5
6
7
8
9
10
11
12
10
12
14
16
18
20
22
24

Figure 8.8

FULL CIRCLE RADIAL VANE SEPARATOR DATA SHEET

PG&E MOSS LANDING TEST FACILITY

Date MAY 25, 1961

Time	1:50	2:00	2:10	2:30	2:40	2:50	3:00	3:10	3:20	3:30	3:40	3:50
Steam Flow Mlbs/hr	13.5	13.5	13.5	27	27	27	27	27	27	35	35	36
Recirc Flow Mlbs/hr	200	200	200	200	200	200	300	300	300	300	300	400
X_s Inlet Quality %	6.3	6.3	6.3	11.9	11.9	11.9	8.25	8.25	8.25	10.4	10.4	8.25
Total Volume Flow ft^3/hr	10.24	10.24	10.24	16.16	16.16	16.16	18.32	18.32	18.32	21.83	21.83	24.43
Vessel Pressure psig	1000	1000	1000	1000	1000	1000	1000	1000	1000	980	1000	1000
ΔP Separator psi	.45	.499	.572	.705	.852	.901	.879	1.03	1.08	1.26	1.41	1.32
Vessel Exit Temp.	545	550	542	542	547	547	547	547	547	542	547	547
% Moisture Sample Tube C_3	3.7	3.9	2.6	72.5	69	70.5	97.5	100	100	86.3	77.0	78.8
% Moisture Sample Tube C_4	0.05	0.07	0.05	21.4	20.8	21.6	40.7	43.8	44.3	47.1	40.0	43.7
% Moisture Sample Tube C_5	0.08	0.04	0.08	22.1	32.0	25.1	83.5	84	91.5	63.8	51.4	53.1
% Moisture Sample Tube C_6	0.61	0.08	0.19	40.8	39.8	39.6	86.1	86.8	91.8	80.5	71.5	65.2
% Moisture Sample Tube C_7	0.04	0.03	0.08	0.73	0.69	0.66	1.64	1.31	1.65	40.9	43.7	40.0
Water Level	15	15	14	15	15	15	15	15	15	15	13	15

Figure 8.9

FULL CIRCLE RADIAL VANE SEPARATOR DATA SHEET

PG&E MOSS LANDING TEST FACILITY

Date MAY 25, 1961

Time	4:00	4:10	4:20	4:30	4:40	4:50	5:00	5:10	5:20	5:30	5:40	5:50
Steam Flow Mlbs/hr	26.5	26.5	26.5	30	29.5	29.5	29.5	29.5	26.0	26.0	26.0	26.0
Recirc Flow Mlbs/hr	400	400	400	400	400	400	400	350	350	350	300	300
X_s Inlet Quality %	6.22	6.22	6.22	6.98	6.88	6.88	6.88	7.75	6.9	6.9	8.0	8.0
Total Volume Flow ft^3/hr	20.26	20.26	20.26	21.8	21.58	21.58	21.58	20.5	18.96	18.96	17.88	17.88
Vessel Pressure psig	1000	1000	1000	1000	1000	1000	1000	1000	1000	1000	1000	1000
ΔP Separator psi	1.55	1.58	1.68	.445	.544	.642	.839	.955	1.03	1.16	1.37	1.45
Vessel Exit Temp.	542	550	550	547	545	547	545	550	545	550	550	550
% Moisture Sample Tube C_3	82.9	84.5	84.9	76.0	77.9	77.5	73.3	73.0	76.8	74.8	68.4	62.7
% Moisture Sample Tube C_4	31.0	29.0	28.7	39.0	42.0	41.0	35.3	35.3	33.2	25.7	33.6	32.8
% Moisture Sample Tube C_5	37.0	37.8	39.8	54.4	53.4	63.8	42.6	41.6	26.1	28.6	33.8	35.0
% Moisture Sample Tube C_6	53.0	55.8	58.8	61.2	65.9	59.0	4.7	4.6	49.0	48.8	43.3	41.1
% Moisture Sample Tube C_7	5.0	4.0	3.9	17.9	17.8	19.8	21.8	19.8	7.37	7.8	10.5	10.2
Water Level	14	15	15	15	15	15	15	15	15	14	15	15

Figure 8.10

FULL CIRCLE RADIAL VANE SEPARATOR DATA SHEET

PG&E MOSS LANDING TEST FACILITY

Date MAY 26, 1961

Time	11:20	11:30	11:40	11:50	12:00	12:10	12:20	12:30	12:40	12:50	1:00	1:10
Steam Flow Mlbs/hr	19.2	19.2	19.2	25.5	25.5	25.5	33.5	33.5	33.5	21.8	21.8	21.8
Recirc Flow Mlbs/hr	300	300	300	300	300	300	300	300	300	350	350	350
X_s Inlet Quality %	6.0	6.0	6.0	7.82	7.82	7.82	10.0	10.0	10.0	5.86	5.86	5.86
Total Volume Flow ft^3/hr	14.9	14.9	14.9	17.66	17.66	17.66	21.17	21.17	21.17	17.12	17.12	17.12
Vessel Pressure psig	1005	993	998	1003	1000	1000	1004	1002	1004	995	995	1000
ΔP Separator psi	.501	.501	.599	.636	.636	.685	.758	.817	.99	1.19	1.19	1.31
Vessel Exit Temp.	548	548	548	548	548	548	548	548	548	548	548	546
% Moisture Sample Tube C_3	14.0	14.5	20.8	91	90.8	93	100	100	86	57	68.5	58.5
% Moisture Sample Tube C_4	2.35	1.46	1.25	31.6	28.6	29.5	55	53	47	6.2	10.4	5.5
% Moisture Sample Tube C_5	2.62	3.0	3.14	65.7	70.4	58.5	77	74.5	61	12.6	10.1	9.2
% Moisture Sample Tube C_6	5.22 ~~3.77~~	5.6	5.13	74.0	71.1	67.0	91.5	91	80	25.2	30.8	27.6
% Moisture Sample Tube C_7	.13	.14	.11	.715	.61	.50	35.2	39.5	42.0	.47	.29	.22
Water Level	15	15	15	15	15	15	10	15	14	15	13	15

Figure 8.11

FULL CIRCLE RADIAL VANE SEPARATOR DATA SHEET

PG&E MOSS LANDING TEST FACILITY

Date MAY 26, 1961

Time	1:20	1:30	1:40	1:50	2:00	2:10	2:20	2:30	2:40	2:50		
Steam Flow Mlbs/hr	30.5	30.5	28.8	27.0	24.7	24.7	24.5	28.5	28.5	28.5		
Recirc Flow Mlbs/hr	350	350	350	350	350	375	400	400	400	350		
X_s Inlet Quality %	8.0	8.0	7.6	7.2	6.6	6.2	5.8	6.7	6.7	7.51		
Total Volume Flow ft^3/hr	20.93	20.93	20.19	19.4	18.39	18.93	19.38	21.14	21.14	20.06		
Vessel Pressure psig	1015	1005	1005	1005	1000	1000	1000	1005	1000	1000		
ΔP Separator psi	1.47	1.52	1.62	1.67	1.7	1.74	1.68	1.38	1.45	1.57		
Vessel Exit Temp.	546	545	545	545	545	545	544	544	545	545		
% Moisture Sample Tube C_3	80.8	86.0	85.0	83.0	80.4	82.9	86.0	86.5		86.5		
% Moisture Sample Tube C_4	45.0	42.9	42.0	33.3	23.7	23.5	26.1	45.0		35		
% Moisture Sample Tube C_5	59.6	59.5	53.0	40.4	17.0	23.1	22.9					
% Moisture Sample Tube C_6	73.3	70.0	64.3	57.5	42.3	42.4	43.0	62.6		61.5		
% Moisture Sample Tube C_7	16.8	19.4	10.6	6.93	1.3	1.5	1.0	7.8	6.9	7.0		
Water Level	15	14	15	15	14	15	15	15	15	15		

Figure 8.12

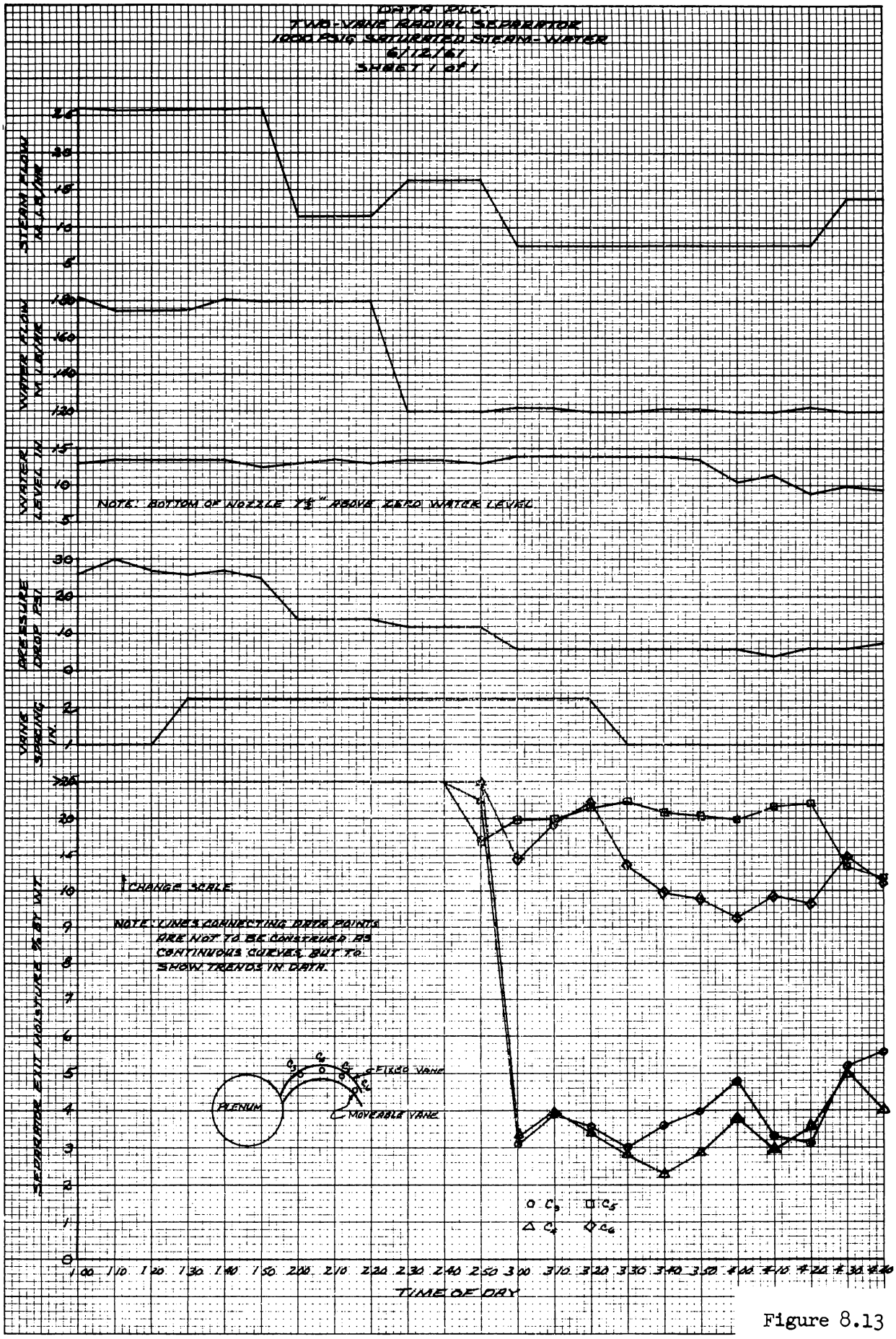
DATA PLOT
TWO-VANE RADIAL SEPARATOR
1000 PSIG SATURATED STEAM-WATER
6/12/61
SHEET 1 OF 1
STEAM FLOW M LB/HR
WATER FLOW M LB/HR
WATER LEVEL IN
NOTE: BOTTOM OF NOZZLE 7½" ABOVE ZERO WATER LEVEL
PRESSURE DROP PSI
VANE SPRING IN.
SEPARATOR EXIT MOISTURE % BY WT
CHANGE SCALE
NOTE: LINES CONNECTING DATA POINTS ARE NOT TO BE CONSTRUED AS CONTINUOUS CURVES, BUT TO SHOW TRENDS IN DATA.
PLENUM
FIXED VANE
MOVEABLE VANE
TIME OF DAY

Figure 8.13

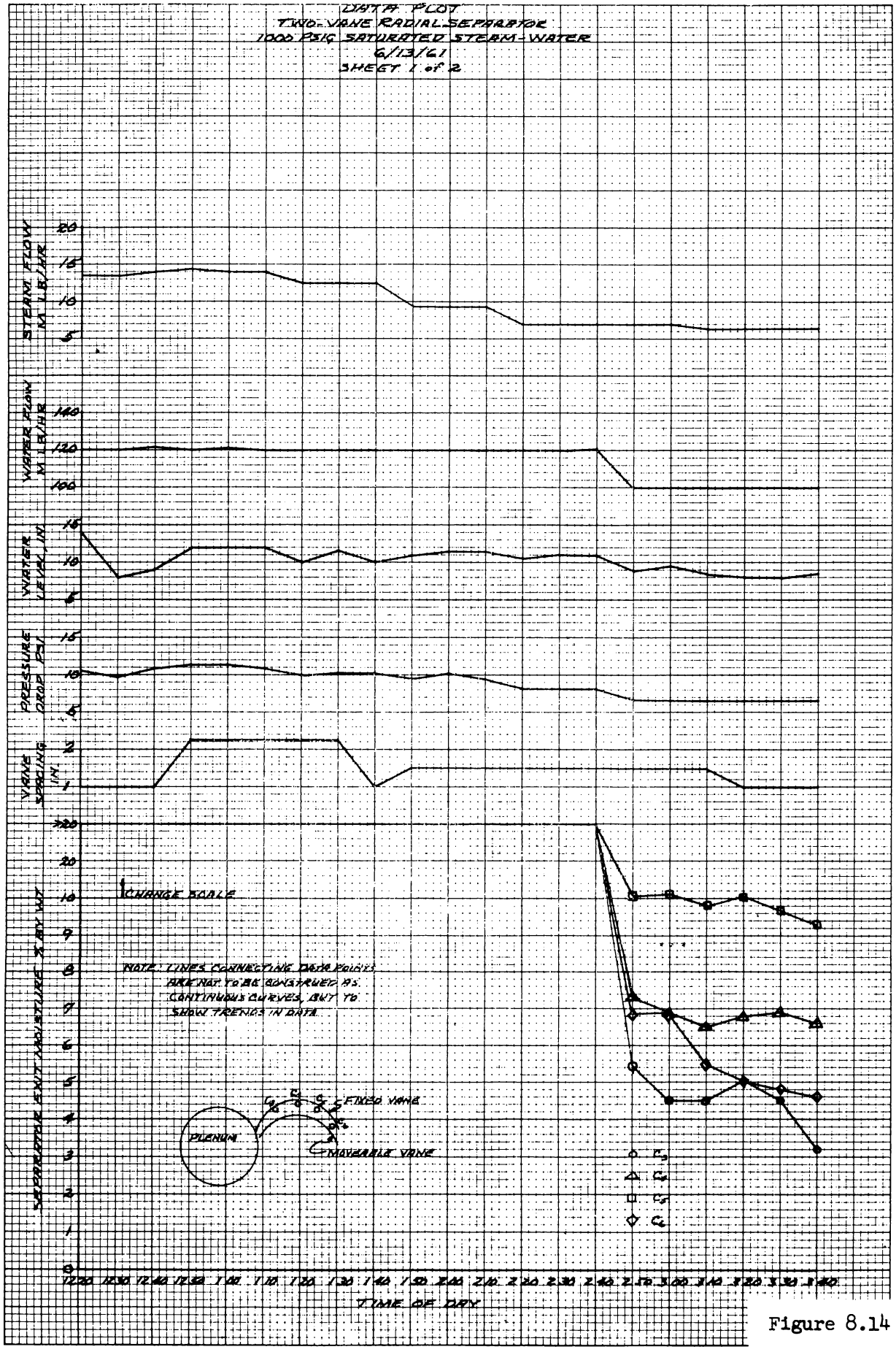
DATA PLOT
TWO-VANE RADIAL SEPARATOR
1000 PSIG SATURATED STEAM-WATER
6/13/61
SHEET 1 of 2
STEAM FLOW M LB/HR
WATER FLOW M LB/HR
WATER LEVEL IN.
PRESSURE DROP PSI
VANE SPACING IN.
SECONDARY EXIT VELOCITY X BY VAT
CHANGE SCALE
NOTE: LINES CONNECTING DATA POINTS ARE NOT TO BE CONSTRUED AS CONTINUOUS CURVES, BUT TO SHOW TRENDS IN DATA
PLENUM
FIXED VANE
MOVEABLE VANE
TIME OF DAY

Figure 8.14

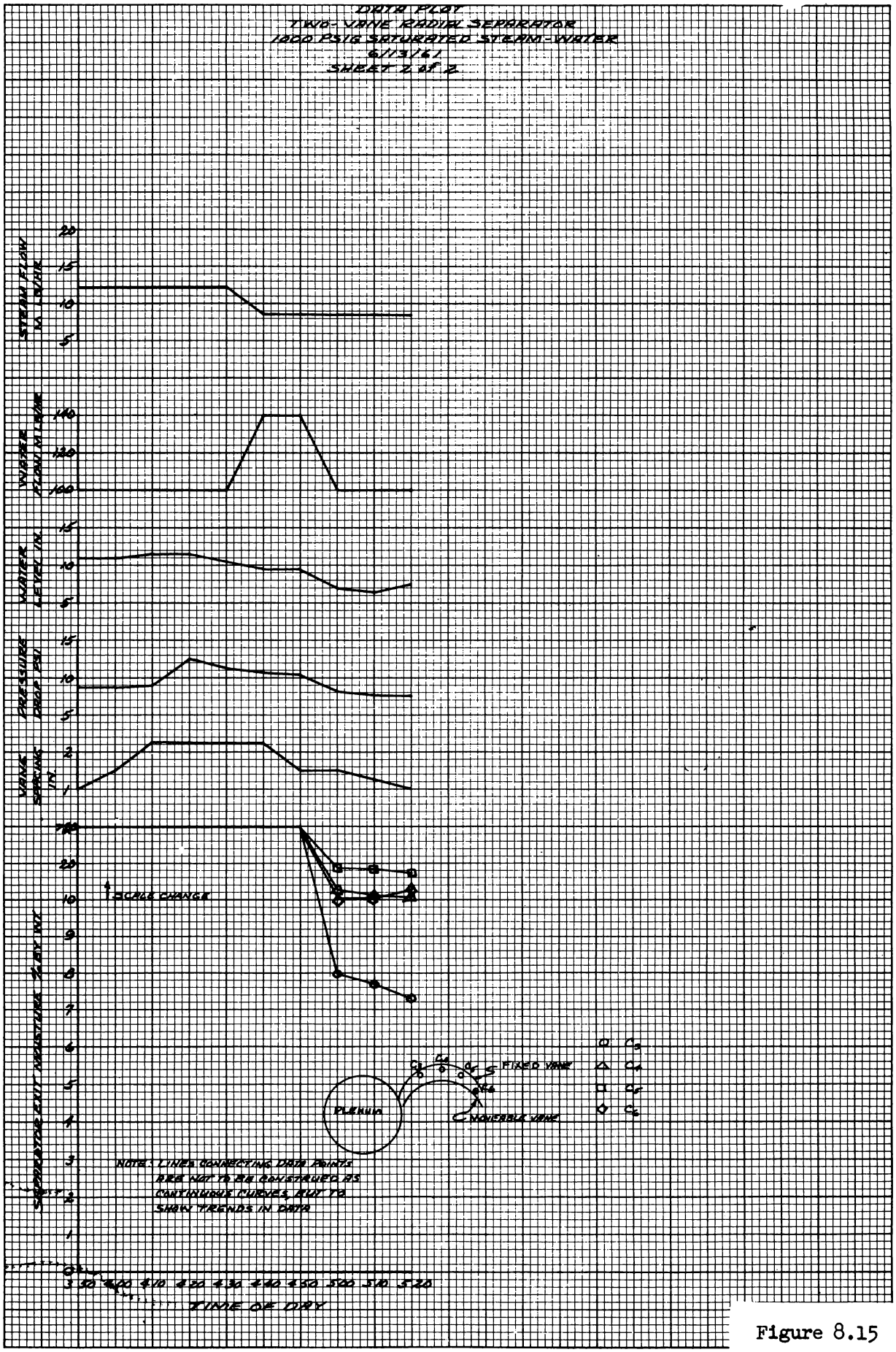
DATA PLOT
TWO-VANE RADIAL SEPARATOR
1000 PSIG SATURATED STEAM-WATER
6/13/61
SHEET 2 OF 2
STEAM FLOW IN LB/HR
WATER FLOW IN LB/HR
WATER LEVEL IN.
PRESSURE DROP PSI
VANE SETTING IN.
SEPARATOR EXIT TEMPERATURE °F BY 10°
SCALE CHANGE
NOTE: LINES CONNECTING DATA POINTS ARE NOT TO BE CONSTRUED AS CONTINUOUS CURVES, BUT TO SHOW TRENDS IN DATA
TIME OF DAY
FIXED VANE
MOVABLE VANE
PLENUM

Figure 8.15

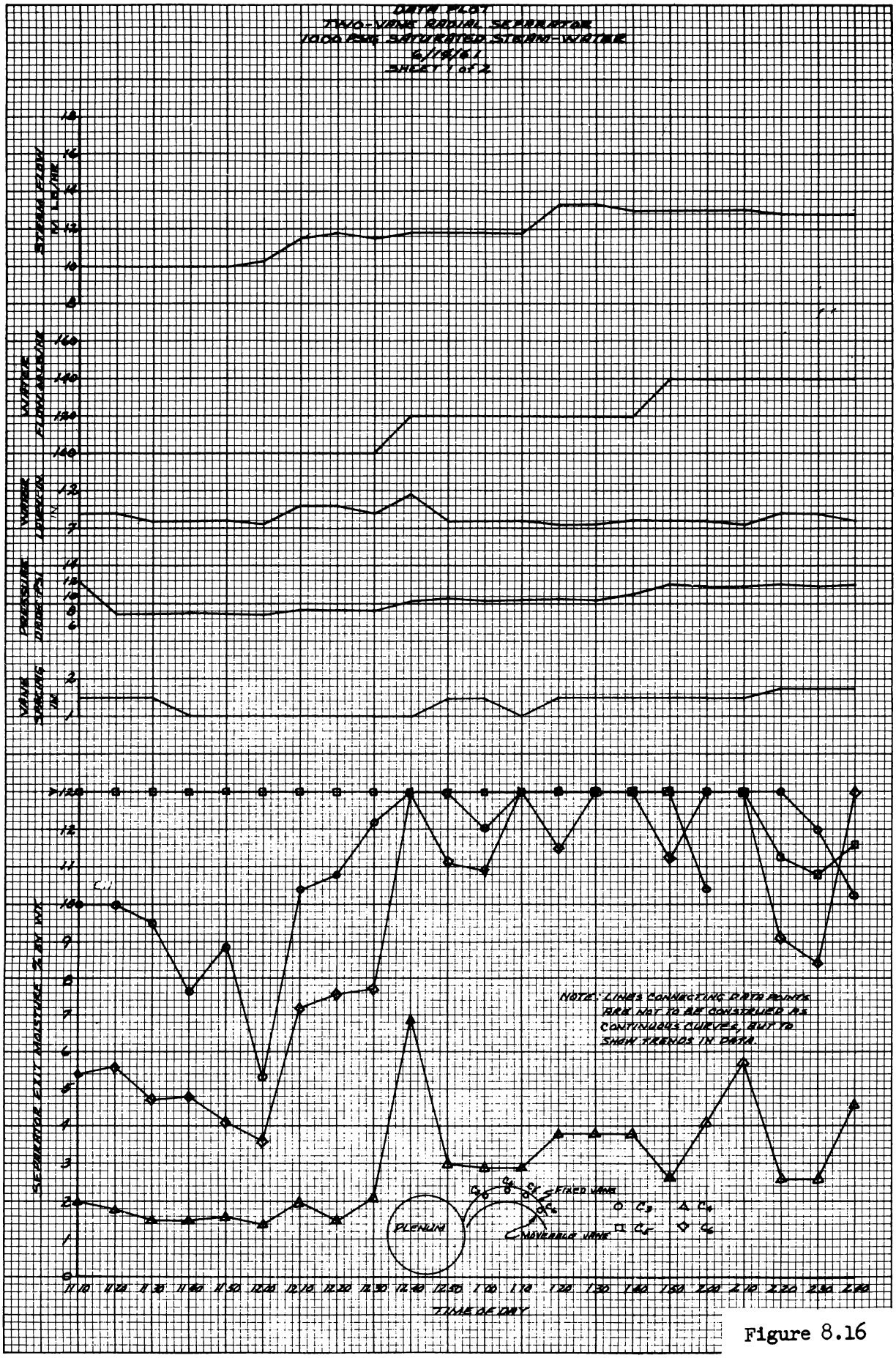
DATA PLOT
TWO-VANE RADIAL SEPARATOR
6/18/81
SHEET 1 of 2
STEAM FLOW
WATER LEVEL
SURGE FLOW
WATER LEVEL
PRESSURE DROP
VANE SETTING
SEPARATOR EXIT MOISTURE
TIME OF DAY
NOTE: LINES CONNECTING DATA POINTS ARE NOT TO BE CONSTRUED AS CONTINUOUS CURVES, BUT TO SHOW TRENDS IN DATA.
FIXED VANE
MOVEABLE VANE
PLENUM

Figure 8.16

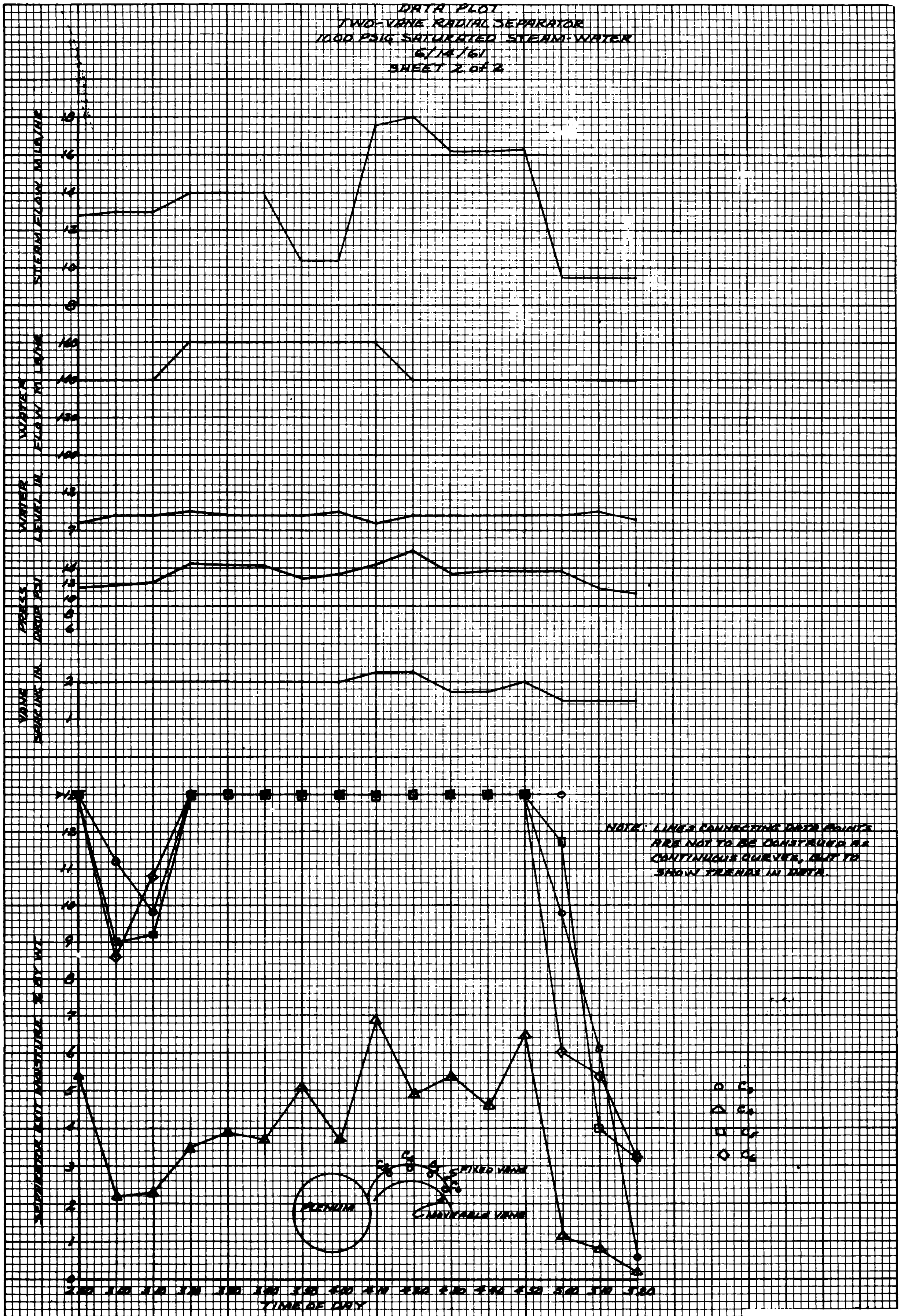
DATA PLOT
TWO-VANE RADIAL SEPARATOR
1000 PSIG SATURATED STEAM-WATER
6/14/61
SHEET 2 of 2
NOTE: LINES CONNECTING DATA POINTS ARE NOT TO BE CONSTRUED AS CONTINUOUS CURVES, BUT TO SHOW TRENDS IN DATA.
PLENUM
FIXED VANE
MOVABLE VANE
TIME OF DAY

Figure 8.17

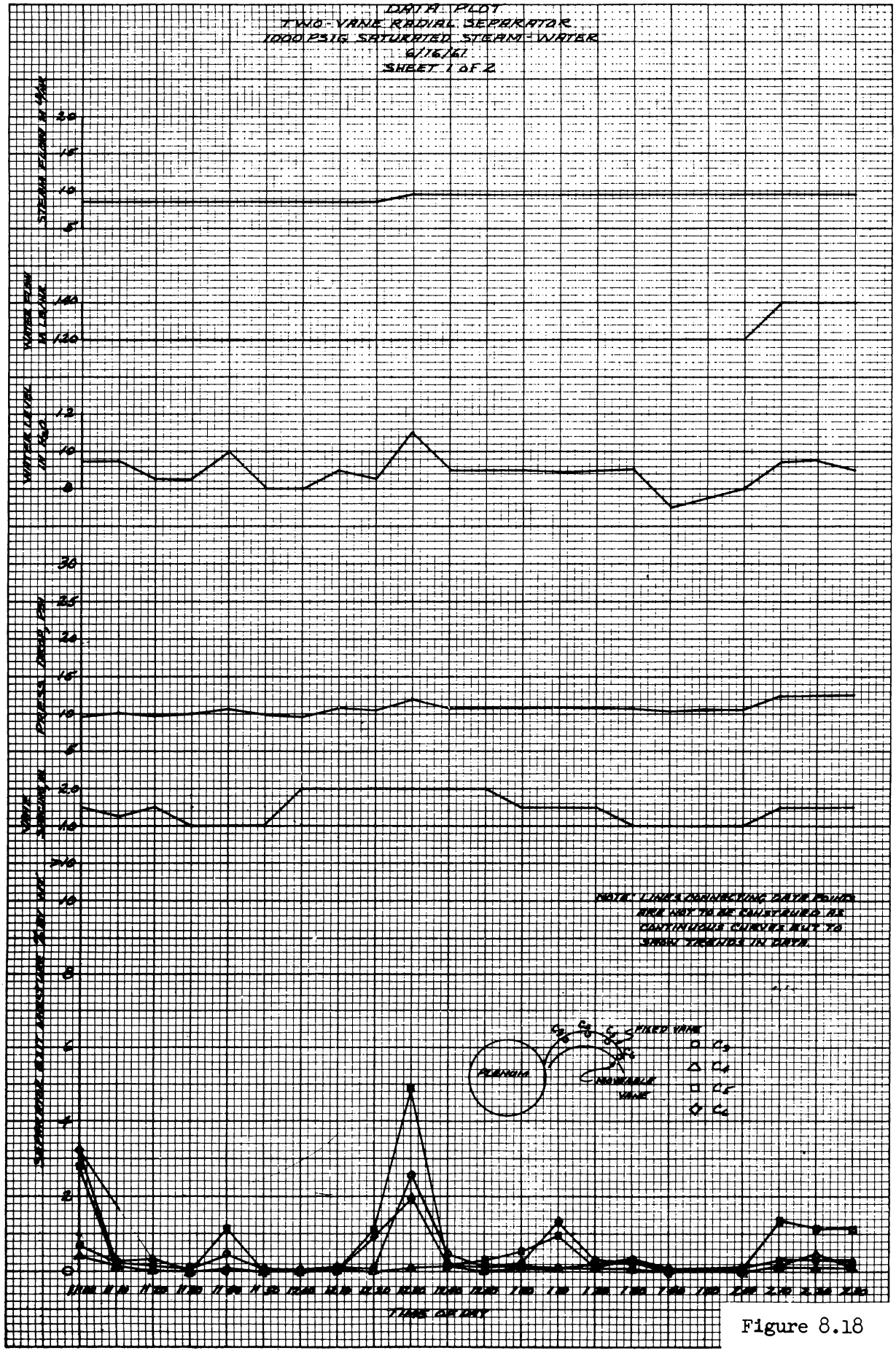
DATA PLOT
TWO-VANE RADIAL SEPARATOR
1000 PSIG SATURATED STEAM-WATER
6/16/61
SHEET 1 OF 2
STEAM FLOW IN 1000 LB/HR
WATER FLOW IN 1000 LB/HR
WATER LEVEL IN INCHES
PRESSURE DROP, PSI
NOTE: LINES CONNECTING DATA POINTS ARE NOT TO BE CONSTRUED AS CONTINUOUS CURVES BUT TO SHOW TRENDS IN DATA.
PLENUM
MIXED VANE
NORMALIZED VALUE
TIME OF DAY

Figure 8.18

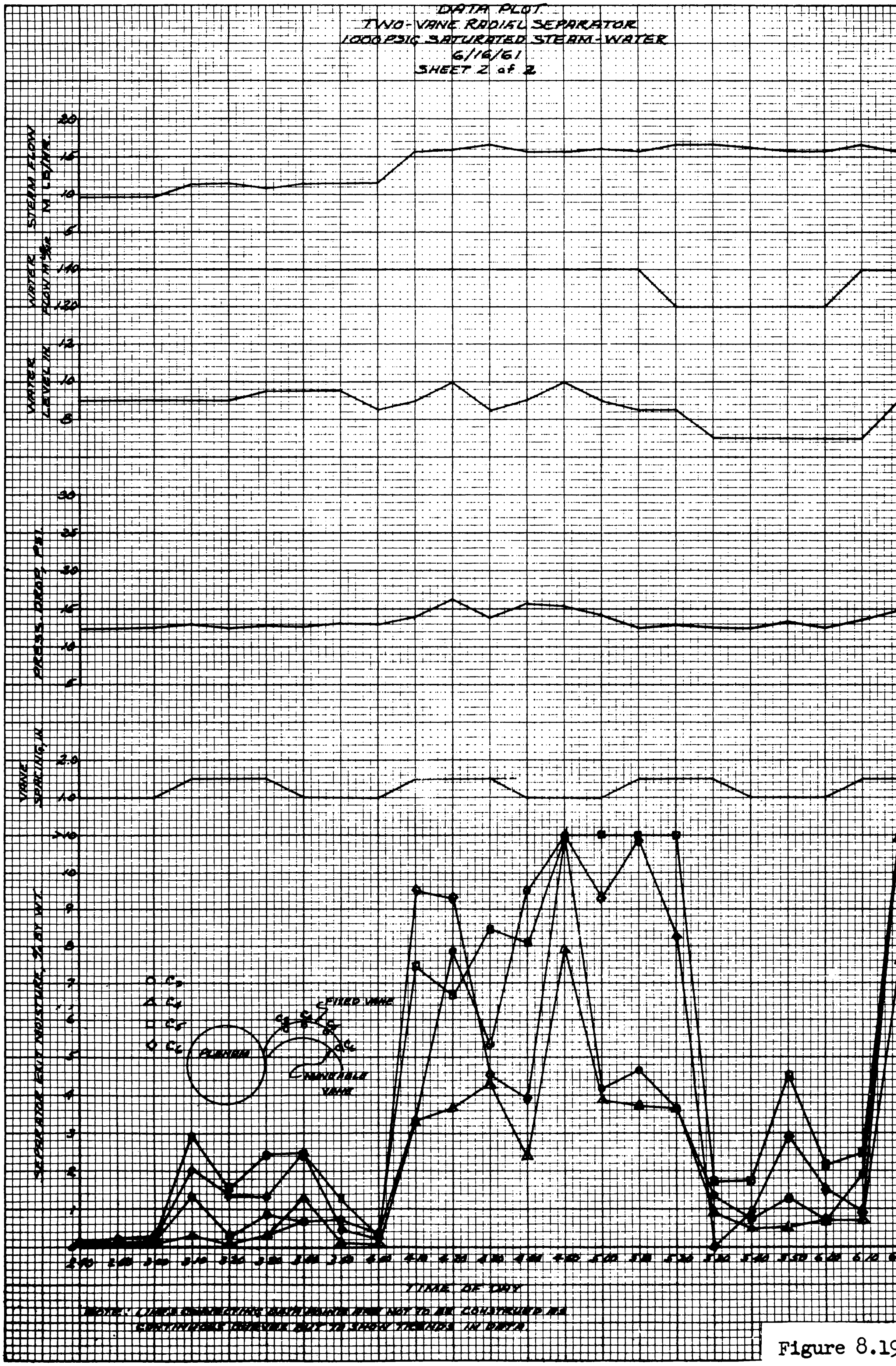
DATA PLOT
TWO-VANE RADIAL SEPARATOR
1000 PSIG SATURATED STEAM-WATER
6/16/61
SHEET 2 of 2
STEAM FLOW M LB/HR.
WATER FLOW
WATER LEVEL IN
PRESS. DROP, PSI
VANE SPACING, IN
SEPARATOR EXIT MOISTURE, % BY WT.
FIXED VANE
PLENUM
MOVEABLE VANE
TIME OF DAY
NOTE: LINES CONNECTING DATA POINTS ARE NOT TO BE CONSTRUED AS CONTINUOUS CURVES BUT TO SHOW TRENDS IN DATA.

Figure 8.19

Although vane spacing and water level show some influence on the carryover results these can be seen to show no significant trend in effect on carryover with the levels and spacings used in the tests. Somewhat better results however, were obtained with water levels below 9 inches than with higher levels. As shown in Figure 8.3, water levels above 7 inches may partially block the nozzle exit.

Impingement on the vessel wall of the water leaving the vanes resulted in splashing and caused a spray of water in the vicinity of the sample tubes. Some of the water droplets may have been picked up by sample tubes C_5 and C_6 and could partially account for the relatively high moisture content of these samples. The greater the vane spacing the greater is expected to be the spray content between vanes. Since samples C_5 and C_6 are nearest the vessel wall these were most effected by the spray.

During these tests some steam probably escaped through the longitudinal gap and out the opening at the lower end of vanes resulting in lower vertical exit velocities than would normally occur. The lack of any significant change in results from vane spacing indicate that good results could be expected from operation with a full circle of vanes at spacing of from 1 to 1 1/2 inches.

8.2 Temperature Actuated Seal Development

8.2.1 Summary

A test program was set up to determine the feasibility and performance of the temperature actuated seal. The results

of these tests are inconclusive at present due to difficulties encountered in the construction of the seals. However, indications are that the seal should perform satisfactorily if construction problems are overcome. A seal incorporating changes designed to eliminate these problems is in the process of construction.

8.2.2 General

Figures 8.20 and 8.21 show the originally proposed temperature actuated seal in detail, and as assembled in a typical installation. The seal is a stainless steel ring with cavities cut around the inside and outside periphery. Between these cavities are slots for the saturated steam flow. Thin (.008") sleeves are welded in place over the cavities, and they are then filled with a low melting alloy (50% Pb - 50% Sn) and sealed by means of filler tubes. As the solder begins to melt (at about 355°F) it exhibits an expansion which deforms the sleeves against the joint and creates a seal.

8.2.3 Test Program

The test program is divided into two phases: (1) Prototype testing, in which the sealing mechanism is to be investigated and evaluated, (2) and environmental testing, in which leackage rates and liquid metal corrosion is to be determined at near reactor conditions. During the course of the prototype tests, methods of constructing the seal are also investigated.

The prototype testing consists of:

8.2.3.1 Tests to evaluate the sleeve expansion as a function of temperature. A model seal is designed which contains a cartrige heater. A mechanical linkage is attached to the sleeve, and connected to a dial indicator, so that

sleeve expansion may be read. The seal temperature is determined by means of a thermocouple.

8.2.3.2 Tests to estimate the contact pressure of the sleeve in the pipe joint. This is done by constructing four sleeves 1/32" thick and of varying inside diameters such that the cold clearance varies from .004" to .016" on the diameter. Strain gages are attached to these sleeves to measure circumferential strain. An average contact pressure can be estimated from this data.

8.2.3.3 Tests to determine the effect of increasing the restraint on the upper and lower ends of the sleeve. It is felt that this would increase the sleeve expansion by confirming the solder expansion to a smaller area. This is done by making heavy collars which fit over the sleeve at each end, and can be moved progressively closer together. The sleeve expansion vs. temperature is measured at each collar position.

8.2.4 Test Equipment

The environmental test fixture consists of a two-chambered can whose dimensions reproduce the reactor assembly as closely as possible (See Fig. 8.20).

The seal fits between the inner and outer walls of the can. The superheat conditions are simulated by means of small, high-power cartridge heater mounted in the inside chamber (superheat tube), which radiates to the seal. A thermocouple mounted on the other side of the wall measures this temperature. The entire fixture is mounted in an autoclave filled with saturated water at 1000 psi.

The pressure in each of the fixture chambers may be varied independently; and by doing so, leackage flow may be drawn off, condensed, and measured.

The corrosion test consists of stainless steel capsules filled with solder and run at temperature for varying lengths of time. Photomicrographs of these capsules should indicate the effect of the molten solder on the steel.

8.2.5 Test Results

8.2.5.1 Prototype Tests

The results of the prototype tests are inconclusive at present, due to difficulty encountered in the construction of the seals. The two major problem areas are the sleeve weld and the method of filling the seal. The latter problem is the most serious in as much as liquid metal leaks at the closure joints, and air bubbles and gas inclusions in the solder do not allow proper expansion to take place. Qualitatively, the results available indicate that the seal should perform satisfactorily if it can be properly constructed. The results of the restraint tests tend to show that the added expansion of the sleeve is offset by the increased sleeve regidity, so that not much improvement is noted. No other test results are available to date.

8.2.6 Seal Construction

Several modifications in the original seal design (Fig. 8.20 & 8.21) have been made in an attempt to eliminate construction difficulties. Since filling the seal after the sleeve welds are made created problems in closure weld leakage, a method was devised to fill the seal prior to the sleeve weld. In order to eliminate gas voids, this is done in a

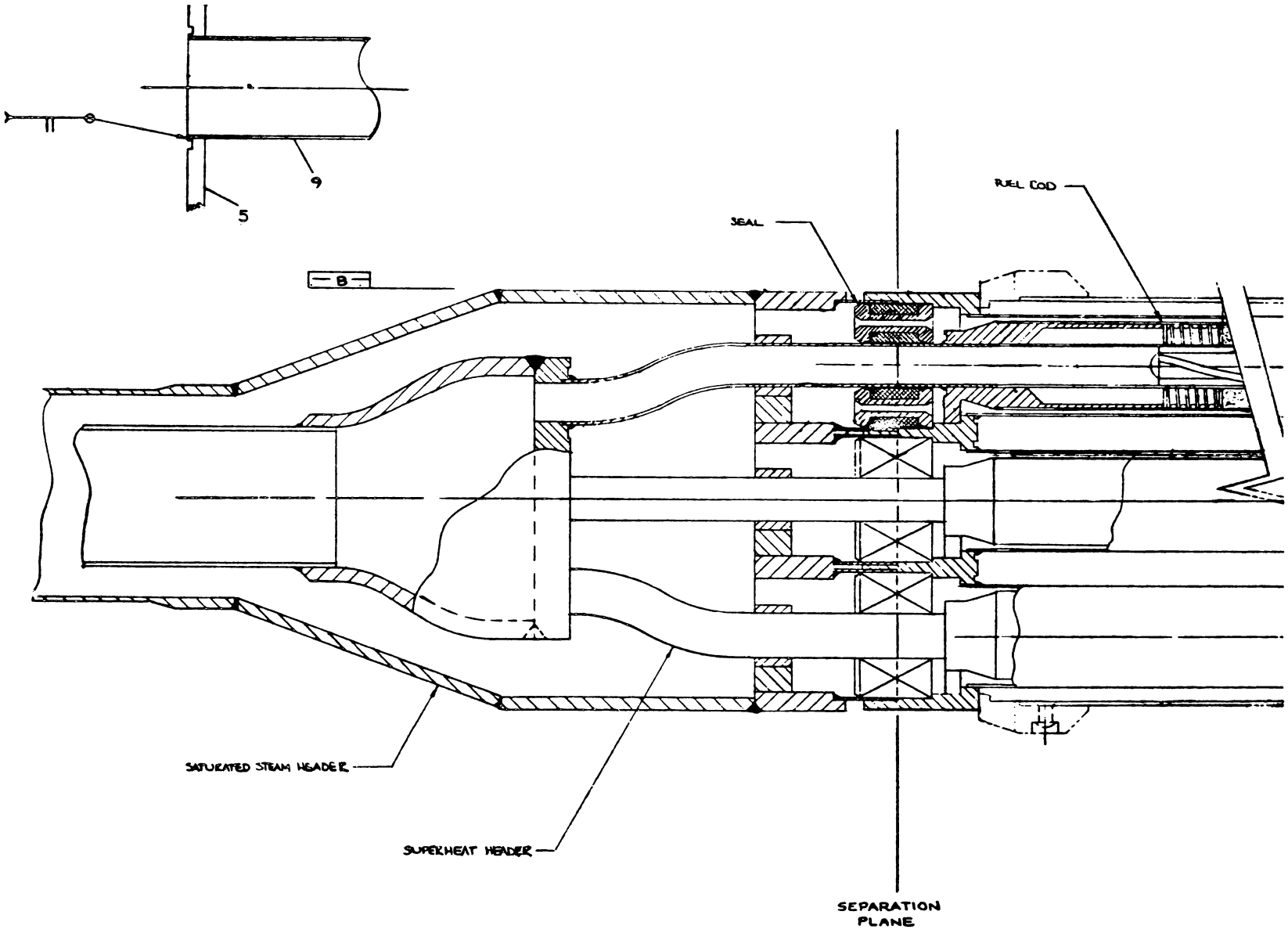

Figure 8.20

FUEL ASSEMBLY

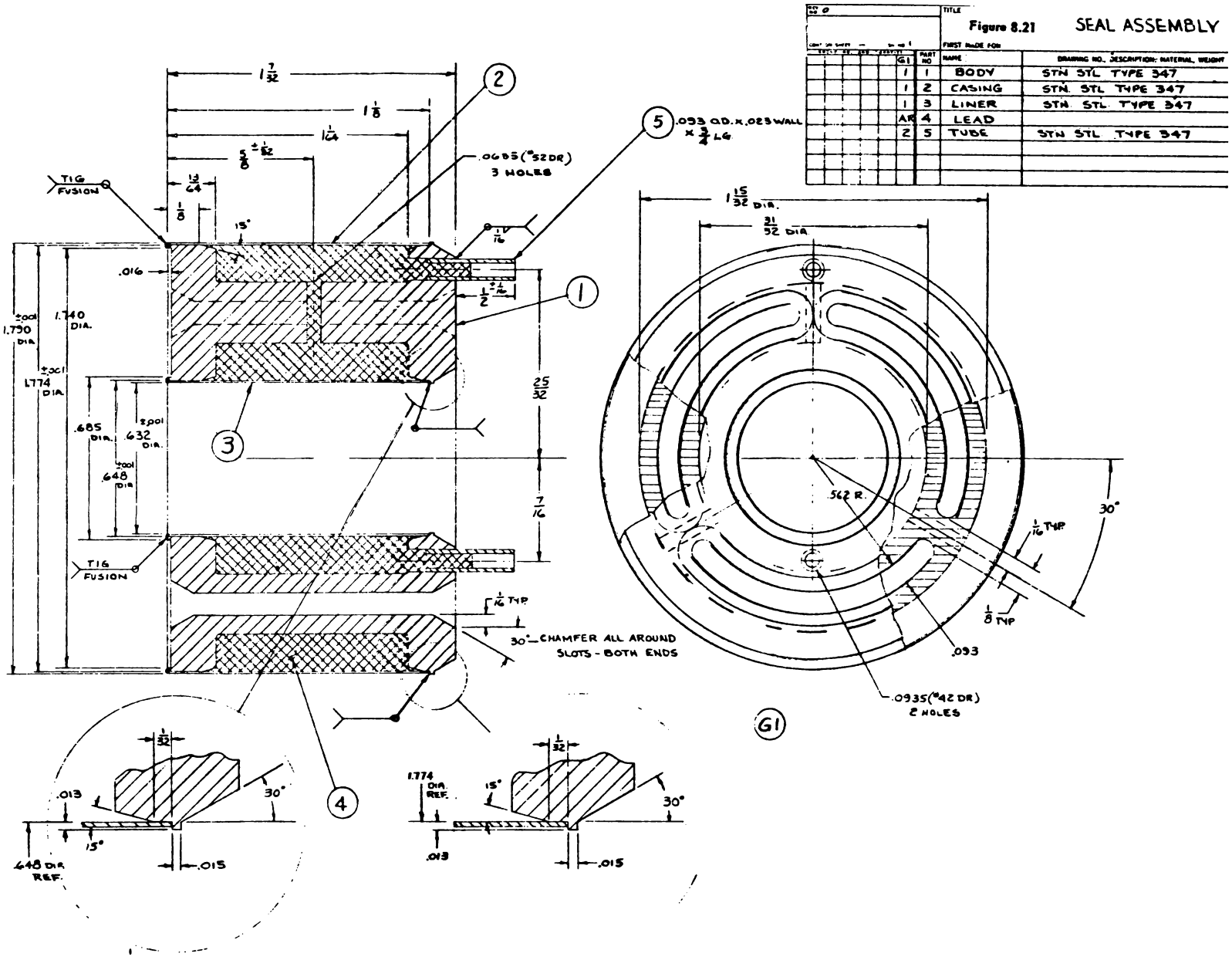
Figure 8.21
SEAL ASSEMBLY
TITLE
FIRST MADE FOR
NAME
DRAWING NO., DESCRIPTION: MATERIAL, WEIGHT
PART NO.
G1
BODY
STN STL TYPE 347
CASING
STN. STL TYPE 347
LINER
STN. STL. TYPE 347
LEAD
TUBE
STN STL TYPE 347
1 7/32
1 1/8
1 1/24
5/8 ±1/32
13/64
1/8
15°
TIG FUSION
.0685 (#52 DR) 3 HOLES
.093 O.D. x .023 WALL x 3/4 LG
1/16
.016
1/2 +1/64
1.740 DIA.
1.790 ±.001 DIA.
1.774 ±.001 DIA.
.685 DIA.
.632 ±.001 DIA.
.648 ±.001 DIA.
25/32
7/16
TIG FUSION
1/16 TYP
30° CHAMFER ALL AROUND SLOTS - BOTH ENDS
1 15/32 DIA.
31/32 DIA.
.562 R.
1/16 TYP
30°
1/8 TYP
.093
.0935 (#42 DR) 2 HOLES
G1
1/32
.013
30°
15°
.448 DIA REF.
.015
1.774 DIA REF.
.013
1
2
3
4
5

vacuum. The solder is essentially cast in place and machined to size. The sleeves are then pressed on and welded in place.

The difficulty encountered in welding the 8 mil. sleeve to the seal was overcome by redesigning the sleeves so that they are 30 mils. at each end, and taper down to the 8 mil. thickness at an 8° angle. This has the added advantage of reducing the stress concentration in the sleeve as expansion occurs.

A seal incorporating these changes is in the process of construction.

9.0 TASK H - SADE AND E-SADE

9.1 Sade

9.1.1 Sade Irradiations

9.1.1.1 SH-4B

Operation of VBWR was resumed at the start of this report period, after completion of changes of materials and some revision in design details to the reactor to avoid difficulties which were being experienced with 17-4 Ph material. Design of SADE equipment was reviewed and all 17-4 Ph material changed to recommended heat treatment specification.

Fuel element SH-4B was reinstalled in the reactor and the irradiation program interrupted by the 17-4 Ph reactor outage was resumed. Because it was expected that reactor operations would reach 33 MW, at which power the expected power from SH-4B would reach 111 kw, revised operating conditions were calculated for the SH-4B element. Table 9.1 gives information on the expected conditions for the revised reactor power.

TABLE 9.1

SH-4B DESIGN CONDITIONS

	Initial	Revised
Power	100 kw	111 kw
Fuel enrichment (nominal)	4.5% U^{235}	
Fuel enrichment (measured)		4.55% U^{235}
Steam pressure	1000 psia	
Active fuel length	36"	
Outer clad, outside diameter	1.25"	
Inner clad, outside diameter	0.75"	
Clad thickness, outer and inner	0.028"	
Clad material (weld-drawing tubing)	304 S.S.	
Instrument tube, outside diameter	0.50"	
Fuel (UO_2) % theoretical density	95%	
Total fuel loading (UO_2)	3.76 Kg	
Max. clad temperature (STEADY)	1200°F	1200°F

	Initial	Revised
Max. superheat exit Temp. (STEADY)	925°F	925°F
Max. heat flux (STEADY)	332,000 Btu/hr-ft^2	375,000 Btu/hr-ft^2
Min. steam flow rate (STEADY)	1032 lbs/hr	1155 lbs/hr
Maximum fuel temp. (STEADY)	3030°F	3246°F
Maximum clad temperature (Transient*)	1292°F	
Maximum superheat exit temp. (Transient*)	980°F	
Maximum heat flux (Transient*)	330,000 Btu/hr-ft^2	
Minimum steam flow rate (Transient*)	915 lbs/hr	
Maximum fuel temperature (Transient*)	3116°F	

* The transient conditions may be achieved for short intervals to obtain test data; extended operation will be in accordance with the limits for steady conditions.

For the revised operating power transient conditions were calculated based upon a 36 MW reactor power transient as shown in Table 9.2.

TABLE 9.2

SH-4B DESIGN TRANSIENT CONDITIONS

Maximum clad temperature	1276°F
Maximum exit temperature	968°F
Maximum heat flux	408,000 Btu/hr-ft^2
Maximum steam flow (**)	1155 lbs/hr
Maximum fuel temperature	3502°F
Power	121 kw

** This transient assumed that flow was held steady during the power transient of the reactor.

Re-installation of the hot (previously irradiated) element SH-4B in the SADE loop was successfully accomplished, but the re-assembly was difficult since it had to be accomplished in the reactor vessel, working through a refueling port. During reactor start-up, cooling of the element was unsatisfactory therefore, it was necessary to disassemble the equipment and reassemble in a procedure which assured the maximum probability of correct reassembly. This included raising the fuel element

process tube assembly up into the throat of the reactor refueling port to provide better visability to the technicians making the installation. The second reassembly attempt was successful and the testing program continued. Assembly difficulties with seals, remote coupling of coolant flow piping, are more difficult with SADE test loop because of replacement requirements, however; it is expected that these difficulties may be typical of superheat reactors.

Irradiation of element SH-4B continued until May 24. Reactor operational problems resulting from radioactivities seemed to indicate that the SADE loop was adding to high activities present from defected boiling water fuel elements. (See Section 6.0) Further sampling tests of the SADE element inlet and outlet steam confirmed that the SH-4B element cladding was defective and that the element was contributing fission products to the reactor off-gas system. Since reactor operations were very limited under these conditions and the test was not intended as a defected superheat element test, SH-4B was removed from the reactor. Subsequent examination of the element confirmed the defect in the cladding of this fuel element. Details of the examinations on this element are included in Section 3.0.

During the testing of this element, it operated at 1000 psig steam pressure, with superheated steam exit temperatures up to 900°F, and power outputs up to 96 kw thermal. Heat fluxes were calculated to be up to 320,000 Btu/hr-ft^2, and clad temperatures were calculated to be as high as 1150°F. The

operating history of this element is summarized in Section 3.0.

9.1.1.2 SH-4

Fuel element SH-4 was installed early in June and has been operating satisfactorily since that time. Because of the lower enrichment of this element, the power output has been less than was achieved with SH-4B, and heat fluxes were correspondingly reduced. The design conditions for SH-4, in the present VBWR core, are shown on Table 9.3.

TABLE 9.3

SH-4 DESIGN CONDITIONS

Power	73 kw
Fuel enrichment	3.5% U^{235}
Steam pressure	1000 psia
Active fuel lengths	36"
Outer clad, outside diameter	1.25"
Inner clad, outside diameter	0.75"
Clad thickness, outer and inner	0.028"
Clad material (weld-drawn tubing)	304 S.S.
Instrument tube, outside diameter	0.50"
Fuel (UO_2) % theoretical density	95%
Total fuel loading (UO_2)	3.79 Kg
Maximum clad temperature (STEADY)	1200 F
Maximum superheat exit temp. (STEADY)	937 F
Maximum heat flux (STEADY)	240,000 Btu/hr-ft^2
Minimum steam flow rate (STEADY)	750 lbs/hr

The SH-4 incorporates a "gum-drop" experiment in the upper section to determine relative movement between clad and fuel during the operating period.

9.1.1.3 SH-1

The defected SH-1 test program has been planned and the predicted operating conditions calculated for this element. Design operating conditions for this element are shown on Table 9.4.

TABLE 9.4

SH-1 DESIGN CONDITIONS AT VBWR POWER OF 33 MW(T)

Power	70 kw
Fuel enrichment	2.3% U^{235}
Steam pressure	1000 psia
Active fuel length	36"
Outer clad, outside diameter	1.25"
Inner clad, outside diameter	0.75"
Clad thickness, outer clad	0.049"
Clad thickness, inner clad	0.035"
Outer clad material (weld-drawn tubing)	304 S.S.
Inner clad material (weld-drawn tubing)	347 S.S.
Instrument tube, outside diameter	0.500"
Fuel (UO_2) % theoretical density	95%
Max. clad temperature (STEADY)	1200 F
Max. superheat exit temp. (STEADY)	933 F
Max. heat flux (STEADY)	234,000 Btu/hr-ft^2
Min. steam flow rate (STEADY)	710 lbs/hr
Max. fuel temperature (STEADY)	2470 F
Low Flow Transient Conditions:	
Power	70kw
Flow rate	625 lb/hr
Max. fuel temperature	2550 F
Max. clad temperature	1300 F
Max. heat flux	232,000 Btu/hr-ft^2
Overpower Transient Conditions:	
Power	77kw
Flow rate	710 lbs/hr
Max. fuel temp.	2670 F
Max. clad temp.	1280 F
Max. heat flux	258,000 Btu/hr-ft^2

If the power is higher than predicted the operation will continue at the higher power provided the fission product release is not excessive and the element power does not exceed 100 KW. A new design test power will be established upon the basis of measured power generation and the steam flow trip and alarm will be adjusted to correspond to the new power.

9.1.2 Defective Fuel Test (SH-1)

During irradiation of SH-2 in May, 1959, the element developed a crack, allowing the release of fission product into the steam. Accurate

measurements of the amount of release radioactivity were not made at that time.

The irradiation of a defective superheat element was scheduled in order that more accurate data could be obtained concerning the release of fission products and their subsequent carryover to the turbine.

The defect in SH-1 is a 0.040" hole drilled into the upper end plenum.

9.1.3 SADE COUPON TESTING

Design of an instrument tube incorporating cladding test coupons has been completed and fabrication of the assembly initiated. This arrangement provides for exposure of a number of coupons to the superheated steam and to the neutron flux which is encountered by the fuel cladding. Plans are to utilize this instrument tube during the irradiation of SH-5 fuel element.

Test coupons, cut from tubing samples which are suitable for fuel cladding, have been preapred. Materials included are 304, 304E, 304L, 316, and 347. Most coupons were prepared from a transverse section of the tubing from which the coupons were cut, but a few coupons of 304 material were prepared to provide a longitudinal section for test. Figure 9.1 shows this instrument tube assembly. Previous plans, which were to irradiate coupon samples within a fuel element section, have been revised to substitute this arrangement for obtaining irradiated cladding samples. Greater flexibility, an increased number of specimens, and less interference with fuel elements tests are provided by this method.

9.1.4 NUSU IRRADIATION

Drawings of the special equipment necessary for installation of the NUSU fuel element in the SADE loop were prepared and orders were placed on the shop for this special equipment. The NUSU fuel element is to be attached

REV NO.	D12
DRAW NO.	762D273
CONT ON SHEET	SH NO.

TITLE ASSEMBLY — CONT ON SHEET — SH NO.
INSTRUMENT TUBE
FIRST MADE FOR SADE FCF

DRAW NO.	CHD	QUANTITY G2	QUANTITY 61	PART NO.	NAME	DRAWING NO., DESCRIPTION, MATERIAL, WEIGHT
			1	1	TUBE	ASTM A-269 TP 304 WD STN. STL
			2	2	SEPARATOR	ASTM A 167 TP 304 STN. STL.
			4	3	SUPPORT	ASTM A 167
			12	4	SPACER	ASTM A 167
			1	5	PIN	ASTM A 276
			1	6	NOSE	ASTM A 276 TP 304 STN. STL
		X	1	7	TEST ASM	G2 THIS DWG
		1		8	SUPPORT	ASTM A 167 TP 304 STN. STL.
		AR		9	SPECIMEN	RAD MAT, SPECIMEN PER ENG INST.
		AR		10	WIRE	PER ENG INST

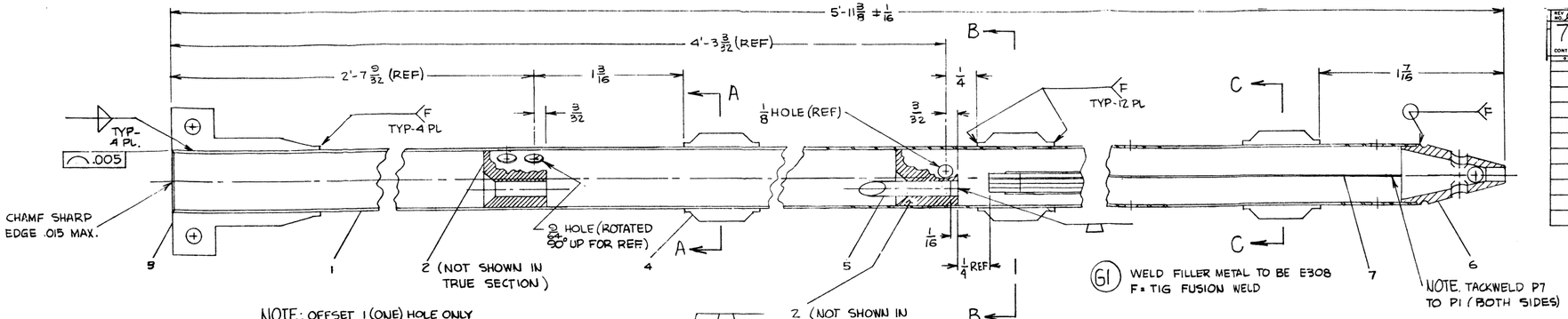

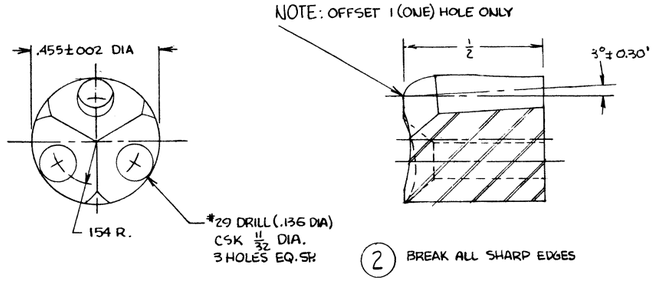

(2) BREAK ALL SHARP EDGES

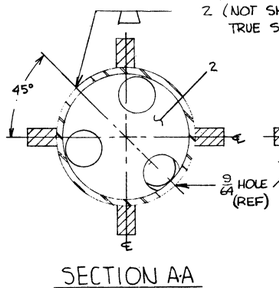

SECTION A-A

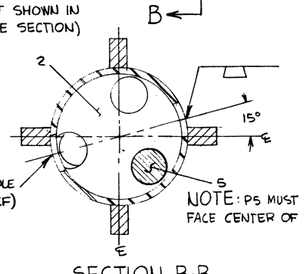

SECTION B-B

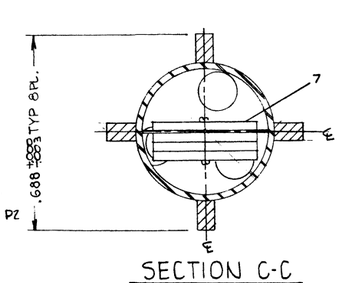

SECTION C-C

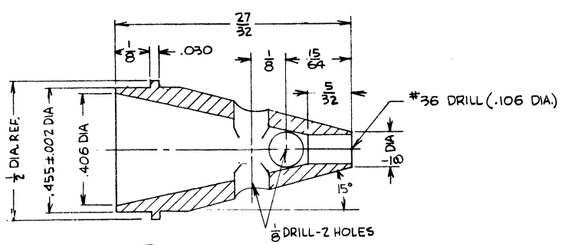

(6) 1/2 DIA BREAK SHARP EDGES

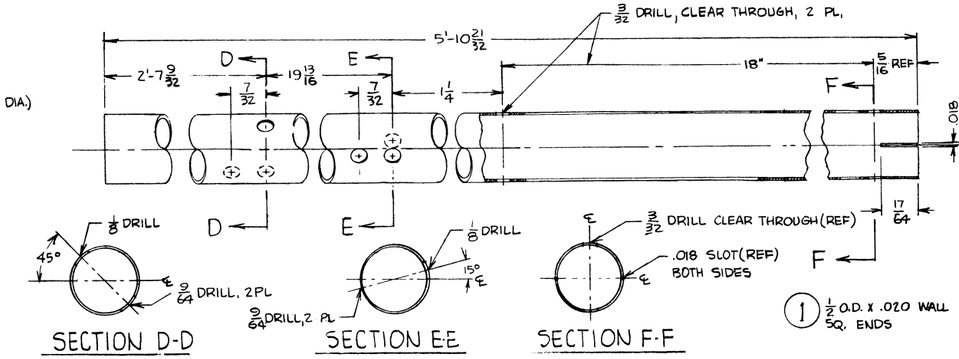

SECTION D-D SECTION E-E SECTION F-F

(1) 1/2 O.D. X .020 WALL SQ. ENDS

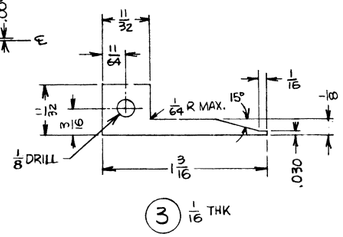

(3) 1/16 THK

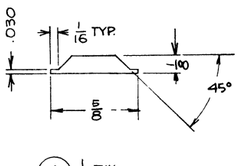

(4) 1/16 THK.

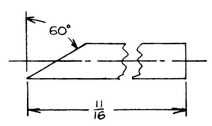

(5) 1/8 DIA

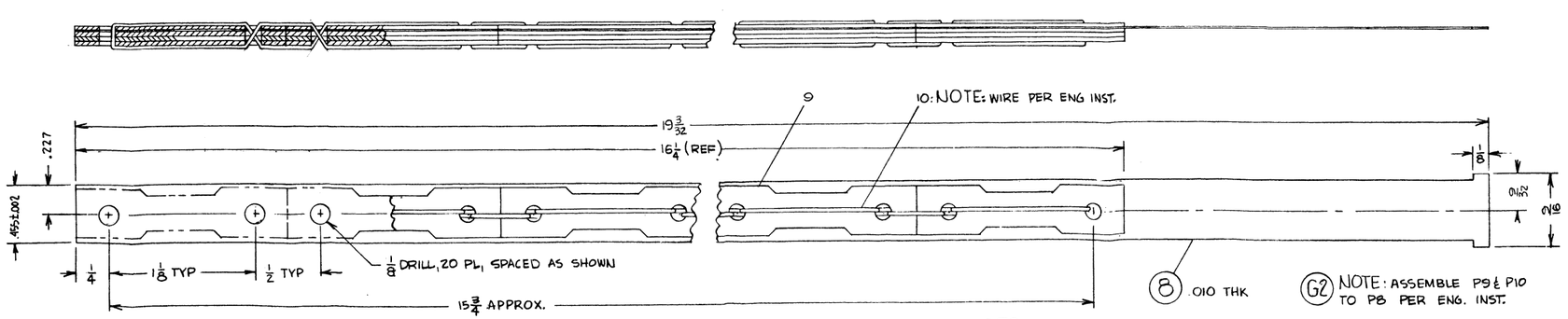

(8) .010 THK

(G2) NOTE: ASSEMBLE P9 & P10 TO P8 PER ENG. INST.

Figure 9.1

by welding to the hardware required for this installation, with the fuel element functioning essentially as the process tube in a standard SADE installation. The large upper flange required on the NUSU fuel assembly, to adapt it to the SADE loop, has necessitated the design of a special container for this element. The container dimensions are such that it will require the E-SADE cask to handle this element when in the container.

Figure 9.2 shows the installation of this element.

The NUSU combination-boiling superheat element is 3.5% enriched, with the predicted operating conditions shown in table 9.5.

The following considerations led to the present values selected for use in this table:

1) The use of 150 instead of 500 Btu/hr-ft^2 as a more realistic value for the clad-to-fuel contact coefficient for the inside fuel cladding.

2) The use of the latest axial power profile for the SADE loop position with a 1.58 peak to average ratio.

3) The use of a correction factor for the steam film coefficient, so that the temperature used to evaluate it is the average film temperature instead of the bulk steam temperature.

4) The use of the burn-out heat flux correlation that is presently used by VBWR Operations, instead of the correlation used in the COF2 code.

TABLE 9.5

NUSU OPERATING CONDITIONS AT VBWR POWER OF 36 MW(E)

Power	122 kw
Fuel enrichment	3.5% U^{235}
Steam pressure	1000 psia
Active fuel length	34.5"
Outer clad, outside diameter	1.50"
Outer clad thickness	0.028"
Outer clad material	347 S.S.
Inner clad, outside diameter	1.072"
Inner clad thickness	0.025"
Inner clad material	Inconel X

104R654

SADE NUSU TEST INSTALLATION
FIRST MADE FOR GEN NUCLEAR ENG. CORP

PL ISSUED

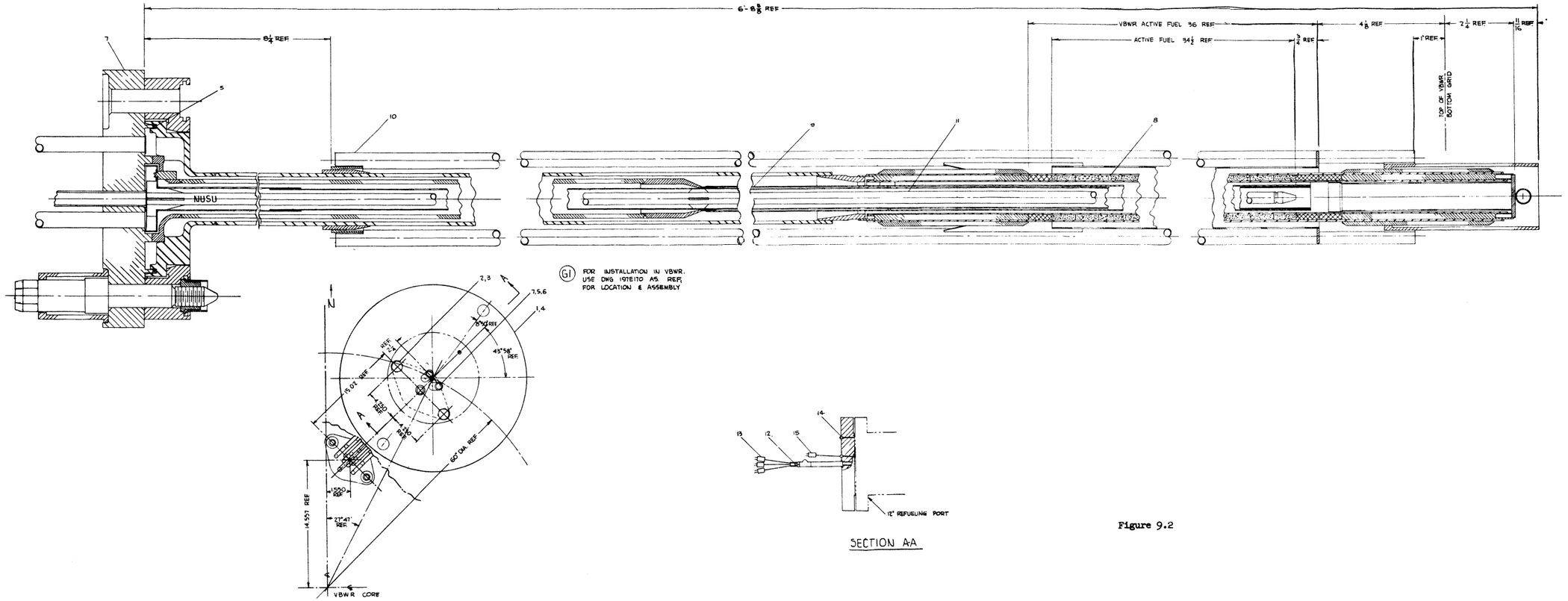

Figure 9.2

Outer steam supply tube, outside diameter	0.814"
Water flow tube, outside diameter	2.00"
Water flow tube thickness	0.049"
Fuel (UO_2) % theoretical density	95%
Total fuel loading (UO_2)	4.248 kg
Maximum clad temperature (STEADY)	1192 F
Maximum superheat exit temperature (STEADY)	743 F
Maximum steam side heat flux (STEADY)	248,000 Btu/hr-ft^2
Maximum water side heat flux (STEADY)	413,000 Btu/hr-ft^2
Minimum steam flow rate (STEADY)	755 lbs/hr
Minimum burnout ratio (STEADY)	2.42
Maximum fuel temperature (STEADY)	3330 F
Maximum clad temperature (TRANSIENT*)	1280 F
Maximum superheat exit temperature (TRANSIENT*)	781 F
Maximum steam side heat flux (TRANSIENT*)	244,000 Btu/hr-ft
Maximum water side heat flux (TRANSIENT*)	416,000 Btu/hr-ft
Minimum steam flow rate (TRANSIENT*)	645 lbs/hr
Minimum burnout ratio (TRANSIENT*)	2.40
Maximum fuel temperature (TRANSIENT*)	3370 F
Inside clad-to-fuel contact coefficient	150 Btu/hr-ft^2-^{o}F
Outside clad-to-fuel contact coefficient	1000 Btu/hr-ft^2-^{o}F
VBWR Power	36 MW
Axial peaking factor	1.58

* The transient conditions may be achieved for short intervals to obtain test data; extended operation will be in accordance with the limits for steady conditions.

9.2 E-Sade

9.2.1 Summary

Design and procurement of equipment for the E-SADE test loop continued throughout this report period. This covered all phases of this activity, including fuel, the instrumentation and control system, reactor internals, all piping systems, condenser and auxiliary equipment and the new reactor enclosure penetration required for instrumentation and control system circuits and the secondary cooling system. The safeguards report for the E-SADE system was completed and forwarded to AEC, see Section 11.0.

9.2.2 Incore Assembly

The initial design of the reactor in-core assembly provided for nine removable fuel elements, but because of space limitations in the reactor core, it was necessary to provide for the fuel spacers for

this arrangement to be part of the process tube assembly. It was decided that this limitation was serious enough to consider other arrangements which provided means for having spacers attached to the fuel element. A design was completed, providing for such spacer arrangements, but providing replacability only for the center fuel element, with the remaining eight assemblies installed in welded process tube assemblies. Thus, this arrangement does not provide the flexibility with regard to installation and exchange of fuel elements furnished in the first design. This design is shown in Figure 9.3. Design of remaining reactor internal equipment was completed and checked, and orders for manufacture of these components were placed with the APED shop. Procurement of materials for this equipment is in progress.

9.2.3 Fuel Assembly (ESH-1)

The assembly is being manufactured for installation as the ESH-1 (initial E-SADE test fuel section) test assembly. The characteristics of the first nine fuel assemblies to be installed are shown on Table 9.6. The elements will be of the bayonet type similar to the SADE series, 8 of these being nonreplaceable, one in the center being replaceable. The analytical work completed consisted of the determination of thermal and hydraulic characteristics, fission gas release and internal pressure buildup, and stress analysis for the prediction of cycles to failure on the cladding material.

Upon completion of the analytical study, detail design drawings of these elements were completed and issued. The general design description is as follows:

198E282

TITLE: NINE ELEMENT FUEL ASSEMBLY
FIRST MADE FOR SHNEE II FCF 7178E79

PL ISSUED

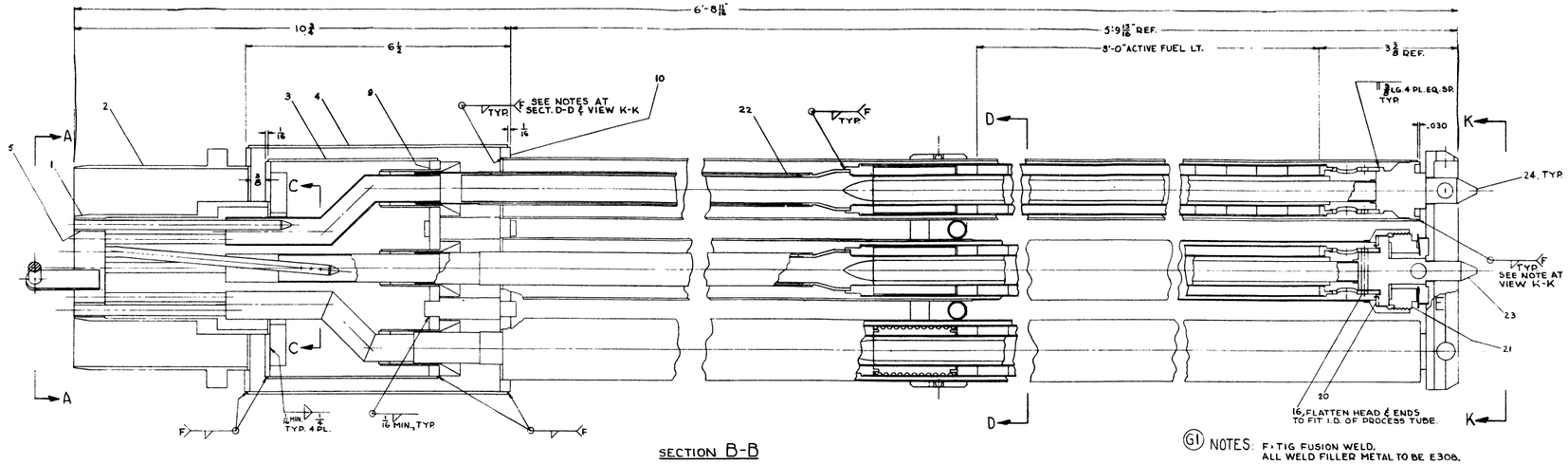

SECTION B-B

(G1) NOTES: F: TIG FUSION WELD.
ALL WELD FILLER METAL TO BE E308.

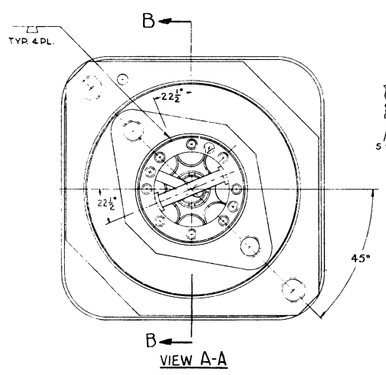

VIEW A-A

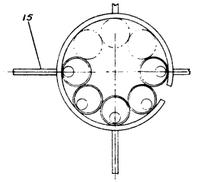

SECTION C-C
DO NOT WELD PT OF B TO P15

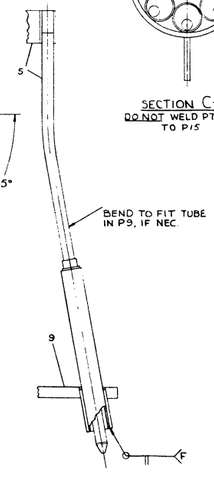

SECTION H-H

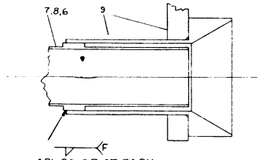

4 PL. EQ. SP. AT EACH TUBE LOCATION

SECTION G-G

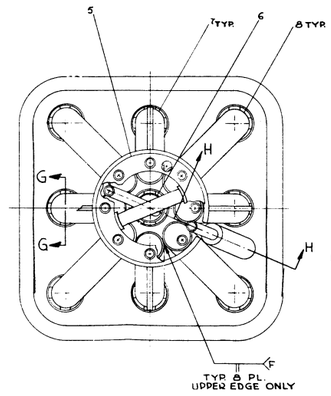

VIEW A-A
(P1,2,3 & 4 REMOVED)

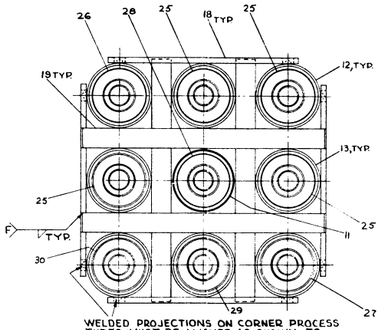

WELDED PROJECTIONS ON CORNER PROCESS TUBES MUST BE ALIGNED AS SHOWN, TO LOCATE AND HOLD PARTS 18 & 19.

SECTION D-D

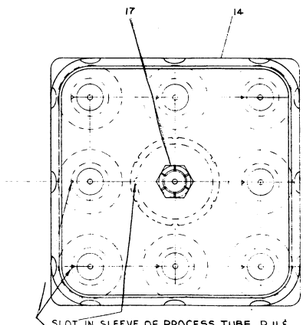

SLOT IN SLEEVE OF PROCESS TUBE P11 & V NOTCHES ON PLUG OF VELOCITY BOOSTER TO BE ALIGNED TO FACE DIRECTION AS INDICATED BY LETTER "E" ON SIDE OF ELEMENT SPACER, P14.

VIEW K-K

Figure 9.3

Fuel O.D. = 0.250"

Fuel I.D. = 0.694"

Velocity booster O.D. = 0.500"

Outer pass flow gap = 0.075"

Inner pass flow gap = 0.097"

Active fuel length = 36'

Fuel cladding material = Type 304 Stainless Steel

Fuel cladding thickness = 0.028" and 0.016"

TABLE 9.6

E-SADE INITIAL FUEL LOADING

Element	UO_2 Enrichment (%)	Weight of UO_2 Element (grams)	Gap Between Pellet and Outer Clad (mils)	Outer Clad Thickness (mils)	Type of Element Spacers
A	8	4,550	Swaged	16	Spiral Wires
B	8	4,550	Swaged	16	Spiral Wires
C	10	4,550	Swaged	16	Spiral Wires
D	8	4,550	Swaged	16	Spiral Wires
E	10	4,300	4	28	Spiral Wires
F	8	4,550	Swaged	16	Spiral Wires
G	6	4,300	6	28	Spiral Wires
H	6	4,300	4	28	Fins
I	8	4,300	6	28	Fins

9.2.4 Fuel Assembly (ESH-2)

During this reporting period the design of the second fuel assembly, ESH-2 was initiated. The ESH-2 assembly will consist of nine fuel elements with single pass or one through flow configuration, all fuel elements replaceable. The thermal and hydraulic analysis

of these elements have been completed and hydraulic flow gaps sized. The spacing technique to be used is spiral wires in all cases. Detail drawings of these elements are in progress.

A brief description of the fuel is:

Fuel O.D. = 0.875"

Fuel I.D. = 0.406"

Outer pass flow gap = 0.075"

Active fuel length = 36"

Fuel cladding material = Type 304 Stainless Steel

Fuel cladding thickness = 0.010" and 0.020" O.D. thickness
0.016" I.D. thickness

9.2.5 External System

Design of the external system was also essentially completed during this period and orders have been placed for most major components. Some equipment is already on site and additional items, including the main condenser are in transit. System changes were required as a result of more detailed safeguards analysis. Work is now in progress to determine the effect of these changes on overall E-SADE construction and operation schedule.

Considerable difficulty was encountered in procuring plate material for the new penetration of the reactor enclosure, because of the low temperature ductility specification imposed by this application. Satisfactory material was finally obtained and shop fabrication of the patch assembly is being completed. Installation of the assembly into the reactor enclosure is presently scheduled for September.

Procurement delays plus the desirability of providing maximum utilization of SADE to determine characteristics of chloride stress corrosion would seem to establish a strong motivation for delay of E-SADE start-up.

9.3 Fretting Corrosion Tests

A parasitic attachment to the F-2 superheat loop has been installed for studying

(1) fuel element spacer geometrics to determine whether fretting or wear corrosion is a problem,

(2) pressure drops associated with each configuration, and,

(3) integrity of wire attachments.

The loop shown on Figure 9.4 (DWG 124F743) will provide superheated steam at 950°F with operating pressures ranging from 800 to 1400 psi. Present instrumentation will allow separate measurement of pressure drops caused by the wire spacers on the fuel O.D. and the velocity inducer. Fuel element attachments and loop flow passages have been designed to conform to E-SADE parameters.

The first test specimen shown on Figure 9.5 (DWG 124F761) is a .028" wall clad, 1 1/4" OD, annular fuel element with three wire spacers; each wire making one complete revolution along the fuel length. Spacer wires are attached to both end plugs only (no attachment on the fuel clad). Wires were fastened to the top and bottom end plug by fusion welding. One wire was put on somewhat looser than the other two to determine the effects, if any, on fretting corrosion and wire attachment integrity. This test is scheduled to commence in September, 1961.

Other configurations to be investigated include:

(1) a .016" wall clad element,

124 F 743

TITLE FUEL TEST FACILITY

FIRST MADE FOR AT(04-3)-189 PA #13

P.L. ISSUED

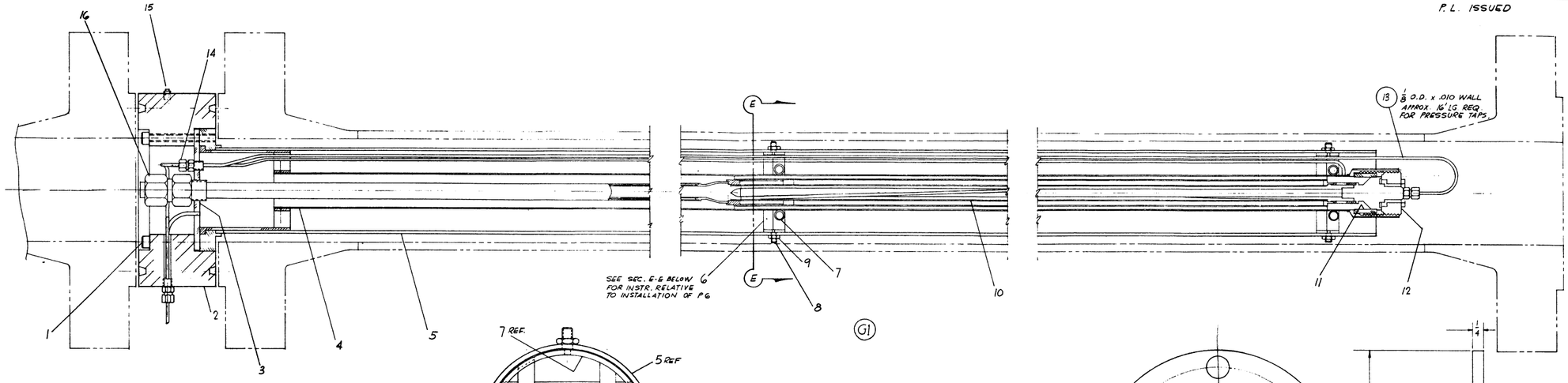

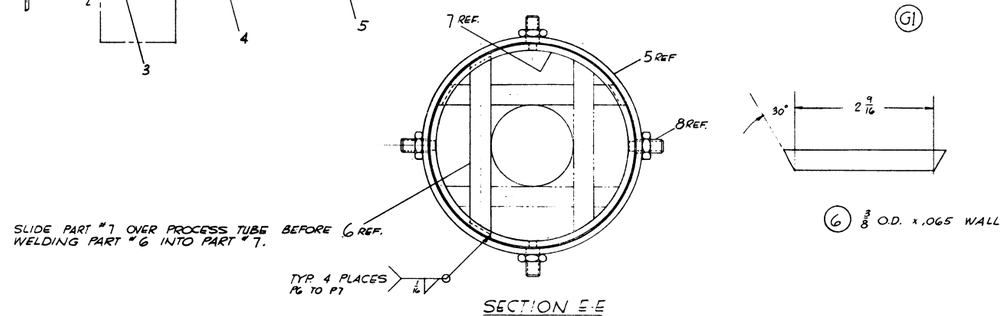

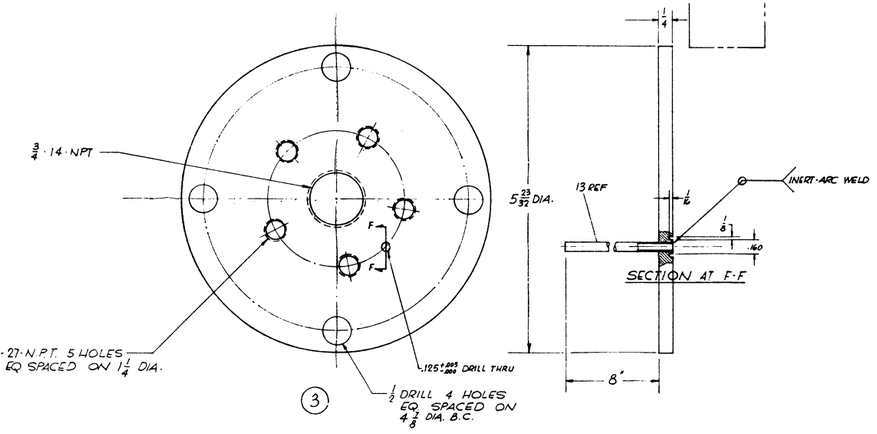

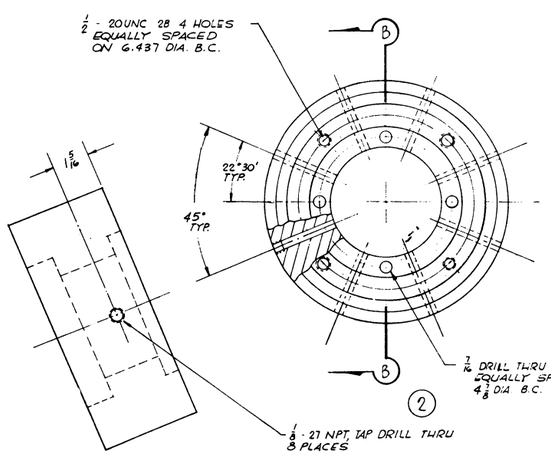

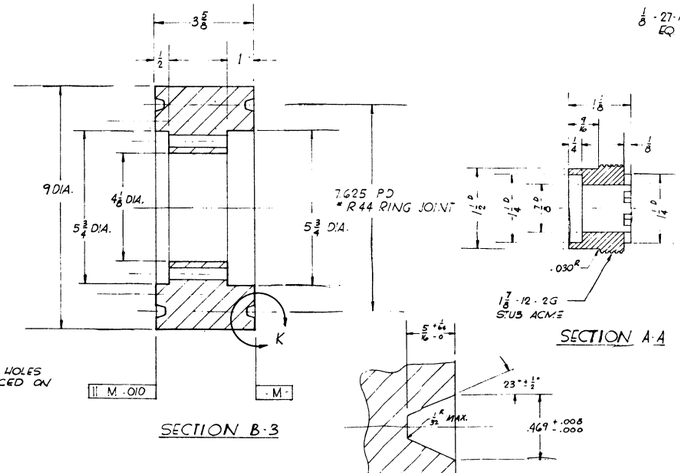

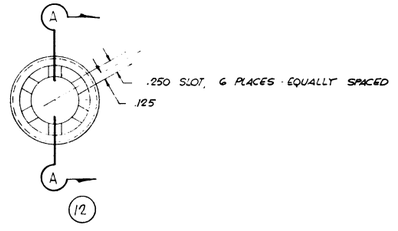

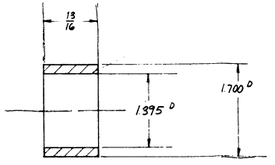

Figure 9.4

124 F 761

TITLE
FUEL ELEMENT
FIRST MADE FOR AT (04-3)-189 PA "13

PL ISSUED

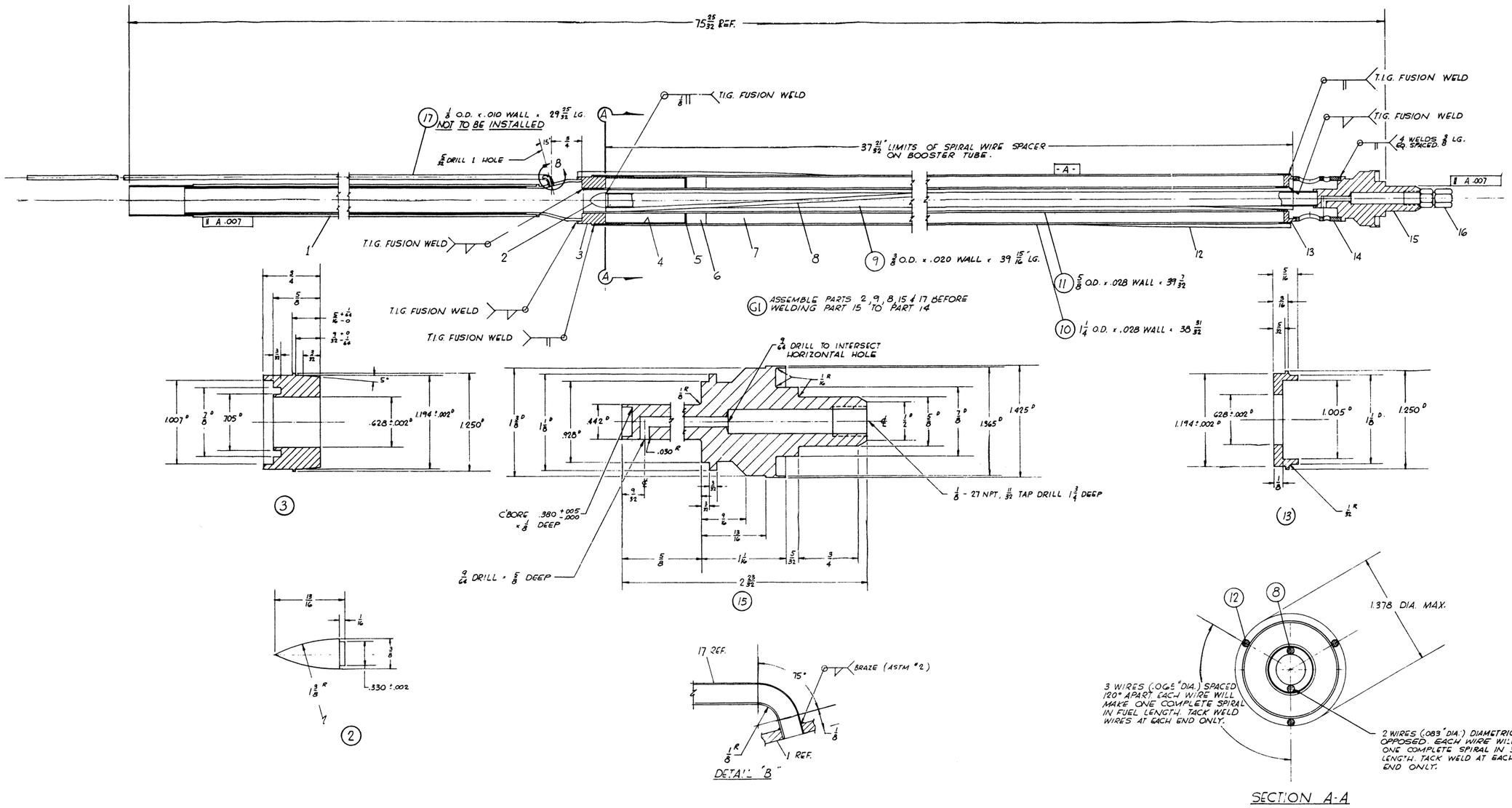

Figure 9.5

(2) more .028" wall clad elements with the spacers attached to (magnetic force welding) or an integral part of the fuel clad (chem-milled to size).

It is also deemed feasible to simultaneously test promising concepts of insulated process tubes. These tests will require minor modifications to the test facility.

10.0 TASK H - MIXED SPECTRUM SUPERHEATER DESIGN STUDY

10.1 Prototype Reactor Design

Work was initiated on the design of a small prototype reactor to demonstrate the important features of a Mixed Spectrum Superheater. As has been noted previously, the physics of the MSS is strongly size dependent so that information from very small reactors would not be readily extrapolated to the operation of a large sized reactor. Of primary concern in this respect are the characteristics of the core during flooding and unflooding of the superheater, the doppler effect in the fast superheating section and the control and coupling between the superheating and boiling sections of the core. In the present work, the requirement was set that the prototype reactor would have similar characteristics to the large 300 MW(e) reference iesign described in GEAP 3590. In addition, for the initial work, the following design requirements were placed on the thermal hydraulics of the system.

Outlet Temperature	$\sim 950^{\circ}F$
Central Fuel Temperature	$\sim 4500^{\circ}F$
Maximum Surface Temperature	$1250^{\circ}F$
Maximum Flow Velocity	250 ft/sec

The temperature requirements together with the requirement of physics simulation determine the form of the reactor.

10.1.1 Thermal-Hydraulics

Studies indicate that the physics characteristics of the reactor are largely determined by the uranium to plutonium ratio in the core. (Since the neutron spectrum is primarily determined by this ratio). A number of studies involving the inter-play of physics and mechanical design determined that a core of approximately 30 $in.^3$ in which the steam volume was reduced over that in the reference design would permit plutonium enrichments comparable to that of the

reference design and would have physics characteristics which are similar. An investigation of the thermal hydraulics of a core of this size indicated that the major limitation would be caused by a tendency towards high clad temperatures at low power levels. Paradoxically, the lower the power level of the system, the higher is the resulting maximum surface temperature of the fuel. This is due to the fact that the steam production is proportional to the power of the reactor because the ratio of power in the fast and thermal cores is held fixed. Therefore, an increase in power causes an increase in steam velocity through the core which results in better heat transfer. Also, to maintain a given fuel central temperature, the increased power requires a reduction in fuel rod diameter and thus an increase in surface area in the core. The net effect is that the improvement in heat transfer and surface area more than compensate for the increase in power and one obtains a lower film drop and a lower surface temperature as the power is increased. Thus, a restriction on the fuel surface temperature with a given central temperature, core size and minimum pitch to diameter ratio, will set a minimum power level for the core.

These points can be illustrated by the following calculations. If one assumes a power in the superheater of 20 MW thermal and a minimum allowable pitch to diameter spacing of 1.04, the hot channel flow velocity is only 64 ft/sec and the resultant film drop is $410^{\circ}F$, leading to a maximum surface temperature of $1480^{\circ}F$. If one allows the outlet temperature to drop from the design point of $950^{\circ}F$ to $825^{\circ}F$, the surface temperature will be $1270^{\circ}F$. If the power is doubled to 40 MW thermal in the superheater, then the hot channel flow velocity

increases to 128 ft/sec, the hot channel average film drop is reduced to 292°F and the maximum surface temperature is 1325°F. The outlet temperature must be reduced from 950 to less than 875°F to keep from exceeding a 1250°F surface temperature. From these examples, one may conclude that the power requirements of a single pass reactor core will be very high if one expects to meet the requirements set forth above.

For these reasons, it was decided to investigate a design based on a two-pass flow scheme. In essence, two-pass flow is beneficial in keeping the surface temperature low because it affords a means of reducing the flow area in a single pass and thus increasing the steam velocity in the superheating core. There is another advantage in the two-pass system in that there is an extra degree of freedom. One is able to adjust the characteristics of the two regions of the core separately to achieve desired results. Thus, it becomes possible to utilize a higher pitch to diameter ratio in the second pass where the temperature conditions are closer to the limits. In the initial set of calculations, a pitch to diameter ratio of 1.10 was chosen for the second pass in order to simulate closely the reference design fuel. In the first pass where greater peripheral heat transfer variations can be tolerated, a pitch to diameter ratio of 1.04 was chosen. One still has freedom to vary the relative sizes of the two regions of the core and thus, the temperature rise through each pass. Figure 10.1 contains curves which show how the maximum surface temperature in each of the two regions varies as the power split between the regions is changed. Since the hottest gas is present in the second pass, surface temperature will tend to be higher in the second pass than the first

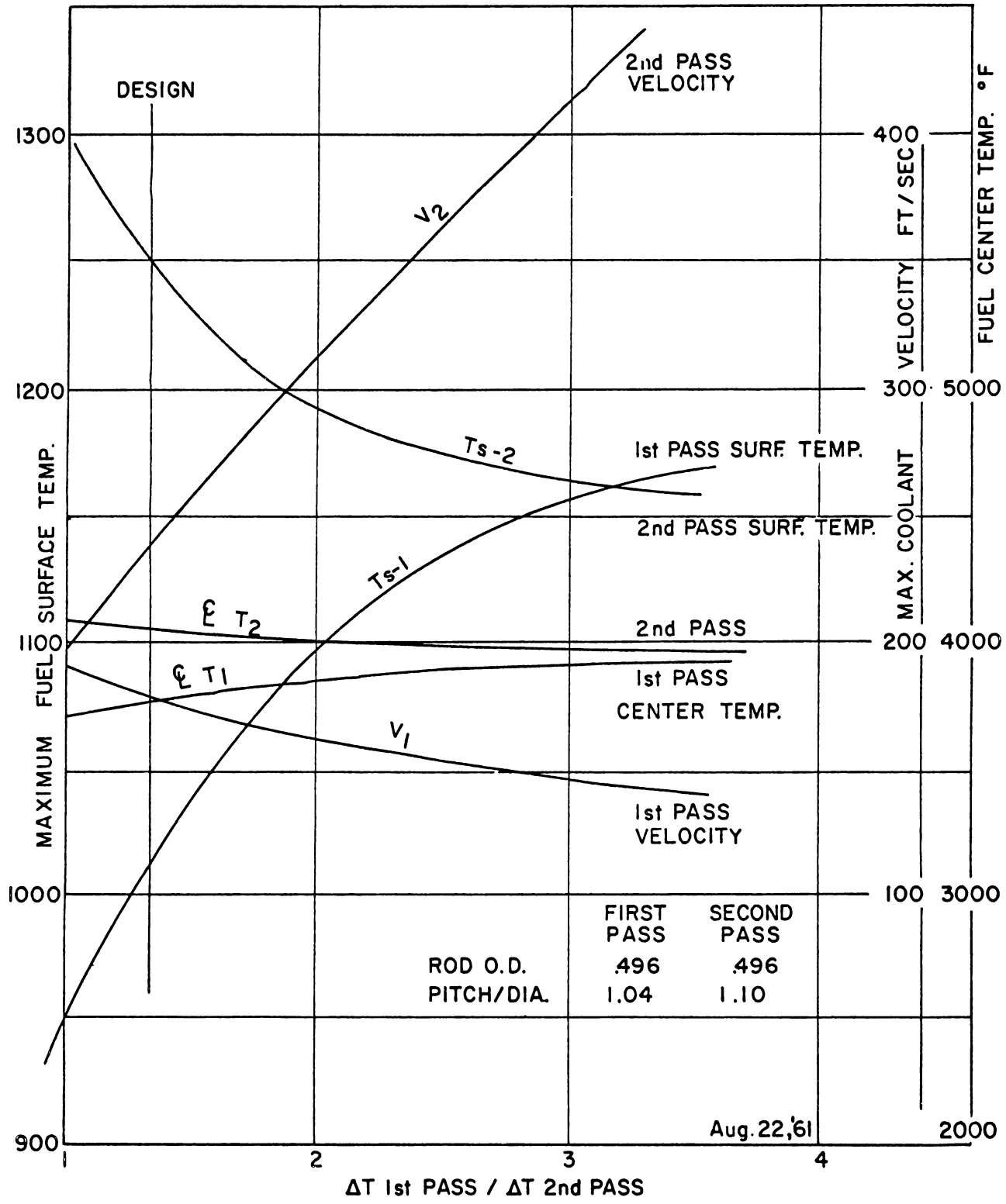

40 MW MIXED SPECTRUM FAST CORE 1000 psi - 950° SUPERHEAT
FIGURE 10.1

for equal power sharing. As the ratio of power in the first pass to that in the second pass increases, the maximum surface temperature decreases in the second pass and increases in the first pass.

Shown in the figure is a design line. Along the design line, one notes that the maximum surface temperature for a 40 MW prototype will be 1250° on the second pass, that the steam velocity on the second pass is 230 ft/sec and that the center line temperature during normal operation is 4000°F. Thus, with this two-pass core operating at 40 MW, the nuclear characteristics of the Mixed Spectrum Superheater are well simulated and the fuel operating temperatures and conditions in the second pass are also close to those in the reference design.

10.2 Reference Prototype Design

In assessing the size of a small prototype which would give meaningful data on a large economic mixed spectrum reactor, the two-pass core and the 40 MW thermal power level for the superheating section was chosen. Conditions are those shown in Figure 10.1, and tabulated in Table 10.2 below. As a start, an attempt is being made to ascertain whether a reactor of this size can be built in a vessel of the size used in the Vallecitos Experimental Superheat Reactor (7 ft. I.D.). Figure 10.2 shows a preliminary core schematic. The hexagonal grid is used in the fast core section in order to conserve space since initial work indicated that such an arrangement would facilitate a match of the core boundary to the vessel of circular cross-section.

10.2.1 Prototype Physics Studies

Design calculations for the prototype reactor were carried out using 18-group one-dimensional diffusion theory. A fast superheating core

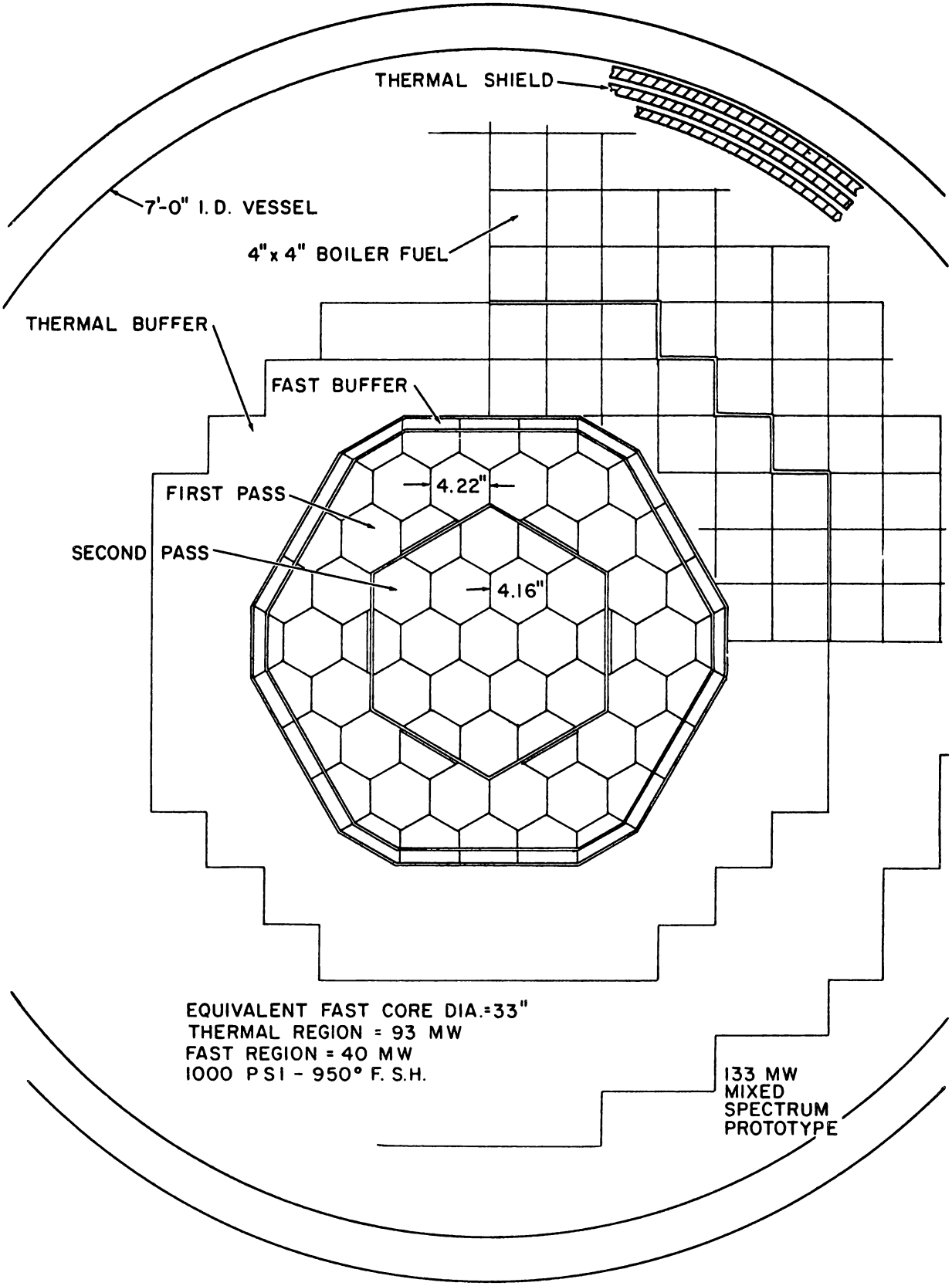

PRELIMINARY CORE SCHEMATIC

Figure 10.2

TABLE 10.2

MIXED SPECTRUM SUPERHEATER PROTOTYPE

Core Data Sheet

	1st Pass	2nd Pass
Max. V ft/sec	175	240
Max. Surf. T ^{o}F	1015	1250
Max. Center-line T (steady state power)	3880	4050
$\frac{\Delta T \text{ first pass}}{\Delta T \text{ second pass}} = 1.35$	-	-
Coolant Bulk Rise ^{o}F	230	170
Coolant Flow #/Hr	4.82×10^{5}	4.82×10^{5}
Total Heat/Pass Btu/Hr	8.83×10^{7}	4.82×10^{7}
Outlet Temp. ^{o}F	775	950
Rod O.D. in.	.496	.496
Rod Clad in.	.040	.040
Number Rods	2060	1120
Ave. Q/A Btu/hr ft^{2}	134,000	134,000
Max. Q/A Btu/hr ft^{2}	300,000	300,000
Hot Channel h Btu/hr ft^{2} ^{o}F	1530	1230
Core Area $in.^{2}$	501	304
Power Split %	65	35
Pitch/Rod Dia. Ratio	1.04	1.10

in the shape of a 30" cube was used to determine the required plutonium loading and power distribution. Results illustrated in Table 10.1 show that if the prototype were fueled with plutonium, an enrichment of between 12 and 13% would be required. This is close to the enrichment required by the 300 MWe reference design. Table 10.1 also indicates that a plutonium inventory of approximately 290 kg would be required for this size core.

Case 5 shows that the power split between the fast core and the boiling core is quite sensitive to control insertion in the slow buffer. The Boron 10 concentration shown in the slow buffer for Case 5 is equivalent to the insertion of controls in the buffer region. The power distribution obtained for Case 4 is shown in Figure 10.3 and indicates that the fast buffer design (divided into two parts) must be modified in order to reduce the large power peak.

A two-dimension, four-group calculation of the power distribution was made using the PDQ code. The power distribution was consistent with the one dimensional calculation but a considerable difference (about 10%) occurred in the criticality factor. There are a number of possible sources of this difference of criticality factor, the most probable one involving the method of condensing the 18-group cross-section set into the 4-groups, to which PDQ is limited. Further work on this point is planned.

Neutron lifetimes were calculated for several conditions of the 300 MWe reference design Mixed Spectrum Superheater and for the small prototype. Neutron lifetimes were also calculated for the boiler alone and for the superheater alone.

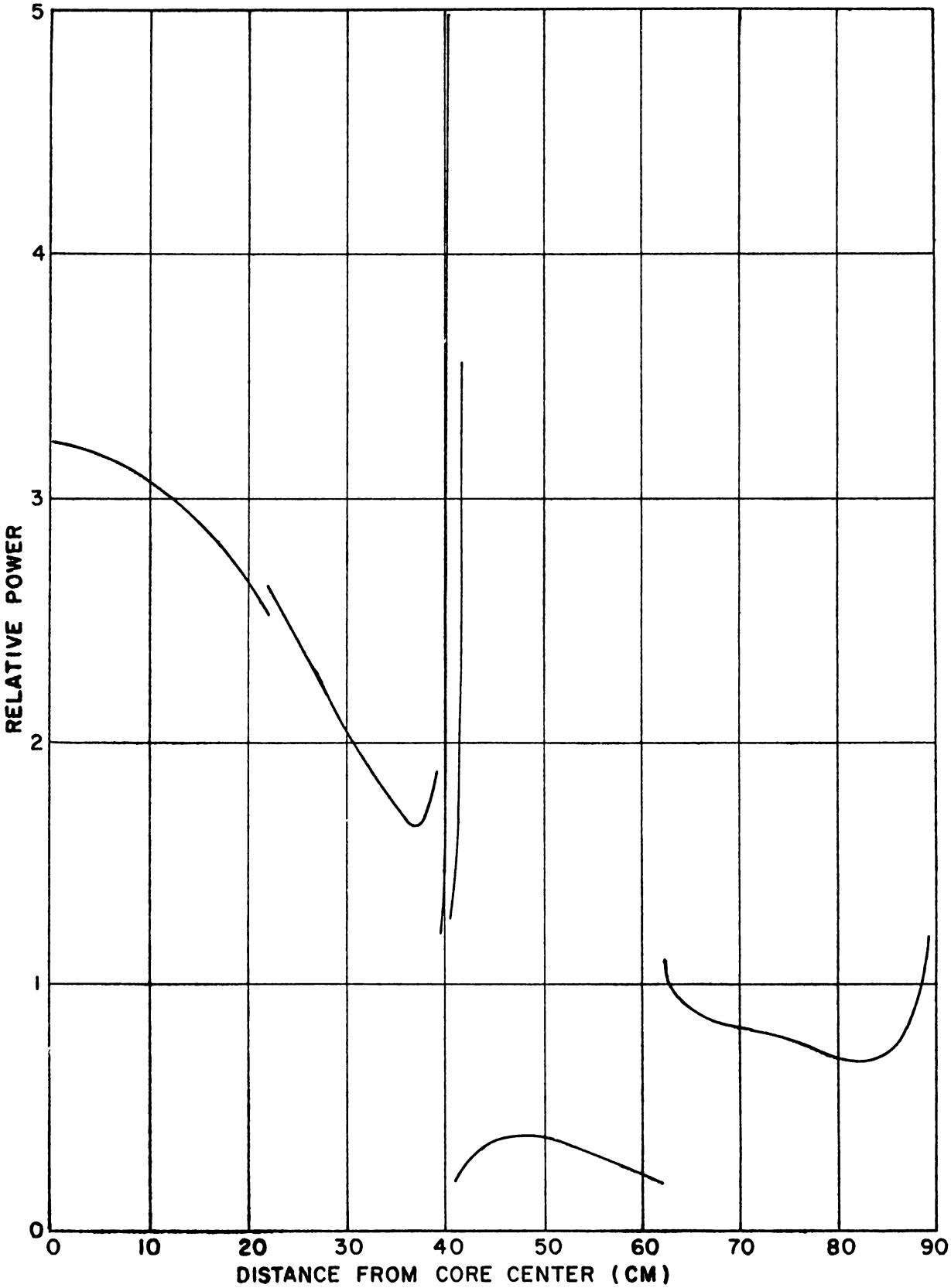

POWER DISTRIBUTION IN PROTOTYPE MSS
FIGURE 10.3

The lifetime was calculated by adding a $\frac{1}{v}$ absorber to all regions of the reactor and using the relation $\ell = \frac{\Delta k}{C}$ where Δk is the difference in criticality factor in the reactor with and without the $\frac{1}{v}$ poison, and C is chosen so that the macroscopic cross-section of the absorber is $\frac{C}{v}$. Table 10.3 shows the results. It can be seen that the lifetime of the Mixed Spectrum Superheater has been that of the fast and slow core and that its effective value is sensitive to the percentage of power generated in the superheating section. It is significant to note that even for the case of 58% of the power in the superheating section (in operation a maximum of 30% of the power would be generated in the superheater) the neutron lifetime is about 5 times the value of that of an uncoupled fast core alone.

The neutron lifetime for the prototype lies in the range of that of the reference design but is somewhat higher for the same power split. This can be explained on the basis of a closer coupling of the smaller prototype between the fast section and the thermal core.

The significance of neutron lifetime in terms of the safety of the reactor is not plain at present. There appears to be some circumstances where it is advantageous to have a short neutron lifetime and other cases where a long neutron lifetime is of advantage. Two extreme examples are the following. If one has an accident in which reactivity is inserted at a constant rate until some shut-down or disassembly mechanism occurs above a given energy threshhold, then the damage which occurs will depend upon the overshoot in power above this energy threshhold. In this case, a larger overshoot will occur for the reactor with the shorter lifetime and thus, there will be a larger

energy release. On the other hand, if one has a shut-down mechanism which is proportional to temperature, then a short lifetime will cause the power to increase rapidly and the shut-down mechanism becomes effective before much reactivity is inserted, while a long lifetime can lead to the introduction of considerable reactivity before the shut-down mechanism becomes effective. General calculations indicate that there can be a factor of 2 difference in the peak temperature reached between a very short and a very long neutron lifetime.

TABLE 10.1

Case	Pu Enrichment Fast Core	Pu Enrichment Outer Half Fast Buffer	Superheat Pu Inventory	N_{B10} Slow Buffer	k	Fraction Power in Superheater
1	13.0	3.0	292	0	1.0153	-
2	12.8	3.0	288	0	1.0081	.39
3	12.6	3.0	284	0	1.0011	.36
4	12.6	1.75	284	0	0.9924	.37
5	13.0	1.75	292	$.7 \times 10^{-5}$	1.0319	.09

10.3 Fast Core Meltdown

To assess an important factor with regard to the safety of the Mixed Spectrum Superheater, a calculation was performed to simulate an extreme case of melting in the superheater core. In this calculation, it was assumed that the superheater section melted and slumped so that all the steam volume was removed from the core. The volume of fuel and steam in the core and all radii were conserved. The height of the fast core was reduced. The calculation showed that in the case of the reference design,

4% in reactivity would be added, while in the smaller prototype with the higher leakage from the fast section, a reactivity increase of 9% would result.

10.4 Flooding of the Fast Core

From the inception of the work on the Mixed Spectrum Superheater, it has been clear that the problem of accidental flooding or unflooding of the superheating section would be of major importance with regard to the safety of this type of reactor. Intensive study of the effect of flooding in a Mixed Spectrum Superheater has been made during this quarter, and recorded in a topical report GEAP 3737. In GEAP 3737, results on the uniform flooding of the Mixed Spectrum Superheater were reported and the methods used in the analysis are described. Results described in GEAP 3737 will not be repeated here. However, additional work on this problem has been performed which involves flooding of the superheater in nonuniform ways. In particular, the following situations were considered.

(A) Flooding (and unflooding) the superheater steam section by varying the water level in the superheater.

(B) Flooding and unflooding with water density decreasing from bottom to top of the superheater core.

(C) Uniform flooding and unflooding (reported in GEAP 3737).

Calculations for these cases were carried out for the 300 MWe Mixed Spectrum Superheater which contains .3% by volume europium as an epithermal poison. The results are illustrated in Figure 10.4. This schematically indicates the condition of the core for the various calculations made and shows the change in reactivity from the operating condition.

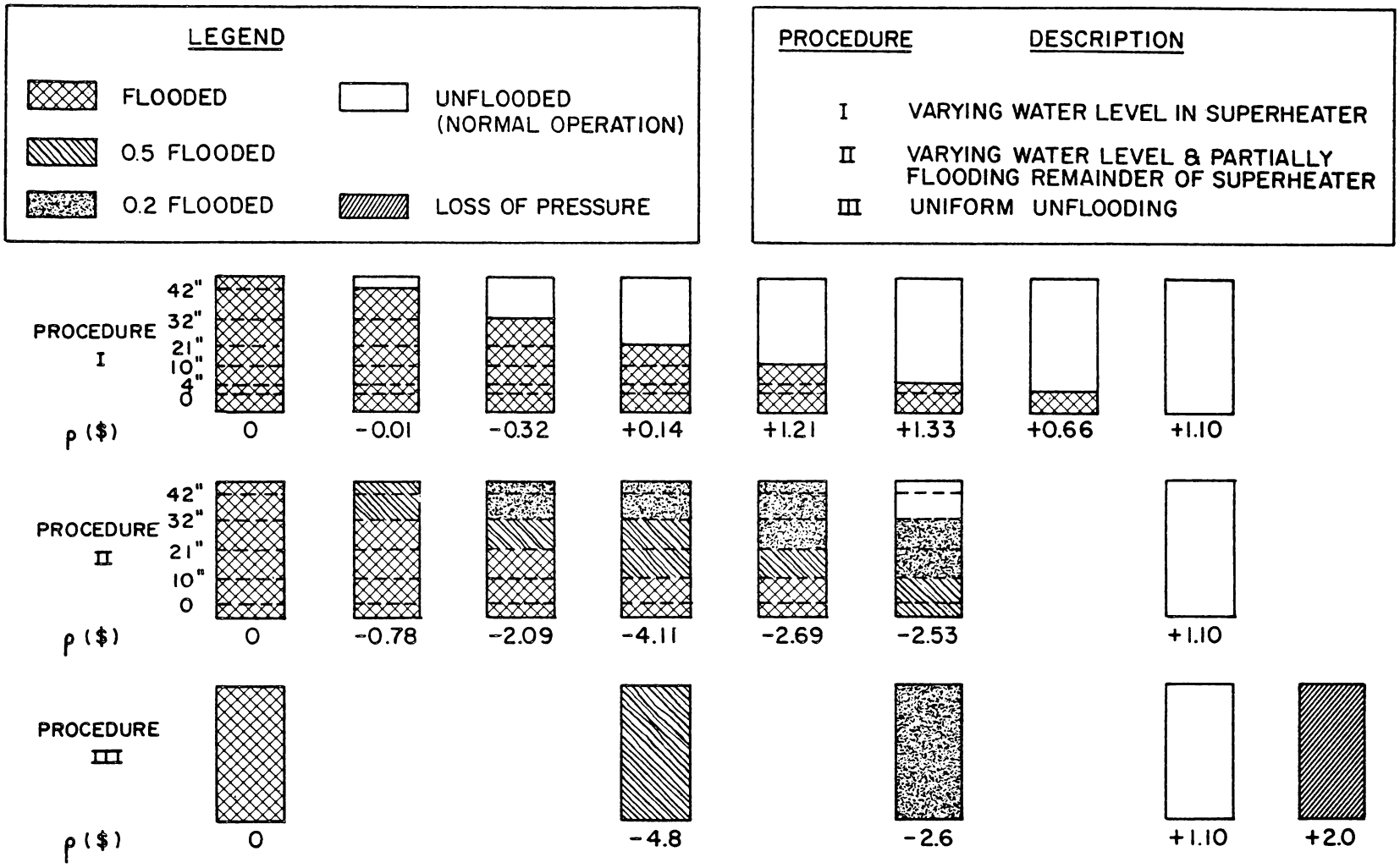

REACTIVITY RESPONSE FOR VARIOUS UNFLOODING PROCEDURES

Figure 10.4

TABLE 10.3

Reactor	Fraction Power in Superheater	k	ℓ (sec)
Fast Core	1.00	1.05889	0.48×10^{-6}
Slow Core	0	1.02600	32×10^{-6}
300 MW(e) MSS	0.58	1.0004522	2.36×10^{-6}
300 MW(e) MSS	0.33	0.99809615	2.40×10^{-6}
300 MW(e)	0.02	1.008175	33.8×10^{-6}
50 MW(e) Prototype MSS	0.37	1.001130	7.75×10^{-6}

TABLE 10.4

Power Distributions (300 MW(e) MSS)

Case	Pu Enrich. in Superheater (%)	N_B10 in Slow Buffer (atoms/cm^3)	N_B10 in Boiler (atoms/cm^3)	k	Fraction of Power In Superheater
1	13.0	0	0.7×10^{-5}	1.0005	0.58
2	12.9	0	0.475×10^{-5}	0.9981	0.33
3	12.8	0	0.475×10^{-5}	0.9932	0.28
4	12.75	0	0.500×10^{-5}	0.9907	0.32
5	12.75	0	0.525×10^{-5}	0.9907	0.37
6	12.5	0	0.35×10^{-5}	1.0082	0.02
7	13.0	1.4×10^{-5}	0.35×10^{-5}	1.0055	0.03

As can be seen, the change in reactivity between the flooded and unflooded conditions is small although the way in which reactivity changes during the flooding operation is quite different for the various cases studied.

10.5 Power Distribution

The split of power between the superheater and boiler was studied as functions of plutonium enrichment in the superheater, boron concentration in the boiler and boron concentration in the thermal buffer. These three parameters are related to the control in each of the regions since in the fast core, control is accomplished by inserting and removing fuel while in the thermal buffer and boiler, poison control elements are utilized. The results are presented in Table 10.4. It is observed that a 0.1% increase in superheater enrichment increases the fraction of the power produced in the superheater by about 5% and the criticality factor by about 0.005. A 5% change in boron-10 concentration in the boiler changes the fraction of power in the superheater by about 5% but produces a very small effect on criticality. The effect of boron in the thermal buffer, Case 7, is to decouple the cores. The calculations are in agreement with previous work which indicated that the power split between the fast and thermal core can be varied and is sensitive to the placement of control elements in the various regions.

10.6 Critical Experiment

Work was initiated on consideration of the critical experiment design to demonstrate the characteristics of the Mixed Spectrum Superheater. One scheme envisioned consisted of a water tank supported approximately 6 ft. above floor level. The center of the water tank contains a vertical stand pipe into which the fast assembly can be raised by a mechanical ram.

The ram at its lowest position carries only the central portion of the fast region. As it is raised, it picks up the rest of the fast region from a pedestal and finally inserts the entire fast region into the core. Control rods and scram rods will be inserted into the thermal region. Different grid arrangements will be used to alter the center region and the buffer zones. Special source drives, interlocks and water metering equipment will be used to examine reactivity during various conditions of flooding. The assembly would be monitored by means of a closed circuit TV system.

10.7 Preliminary Safeguards Summary

10.7.1 Introduction

As part of the initial work on the safety of the Mixed Spectrum Superheater, the pertinent material from GEAP 3590, together with additional available information, was put in the form of a preliminary safeguards review which will serve as a base for further work. This review has been circulated internally within G. E. to those expert in safeguards evaluation in order to solicit comments and suggestions. The report which includes a description of the important features of the MSS for background perspective, may be of general interest and is included in the following pages.

10.7.2 Summary

The MSS is an 815 Mwt (313 Mwe) integral boiling-superheating reactor contained within a single pressure vessel. Its core consists of an unmoderated, steam-cooled, fast-spectrum central region which is surrounded by a conventional boiling water reactor core. The boiler fuel consists of conventional BWR fuel elements, while the

superheater uses PuO_2-UO_2 rods enriched to about 13 atom percent Pu-239. The superheater produces about 30% of the reactor power.

The MSS simplifies mechanical problems by essentially eliminating the manifolding connections required in the thermal design. Additionally, the fast spectrum superheating core is relatively insensitive to the inclusion of structural materials and thus can take advantage of relatively thick cladding (0.020 inch clad on 0.21 inch pellets).

From the standpoint of safeguards, there are additional advantages of this type of design.

1. The large open nature of the superheat region permits the incorporation of emergency cooling pipes directly in the superheat region.

2. The superheater and boiler are contained in the same vessel and are directly connected so that isolation of the boiler from the superheater, which can occur in a separate superheater design, is eliminated.

3. It appears that the flooding reactivity effect can be minimized by the inclusion of epithermal poisons with the superheater fuel. Recent calculations indicate that the reactivity effect would be $\sim$ 12% Δk ($\sim$30 dollars) without poisons as compared to less than 1 dollar with poisons. The poisons are effective only when the core is flooded and produce small effect during normal operation. This is obviously a tremendous advantage if the use of epithermal poisons is feasible; however, this must be demonstrated and if the poisons prove unuseable, the large flooding-effect would be a serious problem.

The reverse problem of unflooding, with the addition of the poisons, is somewhat complicated because the reactivity change is first negative and then positive as the core goes from flooded to unflooded. The net reactivity change may be limited to less than 1 dollar; however, the reactivity swing, first negative and then positive, could amount to several dollars. We have not evaluated fully the safety aspects of this feature and its desirability or undesirability is unclear at this time. However, recent calculations indicate that there is flexibility in adjusting the reactivity swing and indicate that further work may alleviate this peculiar aspect.

A major concern in the MSS reactor involves the meltdown accident. As is the case with any unmoderated reactor, a compaction of the superheater core will increase reactivity. Undetailed but pessimistic calculations indicate that the worst core meltdown accident could result in estimated energy releases equivalent to as much as 300 lb. of TNT.

The core meltdown accident, coincident with a primary system rupture, is taken as the "maximum credible accident" which is the basis for the containment design pressure (26 psig). The blast and missile shields are designed to contain the blast effects of the meltdown accident.

10.7.3 DESCRIPTION OF THE REACTOR

10.7.3.1 General

The Mixed Spectrum Superheater is a nuclear reactor plant intended for the production of central station power. The power rating for the present reference design of the 1968 plant is 313 MWe based on a thermal output of 815 MW. Approximately 30 per cent of the total thermal output is generated in the superheater. Reactor plant characteristics and performance data are summarized in Table I0.5

The conceptual design of the MSS combines an unmoderated, fast-spectrum superheater with a thermal boiler. The neutron spectrum varies from fast in the superheater to thermal in the boiler; hence, the name Mixed Spectrum Superheater. The core consists of four annular regions, which, in going from the inside to the outside, are: an inner unmoderated superheating region, an inner unmoderated buffer region, an outer moderated buffer region, and an outer thermal boiling region. The boiler is similar in composition and arrangement to a conventional boiling-water reactor core. The superheating core is an unmoderated, fast-spectrum reactor cooled by forced steam flow past the fuel. Thirty-six fuel bundles, including four which serve as control elements, make up the fast core. The fast fuel consists of mixed PuO_2-UO_2 rods clad with stainless steel.

An essential feature of the MSS is that the fast core cannot normally be made critical when it is isolated nuclearly from the thermal core. It depends upon neutron leakage from the thermal core to achieve criticality. Thus the fast core can be shut down by motion of nearby control rods in the thermal core. In addition, the transient nuclear behavior of the reactor tends to approach that of a thermal BWR.

Figure I0.5 shows schematically the basic features of the Mixed Spectrum Superheater. The flow is two-pass. The steam-water mixture formed in the outer boiler region passes up through parallel sets of radial-type steam separators. The separated steam passes through steam dryers and then flows down through an offset pipe to the inner vessel which houses the superheating core. Water surrounding the offset

TABLE 10.5

SUMMARY OF REACTOR PLANT CHARACTERISTICS

DESCRIPTION	FAST	THERMAL
A. Heat Balance		
1. Net Plant Power, MW(e)		313
2. Total Reactor Power, MWt	245	570
B. Turbine Cycle Conditions		
1. Throttle Temperature, °F		950
2. Throttle Pressure, psia		1450
3. Total Steam Flow, lb/hr		2.8×10^6
C. Reactor Description		
1. Reactor Vessel		
a. Inside Diameter, ft.		12-1/2
b. Inside Height, ft.		41
c. Wall Thickness, in.		7-3/4
d. Design Pressure, psig		1800
e. Design Temperature, °F		650
2. Reactor Core		
a. Equivalent Diameter, in.	46	120
b. Active Height		
Superheater/Boiler, in.	41.5	101
Buffer, in.	41.5	44
Reflector, in.	12-11/16	
c. Active Core Volume (incl. Buffer), ft^3	39.8	563
d. Fuel Loading		
Superheater, Kg Pu & U	4020	
Boiler		
Standard Rods, Kg U		30,7000
Corner Rods, Kg U		3,910
Buffer, Kg U	258	4,310
Reflector, Kg U	2120	
e. Enrichment		
Superheater, a/o Pu-239	13	
Boiler		
Standard Rods, a/o U-235		2.3
Corner Rods, a/o U-235		1.8
Buffer, a/o U-235	5	Depleted
Reflector, a/o U-235	Depleted	

			FAST	THERMAL
2.	f.	Structural Material	SS	Zr-2
	g.	Neutron Moderator	None	H_2O
	h.	Moderator to Fuel Ratio		
		Boiler		2.2
		Buffer Side Channels		1.2
		Buffer Corner Channels		1.3
3.	Reflector			
	a.	Material	Depleted U	H_2O
	b.	Axial Thickness, ft.	1.0	4
	c.	Radial Thickness, ft.		1
4.	Fuel Elements (for each type)			
	a.	Fuel Material	PuO_2-UO_2	UO_2
	b.	Fuel Element Geometry	Rods	Rods
		Pitch arrangement	Triang.	Square
	c.	Clad Material	SS	Zr-2
	d.	Fuel Material Outside Diameter		
		Superheater, in.	.24	
		Boiler		
		Standard Rods, in.		.392
		Corner Rods, in.		.370
		Buffer, in.	.24	.750
		Reflector, in.	.50	
	e.	Clad Thickness		
		Superheater, in.	.020	
		Boiler		
		Standard Rods, in.		0.026
		Corner Rods, in.		0.038
		Buffer, in.	.020	.040
		Reflector, in.	.030	
	f.	Fuel-Clad Gap (cold), in.		
		(Equilibrium)	~0	~0
	g.	End Plenum Length		
		Superheater/Boiler, in.	3.5	3
		Buffer, in.	3.5	1.0
		Reflector, in.	.5	
	h.	Gap Filler Material	He	He
5.	Fuel Assemblies			
	a.	Number of Channels		
		Superheater/Boiler	36	76
		Buffer, Corner	4	4
		Buffer, Side	20	16

			FAST	THERMAL
5.	b.	Number of Assemblies/Channel		
		Superheater/Boiler	3	1
		Buffer	3	2
	c.	Number of Rods/Channel		
		Superheater	416	
		Boiler		
		Standard Rods		193
		Corner Rods		32
		Buffer Corner - Buffer	44	64
		Above Buffer		179
		Buffer Side - Buffer	38	72
		Above Buffer		193
		Supperheat Control	321	
		Reflector - Standard Channel	81	
		- Control Channel	64	
	d.	Cross Section Dimensions (Inside)		
		Superheater/Boiler, in.	6.08 x 6.18	9.15 x 9.15
		Buffer Corner, in.	7.25 x 0.75	8.50 x 7.32
		Buffer Side, in.	6.25 x 0.75	9.15 x 7.32
		Superheater Control, in.	5.50 x 5.50	
	e.	Lattice Spacing, in.	6.5	10.0
	f.	End Fitting Material	SS	SS
6.		Reactor Control		
	a.	Method of Control	Fuel	Poison
	b.	Absorber Material		Boron-SS
	c.	Number of Control Elements		
		Superheater/Boiler	4	52
		Buffer		8
	d.	Cross-Section Dimensions		
		Superheater (Square Shaped), in.	5-3/8x5-3/8	
		Boiler (40 cross Shaped), in.		8-3/8x8-3/8
		Boiler (12 T-Shaped), in.		12-1/2x4-1/8
		Buffer (T-Shaped), in.		16-3/4x2-3/8
	e.	Effective Length		
		Fuel/Poison Section, in.	41.5	100
	f.	Type of Drive	Twin Screw	Locking Piston
7.		In-Core Flux Monitors		
		Number		60
		Number per Channel		4
		Number of Channels		15

		FAST	THERMAL
D.	Performance Data		
1.	Reactor Coolant	Steam	Water
2.	Reactor Coolant Outlet Temperature, °F	950	600
3.	Reactor Coolant Inlet Temperature, °F	600	592
4.	Primary System Operating Pressure, psig	1500	1500
5.	Primary Coolant Flow, lbs/hr	2.8×10^6	30×10^6
6.	Ave. Core Coolant Velocity, ft/sec	122	8
7.	Max. Fuel Center Temperature, °F	4500	4500
8.	Max. Cladding Surface Temperature, °F	1250	628
9.	Burnout Safety Factor		1.8
10.	Max. Core Heat Flux, Btu/hr ft^2	610,000	362,000
11.	Ave. Core Heat Flux, Btu/hr ft^2	224,000	99,000
12.	Ave. Core Power Density, kwt/ft^3	6150	1010
13.	Peak to Average Power Ratio	2.62	3.65
14.	Ave. Specific Power, kwt/kgU	57	16
15.	Fuel Management	4 batch	5 batch
16.	Ave. Fuel Burnup, MWD/MT	38,500	19,000
17.	Peak to Average Burnup Ratio (including local peaking)	1.3	2.04

E.	Suggested Containment	
1.	Design Criteria	ASME Code
2.	Type	Dry
3.	Primary Loop Coolant Inventory, lbs	155,000
4.	Geometry	Sphere
5.	Diameter, ft	160
6.	Design Pressure, psig	25.8
7.	Material	ASTM A-201 Grade B

197E971

TITLE MIXED SPECTRUM SUPERHEAT REACTOR ASSEMBLY
FIRST MADE FOR USEC CONTRACT AT (04-3)-189

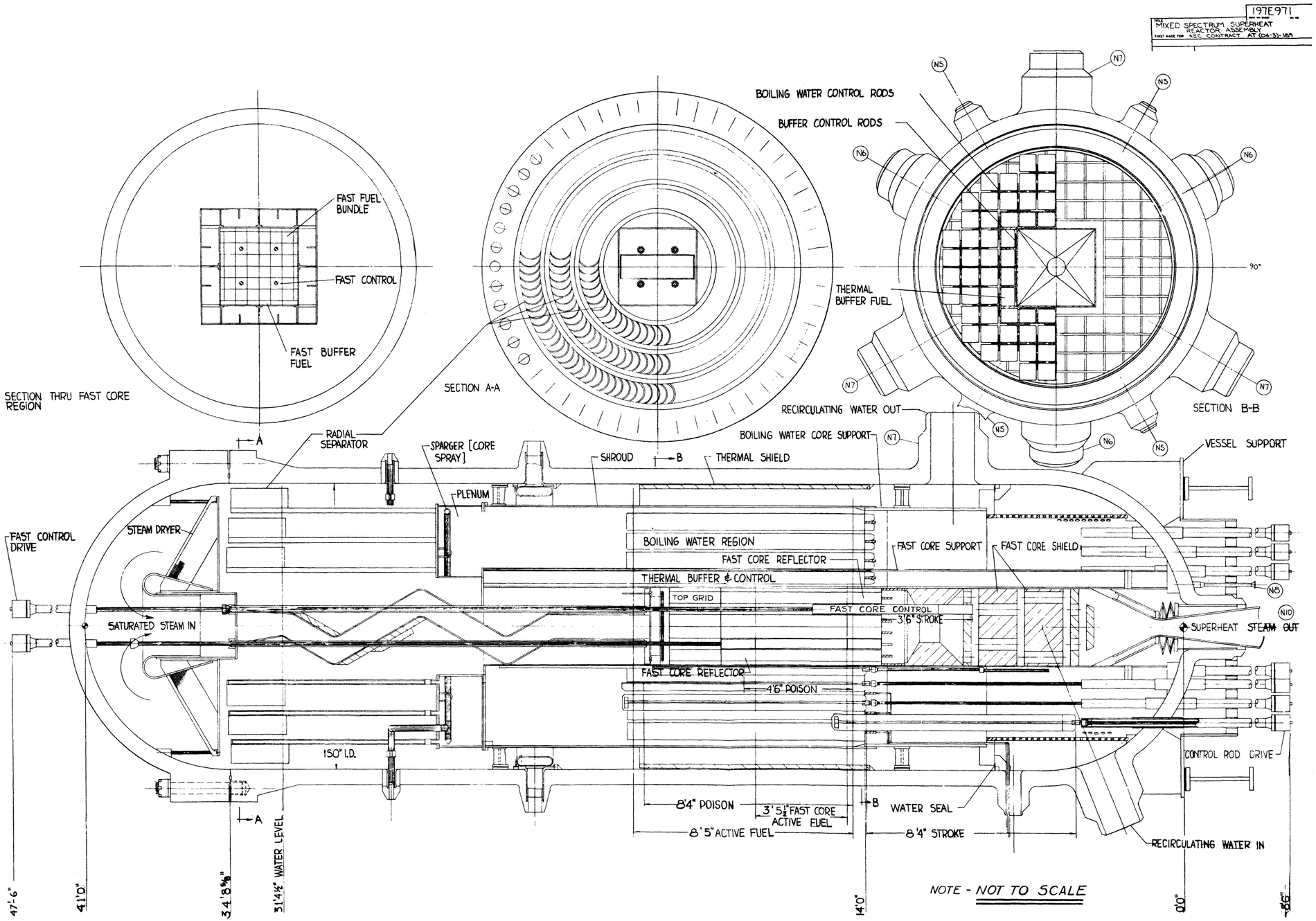

NOTE - NOT TO SCALE

Figure 10.5

pipe reduces radiation streaming to the vessel head. The superheated steam leaves the pressure vessel through a pipe penetrating the vessel bottom. Within the pipe beneath the superheating core are a series of shielding plugs which reduce radiation streaming to the vessel bottom. A venturi at the outlet serves to limit mass flow rate in the event of a pipe rupture external to the vessel. Isometric drawings (Figures 10.6 and 10.7) illustrate more clearly the mechanical arrangement of the various components.

The reactor is pressurized to 1550 psia. Superheated steam is supplied to the turbine at 1450 psia and 900°F. Feedwater is returned to the reactor vessel at a temperature of 425°F. Recirculating water leaves the reactor vessel through three outlet nozzles and is returned by three parallel mechanical-seat-type pumps through three inlet nozzles.

10.7.3.2 Boiler Fuel

The fuel bundle for the boiler section, shown in Figure 10.8, consists of a 15 x 15 array of fuel rods. The first core will utilize stainless steel clad, while the equilibrium core will take advantage of the better nuclear properties of zircaloy, provided the fuel development programs now in progress are completed successfully. In general, it is intended that the boiling section of the core be identical in important respects to standard APED products and that it incorporate all important safety features, particularly with regard to reactivity worths of individual fuel bundles.

10.7.3.3 Superheater Fuel

The fuel for the initial load of the superheater is in the form of solid UO_2 cylinders. In the equilibrium core, this fuel will contain a mixture of PuO_2 and UO_2. The cladding will be free-standing stainless steel for both cores. A triangular array of 416 fuel rods make up a standard sub-assembly as shown in Figure 10.9. The rods are held loosely top and bottom by tie plates. Spacing is accomplished by wires twisted around individual rods. Every third rod has no wire wrap and is supported by six surrounding wire-wrapped rods. The wire wraps are arranged with alternate directions of twist to provide "pumping action" to enhance flow mixing. Figure 10.1 shows the assembled fuel bundle consisting of the central fuel section and the upper and lower reflector sub-assemblies. The reflectors are made up of 81 depleted UO_2 rods approximately one foot long and clad with stainless steel. The maximum surface temperature of the superheater fuel is 1250°F. Dimensions and other pertinent data for both boiler and superheater fuels are summarized in Table 10.5.

10.7.3.4 Buffer Fuel

Depleted and slightly enriched UO_2 fuel is placed in the region between the fast and thermal cores where it is held down by the differential

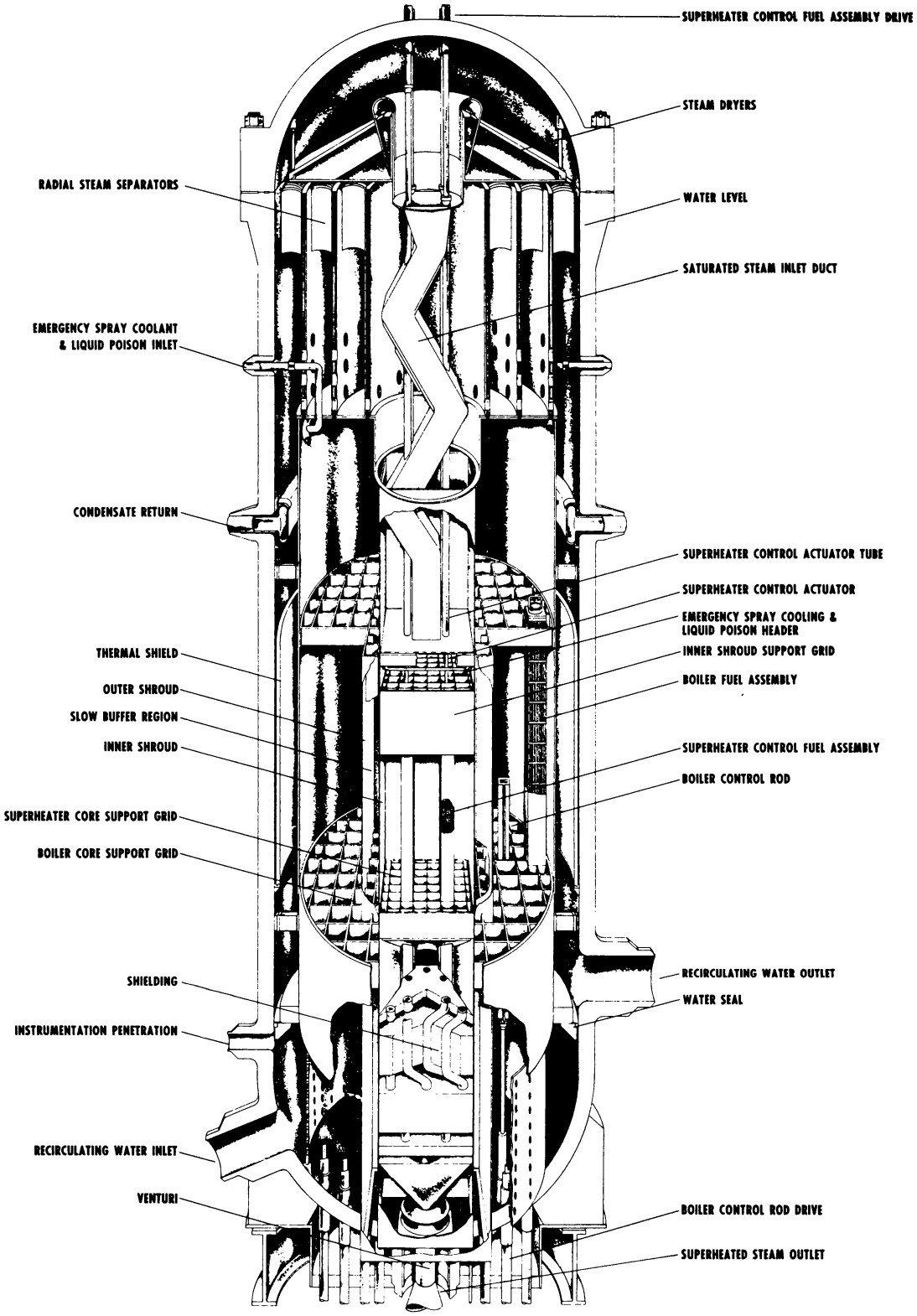

ISOMETRIC VIEW OF MIXED SPECTRUM SUPERHEATER

Figure 10.6

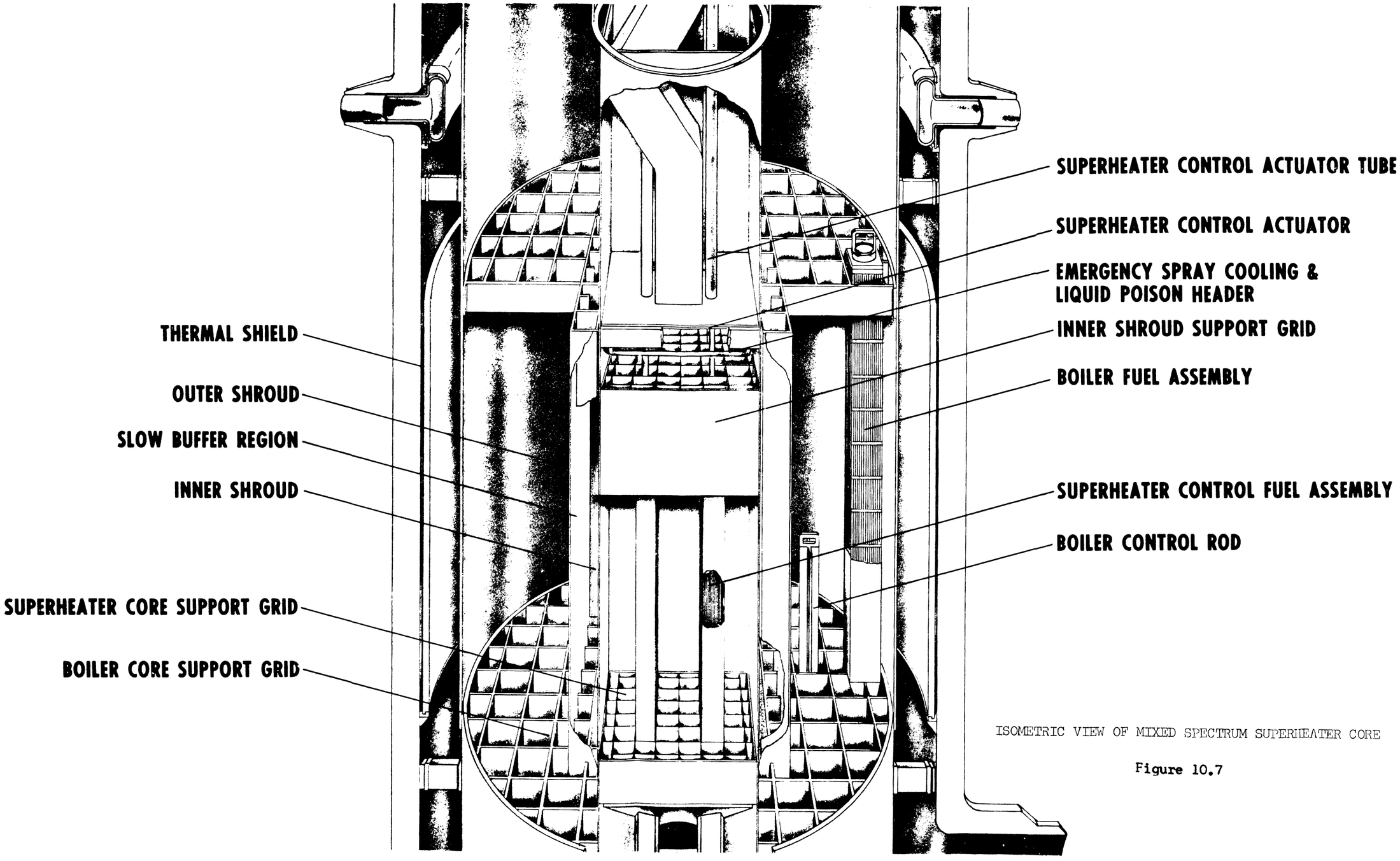

ISOMETRIC VIEW OF MIXED SPECTRUM SUPERHEATER CORE

Figure 10.7

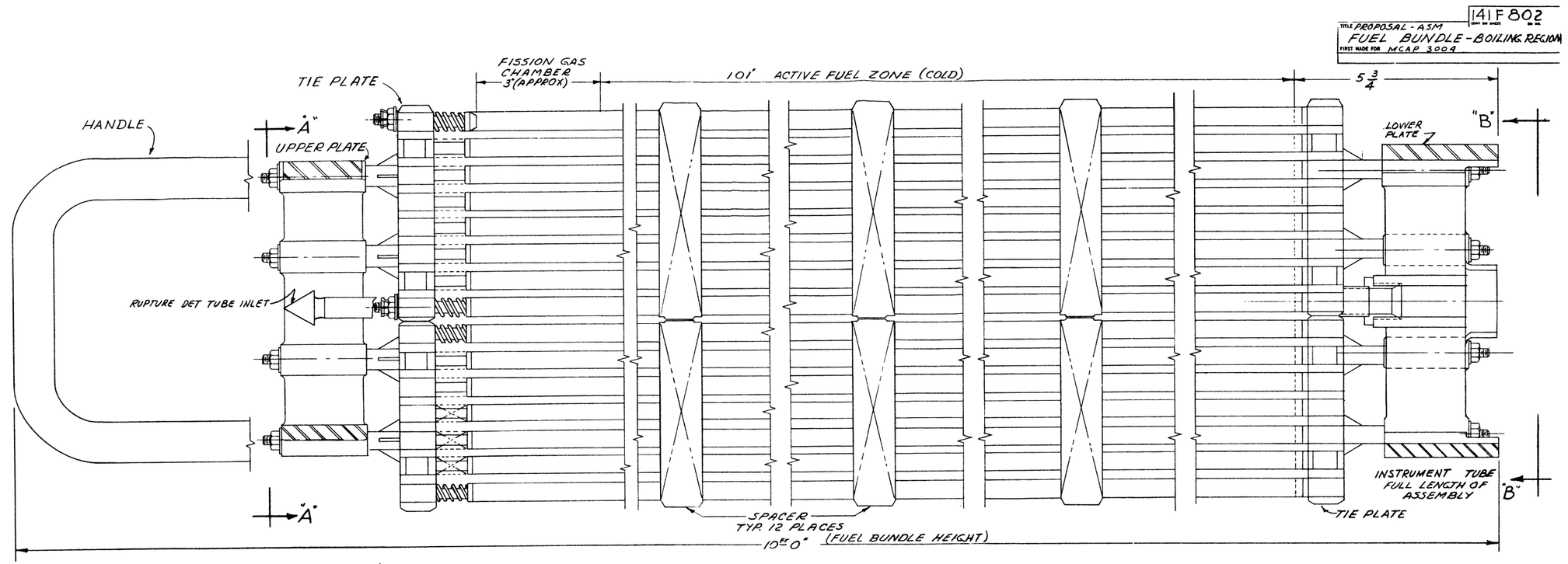
141F802
TITLE PROPOSAL - ASM
FUEL BUNDLE - BOILING REGION
FIRST MADE FOR MCAP 3004
FISSION GAS CHAMBER 3"(APPROX)
101" ACTIVE FUEL ZONE (COLD)
5 3/4
TIE PLATE
HANDLE
"A"
UPPER PLATE
"B"
LOWER PLATE
RUPTURE DET TUBE INLET
INSTRUMENT TUBE FULL LENGTH OF ASSEMBLY
SPACER TYP 12 PLACES
TIE PLATE
10'-0" (FUEL BUNDLE HEIGHT)
49 ROD FUEL BUNDLE (2 REQ'D PER ASM.)
63 ROD FUEL BUNDLE (2 REQ'D PER ASM.)
SECTION "A-A"
VIEW "B-B"

Figure 10.8

TITLE:
FUEL BUNDLE - SUPERHEATING REGION

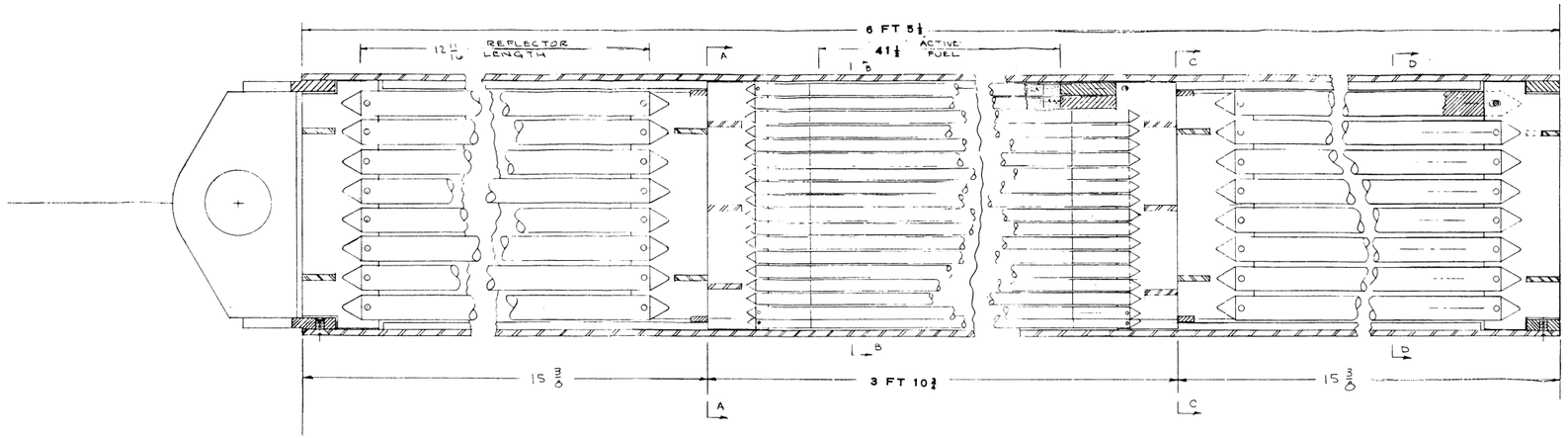

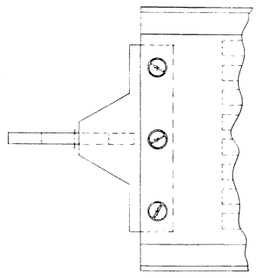

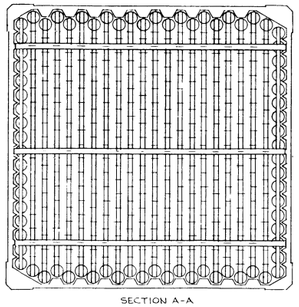

SECTION A-A

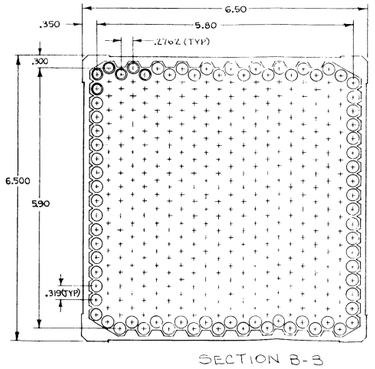

SECTION B-B
416 RODS .280 O.D.

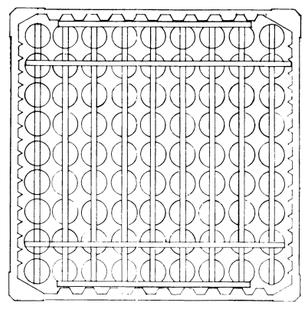

SECTION C-C

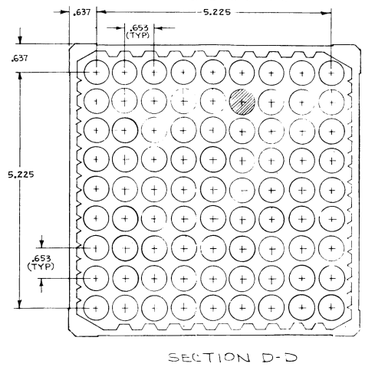

SECTION D-D
81 RODS - 9/16 O.D.

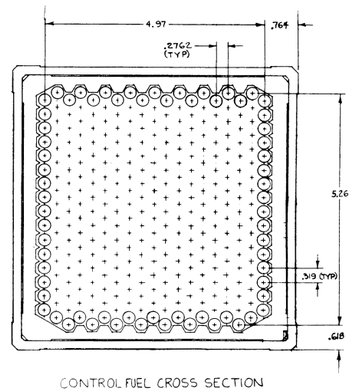

CONTROL FUEL CROSS SECTION
321 RODS - .280 O.D.

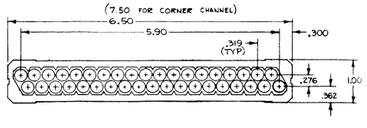

BUFFER FUEL - (SIDE CHANNEL)
38 RODS - .280 O.D (SIDE CHANNEL)
44 RODS - .280 O.D. (CORNER CHANNEL)

Figure 10.9

pressure between the cores. Its function is to act as a nuclear buffer to provide a means of matching the power densities of the two cores at their boundary. A more detailed discussion of the function of the buffer is given in the section on Reactor Physics.

The buffer region is divided into two zones: the water-moderated buffer zone of the boiler and the unmoderated buffer zone of the fast core. The assemblies in the boiler buffer zone consist of 0.830-inch diameter rods in the lower section adjacent to the superheater fuel and standard (0.416-inch O.D.) rods in the upper region. The lower section has a low water-to-fuel ratio.

The fast core buffer section contains fuel assemblies similar to those in the fast core except for the number of rods per assembly. The corner buffer assemblies contain 44 rods and the side assemblies 38 rods. The standard fast core assembly contains 416 rods. The fast buffer rods contain slightly enriched (5%) uranium oxide. Depleted uranium reflector elements are positioned above and below the fast buffer rods.

E. Reactor Physics

1. Introduction

The Mixed Spectrum Superheater differs from conventional reactors in the complexity of its neutron spectrum which results from the presence in one reactor core of a number of regions of widely varying nuclear properties. For this reason, its nuclear analysis is considerably more difficult. The preliminary physics analysis of the MSS concept was performed with methods already developed at General Electric for fast reactor analysis (on the Fast Oxide Breeder program) and for its boiling water reactors. The analysis benefited greatly from these methods; however, it was evident from this work that new tools are required for efficient analysis of the MSS concept.

A summary of the physics of the Mixed Spectrum Superheater is presented below. These results were in general obtained from an 18-group, one-dimensional analysis, although 4-group calculations for scoping purposes were performed in the early stages.

2. Core Geometry

As can be seen in Figure 1, the superheating core of the Mixed Spectrum Superheater occupies a vertical height of only 42 inches as compared to 101 inches for the boiler section. The advantages accuring from this arrangement are as follows:

a. With a more nearly spherical geometry of the fast core the inventory is reduced.

b. Making the fast core shorter and wider reduces leakage which in turn reduces reactivity effects upon flooding.

c. The short core has benefits from the standpoint of heat transfer and fluid flow. The lower pressure drop permits close packing of the fuel rods so that the self-spacing, wire-wrapped pin design can be used. In addition, the close packing reduces the void space in the core and thus the reactivity effects upon flooding.

d. Placing the fast core near the bottom of the boiling core reduces the interacting effect of voids on the fast core and the perturbing effect of flux distortion on heat transfer limitations in the thermal core.

3. Core Inventory and Conversion Ratio

In the superheating core, an inventory of approximately 525 kilograms of Pu-239 is required if 30 per cent of the total power is to be produced by the superheater. If U-235 is used instead of plutonium, the required inventory is about 700 kilograms.

A potential conversion ratio of 1.3 is achievable for the superheating section. This ratio is defined as the number of atoms of fissionable material produced in the superheater, core blanket, core reflector, and buffer regions per fissionable atom destroyed in these regions. The internal conversion ratio, the number of fissionable atoms produced within the superheating core per atom destroyed, is 0.75. This large internal conversion ratio results in a small net percentage fissionable material burn-up in the core and, therefore, a small reactivity swing between refueling.

4. Power Distribution

Figure 10.10 shows the radial power distribution through the center of the superheating core and the adjacent lower region of the boiling core obtained with an 18-group, one-dimensional calculation. Flux distributions for several representative energy groups are shown in Figure 10.11, The power distribution shown represents a power split such that 27 per cent of the power is produced by the superheater. In determining the power split from the one-dimensional plots of Figures 10.10 and 10.11, the shorter length of the superheating core must be taken into account.

5. Use of Buffer Regions

The steam-cooled, fast buffer section is composed of fuel identical to that in the main part of the superheating core but is enriched

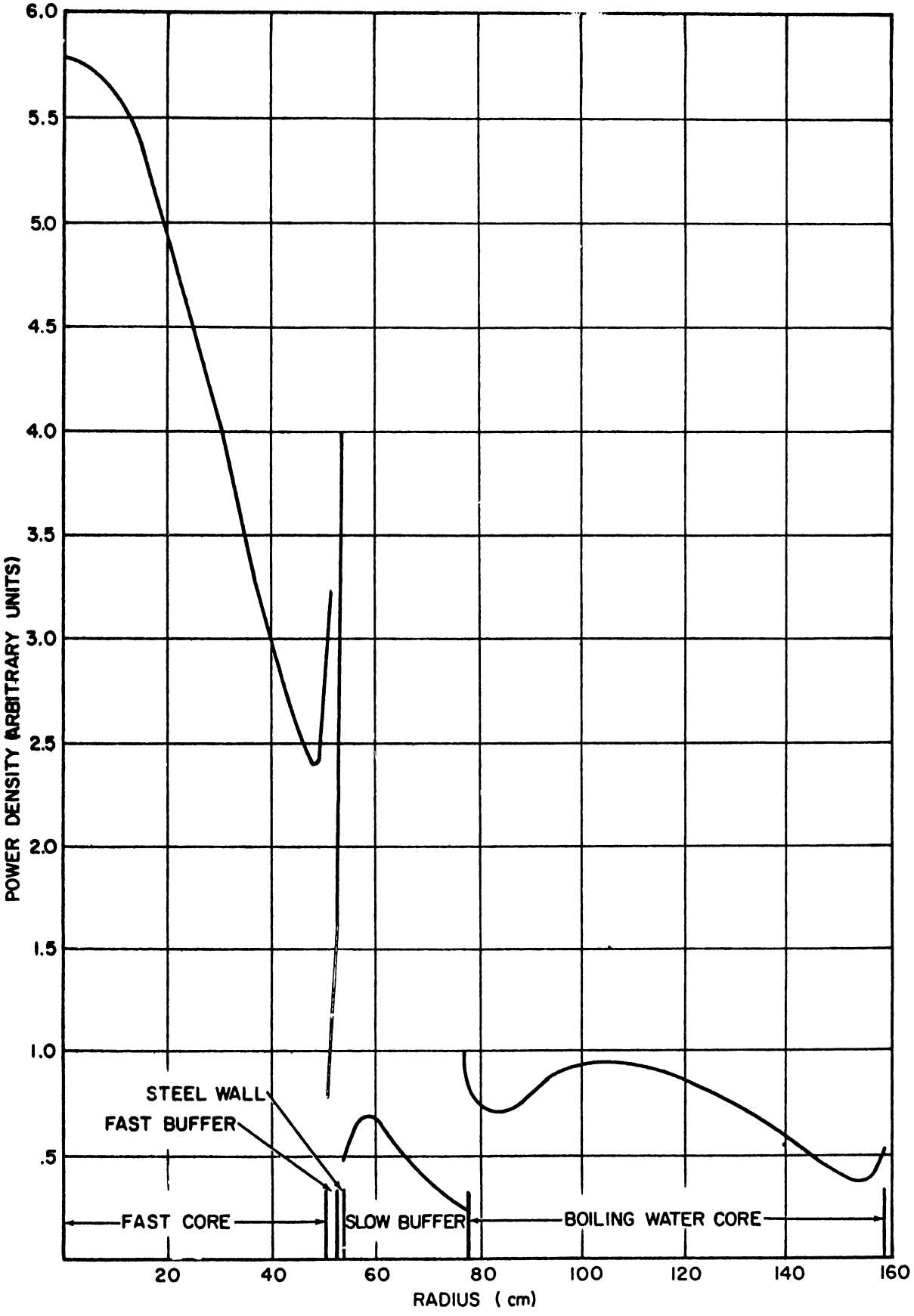

POWER DENSITY AS A FUNCTION OF RADIUS

FIGURE. 10.10

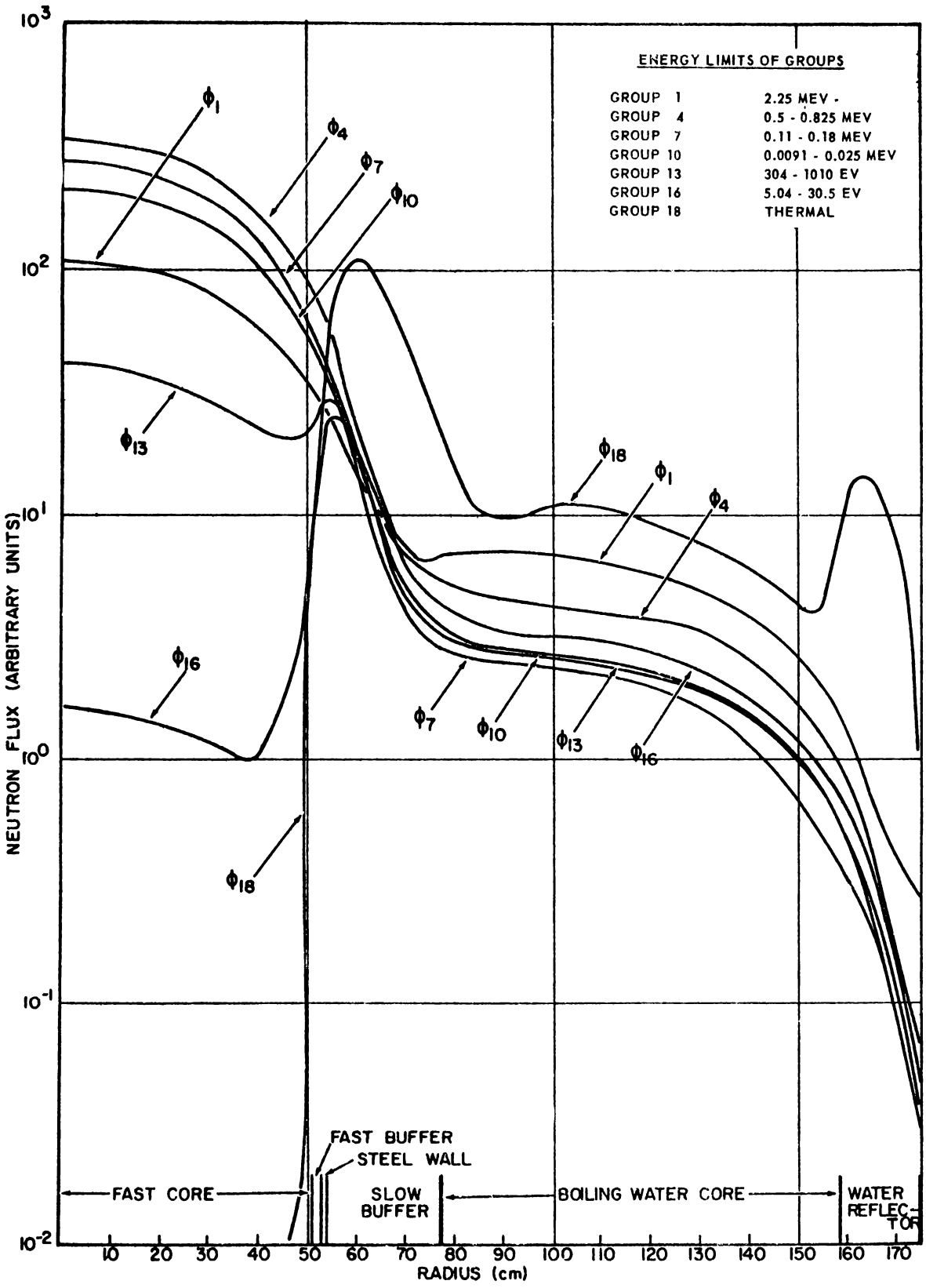

EIGHTEEN GROUP NEUTRON FLUXES AS A FUNCTION OF RADIUS

FIGURE 10.11

to 5 per cent U-235 instead of 13 per cent Pu-239. This buffer has two purposes. First, it is designed to prevent a large power spike at the edge of the superheating core which, without the buffer, would be caused by leakage of thermal neutrons from the water-moderated core. Second, it is designed to perform at high power density as a result of fissions caused by leakage of thermalized neutrons from the water region. The fast buffer region plays a significant role in determining the dynamic behavior of the reactor and is in large measure responsible for the relatively long neutron lifetime (10^{-5} second) as compared to the lifetime of a fast reactor with no thermal coupling (about 10^{-7} second).

Figure 10.0 indicates the possible presence of rather sharp gradients in power density in the fast buffer region. This may result in excessive thermal stresses in the buffer fuel elements. These stresses will be examined in future detailed design studies. If necessary, modifications will be made to keep stresses below allowable levels. One possibility in this direction is the use of thin plates in this region rather than rods.

The slow buffer region consists of depleted uranium oxide in rods 0.75 inches in diameter with the water-to-fuel ratio set at 1.2 to 1.3. Its purpose is again twofold. Its primary function is to isolate the very high-power-density superheating core from the lower-power-density boiling core. Without this buffer, the power at the edge of the boiling core would be excessive. The buffer region prevents this by absorbing leakage neutrons from the fast core. In so doing, the buffer performs its second function which is to produce fissionable material.

Figure 10.1 shows the effectiveness of the buffer in allowing tolerable power distributions in each of the sections of the core; however, calculations of build-up of fissionable material indicates that power generation in the buffer at the end of life could be excessive. In the preliminary studies, it has been assumed that the excessive heat generation can be controlled by the addition of thermal poisons. In future studies, the design of the buffer will be re-examined to find a more optimum means of controlling the power generation.

6. Reactivity Requirements

Table 10.6 shows the reactivity control requirements for the different regions of the core. It should be noted that the reactivity effects in a particular region of the core depend upon the relative power distributions throughout the core. For example, if the superheating core is operating at a very low power level relative to that in the boiling core, the effectiveness of the control elements in the super-

TABLE 10.6

REACTIVITY CONTROL REQUIREMENTS

Fast Core	Reactivity
Fuel cycle	.0. 014
Cold water to cold steam	-0. 010
Cold steam to hot steam	0. 020
Power distribution control	0. 005
Shutdown margin	0. 016
Total Δk controlled by fast core control system	0. 045
Additional shutdown margin in fast core provided by slow buffer control system	0. 040
Boiling Core	
Fuel cycle	0. 070
Cold to hot	0. 005
Hot to boiling	0. 036
Xe and Sm	0. 040
Shutdown margin	0. 036
Total Δk control requirements for boiling core	0. 187
Control system worth in boiling core	~ 0. 21

heating core will be small, and vice versa. In order to avoid this confusion, the reactivity requirements shown in Table 10.6 refer to the superheating and boiling sections as if they were independent systems. In other words, if the superheating section were critical by itself, 2.9% in reactivity would be required for control needs whereas in the boiling section, a change in reactivity of 17% is required over the reactor cycle.

The control system in the boiling core is identical to that in the Dresden reactor. In the fast core, control is obtained by removing fuel and replacing it with blanket material which is primarily U-238. Calculations indicate that the four control elements, which represent 8% of the fast fuel, will have a reactivity effect of 4.5%. Thus, with the 2.9% requirement, the shutdown margin in the fast core with all fuel control out is about 1.6%.

In addition, calculations show that the control rods in the slow buffer region will reduce the reactivity of the fast core by over 4% when they are fully inserted; therefore, the fast core cannot be made critical as long as the buffer elements are fully inserted.

7. Fuel Scheduling

The fuel schedule for the Mixed Spectrum Superheater must consider each of the different fuel regions in the core. The schedule is presently envisioned to be approximately as follows:

a. Superheating Core

Average burnup will be 38,500 MWD/MT corresponding to 50,000 MWD/MT at point of maximum exposure. In the equilibrium fuel cycle, one-fourth of the core will be replaced by new fuel every seven months.

b. Boiler Core

Average fuel exposure will be 19,000 MWD/MT corresponding to a maximum exposure of 35,000 MWD/MT. One-fifth of core is to be replaced every ten months.

c. Buffer and Reflector Regions

The water-cooled slow buffer will remain in the core for 56 months, after which time it will be entirely replaced. The top and bottom superheat reflectors will be exposed for 56 months but will be loaded and unloaded with the superheat fuel. Low exposure reflector pieces will be reloaded into

fresh fuel channels. The steam-cooled buffer will be burned to an average exposure equivalent to that for the standard fast core fuel.

10.7.3.6 Control System

The control system of the MSS has four important functions: to compensate for reactivity changes during normal operation, to provide a continuous means of adjusting the power split between fast and thermal cores, to prevent the occurrence of excessive hot spots, and to provide for scram and shutdown. To carry out these functions, the control system is divided into three parts. One part is located in the fast core, one in the slow buffer region and one in the boiling core.

In the fast core, the control system consists of four fuel assemblies, each of which contains an amount of fuel approximately equivalent to each of the other 32 fuel assemblies in the fast core. The fuel assemblies are inserted by means of motor-driven lead-screw mechanisms located above the reactor vessel to compensate for reactivity lost due to burnup. In the boiling core forty cruciform and 12 T-shaped poison elements presently composed of boron stainless steel provide control for burnup during the operating cycle and for the transition from the cold to operating condition. It is expected that boron carbide will replace the boron stainless steel in accordance with present APED policy. These controls and the buffer controls described below are driven by hydraulic locking piston mechanisms from below the vessel.

The third set of controls in the slow buffer region consists of 8 T-shaped boron carbide and stainless steel rods. These elements permit adjustment of the power split between the fast and thermal cores. For example, if one wished to reduce the amount of power in the superheating core, this would be accomplished by moving the controls in the fast core together with a compensating movement of the controls in the slow buffer region. The net effect would be to maintain the entire system critical while reducing power in the fast core. Some small adjustment of the boiler controls may also be necessary.

It should be noted that the controls in the slow buffer region provide a scram and shutdown mechanism for the fast core independent of the control elements in the fast core. With the control elements of the fast core in their most reactive positions, the fast core will still be subcritical if the buffer control rods are fully inserted.

In addition to these three primary control systems, a back-up, liquid-poison emergency control system is provided to shut down the reactor should the control system malfunction.

10.7.3.7 Instrumentation

The control and instrumentation system provides all the necessary information for normal and abnormal plant operation. The system consists of the necessary control and instrumentation equipment and associated control consoles and panels.

The over-all plant control and safety systems are designed to make the plant safe, reliable, and easy to operate. A centralized system of plant control is provided. Local instrumentation and control boards are included where necessary to supplement the facilities in the central control room. Conventional power plant instrumentation and control is used as far as possible. Safety instrumentation will conform to present APED specifications as recommended by the Hazards Council.

10.7.4 CONTAINMENT PHILOSOPHY

In general, the selection and design of a reactor containment system is based upon a detailed study of postulated "maximum credible" accidents. The study of the Mixed Spectrum Superheater has not reached the point where an analysis of sufficient thoroughness has been performed to delineate the sequence of events occurring during such an accident. Dry containment in the form of a vapor-tight sphere has therefore been provisionally selected for the 1968 plant on the general grounds that the integrity of a vapor-tight sphere is more dependent on the magnitude rather than on the rate of total energy release. It is recognized, however, that further study may demonstrate that the pressure-suppression systems can provide adequate or preferred containment. The maximum credible accident postulated to size the containment sphere was a primary system rupture coincident with core meltdown and reassembly to give a super critical mass which on the basis of pessimistic calculations could result in energy releases equivalent to as much as 300 lb of TNT.

The general criteria used to insure that the containment integrity can be maintained for all credible occurrences are as follows:

A. The design enclosure pressure (25.8 psig) equals or exceeds the peak pressure that could be expected to accompany the maximum credible accident.

B. The leakage rate for the enclosure is not expected to exceed 0.5% of free volume per day at the appropriate design pressure. This limit is subject to review for specific site conditions.

C. A containment spray system will be provided to augment the heat removal mechanism incorporated into the design to reduce enclosure pressure following a severe accident. The spray system may be initiated manually or automatically following an appropriate delay period to permit manual interruption if necessary.

D. Enclosure isolation will be effected automatically in sufficient time following the incident to assure confinement of any significant quantity of radioactive fission products.

E. Adequate provision will be made to protect the containment sphere against possible missiles that may be initiated during the excursion. This will be primarily in the form of the biological and missile shields above the reactor.

10.7.5 REACTOR PRESSURE VESSEL

The reactor vessel is a carbon steel (SA302, Grade B) pressure vessel with a wall thickness of 7-3/4 inches. It is clad on the inside surface with a 1/4-inch thickness of 304 stainless steel. Design pressure and temperature are 1800 psig and 650°F respectively. The reactor will be designed so that the total integrated neutron dose is the minimum compatible with the necessary power densities and maximum available pressure vessel diameters at the time the detailed design studies are carried out. The expected lifetime of the vessel is 40 years. The vessel is shown in detail in Figure 10.5.

10.7.6 GENERAL OPERATING PROCEDURES

10.7.6.1 Normal Operation

For base load operation, the MSS plant will have the following main control features:

1. System steam pressure will be regulated automatically by the turbine control valves. In effect the turbine then becomes a slave to the reactor, and turbine power varies so as to maintain reactor pressure.

2. Power (hence, steam flow) in the boiler region of the reactor core will be controlled manually by positioning the control rods in the boiler.

3. Superheat steam temperature will be controlled manually by adjusting the power in the superheating core by positioning the control fuel elements.

4. Load rejections will be absorbed by means of full-capacity steam bypass valves to the condenser.

5. Conventional steam turbine controls will be utilized to prevent overspeeding due to load rejection or other abnormal occurrences.

Normally, load changes are pre-scheduled or are initiated by communication from the control load dispatcher. As presently envisioned, load changes for the MSS plant will be performed as described below.

For a load (steam flow) increase, the power in the boiling core will be increased a small amount. As a consequence of nuclear coupling, the power in the superheat core will rise also, but not quite as much as needed. The superheated steam temperature will drop. If the reduction is great enough (about 25°F), the superheater control rods are moved to raise the superheat power. The buffer control rods are trimmed to maintain the correct power ratio between boiler and superheater. There is also some nuclear coupling from the superheater to the boiler, but the difference in sizes of the cores makes this interaction relatively small. The respective control rods are moved in incremental steps until the desired steam flow and temperatures are achieved.

A reversed procedure is used for a load decrease. The superheater core power is reduced enough to decrease the outlet steam temperature about 25°F. Steam flow is then reduced by decreasing the boiler power to the point where the steam temperature is raised back to the set value. The steps continue until the desired flow and temperature are achieved.

In-core neutron chambers distributed throughout the boiling core will help the operators to control the flux distribution. The closer nuclear coupling within the fast core indicates that regional flux monitoring may not be necessary. Thermocouples will be provided to monitor the outlet steam temperatures of the fuel channels to detect core hot spots should they develop. Some control of outlet temperature distribution is expected from control rod patterns.

10.7.6.2 Start-up Procedure

1. In the start-up condition, the reactor will be completely flooded with cooling provided by the shutdown heat exchanger.

2. All control elements (fuel) in the fast core are kept in their least reactive position to keep the fast core shut down.

3. Shutdown cooling is stopped, the fast core is slowly drained, and normal water level is established in the thermal core.

4. The core spray is used to maintain safe temperatures in the drained fast core.

5. Vacuum is drawn on the reactor by using a mechanical pump on the condenser and opening the steam bypass valves. Since the boiling temperature will be reduced to about 100°F, boiling will occur quickly to supply steam-flow cooling to the fast core.

6. The boiler section of the reactor is made critical using only the poison control rods in the outer region of the boiling core.

7. Power in the boiler is increased to give a heating rate of less than 100 °F per hour.

8. With steam flowing, the pressure will be allowed to build up while enough steam is dumped through the bypass valves for adequate cooling of the fast core.

9. When the reactor pressure reaches 150 psig (lowest operating setting), the pressure regulator will be placed into service. The pressure and temperature build-up rate then are controlled by moving the pressure set point. The steam-operated air pumps (ejectors) are also put into operation at this time, replacing the mechanical pumps.

10. At rated pressure, turbine rolling and heating begins.

11. As the turbine temperatures approach equilibrium, the superheat temperature is raised slowly by increasing the power in the fast core. This is accomplished by withdrawing rods in the slow buffer region followed by insertion of fuel control assemblies in the superheating core.

12. When rated superheat temperature is reached and turbine temperatures have leveled off, the generator is synchronized into the electrical system. The turbine is then placed under pressure regulator control by backing out the governor set point to 102%.

13. The plant is now on base load operation.

10.7.6.3 Shutdown Procedure

1. Reactor power is reduced, as described in Section A above, until the generator has close to zero output at which time the generator is disconnected from the line. The master (turbine) trip is actuated to close the control and stop valves and to stop the turbine.

2. The pressure regulator will be maintaining pressure and temperature by controlling the bypass valves. This hot condition can be continued if the shutdown is for only a few hours.

3. For a prolonged shutdown, the reactor is made subcritical, although steam will still be generated by decay and stored heat. Cooling is by means of this steam flow through the pressure-regulated bypass valve. The pressure set point is decreased, as required, to maintain the proper cooling steam flow.

4. When steam flow has decreased to the point where cooling of the fast core is insufficient, the core spray system is used to continue the cooling and, eventually, to flood the reactor. The shutdown heat exchanger is also put into operation.

10.7.6.4 Refueling Procedure

After the reactor has cooled sufficiently, the refueling procedure is initiated by removing the top head of the reactor vessel. Removing the top head also removes the steam dryers and the fast core control drives which are attached to the head. The top head cannot be removed unless the four fast core control fuel elements are in their least reactive position and detached from the control drives. After the top head has been removed, the fast core head and steam inlet pipes are removed as a unit. The fast core region is now exposed and can be refueled. Access to the boiling section for refueling is obtained by removing the steam separators, which come out as a unit.

10.7.7 COOLING SYSTEMS

10.7.7.1 Cooling under Normal Operating Conditions

In the process of producing, drying, and superheating steam, adequate cooling is derived to maintain the reactor core at the proper temperatures (maximum surface temperature in superheater is 1250 °F, 628 °F in boiler). The superheated steam leaves the vessel through a single opening in the bottom head and is carried to the turbine through a single, insulated pipe. Return of the feedwater to the vessel is also through a single pipe. The arrangement of piping and components is shown in Figure 10.12.

The recirculating water flows in three parallel loops from the reactor, through three recirculating pumps and back to the reactor inlets. To maintain relatively pure water in the recirculating loop, a reactor cleanup system removes part of the water from the recirculating line and returns clean water to the reactor feedwater line. All loop piping is designed in accordance with applicable ASME or ASA piping codes.

10.7.7.2. Shutdown Cooling System

The reactor shutdown cooling system is capable of absorbing the entire rate of reactor decay heat approximately three hours after reactor shutdown. The system consists of two pumps and two heat exchangers with the necessary piping and valves connecting the system to the primary loop. The heat exchangers receive their cooling water from the plant cooling water system. After seven hours of operation, the shutdown system can reduce the primary loop temperature from 212 °F to 125 °F so that refueling may start.

932C740

TITLE PROPOSAL

FLOW DIAGRAM

FIRST MADE FOR MCAP 3004

REACTOR ENCLOSURE

LIQUID POISON

MSS VESSEL

CLEAN UP DEMINERALIZER SYSTEM

SHUT DOWN COOLING SYSTEM

FUEL POOL COOLING SYSTEM

FROM ROD FEED PUMPS

EMERGENCY CONDENSER

DE-SUPER HEATER

TURBINE BUILDING

CORE SPRAY COOLING

CONDENSATE STORAGE

DEMIN. WATER TRANSFER

DEMIN. WATER STORAGE

MAKE UP DEMIN.

RAW WATER

FROM COND. PUMPS

COND. TRANSFER

STEAM BYPASS CONTROL SYSTEM

HIGH PRESSURE TURBINE

LOW PRESSURE TURBINE

GENERATOR

CONDENSER

HOTWELL

GLAND SEAL REGULATOR

TO COND. STORAGE

CONDENSATE PUMPS

BOILER FEED PUMPS

FEED WATER HEATER

FEED WATER HEATER

FEED WATER HEATER

FEED WATER HEATER

FEED WATER HEATER

GSC

AEJ

CONDENSATE DEMINERALIZER SYSTEM

TO FILTERS AND STACK

DRAINS

DRAINS

TO DE-SUPER HEATER

ROD FEED DRIVE PUMPS

RADICACTIVE WASTE DISPOSAL

TO WASTE

TO CONDENSATE STORAGE TANK

Figure 10.12

10.7.7.2 **Emergency Cooling System**

The emergency cooling system consists of three high-capacity dump valves which can pass steam to an emergency condensation tank located within the sphere, an emergency condenser vented to the atmosphere, and a desuperheater with associated equipment to remove superheat from the initial steam flowing to the emergency condenser. Figure 9 shows a schematic diagram of the system.

Fully automatic controls are provided to put the emergency cooling system into operation for any interruption of steam flow. The operational description of the emergency cooling system is summarized in Table III.

At the onset of an emergency condition, an automatic signal scrams the reactor and simultaneously activates the emergency cooling system. The containment isolation valves begin to close instantly, and dump valves open to direct steam to the emergency condensation pool. This results in initial steam flow rates of approximately 50% of rated, which is necessary to assure that the superheater cladding temperatures do not exceed tolerable limits. After approximately 30 seconds, only 6% of rated flow is required. The dump valves are then closed and the emergency condenser and desuperheater utilized to bring the system down to atmospheric pressure at a controlled rate.

The desuperheating system will be sized such as to remove all superheat from the steam flow to the condenser for three minutes of operation, assuming total loss of power. Beyond this time, the steam may leave the unit with some superheat, but by this time the emergency condenser will be adequately warmed and capable of accepting superheated steam.

The emergency condenser is sized to condense approximately six per cent of rated steam flow and is brought into service by either an automatic signal or by manual operation of the discharge valves. The condenser is located at the highest practical elevation to provide sufficient gravity head for natural circulation of the coolant.

10.7.8 REACTOR EMERGENCY POWER

A diesel-engine-driven generator provides emergency power for safety circuits, battery system charger, and selected plant equipment. The following equipment will be tied into the emergency power source, which is automatically started when normal power supply fails:

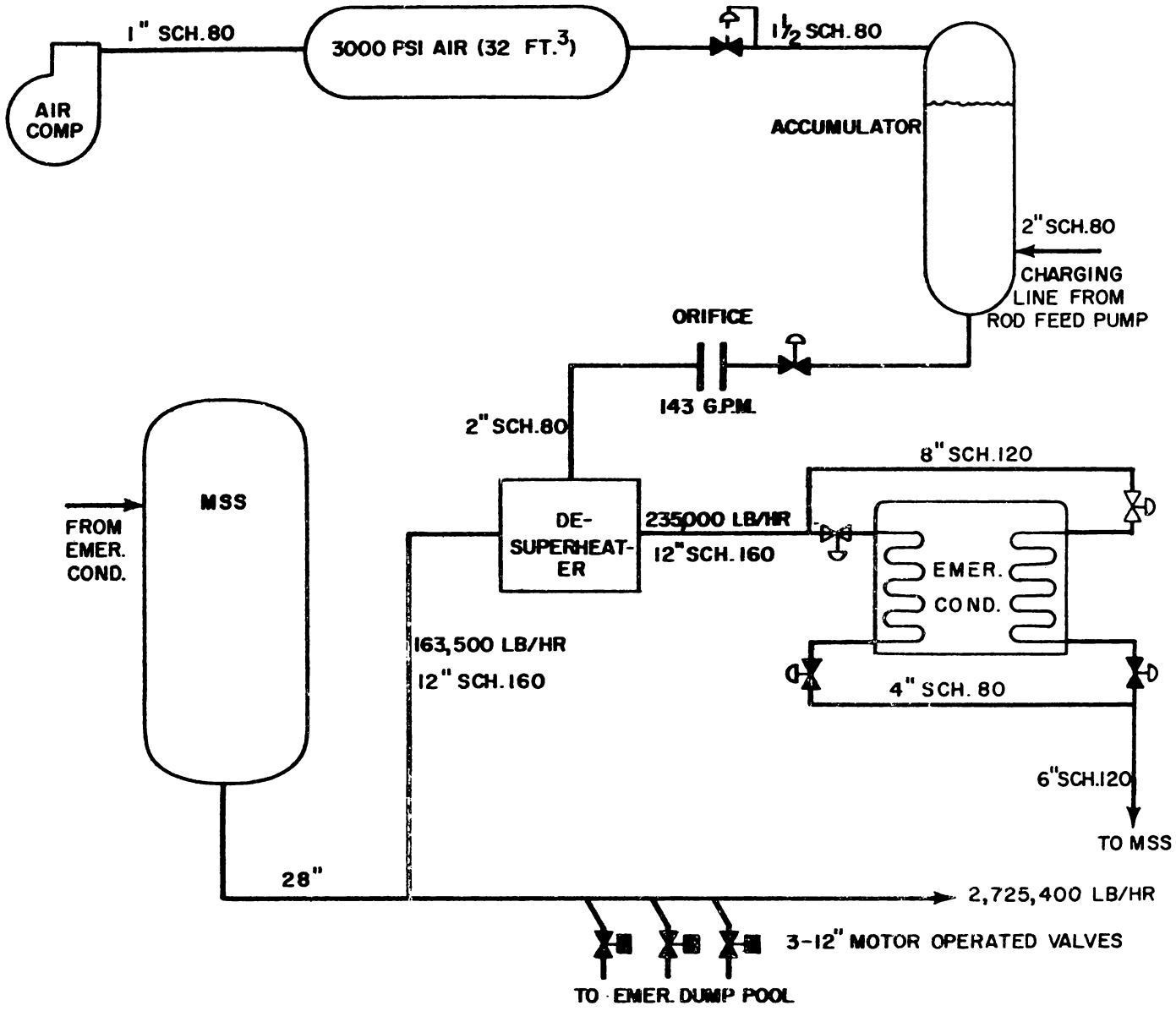

REACTOR EMERGENCY COOLING SYSTEM

FIGURE 10.13

TABLE 10.7

OPERATION OF REACTOR EMERGENCY COOLING SYSTEM

TIME	STEAM FLOW	TEMP.	PRESS.	OPERATIONAL DESCRIPTION
---	up to and including 100% rated flow to turbine	950°	1450 psig	Plant operating normally. All steam flow passing directly to turbine. 1900 lb. pressure maintained in accumulator tank by rod feed pumps. 3000 lb. pressure maintained in air receiver by air compressor.
Scram - 0 seconds	Steam flow drops to 50% of above	950°	1450 psig	Reactor scrams. Incident requiring containment occurs. Containment valves close instantly. Simultaneously, valves open directing steam flow to emergency condensation pool.
25 seconds	10% of rated flow	1300/ 950°	1450	Drain valves on emergency condenser open. Partial flow commences to emergency condenser. Flow of superheater steam activates temperature transmitter and valve opens admitting spray water to desuperheater.
30 seconds	6% of rated flow	1300/ 950°	1450	Emergency dump valves close. Entire flow then passes to emergency condenser. Steam is desuperheated to 580°F. Desuperheater spray of approximately 225 gpm is maintained by accumulator tank for 30 seconds. Make-up will be provided by rod feed pumps when accumulator pressure drops to 1850 lb.
60 seconds	3% of rated flow	1350/ 950°	1450	Entire flow passes to emergency condenser and is desuperheated to 580°F. Desuperheater spray of 113 gpm is maintained by rod feed pumps.

1 Makeup system pump
1 Domestic water pump
1 Service water pump
1 Station battery charger
1 Rod drive feed pump (auxiliary feed)
1 Instrument air compressor system
1 Turbine turning-gear system
1 Diesel oil transfer pump
1 Closed cooling water system pump
1 Post incident cooling water pump
1 Core spray pump
1 Liquid poison pump

10.7.9 SAFEGUARDS CONSIDERATIONS

10.7.9.1 Introduction

Although the present conceptual design of the Mixed Spectrum Superheater has been explored to the point where feasible solutions can be seen for most of the obvious problems, it is recognized that a number of questions remain to be answered. Foremost among these are problems relating to safeguards. APED's experience with boiling water reactors and the more recent work on SADE, ESADE, and VESR will contribute to understanding in this area; however, prototype experience is essentially lacking. Experimental and analytical confirmation of the preliminary results will be required.

Brief discussions of the more significant safeguards problems are given below. For the sake of brevity, consideration has been limited to those problems unique to the Mixed Spectrum Superheater or to superheating reactors in general. The intention here is only to point out the major areas of concern.

10.7.9.2 Flooding and Unflooding Problems

To minimize the flooding coefficient in the MSS, it is planned to add several per cent of epithermal poisons to the fuel in the superheating core. Calculations indicate that without the poisons, flooding of the fast core would add about 12% of reactivity. However, with adjustment of the epithermal poison concentration, the flooding-unflooding effect will be reduced to less than 0.5% of reactivity.

The principle underlying the use of epithermal poisons stems from the degradation of the neutron spectrum in the presence of water. Advantage is taken of this shift in neutron energy by including materials of very high cross section in the epithermal region. The increase in reactivity due to decreased neutron leakage must, of course, be taken into account. In the flooded condition, when the neutron spectrum is degraded, these materials reduce reactivity by absorbing eipthermal neutrons.

The results discussed below, involving the use of europium as the epithermal poison, show that flexibility is available for adjusting the flooding coefficient through the use of epithermal poisons.

Figure 10 and 10 graphically present a summary of the important results. Shown in Figure 10 is the reactivity effect of completely flooding the superheating core as a function of core size and europium content. In all cases, the unflooded operating core is loaded so that it is exactly critical and the reactivity values shown represent the reactivity in the completely flooded core. Except for the 3-1/2 ft. core, all calculations assume that U-235 was used. In the 3-1/2 ft. core, calculations were performed for both U-235 and plutonium. It can be seen that in all cases, the total reactivity effect of flooding can be adjusted to zero or negative values by proper choice of europium content. Figure 11 is a plot of the reactivity change as a function of the fractional flooding of the core. The three cases considered are for the 1-1/2 ft. core containing 3% of europium and a 3-1/2 ft. core containing 0. 2 and 0. 3% of europium. In each case, the flooding is assumed to occur uniformly throughout the core. One notes that the reactivity change with flooding is highly sensitive to the size of the core and the poison content. In particular, whereas the reactivity in the small core rises slightly as the core is initially flooded, the reactivity in the larger core decreases with partial flooding and then increases with further flooding. These effects can be qualitatively understood on the following basis. The small core has a relatively hard spectrum and the decreased leakage due to initial flooding increases reactivity. As the reactor is further flooded, the effect of degradation of neutron spectrum is such that the europium becomes effective and the increased absorption in the europium more than offsets the decreased leakage. In the case of the large reactors, the spectrum is soft enough and the leakage small enough so that even during the initial flooding the increased absorption in the europium has a greater effect that the decreased leakage.

The rise in reactivity in the region of almost complete flooding is due to the degradation of the spectrum into the thermal region. At thermal energies, the europium is not an effective poison and the fissionable material cross section is very high relative to that of the other materials in the core. Thus, essentially all of the neutrons which are thermalized result in capture in the fuel. The shape of the curve can be considerably changed by the addition of the thermal poison as well as an epithermal poison in the core.

The possibility of having a minimum in reactivity during partial flooding may be important in an unflooding accident. The desirability of this is unclear at this time. Under some circumstances, one could envision increased safety since an unflooding accident results initially in a dip in reactivity. Indeed, it appears possible that the dip in reactivity can be made so large that there is not enough excess reactivity

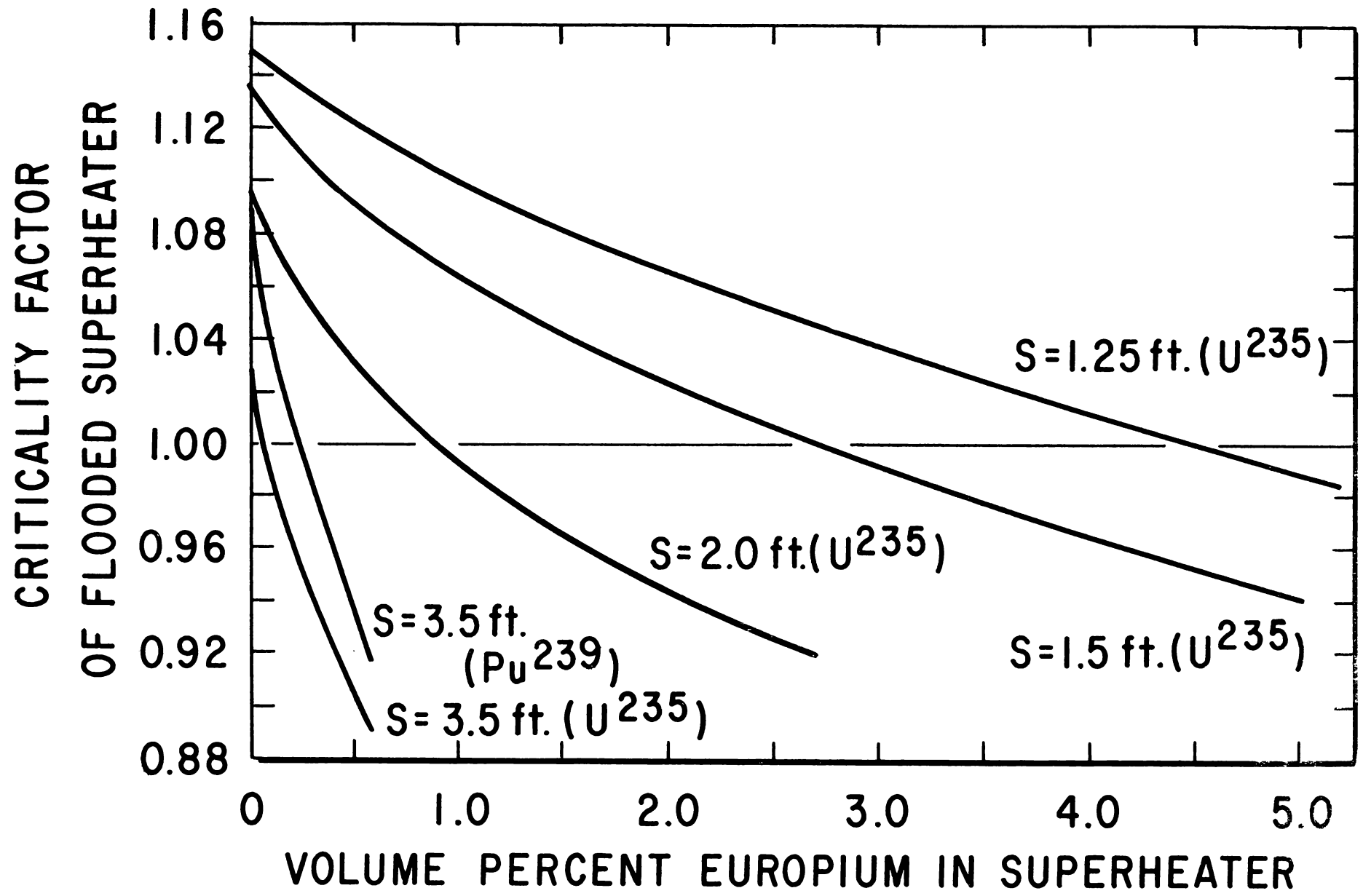
CRITICALITY FACTOR OF FLOODED SUPERHEATER
1.16
1.12
1.08
1.04
1.00
0.96
0.92
0.88
0
1.0
2.0
3.0
4.0
5.0
VOLUME PERCENT EUROPIUM IN SUPERHEATER
S=1.25 ft. (U235)
S=2.0 ft.(U235)
S=1.5 ft.(U235)
S=3.5 ft. (Pu239)
S= 3.5 ft. (U235)

FIGURE 10.14

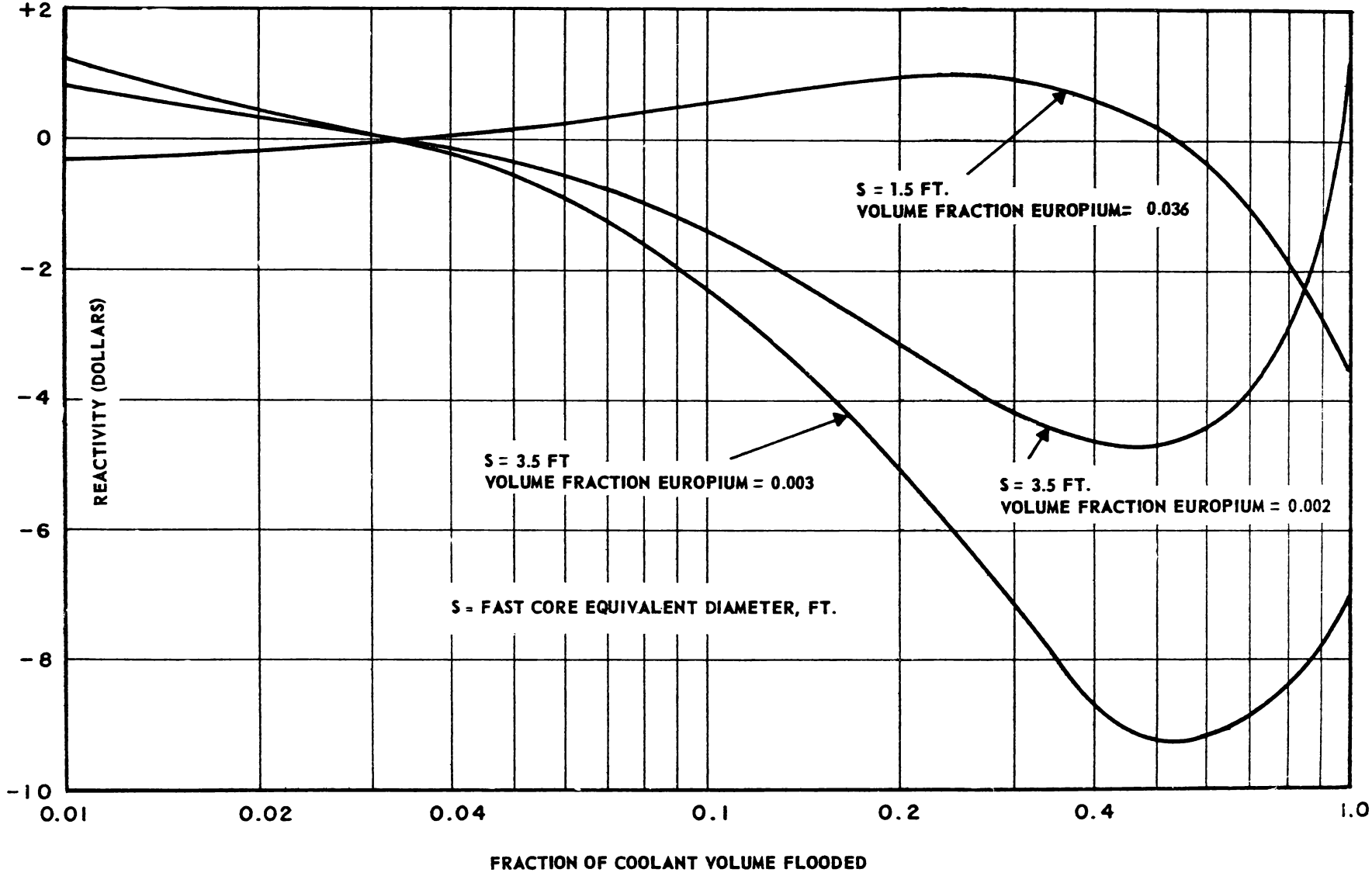

REACTIVITY VERSUS FLOODED CORE FRACTION
FIGURE 10.15

in the core to get past the minimum. On the other hand, the dip means that once the point of minimum reactivity occurs, further flooding increases reactivity. The situation is further complicated by the fact that in an unflooding accident, the reduction of water density will not occur uniformly through the core but will, in general, involve the unflooding of the upper part of the core before the lower part becomes substantially affected.

10.7.9.3 Core Meltdown

Since the central core of the Mixed Spectrum Superheater is essentially a fast reactor, it is recognized that a meltdown of the superheating core can have serious consequences. Assurance is required that a large portion of the fuel cannot slump togehter into an unpoisoned critical mass. Although the seriousness of this event has not been quantitatively examined as yet, it is plain that it represents a hazard not found in a normal boiling water core. The compaction of a high enrichment fast core will increase the reactivity while a similar compaction of a thermal core will cause a decrease in reactivity due to removal of moderator from a low-enrichment material.

The reference design is intended to provide adequate cooling for all foreseeable normal and abnormal conditions. During normal operation, cooling of the superheater is provided by steam generated in the boiling section. The water stored in the boiling section also acts as a source of cooling steam which results from flashing even if the power of the boiling core is reduced to a very low level. Further emergency cooling is provided by the spray cooling system and by the ability to flood the core. These systems appear capable of preventing gross melting in the superheater under operating and emergency conditions, although further detailed analysis is required to assure that temperatures during transient conditions will not become excessive. To provide some perspective it might be noted that at full power, loss of cooling capacity will result in clad melting in less than one second.

10.7.9.4 Start-up Accident

The normal start-up procedure for the MSS is discussed in Section 10.7.6.2 In general, it is planned that the control rods in the buffer region separating the superheating and boiling cores be fully inserted at the time of start-up. This will keep the heat generation in the fast core at a low level until sufficient steam is generated in the boiler to cool the fast core. Various interlocks will be provided to prevent start-up should the controls not be fully inserted.

A "conventional" start-up accident for the Mixed Spectrum Superheater has not been analyzed in detail. It will be made the subject of future work. It is planned that the maximum insertion rate of all control rods

will be limited so that all possible transients can be controlled either by inherent nuclear characteristics or by high-flux scram instrumentation.

10.7.9.5 Pipe System Rupture and Loss-of-Coolant Accident

Studies of major accidents must include an evaluation of major line breaks and loss-of-coolant accidents. Preliminary calculations indicate that explosive decompression due to rupture of the main steam outlet line can result in some distortion of the core, but complete collapse does not appear to be likely. The grid plate can withstand the transient forces imposed upon it during passage of the expansion wave through the fast core. It is expected that the fuel elements in the fast core region can be designed to withstand without collapse the pressure difference exerted during blowdown. The seriousness of the problem is determined by the effect on reactivity of any radial movement of the fuel rods tending towards compaction. On the basis of present calculations, the effect does not seem to be large although confirmation is desirable.

The probability that the fast core may be subject to a strong decompression is markedly reduced by incorporation of a venturi flow stabilizer in the steam outlet nozzle. A venturi limits the mass flow rate passing through it to a value associated with sonic velocity in the throat and, therefore, limits the drag and pressure forces exerted on the fast core during the blowdown period. The nozzle is so designed (9-1/2 inch throat) that choking occurs at a mass flow rate about 50% above rated. This flow condition is reached immediately following pipe break. Subsequently, the flow rate is stabilized until the pressure in the throat reaches ambient pressure. When this happens, the flow becomes unchoked and the mass flow rate is a function of the pressure in the reactor. In effect, the venturi places an upper limit on the pressure drop that can be developed across the fast core by limiting the maximum mass flow to 150% of rated. This protection is available regardless of the steam flow rate prior to the line rupture since the maximum mass flow is a function only of the minimum area ratio of the venturi. This additional safety margin is bought at the price of a small (20 psi) but significant unrecovered pressure drop across the venturi.

Emergency cooling is provided to remove heat from both cores if normal heat removing capability should be lost. This is in the form of spray cooling as discussed previously under core meltdown.

10.7.9.6 Refueling and Control Rod Dropout

The general principle will be followed to prevent damage or injury during refueling or accidental control rod shoot-out or drop-out. The reactivity represented by the maximum size movable unit (fuel bundle or control rod) will be limited to values which when inserted at the maximum possible rate will

not result in damage to the reactor. The analysis at present is not sufficiently complete to assure that this is the case for the reference conceptual design.

10.7.9.7 Main Line Valve Malfunction

Detailed analyses are planned to assure a high degree of reliability in the operation of the turbine bypass and sphere isolation valves and to study the consequences of malfunctions. There are two factors that make it important to do this. The first is the necessity of cooling the superheating core at all times. If the turbine-generator is dropped off the line or if sphere isolation is required, the steam must be bypassed to the main or emergency condenser without interruption. The second factor is related to the fact that the MSS is similar to a single-cycle BWR in that changes in load demand are reflected back in the reactor as pressure changes. If demand is increased, the pressure decrease in the reactor increases the voids, making it necessary to compensate by withdrawing control rods. Conversely, if a main line valve is suddenly closed, a temporary overshoot in power could result. This problem requires further study to assure that the reactor will not be damaged or to provide assurance that flow cannot be interrupted by valve malfunction.

10.7.10 MAXIMUM CREDIBLE ACCIDENT (PRELIMINARY CONSIDERATION)

Current studies indicate that the total energy released in a maximum credible accident for the MSS will not be significantly greater than can be expected for a conventional boiling water reactor. The probability of such a major incident, however, has not been adequately assessed as yet. It is recognized that the presence of the fast core with its possibility of compaction introduces a mechanism by which reactivity can be increased. In contrast, a boiling water reactor will lose reactivity under almost any credible distortion of the core. The sequence of events leading to a maximum credible accident, however, is by no means clearly defined. The safeguards analysis is not complete, and no attempt has been made to define in detail a maximum credible accident.

In order to provide a basis for the present conceptual design, the following hypothetical incident was postulated. Without regard to initiating mechanisms, it was assumed that an excursion occurred in the fast core resulting in meltdown and compaction. On the basis of the analysis for EBR-II, which is an all-fast reactor, it was estimated that the explosive energy released in a worst credible accident could be as much as that equivalent to 300 lbs. of TNT*. It is felt that this estimate is quite conservative. Because of the

* The explosive energy release estimated for the EBR-II maximum credible accident is the equivalent of 300 lbs of TNT. The sequence of events is postulated as follows: It is assumed that somehow the sodium coolant is

negative Doppler coefficient of the MSS not available in EBR-II, the coupling to the thermal core, and the much reduced reactivity effect of compaction as compared to an all-fast reactor.

At the present time, it is debatable whether the pressure vessel will be ruptured by a blast equivalent of 300 lbs. of TNT; however, it is postulated here that the explosive energy will rupture the vessel and release pressurized hot water and steam to the containment building. Missile shielding is provided to insure the integrity of the containment sphere. It is assumed that a significant coincident energy contribution from the thermal core or from a metal-water reaction does not occur simultaneously with the fast core excursion.

The incident is assumed to occur while the reactor is operating under conditions of maximum energy content in the coolant. The total enthalpy, corresponding to approximately 161,000 lbs. of pressurized water and steam, is estimated to be about 1.0×10^8 Btu. Release of this steam-water mixture along with the nuclear energy to the sphere results in peak pressure and temperature of approximately 25.8 psig and 240°F respectively. These figures are based upon the free volume of a 160 ft. diameter sphere with the initial atmospheric state assumed to be 14.7 psia, 100°F, and 100% relative humidity. Accordingly, the conceptual design of the MSS calls for enclosing the reactor and its major components in a vaportight sphere 160 ft. in diameter with a design pressure of 25.8 psig.

11.0 E-SADE SAFEGUARDS

11.1 The following information is from GEAP-3751, "Amendment 46 to License Application for Vallecitos Boiling Water Reactor" dated June 26, 1961.

11.2 Operating Limits for Special Experimental Facilities Expanded Superheat Advance Demonstration Experiment.

TABLE 11.1

OPERATING LIMITS FOR SPECIAL EXPERIMENTAL FACILITIES
EXPANDED SUPERHEAT ADVANCE DEMONSTRATION EXPERIMENT

	Item or Condition	Minimum Value	Design Value	Maximum Value	Units
1.	Outlet temperature	----	1000	1100*	°F
2.	Steam flow during loop operation with steam cooling	80*	100	----	% of calcula. normal operating value
3.	ΔP during loop operation with steam cooling	60*	100	----	% of calcula. normal operating value
4.	Maximum calculated clad surface temp.	----	1250	1400	°F
5.	Water Flow - water cooling	50**	100	----	% of calcula. normal operating value
6.	Calculated maximum element power for steam cooled operation	----	125	156	KW
7.	Calculated maximum element power for water cooled operation	----	12.5	30	KW
8.	Calculated maximum element power during switchover	----	---	2.2	KW

* Automatic Reactor Scram Setting

** Automatic Reactor Run-In Setting

Additional Mandatory Restriction on Loop Operation

(1) A mechanical device similar to the control rod travel limiting stops currently used in the control rod drive system shall be locked on control rod number 4, locking the control rod in the inserted position, before E-SADE loading operations may commence and shall require station supervision cognizance before removal.

(2) It shall be shown by analysis before E-SADE loading operations may commence, that with control rod number 4 inserted, the maximum reactivity change resulting from the installation of E-SADE will not exceed 1% Δk.

11. 3 Expanded Superheat Fuel Demonstration Test Loop

11. 3. 1 Introduction and Summary

The loop is designed to test prototype fuel elements for superheat reactors under environmental conditions. The initial design provides for nine elements in parallel flow channels.

The test facility consists of three fundamental parts

(a) Equipment within the Reactor Vessel shown in Figure 11. 3. 1

(b) Main Loop Equipment outside the Reactor Vessel shown Schematically in Figure 11. 3. 2

(c) Gas Collection & Filtering System shown Schematically in Figure 11. 3. 2

The primary loop coolant is steam which is collected in the upper region of the reactor vessel adjacent to the access port. The steam flow is down around the outside of the nine parallel tubular fuel elements and up through the center of each element. The superheated steam passes to the external piping through a flanged connection at the access port. The steam is then directed by piping outside the reactor through two parallel flow control valves, a condenser, and, finally, to the reactor condensate system.

A detailed description of the facility and a discussion of proposed system operation are given in Section 11. 3. 2 through 11. 3. 4. In Section 11. 3. 5, the provisions for controlling release of radioactive gas are described. Heat transfer and physics characteristics are discussed in Sections 11. 3. 6 and 11. 3. 7, and Section 11. 3. 8 is devoted to the possible hazards associated with the loop operation and the safety features included to mitigate the severity and probability of accidents.

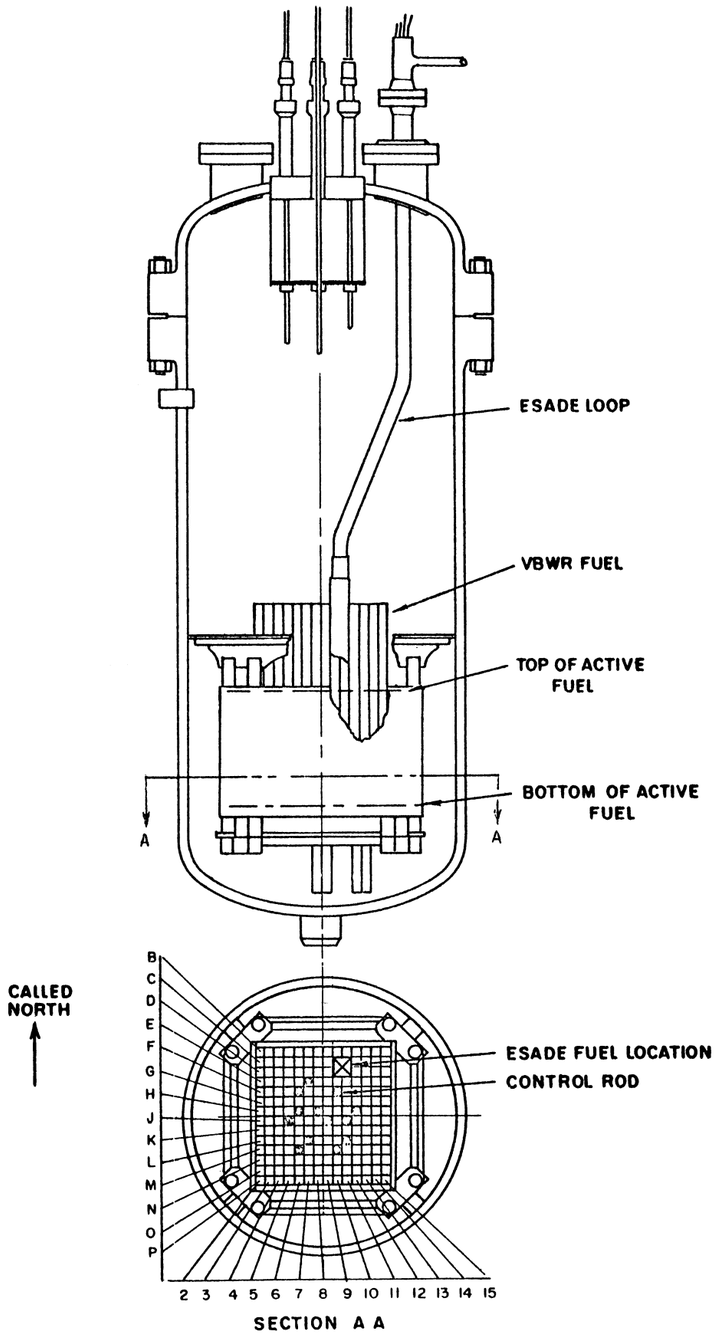

LOCATION OF ESADE IN VBWR REACTOR

FIGURE II. 3.1

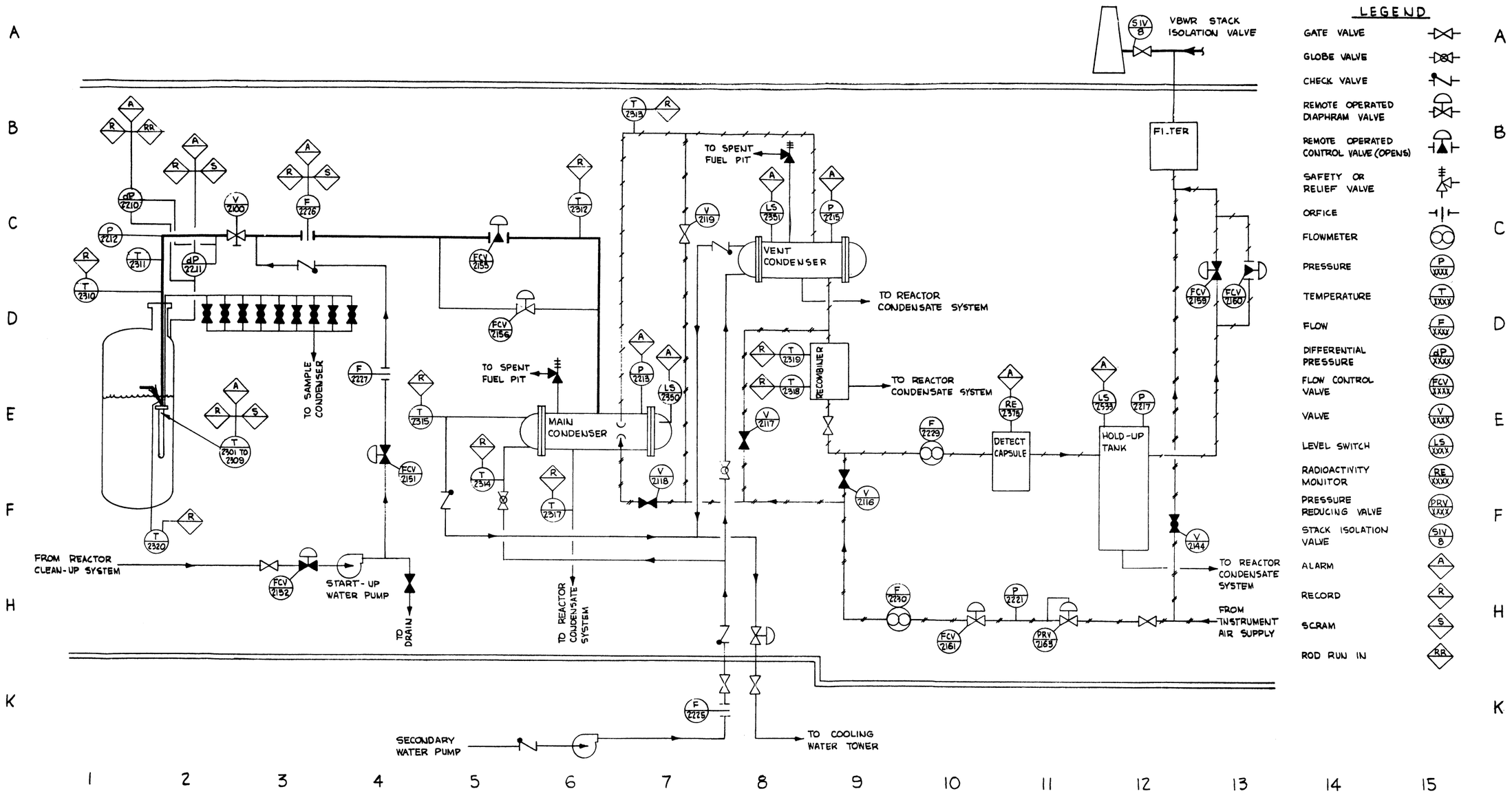

E-SADE PIPING AND INSTRUMENTATION DIAGRAM

FIGURE 11.3.2

11. 3. 2 Equipment within the Reactor Vessel

A view of the equipment within the reactor vessel is shown in Figures 11. 3. 3 and 11. 3. 4

The loop facility tube is installed through the northeast refueling port of the VBWR reactor vessel. As shown in Figure 11. 3. 1, the nine superheat elements are located in the four VBWR fuel positions 10C, 11C, 10D, and 11D. These normal VBWR fuel positions are replaced with nine positions identified as shown in Figure 11. 3. 5.

Four VBWR fuel elements and the corresponding fuel channels are removed to provide a location for this equipment. A test section approximately 6. 2 inches square by 3 feet long is available for test installations.

The assembly provides for installation of nine bayonet-type annular fuel elements. A typical fuel element of this type is shown in Figure 11. 3. 6. Each element is in an individual tube, with steam flow down the outside annulus between the fuel and the process tube, and flow returning up through the center annulus between the fuel element and a velocity boost tube. The steam passes from the outer annulus to the inner annulus through six 3/8-inch diameter equally spaced holes at the lower end of the fuel element. All elements are installed in parallel, with steam drawn directly from the reactor dome through a demister or steam dryer, flowing down the annulus of the facility tube to an inlet plenum, through the test sections to an outlet plenum, and finally through the inner pipe of the facility tube to discharge the superheated steam to the E-SADE external test loop.

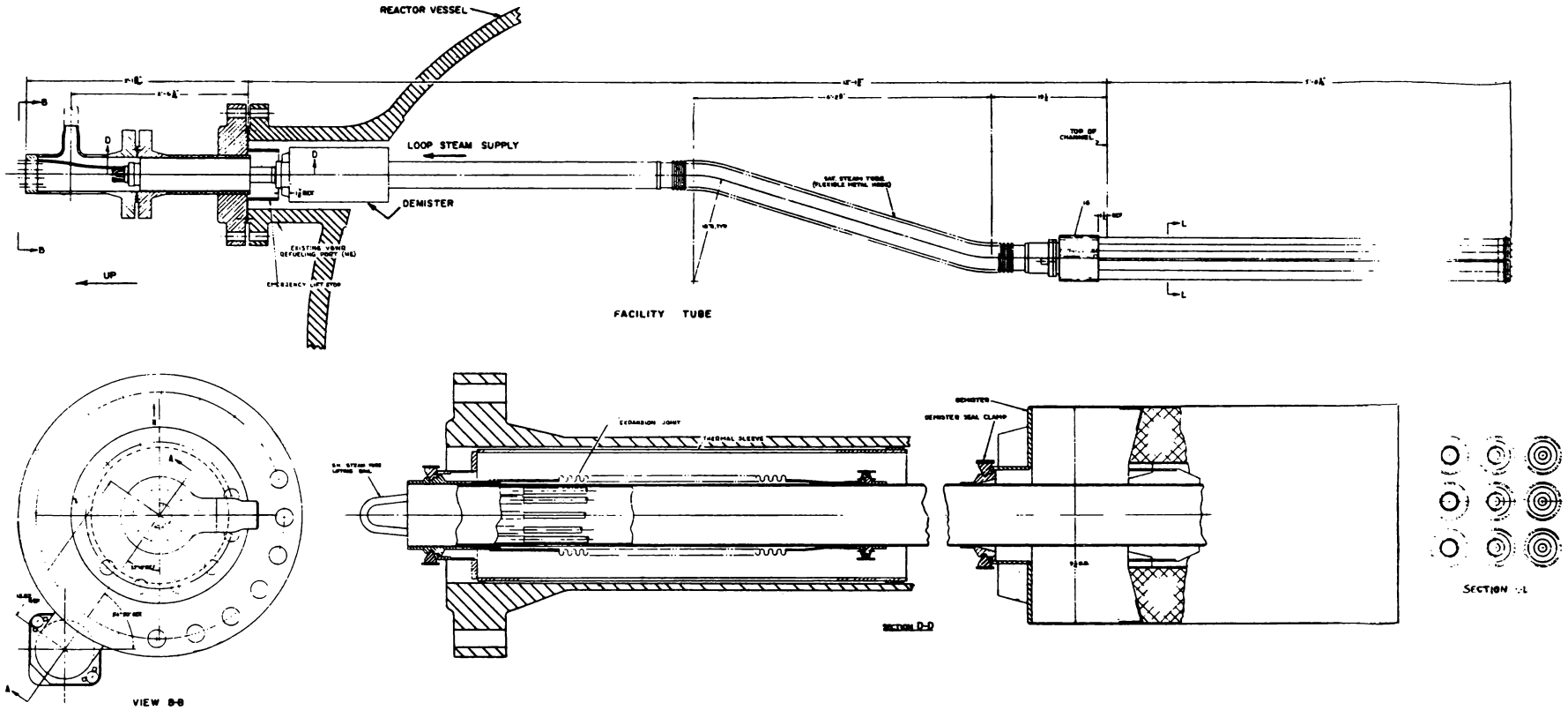

FACILITY TUBE
FIGURE 11.3.3

Note: All dimensions are approximate.

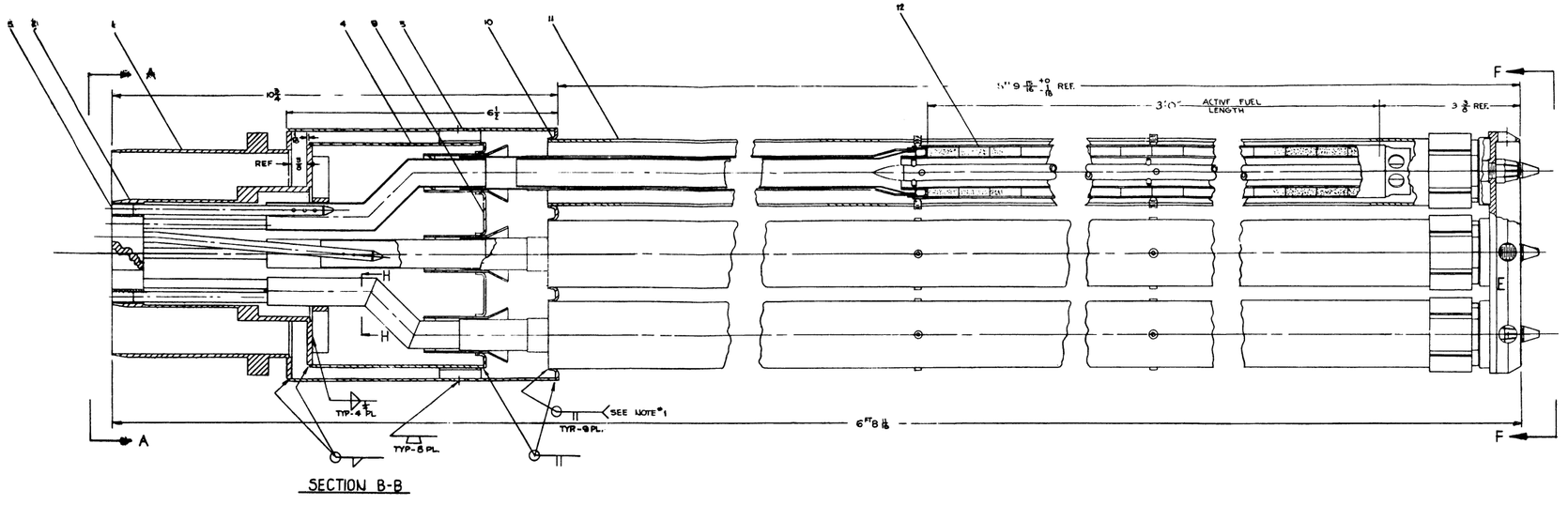

Thermocouple Well

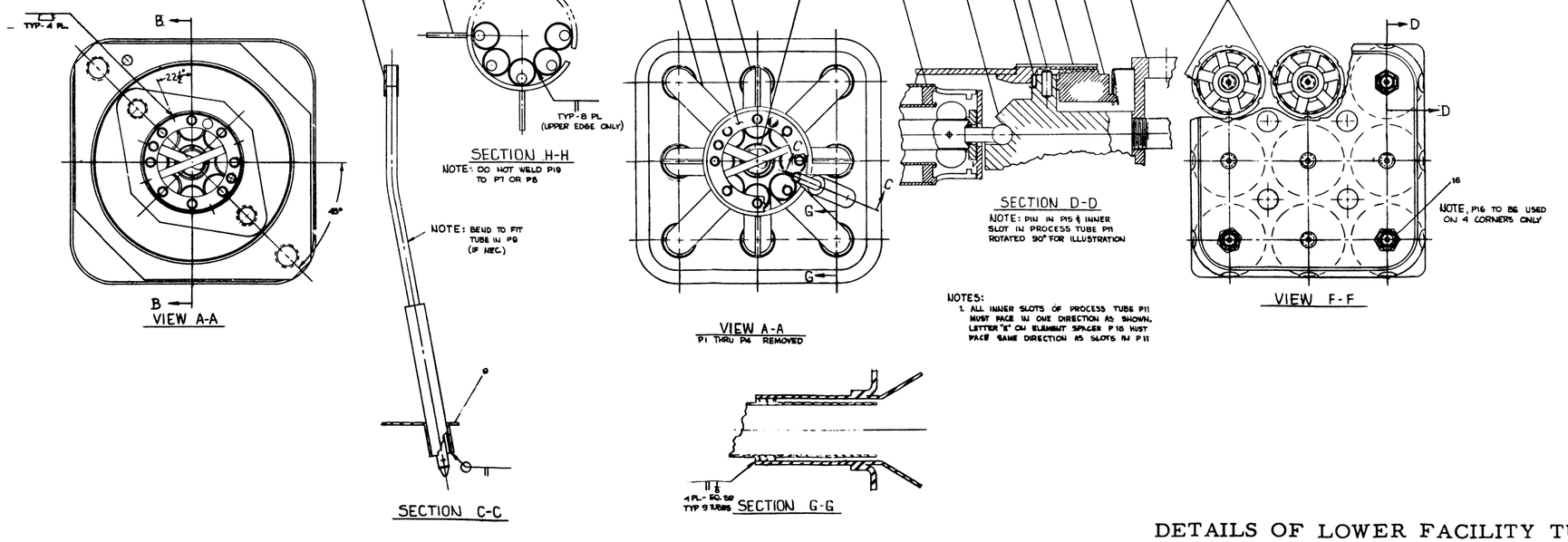

DETAILS OF LOWER FACILITY TUBE
FIGURE 11.3.4

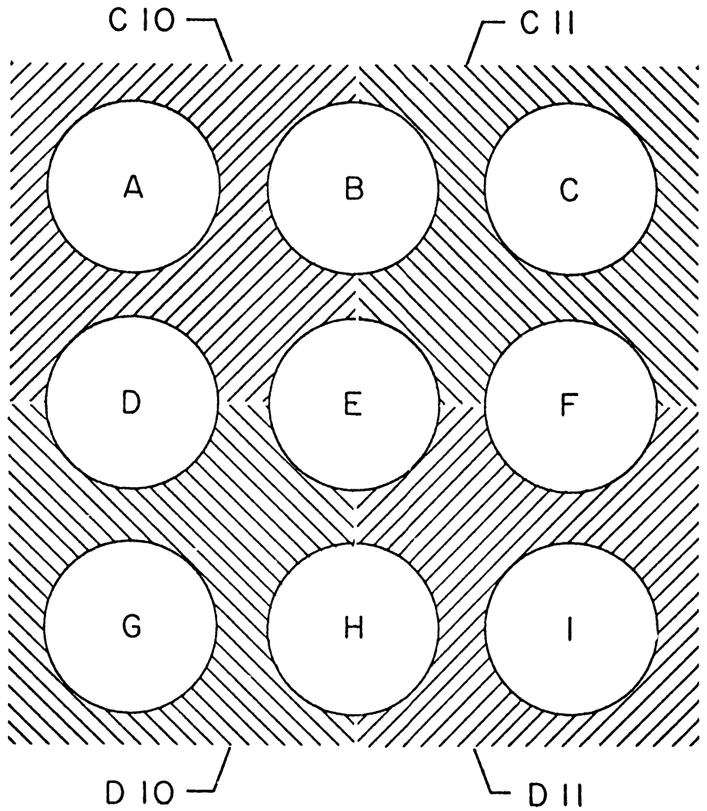

FUEL POSITIONS

FIGURE 11.3.5

The location of the demister is shown in Figure 11. 3. 3. Thermocouples monitor the discharge superheat temperature from each element at each process tube discharge end to assure that the elements are operating at satisfactory temperatures. The thermocouples' locations are shown on Figure 11. 3. 4.

Fuel elements are not individually removable from the assembly while the assembly is in the reactor. Variation in fuel element configuration is planned and will be achieved by means of flow tubes which will permit tests of rod-type elements or annular elements of reduced diameter. Some fuel designs for superheat reactors include rod-type elements. This type of element may be tested, using the re-entry type test assembly design similar to that shown in Fig. 11. 3. 7. In this design the steam flow is down the outside of the outer baffle through the lower fuel assembly ports and up between the inner baffle and the fuel rod. The design concept is representative of the variations in fuel assembly design that may be tested in the facility.

The E-SADE assembly, including inlet and outlet piping, is supported from the VBWR grid plate. It is guided and positioned at the lower end by an alignment plate which fits inside the special channel assembly required for this installation. One view of this alignment plate is shown on Figure 11. 3. 4. The upper end of the assembly is guided by a sleeve but is free to move vertically within the sleeve, thus accommodating differences in thermal expansion between the reactor and E-SADE assembly. This thermal sleeve is shown on Figure 11. 3. 3, Section D-D. An expansion bellows prevents leakage of saturated steam in the reactor dome directly into the superheated steam discharge line. The expansion bellows is also shown on Figure 11. 3. 3, Section D-D.

The first series of tests will be conducted with nine fuel elements of the annular-bayonet type, similar to that shown on Figure 11. 3. 6.

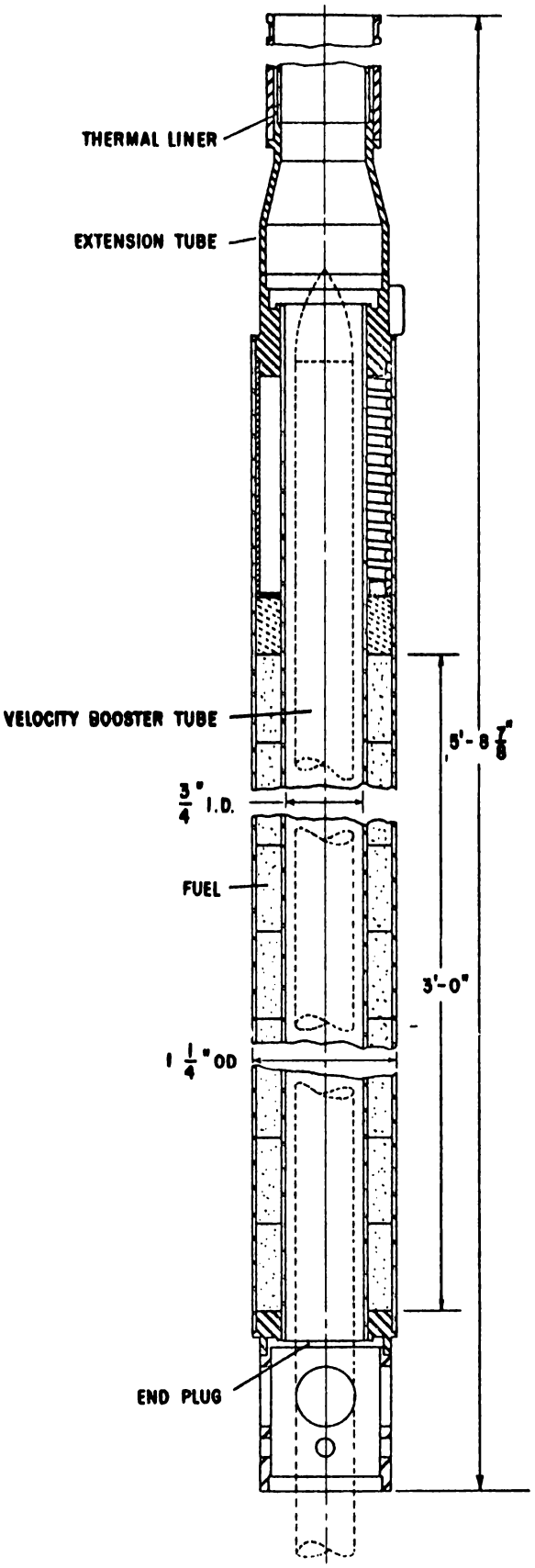

FUEL ELEMENT ASSEMBLY

FIGURE 11.3.6

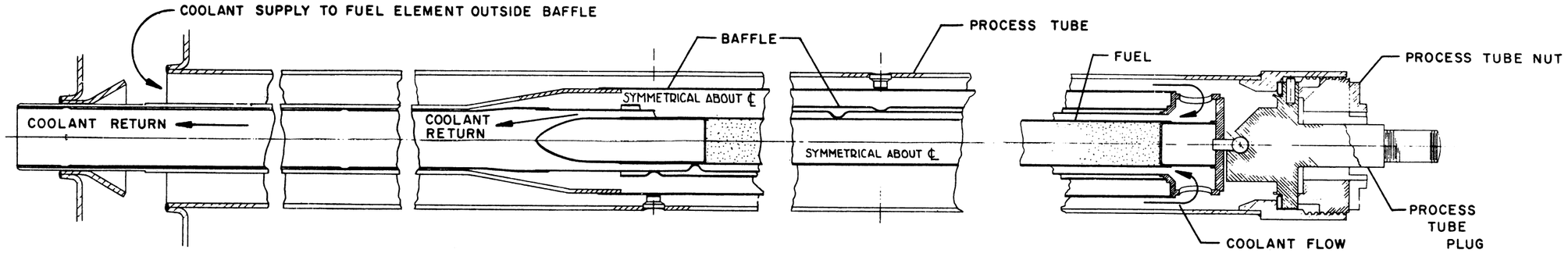

FACILITY TUBE ADAPTED FOR
A ROD FUEL ELEMENT

FIGURE 11.3.7

Details of the fuel design are given below. Although revisions to this information are anticipated, it is included to represent the type of data that will be available before loop operation.

All nine elements of the first test planned will have approximately the same outside dimensions. The outer diameter of the fuel is 1.21", with the wall thickness given in Table 11.3.1. The inner element diameter is 0.750", with 0.028" wall thickness, and the active fuel element length is 36". The cladding material in all cases is 304 stainless steel, and the fuel is UO_2 pellets. All elements have a 2" long gas plenum at the upper end of the element.

Elements A, B, and F (see Figure 11.3.5 for core position) will be identical —— each will have an outer clad .016" thick, 8% enriched pellets, and they will use the spiral wire spacing technique.

Elements C and E will be the same as A, B, and F in all respects except that the fuel will have an enrichment of 10%.

Elements A, B, C, E, and F will contain 4,550 grams of UO_2 each, and the cladding will be swaged over the pellets to zero gap. The void plena in these elements will be supported by solid sleeves.

The remaining four elements — D, G, H, and I — will all have an outer clad .028" thick and contain 4,300 grams of UO_2. The plena in these elements will be supported by close wound ground springs.

Element D will have 8% enriched fuel, spiral wire spacers, and a .004" initial gap between fuel and outer cladding.

Element G will have 6% enriched fuel, spiral wire spacers, and a .006" initial gap between fuel and outer cladding.

Element H will have 6% enriched fuel, fin-type spacers, and .004" initial gap between fuel and outer cladding.

Element I will have 8% enriched fuel, fin-type spacers, and .006" initial gap between fuel and outer cladding.

TABLE 11.3.1

Element	UO_2 Enrichment (%)	Weight of UO_2/ Element (grams)	Gap Between Pellet and Outer Clad (mils)	Outer Clad Thickness (mils)	Inner Clad Thickness (mils)	Method of Plenum Support	Type of Element Spacers
A	8	4,550	Swaged	16	28	Sleeve	Spiral Wires
B	8	4,550	Swaged	16	28	Sleeve	Spiral Wires
C	10	4,550	Swaged	16	28	Sleeve	Spiral Wires
D	8	4,300	4	28	28	Springs	Spiral Wires
E	10	4,550	Swaged	16	28	Sleeve	Spiral Wires
F	8	4,550	Swaged	16	28	Sleeve	Spiral Wires
G	6	4,300	6	28	28	Springs	Spiral Wires
H	6	4,300	4	28	28	Springs	Fins
I	8	4,300	6	28	28	Springs	Fins

The spiral wire spacer technique consists of three wires spaced 120° apart around element periphery, each making one complete spiral in the length of the element.

The fin-type spacers consist of four fins spaced 90° apart and attached to the fuel cladding to eliminate fretting corrosion. The elements are spaced at each end and at the mid-point.

Fuel elements in ESH-1 will be irradiated for long periods of time in E-SADE. To offset excessive stresses on the clad from the internal fission gas buildup, a 2" void plenum is provided at the top of each fuel segment. The plenum length was computed, using the following assumptions:

1. Fission gas release, 5% of that produced.
2. Water content in pellets (after the grinding operation) is maintained at or below 0.6 mg/20 gms of UO_2. The effect of moisture on plenum pressure is given in Figure 11.3.8.
3. No space is present between jacket and pellets during operation; therefore, all gases must be accommodated at the plenum.
4. Plenum temperature is equal to Tp = 1/2 (((Maximum Temperature of Top Pellet) - (Temperature of End Plug))), with the end plug temperature at 545°F.
5. Irradiation exposure to continue up to 3000 MWD/T.

Since cladding of thickness of 0.028" and 0.016" are not self-supporting under the proposed test conditions, the cladding expands with the fuel making fuel expansion and thermal cycling important cladding lifetime parameters. Experiments in GETR show that the strain may be as high as 0.023. Under these conditions, the reversed plastic strain will be about 0.01, and the number of cycles to failure due to load cycle fatigue is expected to be about 1270. The maximum number of shutdowns from full power during any currently planned exposure of the fuel should be much less than 1000. Smaller power fluctuations will produce much less strain and consequently will require greater number of cycles to reach failure. Up to 3000 MWD/T, the maximum irradiation exposure, the number of cycles predicted is under 200 (one complete shutdown every day).

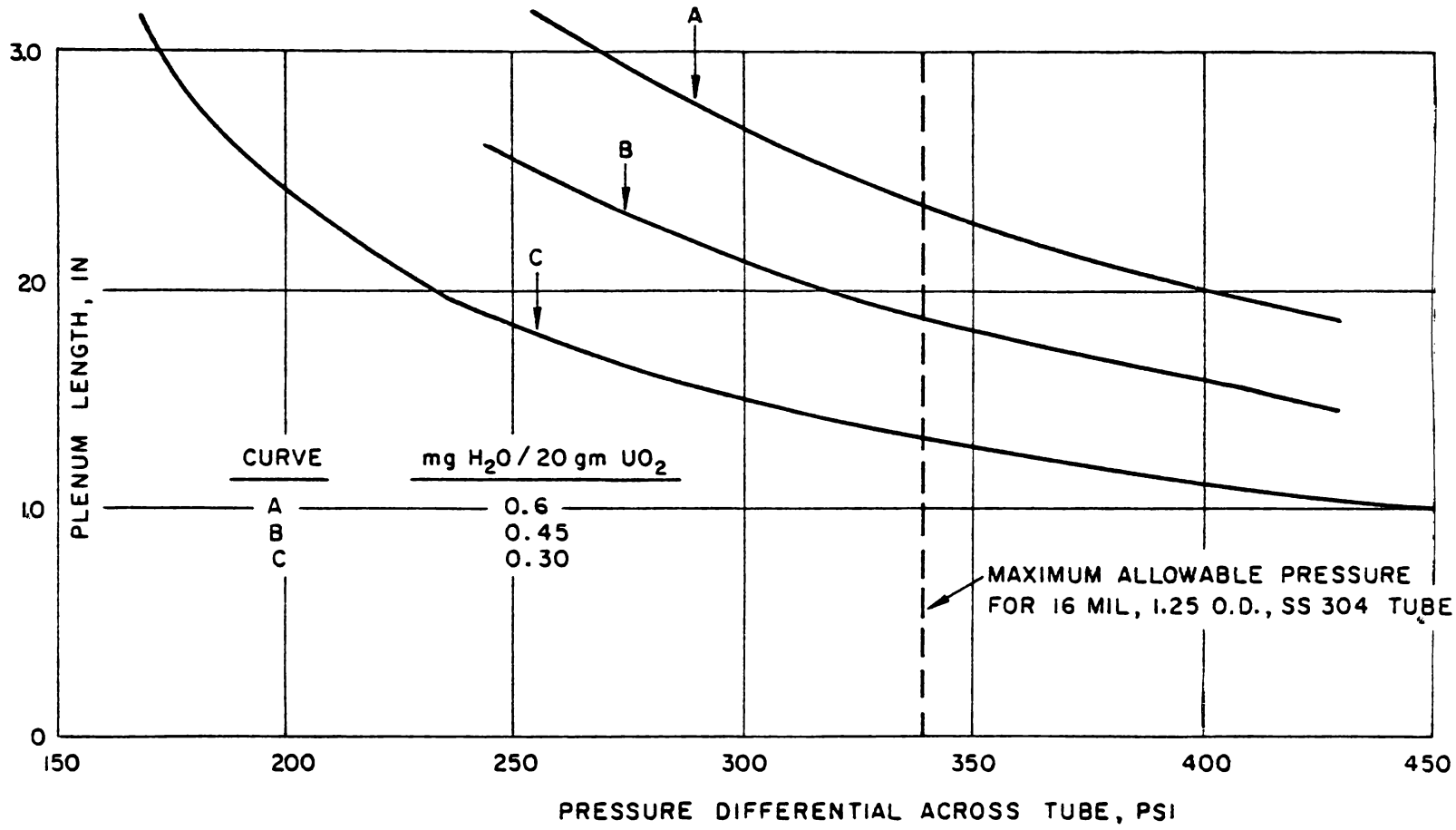

EFFECT OF MOISTURE ON PLENUM PRESSURE DIFFERENTIAL

FIGURE 11.3.8

Data on 304 stainless steel at superheated conditions (not in a reactor environment) show that the corrosion penetration rate is 0.95 to 1.55 mils per year at temperatures of 1300°F. For temperatures of 1100°F to 1300°F, in an out-of-pile loop (with controlled high oxygen), the corrosion in 1000 hours was a maximum of 0.23 mils, or about 2 mils per year upon linear extrapolation of the above-mentioned exposure time. In addition, the corrosion rate at a given temperature will decrease after 1000 hours; thus a linear extrapolation of 2 mils per year is overly pessimistic.

For the proposed irradiations in E-SADE, the 3000 MWD/T can be accumulated within nine months of operation in VBWR. Therefore, a total loss in metal thickness at 1300°F (maximum local hot spot) will be less than 0.6 mils, which is not considered an appreciable loss of clad integrity.

Pellets will be fabricated in a manner described in the General Electric Report, GEAP-3387*. Fuel elements with 0.016 mil clad (outer clad only) will be swaged-over pellets, using a low energy swaging die. This method produces fuel elements with essentially zero clearance between clad and UO_2 (to prevent wrinkling of the clad during reactor exposure) without breaking up the pellets. Fuel elements produced by the swaging technique have been shown by experiment to have low strain ranges under plastic strain cycling. This permits significantly greater number of cycles before clad failure due to load cycle fatigue.

---

*"Nuclear Superheat Project Fabrication Irradiation and Evaluation of Superheat Fuel Elements SH-1 and SH-2" by E. S. Lees, R. F. Boyle, and C. N. Spalaris.

The void plenum, designed to accommodate the fission gases produced during irradiation, must be internally supported to avoid collapse. The support is provided by an Inconel spring in the 0.028" thick clad and by a solid sleeve in the case of the 0.016" clad. Both supports are presently being tested in a high temperature (1400°F) autoclave to pressures up to 1200 psi.

Nondestructive techniques for tubing quality include ultrasonic and eddy current tests with a defect detection sensitivity of 10% of the wall thickness. All tubing is nondestructively tested before use in any fuel element fabrication. Welds are inspected visually and by X-ray radiography. The absence of leaks is tested with a helium mass spectrometer with a sensitivity of 10^{-8} cc/sec. leak rate.

Leakage tests designed to simulate cladding failure under actual operating conditions are planned. These tests will be conducted under carefully controlled conditions, first with fuel fabricated as outlined above, then with a defect of specific dimensions.

The flow booster tubes in some of the fuel elements may contain corrosion and tensile coupons. These are inserted in the tube interior, the tube walls being perforated to allow steam to come into contact with the specimens. Other than slight neutron flux depression, no other effects are expected because of these test coupons. It should also be noted that dummy fuel elements may occupy some of the positions shown in Figure 11.3.5.

11.3.3 Main Loop Equipment outside the Reactor Vessel

Steam from the fuel elements flows through a two-inch diameter schedule 80 stainless-steel pipe (ASTM-A312 TP 347) to the main condenser. Pressure differential and flow sensing elements are located in the line upstream from the flow control valves.

Flow through the fuel is manually regulated by the flow control valve 2155. The valve is designed so that at least 30 seconds are required for complete valve closure. In addition, a bypass line is provided that maintains at least 6% flow when the main valve is completely closed. The bypass valve is designed to remain open approximately 40 minutes following a scram signal. This value is applicable to the reference design and must be re-evaluated for each new fuel assembly. It will also remain open if instrument air or power is lost.

The main condenser is designed to condense the superheated steam from 1000°F and approximately 1000 psia. The condensate from the condenser will be drained to a tank in the enclosure. The operating conditions are as follows:

Steam/initial pressure	800 - 1000 psia
Reduced pressure	250 psia
Temperature	1000°F
Condensate	
Pressure	Atmospheric
Temperature	200°F
Flow	15,000 lbs/hr
Cooling water	
Flow	400 gpm
Temperature inlet	80°F
Temperature outlet	180°F

The design, construction, inspection, and testing of the condenser will comply with Section VIII of the 1959 ASME Boiler and Pressure Vessel Code, including all applicable nuclear case interpretations. The cooling water for the condenser is supplied from the VBWR cooling tower, and the condensate is pumped from the main condenser to the reactor condensate system.

A water circulating system consisting of a pump, flow control, and appropriate control valve is designed to provide cooling for the fuel during startup operations.

The main loop piping and instrumentation drawing, Figure 11.3.2, shows the primary loop components; and Figures 11.3.9 and 11.3.10 are a plan view and section showing location of major loop components within the VBWR enclosure.

The cooling water pump specifications are as follows:

Temperature	100 - 500°F
Capacity	110 gpm
Total dynamic head	135 ft
Suction head	0 - 700 ft
Discharge head	135 - 835 ft
Maximum pressure on pump casing	1250 psig

A sampling system which includes a sample line from each fuel element, flow control valve, detector, and condenser is provided. This system is designed to locate a single defective fuel assembly and obtain quantitative information regarding fission product release rates.

This system is not considered essential for safe loop operation and may not be used in all cases when the loop is in service.

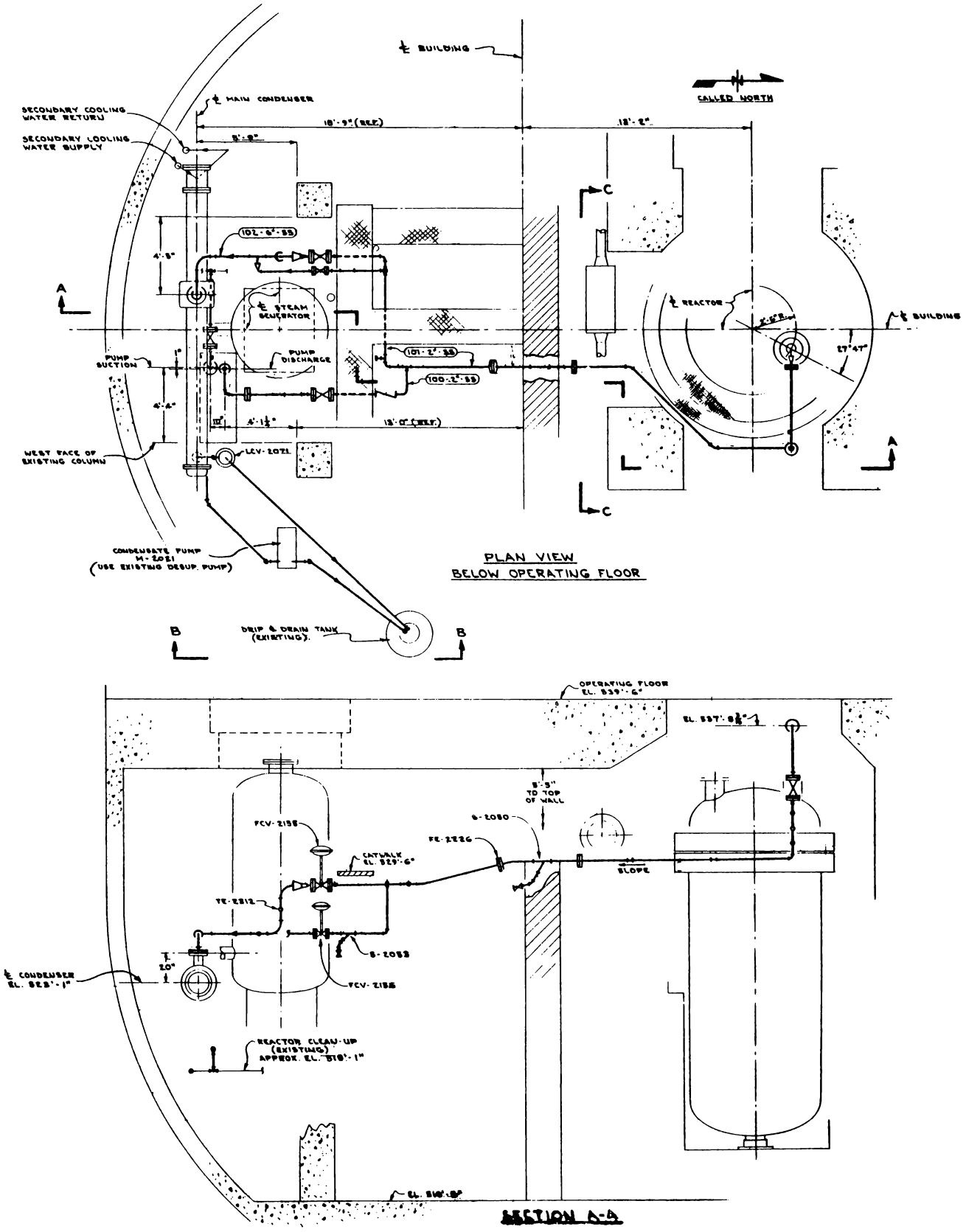
℄ BUILDING
CALLED NORTH
SECONDARY COOLING WATER RETURN
SECONDARY COOLING WATER SUPPLY
℄ MAIN CONDENSER
18'-9" (REF.)
18'-2"
5'-9"
102-6"-SS
4'-8"
℄ STEAM GENERATOR
PUMP DISCHARGE
101-2"-SS
100-2"-SS
PUMP SUCTION
4'-6"
4'-1½"
13'-0" (REF.)
WEST FACE OF EXISTING COLUMN
LEV-2021
℄ REACTOR
℄ BUILDING
27°47"
CONDENSATE PUMP M-2021 (USE EXISTING DEBUP. PUMP)
DRIP & DRAIN TANK (EXISTING).
PLAN VIEW
BELOW OPERATING FLOOR
OPERATING FLOOR EL. 839'-6"
EL. 837'-8½"
5'-5" TO TOP OF WALL
B-2080
FCV-2158
FE-2226
CATWALK EL. 829'-6"
SLOPE
FE-2212
B-2083
20"
FCV-2155
℄ CONDENSER EL. 828'-1"
REACTOR CLEAN-UP (EXISTING) APPROX. EL. 818'-1"
EL. 816'-8"
SECTION A-A

FIGURE 11.3.9

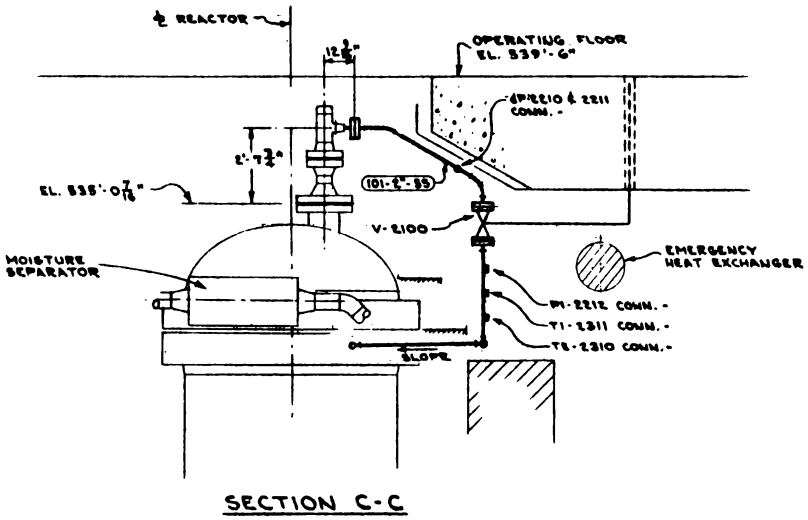

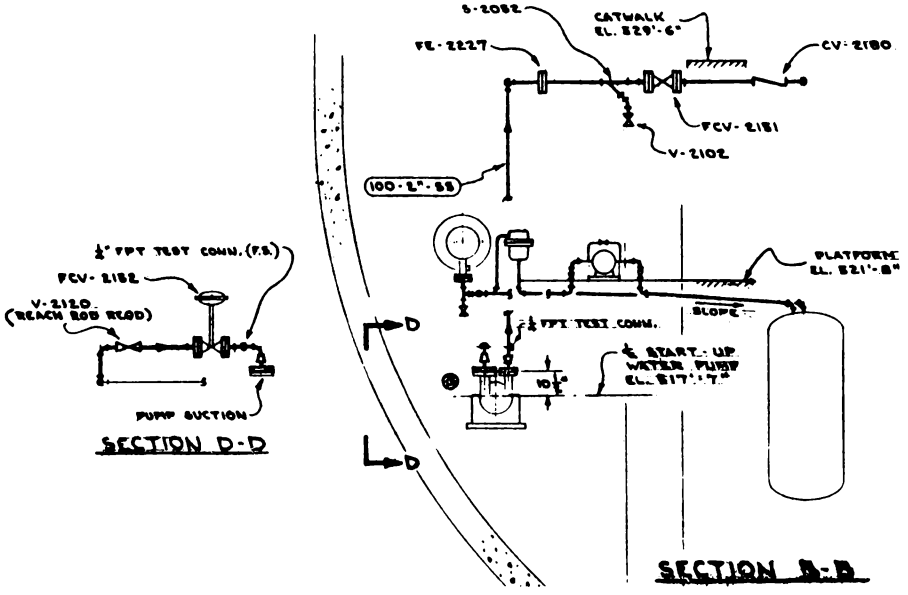

FIGURE 11.3.10

11. 3. 4 Loop Operation

Before the loop is placed in operation and the reactor is started, the loop and its associated equipment will be thoroughly checked. This checkout prior to startup will be facilitated by means of valve and equipment check lists. Completion of this checkout procedure will place all valves and equipment in the position or condition ready to bring the reactor to criticality and cool the E-SADE loop with water by means of the startup section of the loop.

To place the loop into operation, the cooling water circulator is started, and pressure and flow instrumentation are observed to verify establishment of proper conditions. The reactor is then brought to a power of about 3 Mw following normal startup procedures. The reactor will be held at about 3 MW for a sufficient time to reach a reactor pressure adequate for transferring the E-SADE loop to steam cooling. This pressure is estimated to be about 500 psi; however, the pressure may be varied according to experience gained from actual operation.

After reactor pressure is established and normal operation of the reactor and loop is observed, the reactor power will be reduced to about 1.5 Mw. The loop transfer scram selector switch is set for transfer from water to steam cooling. The loop water coolant is stopped, and the water cooling isolation valves are closed. After panel lights indicate that the valves are closed, the steam coolant flow control valve is opened slowly while observing the steam flow indicator.

The steam flow is set for 1500 lbs/hr, the scram selector switch* is set at position "I - Steam Operation," and reactor power is raised from 1.5 Mw to a maximum of 7 Mw. The reactor power is held at this value for a sufficient time to:

(1) Complete reactor pressurization,
(2) Show by the exit thermocouples that steam flow has been established in all channels, and
(3) Assure that any water trapped within the loop piping has been removed.

The flow and ΔP scram settings for position "I - Operation" will be adjusted to provide a minimum flow of 1500 lbs/hr or the minimum flow required to maintain the fuel cladding temperature below 1000°F. The levels at this position must be set before reactor startup.

After normal operation of the loop and reactor has been observed at or less than 7 Mw, the loop coolant flow will be increased to exceed the minimum ΔP flow scram values for the next mode of operation and the scram selector switch set at position "II - Steam Operation." The reactor power may then be increased to a maximum of 15 Mw.

The flow and ΔP scram settings for position "II - Operation" will be adjusted to provide a minimum flow which is the calculated minimum flow required to provide a sufficient ΔP through the loop to remove water from the facility tubes or the flow required to maintain the maximum fuel cladding temperature at less than 1250°F, whichever is larger. The power in this position will not exceed 15 Mw, and the instrumentation must be adjusted prior to reactor operation.

---

* The "scram selector switch" is the functional name of part of the instrumentation system logic which provides a means of activating appropriate scram circuitry during water cooling, of bypassing loop flow scram circuitry during switchover from water to steam cooling and of activating appropriate scram circuitry in three steam cooling operating positions.

Since the reactor power is varied during any operating cycle, it is necessary to adjust the loop operating conditions to the mode of reactor operation. This is achieved by including a third scram selector switch position "III - steam operation".

The flow limitations stated in Table 1. 5 are intended to mean that the flow conditions will be adjusted to obtain a calculated fuel cladding temperature of about 1250°F at the maximum planned reactor power and that the flow condition will be adjusted during operation to match planned variations in reactor power. This scram selector switch position "III - steam operation" is set during operation to the limits calculated for the current operating mode. Under these conditions, if the flow drops to 80% of the calculated design value, the fuel cladding temperature will not exceed about 1400°F even under some loss of flow conditions. A discussion of flow and fuel temperature transients is given in the safety evaluation section 11. 3. 8.

To shut down, the reactor is reduced in power and the loop flow control valve is gradually closed. Although it is not anticipated as a requirement, the scram selector switch positions "I - steam operation" and "II - steam operation" may be used during gradual reduction in power. Sufficient coolant is assured during and following shutdown by the time delay of the main flow control valve and the bypass valve. As shown in Figure 11. 3. 23, Section 11. 3. 8, after the reactor has been shut down about 15 minutes, complete loss of flow will not cause the clad temperature to exceed 1530°F.

A thermocouple is located in the exit channel of each process tube. During the startup of each new fuel bundle and until full power has been achieved for a sufficient time to determine the relative power

of the various channels, all thermocouples must be operative. All thermocouples must also be operative for any revision to the loop which would be expected to change the relative power produced in the various elements. After relative element power has been established, the loop may be operated provided not more than four thermocouples and not more than two in a straight line, except for diagonals (fuel position CEG and AEI, Fig. 11.3.5), are inoperative.

11.3.5 Gas Collection and Filtering System

The coolant passing through the fuel element under normal conditions will be radioactive primarily from N^{16} as a result of O^{16} (n,p) N^{16} reaction. The loop piping and main condenser are located under the reactor operating floor (about 4 ft of concrete), which offers adequate protection for operating personnel. The purpose of the gas collector and filtering system is to collect, hold for decay, and filter radioactive gases arising from the loop operation. The system is also designed to measure and contain contaminated gas within the loop piping if the VBWR stack emission limit is approached.

The system is composed of seven elements. These elements are: (1) vent condenser, (2) H_2-O_2 recombiner, (3) detector, (4) holdup tank, (5) charcoal filter, (6) purge air system, and (7) the remote and automatic isolation system.

Under normal operation, dilution air flow is provided which sweeps the off gas out of the main condenser to the vent condenser and on to the recombiner. Any gas left is then routed to the activity detector, to the holdup tank, through the filter, and finally to the stack through the VBWR stack isolation valve (see Figure 11.3.2).

Saturated off gas and dilution air enters the vent condenser to be dried in preparation for the recombiner action. The vent condenser condensate level is maintained by a level controller, and an alarm is annunciated if the level exceeds a preset limit.

A pressure sensor and associate pressure switch monitor and indicate the outlet vent condenser and inlet recombiner pressure. The pressure sensor is set at 90 psia to annunciate an approach to the limit of the off-gas system static pressure. A relief valve is set at 100 psia to relieve the vent condenser to the fuel storage pool, protecting the off-gas system from excessive pressure.

The recombiner recombines free hydrogen and oxygen in the off gas, holding the resulting water along with condensate. The recombiner efficiency is a function of inlet and outlet temperatures. Inlet and outlet temperature sensors measure and indicate the recombiner temperature gradient.

The flow rate of the off gas and dilution air that leaves the recombiner is measured by a flow meter.

The off-gas activity monitor is a gamma-sensitive spectrometer system. The off gas and dilution air flow through a sample chamber which is monitored by a photomultiplier tube with a sodium-iodide scintillator crystal. This photomultiplier tube is part of a single channel analyzer.

Loop off-gas isolation is controlled by a remote automatic control valve, which controls the on-off air supply as shown in Figure 11.3.2.

The off-gas holdup tank will permit the short half-life isotopes to decay to a safe level before being released to the stack. The actual holdup time depends upon the dilution air flow, which will vary from approximately 0.25 to 1.0 ft^3/min. Since the holdup tank volume is approximately 3.3 ft^3, the holdup times will vary from approximately 3 to 13 minutes.

The condensate accumulation is relieved by a level control valve, and an excessive condensate level will be annunciator-alarm indicated by level switch.

The off-gas system operation, in particular the off-gas activity monitor, requires a smooth continuous flow of off gas. A dilution air flow is supplied and available by manual valving at three points in the off-gas system. It is available at the main condenser, at the inlet to vent condenser, and at the inlet to the recombiner, as shown on Figure 11.3.2. The anticipated best dilution air addition point is at the vent condenser inlet.

Instrument air that is pressure regulated, flow controlled, and measured, is used as the dilution air. Pressure setting and regulation is accomplished through PRV2163, with the regulated pressure indicated by P2221 . Flow is measured and indicated by the flow meter F2230.

A remote control isolation valve is a part of the safety isolation system to contain the off gas. In case of a high activity indication, the dilution air supply will automatically be shut off.

Automatic and remote control valves provide a means of containing the off gas in case of high activity, and also provide a means of bleeding and blending the off gas with dilution air to release it safely to the stack.

A high activity will alarm and a higher activity will automatically isolate the off-gas system.

With isolation of the off-gas system, the high activity gas is contained. The blending system valves will permit dilution mixing and slow and controlled release of the contained off gas to the stack.

It is planned as part of the experimental program to operate purposely defective fuel assemblies in the loop. Similar experiments have previously been performed in the VBWR.

Comparing the power and temperature of the previous defective rod-type element experiments in the VBWR and the E-SADE element, the release of radioactive material from the E-SADE element should be about a factor of three higher under comparable conditions. The decontamination factor from the fuel region of E-SADE to the VBWR stack has been designed to be comparable with the existing decontamination factor from the VBWR fuel to the stack. Thus, the release rates for the loop to the stack are expected to be of the same order of magnitude as those previously experienced in similar defective fuel tests.

The loop monitoring system, discussed above, is an additional precaution, which makes possible the retention of radioactive contaminants within the loop or reactor cooling system in the event that higher than expected release rates occur. The holdup volume available is sufficient to provide at least two hours of operation at power with the off-gas system isolated.

The final protection against release of radioisotopes in excess of those specified in License No. DPR-1, Table 1.2, Part 1, is the VBWR stack monitoring system.

11.3.6 Heat Transfer and Fluid Flow

The loop under normal operating conditions uses saturated steam from the reactor vessel as the primary coolant. A heat balance for a typical operating condition is given in Figure 11.3.11.

A list of typical operating parameters is given in Table 11.3.2. These values were computed, using a digital computer code. The values listed in Table 11.3.2 and those given in the heat balance are intended to be representative of a possible steady-state operating condition. These values are considered as a reference condition and are, therefore, not limiting values, nor are they necessarily related to any experiment that will be conducted.

For the reference condition, an analysis was performed to determine the longitudinal and radial temperature profiles of the element in which the maximum temperature occurs. This element is located in E-SADE position G. The results of this analysis are shown in Figures 11.3.12 and 11.3.13.

Under steady-state conditions with the fuel assembly shown in Figure 11.3.6, the steam enters at the saturation temperature of 545°F (1000 psia). Flow downward past the outer fuel surface raises the steam temperature to about 715°F, and flow up past the inner fuel surface raises the steam temperature to about 930°F. Of the total 125-kw element power, approximately 106 kw are transferred to the steam coolant, and about 19 kw are lost to the moderator water.

During startup, heat is removed from the fuel by forced circulation of reactor water in the reverse direction from that of the steam flow. A 110-gpm pump provides a coolant velocity of about 10 ft/sec through the fuel assemblies which is estimated to be more than twice the velocity required to sweep bubbles through the fuel elements. An analysis of the fluid flow and heat produced in the element during the startup period shows that with the circulating pump operating, a burnout margin of greater than 20 exists with the element at a power of $\sim$ 12.5 kw.

HEAT BALANCE
E SADE

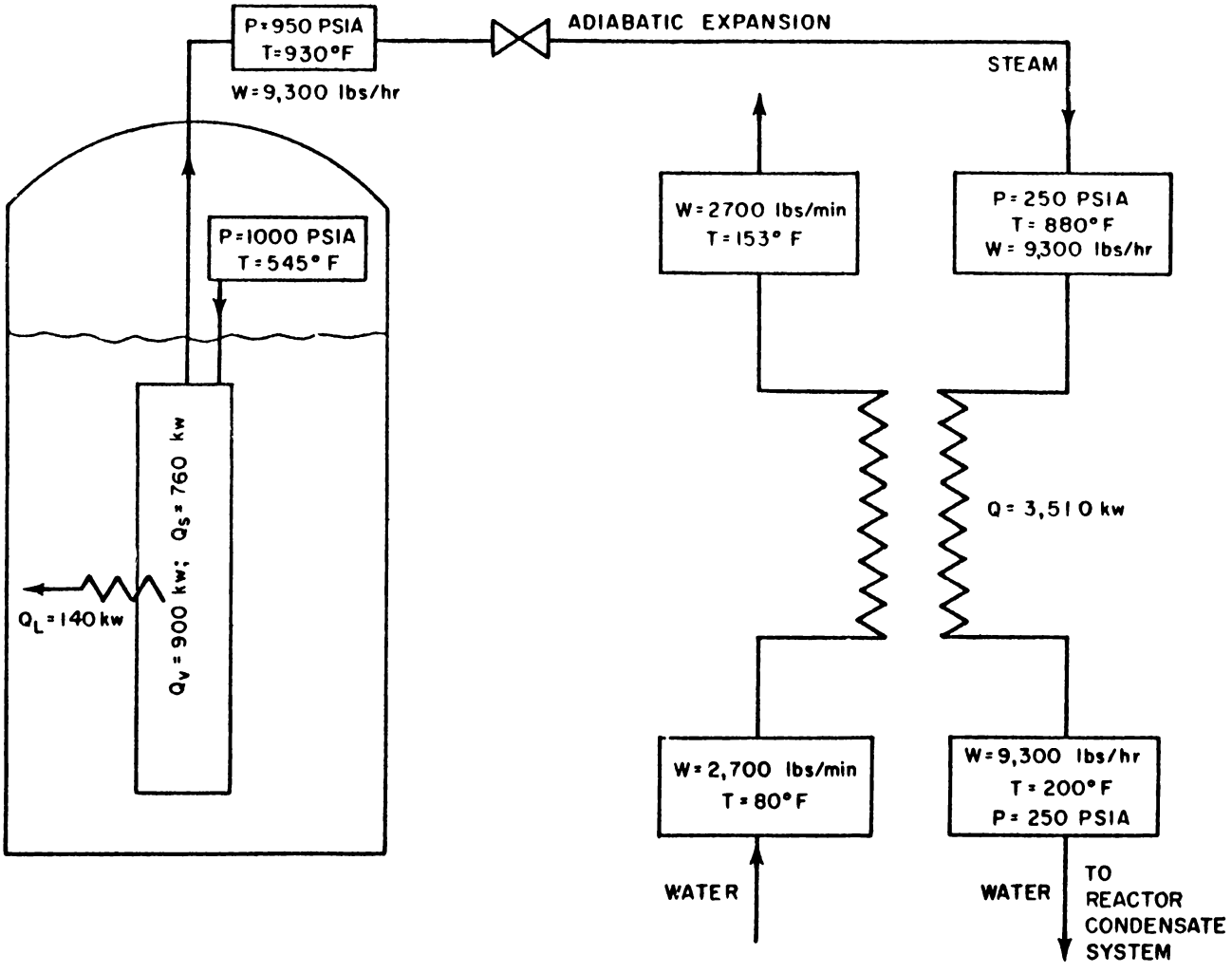

HEAT BALANCE
E-SADE

FIGURE 11.3.11

TABLE 11.3.2

TYPICAL OPERATING PARAMETERS

Fuel Element Design Conditions

Element power	125 kw
Steam pressure	1000 psia
Active fuel length	36"
Fuel element outside diameter	1.25"
Fuel element inside diameter	0.694"
Clad material	304 S.S.
Velocity boost tube, outside diameter	0.5000"
Velocity boost tube thickness	0.028"
Process tube, outside diameter	1.562"
Process tube thickness	0.060"
Maximum clad surface temperature	1250°F *
Maximum superheat exit temperature	930°F
Maximum heat flux	438,000 Btu/hr-ft^2
Minimum steam flow rate	1330 lbs/hr
Maximum fuel temperature	3620°F
VBWR power	40 Mw
Axial peak to average power	1.43

* Factors affecting the selection of a 1250°F cladding temperature are given in Ammendment No. 45 to License Application for VBWR, dated March 13, 1961.

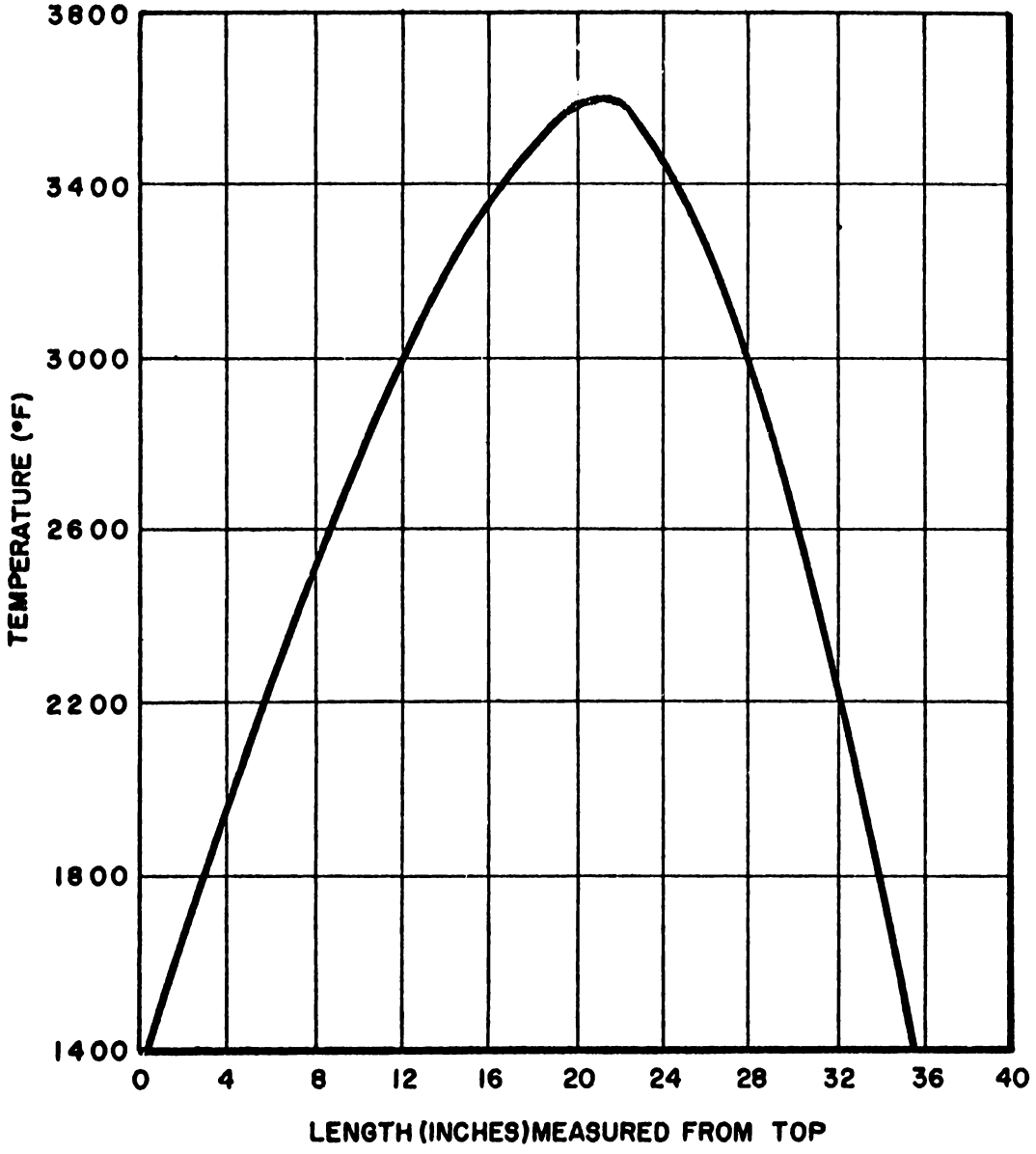

MAXIMUM FUEL TEMPERATURE LONGITUDINAL DISTRIBUTION

FIGURE 11.3.12

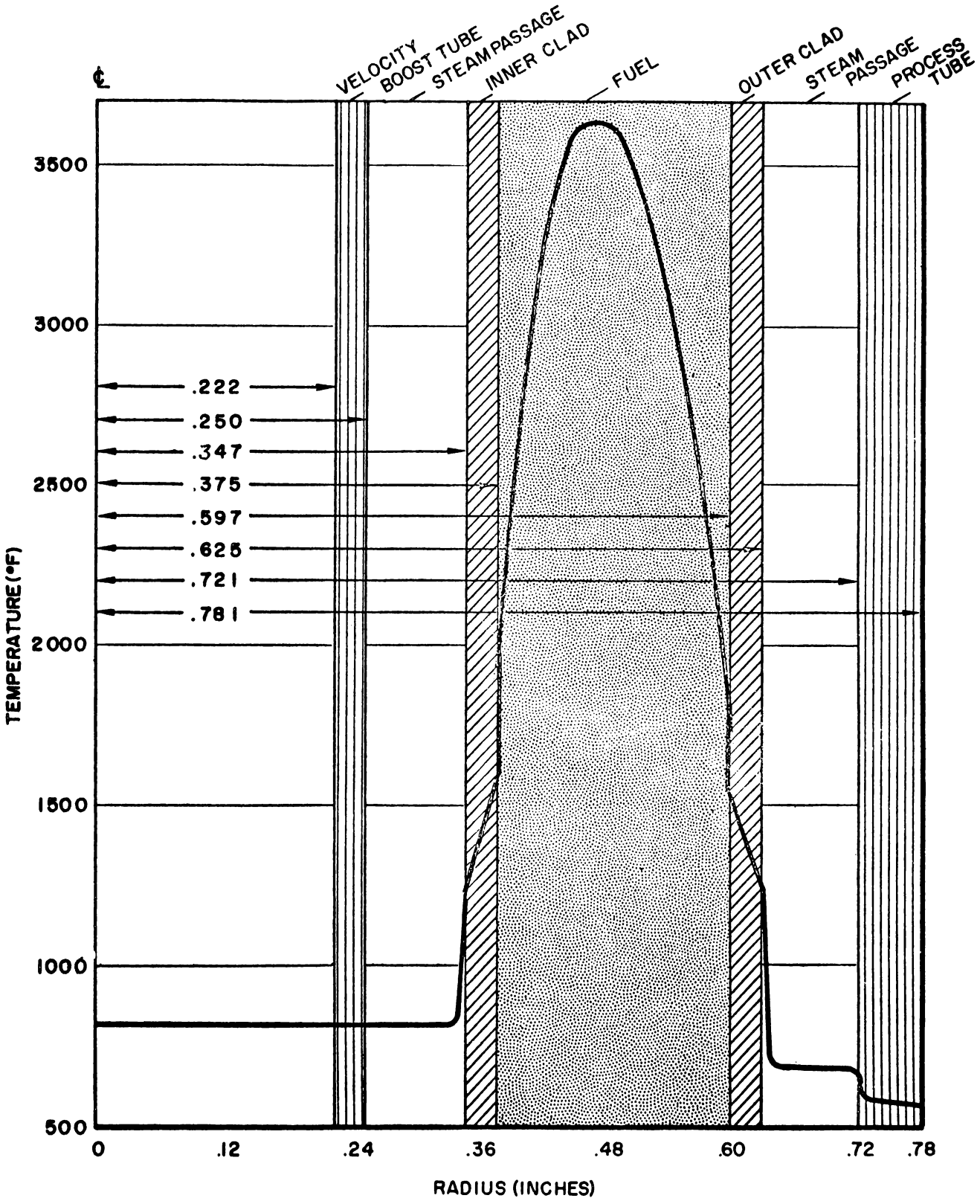

RADIAL TEMPERATURE DISTRIBUTION

FIGURE 11.3.13

The maximum reactor power anticipated for pressurization is about 4.0 Mw, corresponding to an element power of about 12.5 kw, with control rod 4 withdrawn and to about 8.0 kw with the control rod 4 inserted. After the reactor is pressurized, the power is reduced to about 1.5 Mw, and control rod 4 is inserted to a position such that the element power does not exceed 2.2 kw. At 2.2 kw, the maximum clad temperature is estimated to reach about 1400°F with no flow and complete steam blanketing. Thus, the reactor could be held at $\sim$1.5 Mw indefinitely without damaging the test element fuel cladding.

11.3.7 Physics

Estimate of a typical steady-state power distribution across the E-SADE loop was obtained from a two-dimensional diffusion calculation. The VBWR core was assumed to contain 110 elements, including Consumer High Power Density fuel, AEC Fuel Cycle Program fuel, Dresden test elements, and APED driver elements. The core power was assumed to be 40 Mw, and nine rod Dresden elements were assumed to be adjacent to the loop on three sides, with the exception of a control rod fuel follower, and water on the fourth side. The dimensions and thickness of material used in the analysis were essentially those associated with Figure 11.3.6. The effect of enrichment on the relative thermal neutron flux across a single process tube is given in Figure 11.3.14, and the average thermal neutron flux in each tube may be estimated from the flux map given in Figure 11.3.15.

Estimates of the mid-plane heat flux are given in Table 11.3.3.

TABLE 11.3.3

Position	Enrichment	Clad Thickness (inside and outside)	Mid-plane Heat Flux $Btu/ft^2/hr$
A	8%	0.016	342,000
B	8%	0.016	268,000
C	10%	0.016	314,000
D	8%	0.028	344,000
E	10%	0.016	310,000
F	8%	0.016	270,000
G	6%	0.028	415,000
H	6%	0.028	327,000
I	8%	0.028	387,000

It has been estimated that the loop will have a negligible effect on the temperature and void coefficient of the VBWR. Estimates and measurements are made in accordance with licensing requirements for the particular core configuration prior to operation.

THERMAL NEUTRON FLUX DISTRIBUTION
THROUGH SADE FUEL ASSEMBLY
0.016" CLAD

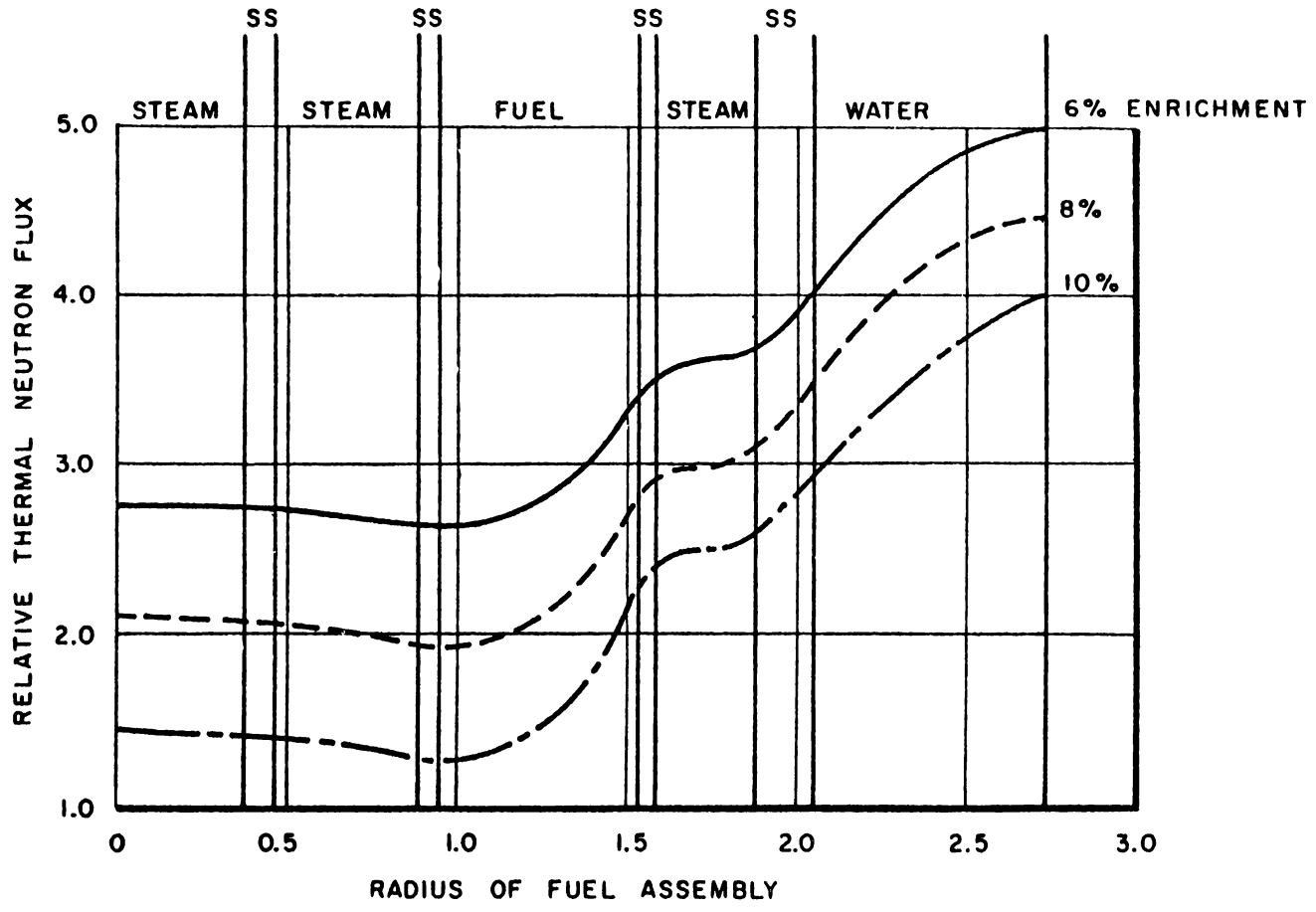

FIGURE 11.3.14

AVERAGE THERMAL NEUTRON FLUX ($X10^{-13}$)

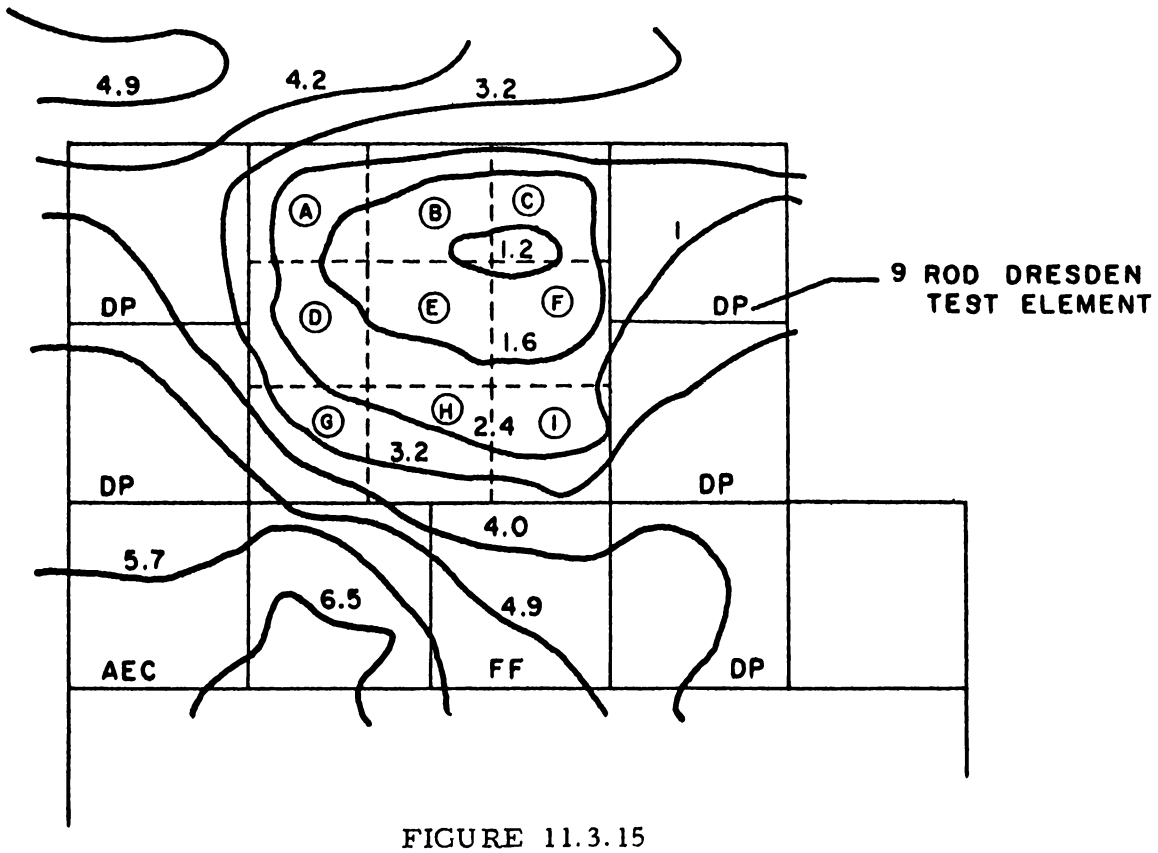

FIGURE 11.3.15

Of considerable interest is the change in reactivity resulting from clearing the loop of water during startup. An estimate was made assuming a full core of E-SADE fuel and then applying the ratio of E-SADE volume to the total core volume, without compensation for the eccentric loop location. The results of this analysis indicated a decrease in core reactivity of about 0.10%. This result is not presented as an accurate estimate of the change in reactivity but, rather, represents a relatively conservative estimate of the probable upper limit to be expected. An accurate estimate of the change in reactivity flooded to unflooded will be determined prior to operation by performing experiments with the SADE loop and relating the results analytically to the E-SADE conditions.

These analyses are representative of only one particular VBWR core loading and of the material compositions listed. Before operation, when an exact core configuration fuel loading and geometry are known, the analyses will be repeated. The analyses will also be reviewed or repeated following significant changes in core or loop which would be expected to affect thermonuclear performance.

11.3.8 Safety Evaluation

Potential hazards in operation and maintenance of the E-SADE loop for the VBWR have been examined and the types of accidents which are believed to represent the worst possible cases are outlined below.

The analysis shows that the reactor can be scrammed and the loop safely shut down without fuel damage. In addition it is shown that the loop maximum credible accident does not increase the probability or severity of the reactor maximum credible accident within the limits of the ability to predict the effects of such an accident.

11.3.8.1 Loss of Coolant

Loss of coolant accidents have been examined on a parametric basis independent of actual mechanisms which could lead to the accident. Types of accidents which could occur are then, by comparison, shown to be a limiting condition of one of the cases analyzed.

In this series of analyses the following general assumptions are used:

1. Element power - 125 KW
2. Loop pressure - 1000 psia
3. Element flow - 1330 lbs/hr
4. Maximum clad temperature - 1250°F
5. The loop power-time relationship follows the curve shown in Figure 11.3.16 and 11.3.17.

With these assumptions five cases were computed as follows:

1. It is assumed that scram occurs and the flow decreases linearly in 30 seconds to 6% of the design value. The resulting temperature-time history of the cladding is shown in Figure 11.3.18.

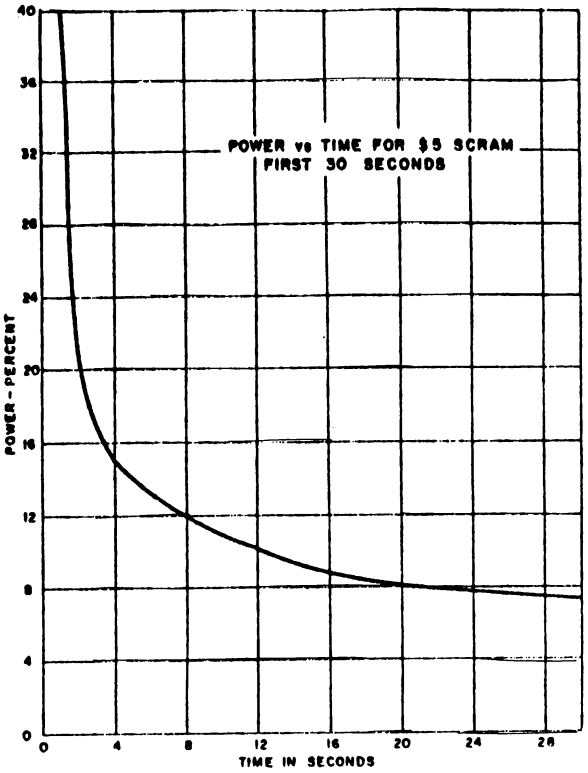

FIGURE 11.3.16

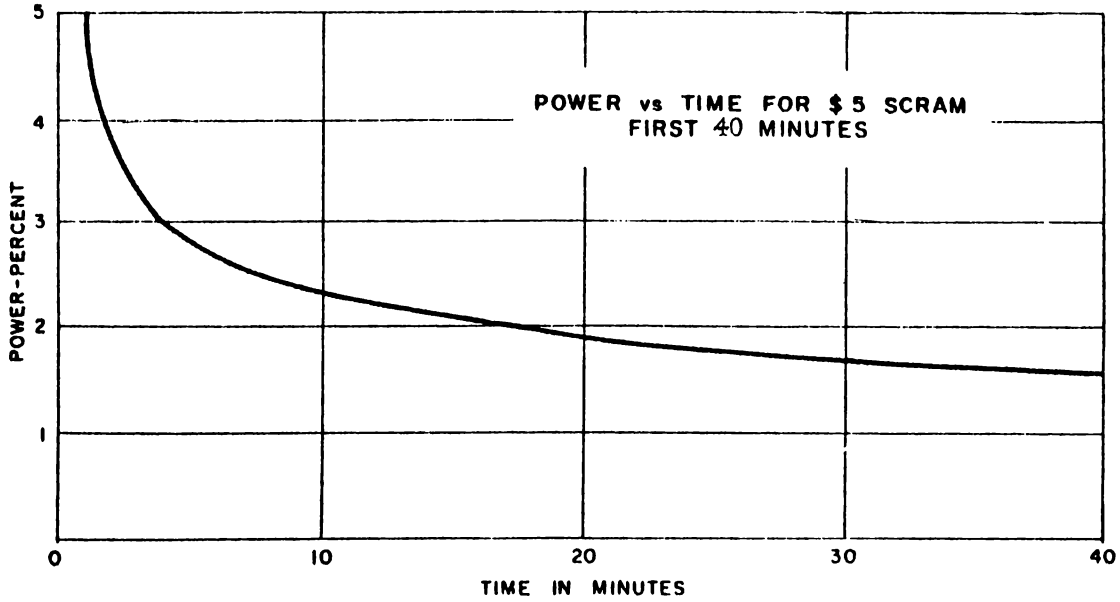

FIGURE 11.3.17

2. It is assumed that flow drops to 80% of design value and in 15 seconds a low flow scram occurs. The flow then decreases linearly over a period of 30 seconds to 4.8% of design value. The time-temperature history of the inner cladding is shown in Figure 11.3.19.

3. It is assumed that, starting with 100% power and flow, a linear increase to 125% power occurs in one second. In 30 seconds the fuel cladding temperature has reached the peak value. A linear flow decrease from 100% to 80% occurs in one second and after 29 seconds the fuel cladding temperature transient is completed. A scram signal is initiated at 60 seconds from time zero and the flow is again decreased to 4.8% of its initial value in 30 seconds. The time temperature history of the cladding is given in Figure 11.3.20.

4. It is assumed that flow is proportioned to pressure and pressure follows the reactor steam line break pressure-time curve shown in Figure 11.3.21. The resulting temperature-time curve of the cladding is given in Figure 11.3.22.

5. Starting after the initial cladding temperature spike which occurs in the first few seconds after scram with no cooling flow, Figure 11.3.23 shows the maximum fuel cladding temperature vs. time. Also shown is the time-temperature history of the fuel cladding for loss of flow starting at 20 minutes following scram and 40 minutes following scram, with initial fuel cladding temperature of about 760°F.

The first loss of flow case, shown in Figure 11.3.18, represents the fuel condition following a scram initiated by any signal other than E-SADE flow, temperature or ΔP which are all assumed to

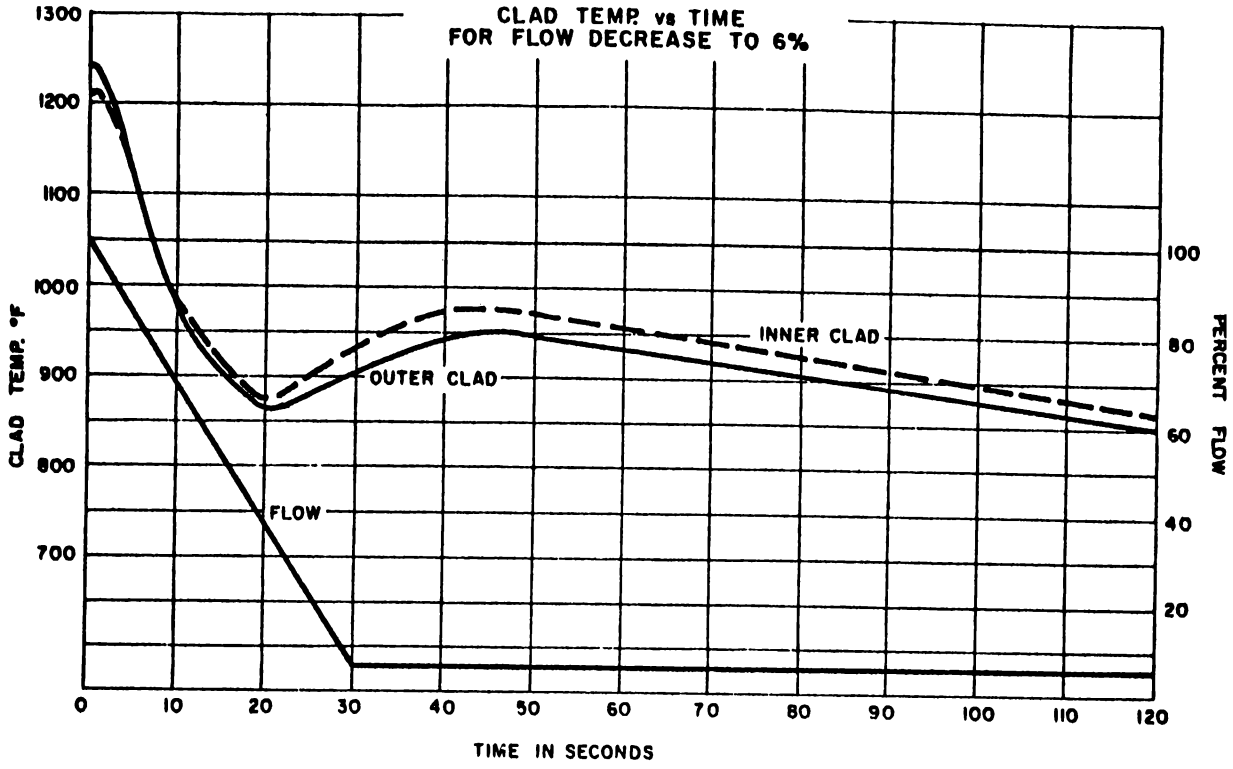

FIGURE 11.3.18

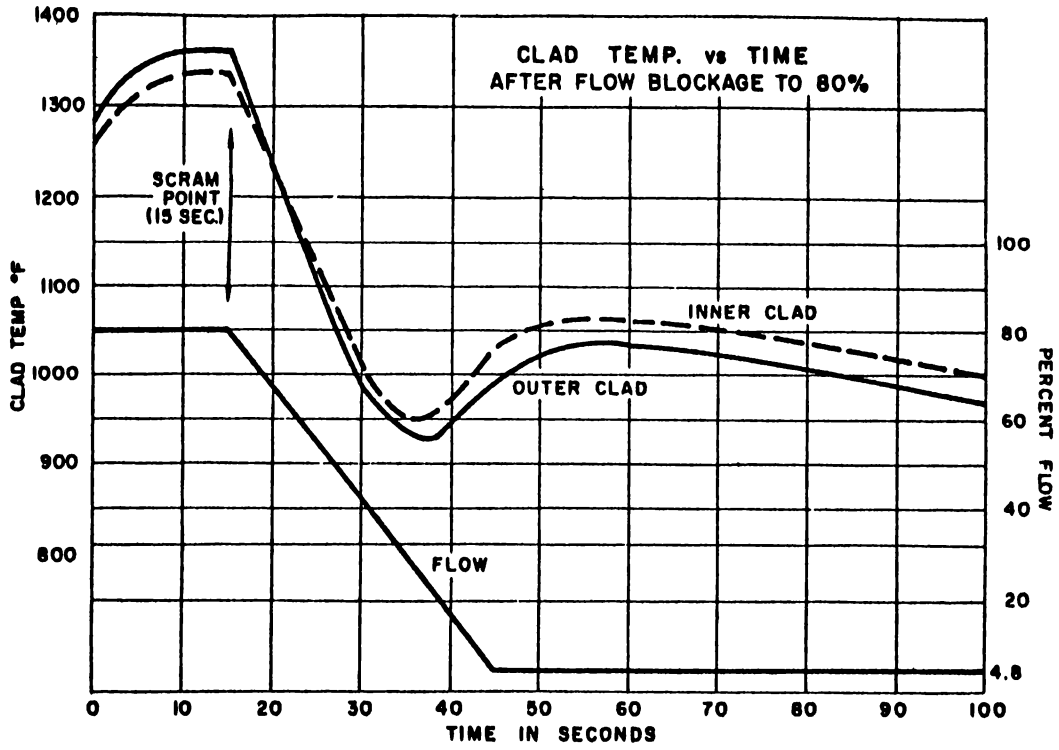

FIGURE 11.3.19

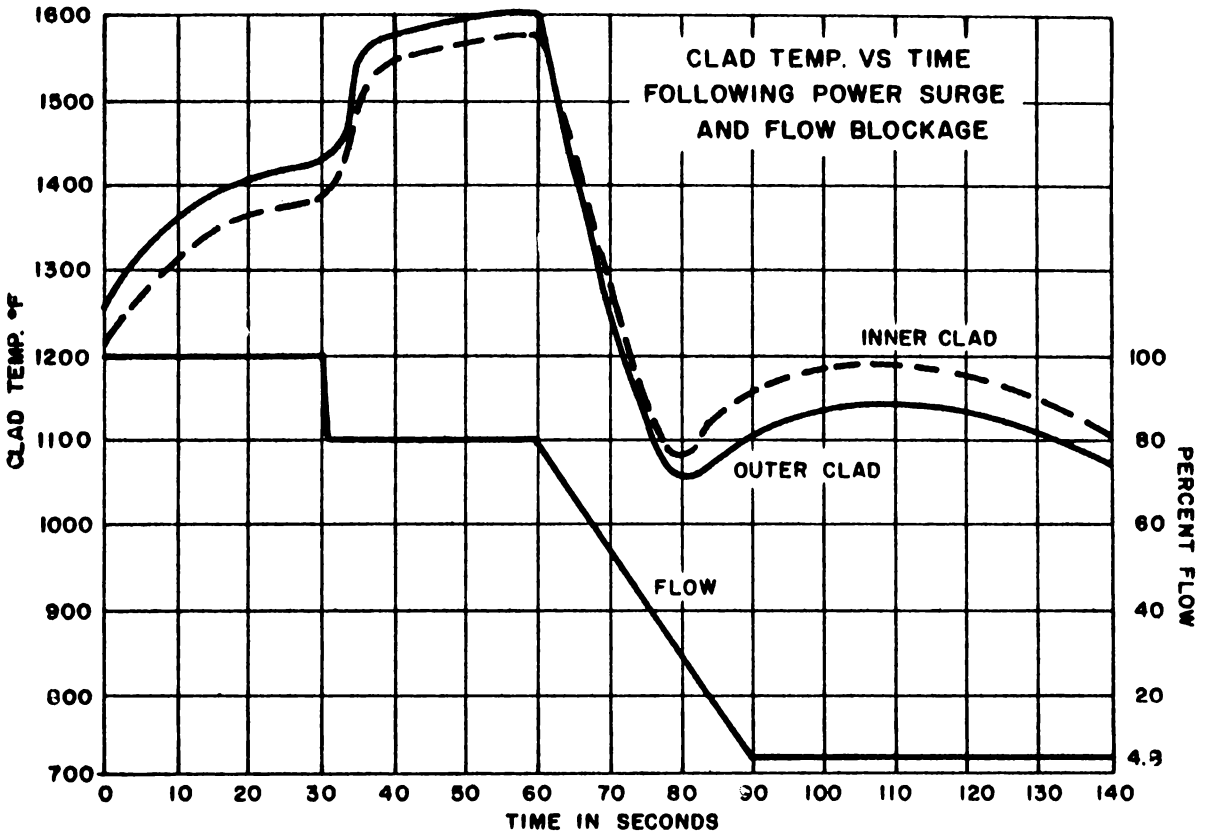

FIGURE 11.3.20

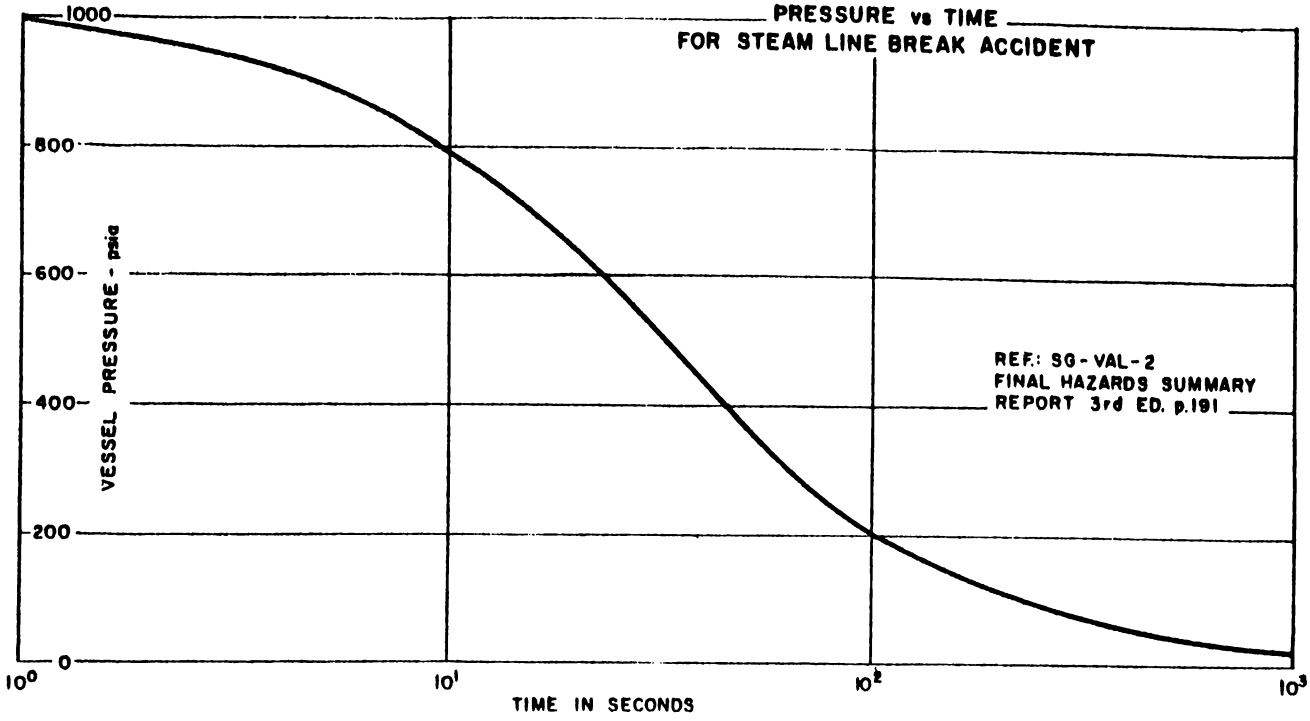

FIGURE 11.3.21

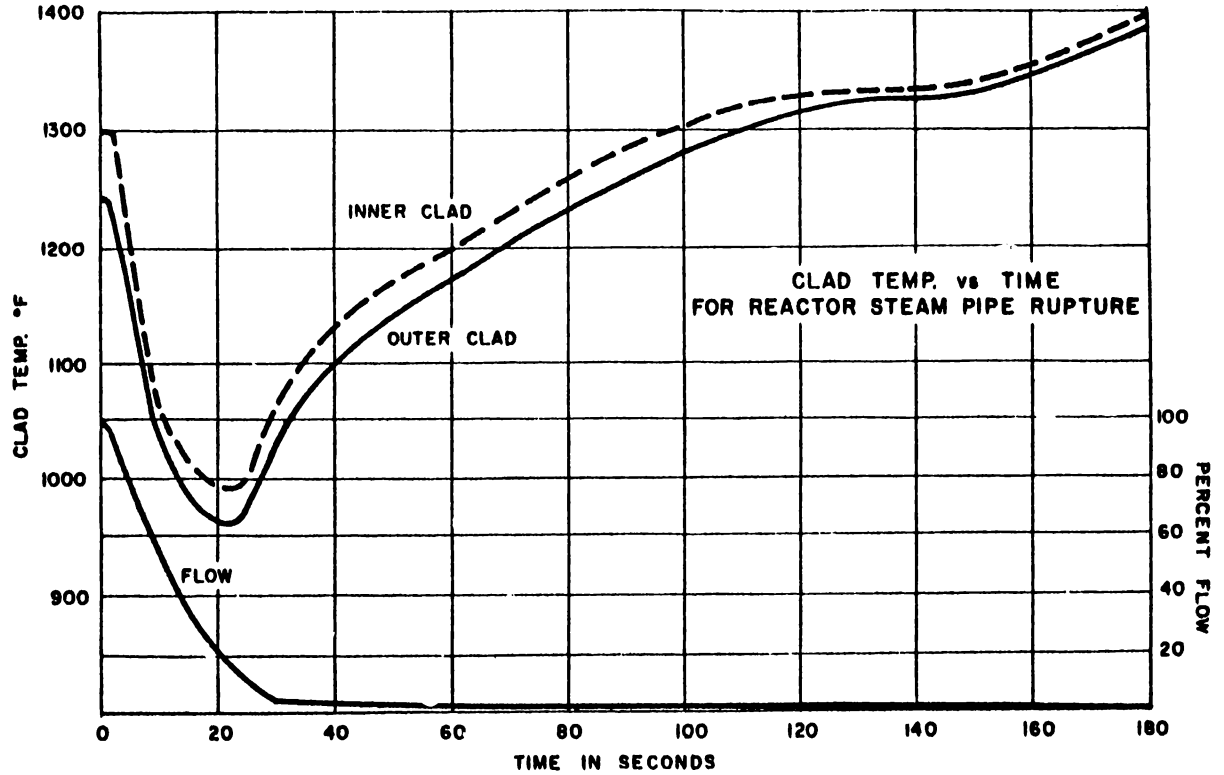

FIGURE 11.3.22

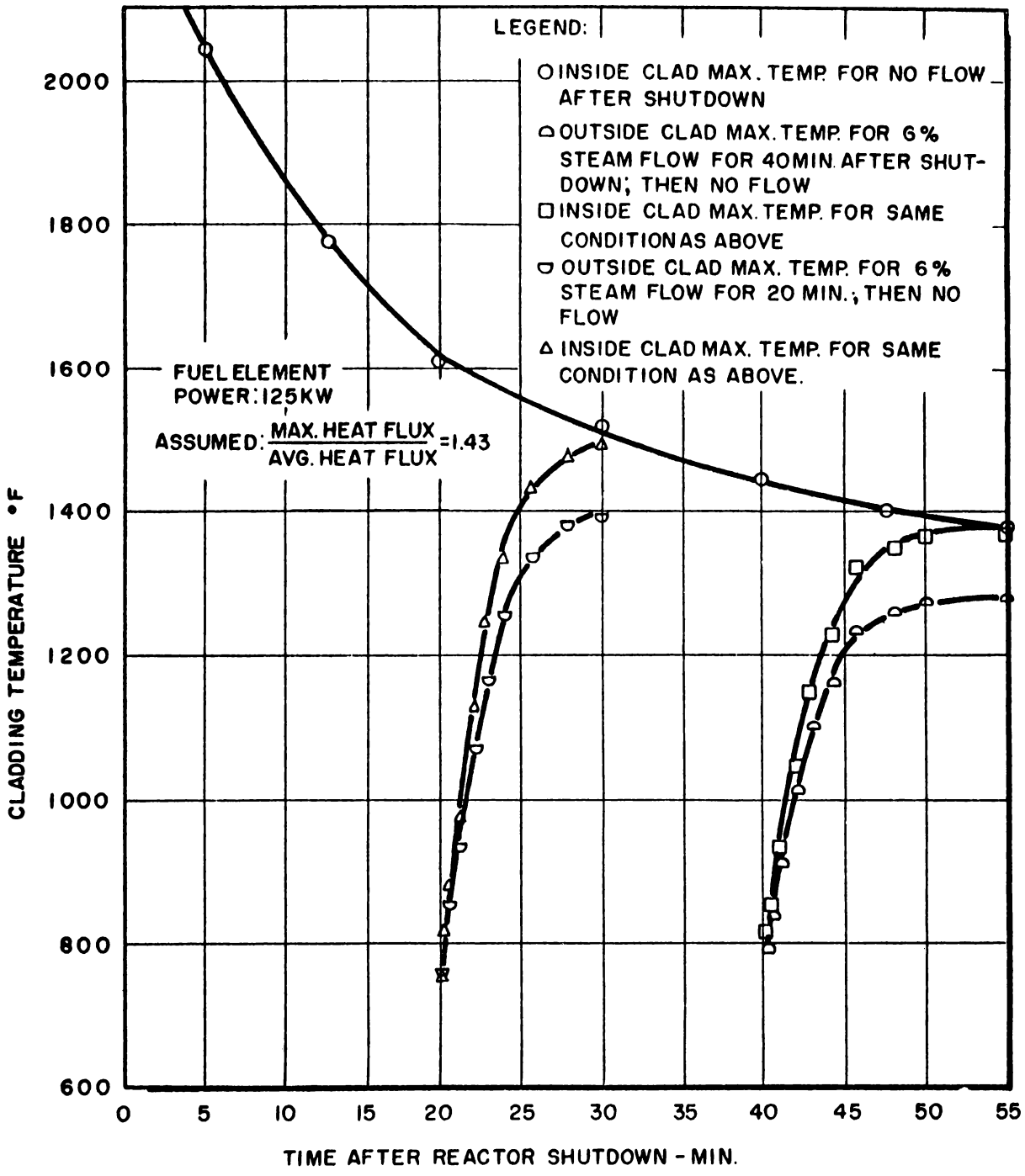

CLADDING TEMPERATURES AFTER REACTOR SHUTDOWN

FIGURE 11.3.23

be normal at time t = 0. The maximum fuel cladding temperature reached in this case is about 980°F.

The second loss of flow case, shown in Figure 11.3.19, represents the establishment of maximum cladding temperature resulting from 80% coolant flow, followed by a scram initiated by the sudden reduction of flow terminating at about 4.8%. The maximum fuel cladding temperature reached during the transient is about 1365°F.

The third loss of flow case shown in figure 11.3.20 represents the unlikely combination of an overpower transient causing maximum cladding temperatures followed by a loss of flow which finally scrams the reactor. This case results in a maximum cladding temperature of about 1600°F.

In this hypothetical accident a scram signal from high exit steam temperature occurs when the cladding temperature reaches about 1550°F. However, this signal has been assumed to be delayed for a sufficient time to allow an additional 50°F rise in cladding temperature.

Since the transient is assumed to occur in less than one minute, considering a purely mechanical cladding failure, the cladding is not likely to fail because the short time tensile properties of 304 stainless steel at 1600°F are superior to the creep properties at 1200-1300°F. It is possible, however, that toward the end of life of the fuel when the fission gas pressure is at a maximum, a failure of the cladding of elements G & I could occur. As discussed in Section 11.3.5, precautions have been taken for detecting and containing radioactive contaminants within the loop or reactor piping if an unplanned fuel rupture should occur.

The fourth loss of flow accident results from loss of reactor pressure. Assuming the maximum rate of pressure loss follows from main steam line pipe rupture, the cladding will reach a temperature of about 1325°F in about 3 minutes as shown in Figure 11. 3. 22. The maximum fuel cladding temperature projected beyond that given in Figure 11. 3. 22, is estimated to be less than 1600°F.

The fifth loss of flow accident is included to illustrate the relative time and maximum temperature that could be reached if the cooling had been supplied in a normal manner at shutdown and the cladding temperature had reached a relatively low value. The coolant is then suddenly removed and the fuel temperature increases from the decay heat to the maximum value shown in Figure 11. 3. 23.

The worst case of loss of reactor pressure other than the piping failure outlined above, involves failure of the turbine admission and turbine bypass valves to close following a reactor scram. The resulting maximum flow rate is about 150, 000 lbs/hr and this results in a maximum clad temperature of about 1300°F.

The steam coolant supply is taken from the reactor vessel through piping across which a pressure difference of only a few pounds exists. A demister covering the entrance is located in the vertical position, offering protection against flow blockage by foreign particles. It is unlikely therefore that complete flow blockage would occur on the inlet side of the steam supply system. The external main loop piping has three valves, 2100, 2155, and 2156 (see Figure 11. 3. 2) which could stop coolant flow. The first valve 2155 is hand operated with a high gear ratio requiring at least 30 seconds to close. Closing the valve at the maximum

rate will result in a reactor scram from low ΔP or low flow. The time from scram to complete valve closure is sufficiently large to prevent fuel cladding failure.

If the valve (2100) is closed at startup, water flow cannot be established and the rods could not be withdrawn. However, contrary to normal operating procedures, this signal could be bypassed by placing the loop safety system in the "switch-over" position. In this case, the hot element is not operated at a power above 2.2kw. At this power the element is sufficiently cooled through radiation and conduction to the moderator water to prevent fuel cladding failure.

If the valve is partially closed so that 50% flow can be achieved, sufficient cooling is available so that damage to the fuel would not occur. If the flow dropped below 50% even momentarily an automatic rod run-in protects the fuel.

The remaining two valves in the steam line are in parallel. One is an air operated valve (2156) held in the open position. A minimum flow of 6% is maintained through a bypass line. A volume chamber and a three-way solenoid valve is arranged so that a scram will cause the bypass to gradually close (about 40 minutes).

It is concluded from the discussion given above that it is highly improbable that coolant will be lost from a piping failure, or by flow blockage by valve closure or by foreign matter to the extent or in the time required to cause fuel cladding failure.

11.3.8.2 Loss of Heat Sink

If the capacity to remove heat from the main condenser was suddenly lost, the pressure in the main condenser will build up to about 330 psi and relieve through a pressure relief valve

(see Figure 11. 3. 2) and the connecting three-inch diameter line to the spent fuel pit. Since the maximum flow to the main condenser is achieved when the pressure beyond the throttling valve is about 450 psi or less, the flow through the test loop will not be reduced appreciably during the transient.

11. 3. 8. 3 Reactivity Effects

The effect on reactivity of removing water from the loop was estimated to reach a maximum of about -0. 25% Δk when the reactor is hot (545°F).

If it is assumed that the loop is suddenly flooded while hot, the power will increase promptly to about 1-1/2 times the initial value and rise on a constant period of about 20 seconds. This increase in power is a relatively minor transient for the reactor (see Sec. 7.12. 2 to 8.12. 4 SG-VAL 2 Third Edition*).

The switch-over from water cooling to steam cooling is accomplished by blowing the water from the loop with reactor steam pressure. If it is assumed that water is partially removed from the loop and falls back in a manner such that a reactivity oscillation is established, since the removal of water produces a negative reactivity effect the neutron production will oscillate from that of criticality to below criticality. However, considering the effect on power of a change in reactivity of 0. 25% as a continuous oscillation, if the frequency of oscillation is in the range between 0. 02 cps and 0. 002 cps, the peak-to-peak reactivity change will yield a peak-to-peak power change of about 36%. By comparison, the magnitude of this power change is not severe.

---

*SG-VAL 2 Third Edition - General Electric Vallecitos Boiling Water Reactor Final Hazards Summary Report, November 30, 1960.

If the frequency of oscillation is greater than 0.02 cps, the power will be reduced and if the frequency is less than 0.02, the power change approaches that obtained by the step function described above.

From the above description it does not appear that a serious excursion would result from clearing the loop of water during startup. However, it is planned to include a period of operation at a reactor power of about 7 Mw, corresponding to a maximum element power of 18 kw, for a sufficient time to insure removal of any water not removed in the initial blowout procedure. The power is selected as the minimum value at which exit steam temperature can be used to verify that all channels are cleared of water.

Estimates have been made for the maximum reactivity worth of the ESADE assembly. These estimates indicate that under extreme conditions, i.e., conditions which are highly improbable, the reactivity worth of the nine (9) element ESADE assembly could reach 3.4% Δk. Because of this potentially high worth of the assembly, the provision has been added to the technical specification specifically prohibiting installation or removal of the ESADE fuel assembly until the mechanical control rod drive lock is in place and it has been shown by analysis that the worth of the bundle is less than 1% Δk. Assuming this restriction is applied the reactivity addition which will occur if the entire ESADE bundle is added to the core, will be less than the 1.1% previously analyzed for the reactor loading accident (Section 8.9 "Loading Accident" SG-VAL 2 Third Edition - General Electric Vallecitos Boiling Water Reactor Final Hazards Summary Report, November 30, 1960).

The effects of reactor reactivity accident on the ESADE assembly have been estimated as follows:
For a reactivity addition accident starting at less than 20% reactor power (about 7 mw) if the loop flow is as low as 20% corresponding to a starting peak fuel temperature of 2000°F, 655 kw seconds is required to cause a peak fuel temperature of 4000°F, corresponding to a cladding temperature of less than 1400°F. This represents a reactor excursion of about 160 mw seconds*.

If the reactor is at full power and a step input of 80¢ reactivity is assumed, some cladding failure of the VBWR core could occur. This assumed accident would result in a maximum ESADE fuel temperature of about 3800°F and a maximum cladding temperature of about 1305°F.

If the loop is being operated with water cooling, 655 kw seconds must be added to raise the fuel temperature 2000°F as stated above. Since about 1000 kw seconds are required to vaporize the water within the fuel element, a sufficient energy sink is available for removing heat stored in the fuel following this hypothetical accident.

These analyses show that fuel cladding failure is unlikely to result from reactor reactivity transients, as hypothesized in General Electric Final Hazards Summary Report SG VAL-2, Third Edition, November 30, 1959.

11.3.8.4 Loss of Power

If the power supplied to the site is lost during power operation

*Startup accident given in General Electric VBWR Final Hazards Summary Report SG VAL-2, Third Edition, November 30, 1959.

of the loop, the reactor will scram and the turbine admission valve will close. The flow control valve (2255 Figure 11. 3. 2) will close in about 30 seconds with the 6% bypass flow valve (2256 Figure 11. 3. 2) held open for approximately 40 minutes. The maximum clad temperature resulting from the transient will be about 980°F as discussed in Case 1, Section 11. 3. 8. 1.

If power is lost while the fuel is water-cooled, a sufficient quantity of water is available within the active fuel region to absorb the energy produced until the decay power is reduced to about 1. 8% of operating power which corresponds to a maximum clad temperature of 1400°F for no steam flow. Actually, a considerably greater quantity of water is available for cooling than that within the active fuel region.

A loss of power will stop cooling water flow to the main condenser resulting in the "Loss of Heat Sink" condition discussed in 11. 3. 8. 2.

11. 3. 8. 5 Loss of Instrument Air

If instrument air is lost during power operation of the loop, the reactor will scram and the turbine admission valves will close. The flow control valve (2255 Figure 11. 3. 2) will close in about 30 seconds with the 6% bypass flow valve (2256 Figure 11. 3. 2) held open for approximately 40 minutes. The maximum clad temperature resulting for the transient will be about 980°F as discussed in Case 1, Section 11. 3. 8. 1.

If instrument air is lost while the fuel is water cooled, the cooling water supply would be lost but as stated in 11. 3. 8. 4, sufficient water is present in the fuel region to prevent fuel cladding rupture.

Loss of instrument air would not affect the normal heat removal process in the main condenser.

11. 3. 8. 6 Maximum Credible Accident

The maximum credible accident of the loop is the instantaneous loss of coolant resulting in fuel temperatures shown in Figure 11. 3.24.

The rate of temperature rise is such that the cladding may be considered violated virtually instantaneously.

Since failure of the loop piping will not result in this type of accident unless a complete seal is effected, it is assumed that the resulting fission products are contained within the loop piping.

The fission products would be only about 2% of that released in the VBWR maximum credible accident, assuming the same percentage of fission products are released. However, in the case of the ESADE loop the fission products are contained within the loop piping and the peak UO_2 temperature for ESADE fuel is less than the reactor maximum credible accident fuel temperature which would tend to depress the total fission product release.

The maximum reactivity addition that could occur if the loop suddenly filled with water is about . 25% Δk. This value is very small compared to reactivity changes which would be expected to result in fuel damage. Thus, complete failure of the ESADE piping within the reactor would not cause a serious reactor excursion and complete flow blocking would result in negligible release of fission products in comparison to the

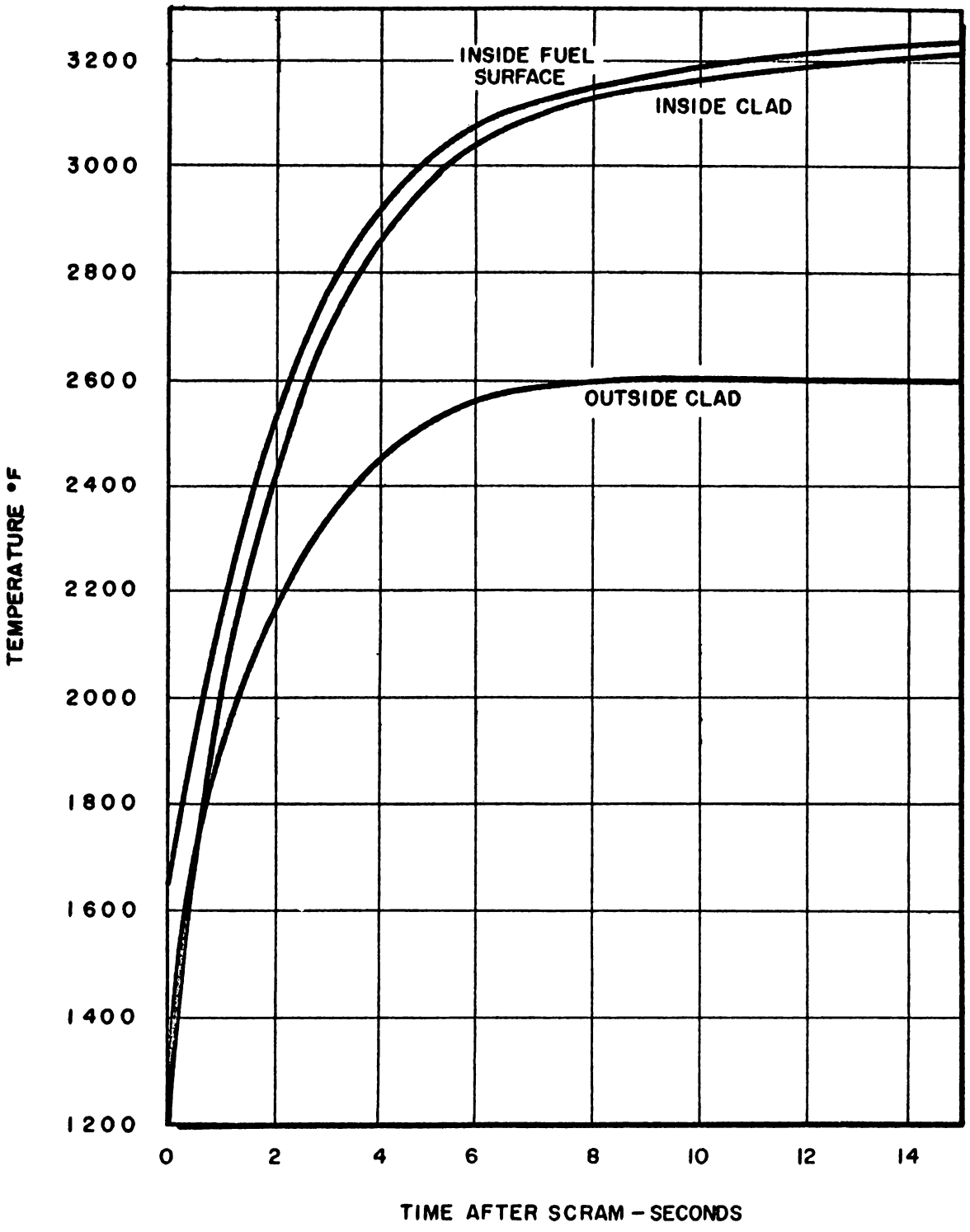

CLAD & FUEL SURFACE TEMPERATURE VS. TIME AFTER SCRAM FOR ZERO FLOW

FIGURE 11.3.24

reactor maximum credible accident.

It is concluded therefore that the experiment does not increase the magnitude or probability of the VBWR maximum credible accident.

6. All other conditions remain the same.